AD_____

Award Number: W81XWH-09-1-0359

TITLE: Role of Stat3 and ErbB2 in Breast Cancer

PRINCIPAL INVESTIGATOR: Mulu Geletu, Ph.D.

CONTRACTING ORGANIZATION: Queen's University
Kingston, Ontario, Canada K7L 3N6

REPORT DATE: October 2011

TYPE OF REPORT: Annual Summary

PREPARED FOR: U.S. Army Medical Research and Materiel Command
Fort Detrick, Maryland 21702-5012

REPORT DOCUMENTATION PAGE

Form Approved
OMB No. 0704-0188

1. REPORT DATE	2. REPORT TYPE	3. DATES COVERED
October 2011	Annual Summary	15 September 2010 ï 14 September 2011

4. TITLE AND SUBTITLE

Role of Stat3 and ErbB2 in Breast Cancer

5a. CONTRACT NUMBER

5b. GRANT NUMBER
W81XWH-09-1-0359

5c. PROGRAM ELEMENT NUMBER

6. AUTHOR(S)

Mulu Geletu, Ph.D.

E-Mail: geletu@queensu.ca

5d. PROJECT NUMBER

5e. TASK NUMBER

5f. WORK UNIT NUMBER

7. PERFORMING ORGANIZATION NAME(S) AND ADDRESS(ES)

Queen's University
Kingston, Ontario, Canada K7L 3N6

8. PERFORMING ORGANIZATION REPORT NUMBER

9. SPONSORING / MONITORING AGENCY NAME(S) AND ADDRESS(ES)
U.S. Army Medical Research and Materiel Command
Fort Detrick, Maryland 21702-5012

10. SPONSOR/MONITOR'S ACRONYM(S)

11. SPONSOR/MONITOR'S REPORT NUMBER(S)

12. DISTRIBUTION / AVAILABILITY STATEMENT
Approved for Public Release; Distribution Unlimited

13. SUPPLEMENTARY NOTES

14. ABSTRACT
Activation of Stat3 has been demonstrated in breast and other cancers. However, the exact mechanisms of its activation as well as the role of Stat3 in these tumors, remain to be determined. This study focuses on the identification of the upstream activators of Stat3 in confluent cells as well as the role of Stat3 in this setting. To explore the nature of cell to cell adhesion molecules responsible for Stat3 activation in breast cancer, we examined the role of cadherin- 11 engagement using mouse Balb/c3T3 fibroblasts, which have high amounts of Cadherin -11. Cadherin-11 knockdown experiments demonstrated that this increase is required for Stat3 activation. Plating the cells on surfaces functionalised with cadherin-11 derived fragments caused a dramatic increase in Stat3-ptyr705 levels, indicating that cadherin-11 can directly activate Stat3, in the absence of cell to cell contact. Our results also demonstrated a reciprocal regulation between cav1 and Stat3. cav-1 downregulation through expression of shRNA activates Stat3, and conversely, cav1 overexpression downregulates Stat3 and induces growth retardation or apoptosis in mouse fibroblasts, as well as in breast cancer lines. In all cases, apoptosis was inhibited by co-expression of the constitutively active form of Stat3, Stat3C. Taken together, these findings point to cav1 as an inhibitor of Stat3 activity. In addition, it was previously demonstrated that cav1 upregulates p53, although the exact mechanism is unclear. Since Stat3 is known to inhibit p53 transcription through direct promotor binding, these data also point to the possibility that cav1 upregulation may, in fact, activate p53 through Stat3 inhibition. We also further demonstrate for the first time that, in a feedback loop, Stat3 inhibition results in a dramatic increase in cav1 levels, indicating that Stat3 also downregulates cav1 expression. Taken together, our findings reveal the presence of a potent, negative regulatory loop between cav1, p53 and Stat3 that plays a crucial role in cellular survival.

15. SUBJECT TERMS
Stat3, ErBb2, Breast cancer, Cadherin-11, Caveolin-1

16. SECURITY CLASSIFICATION OF:			17. LIMITATION OF ABSTRACT	18. NUMBER OF PAGES	19a. NAME OF RESPONSIBLE PERSON
a. REPORT	b. ABSTRACT	c. THIS PAGE			USAMRMC
U	U	U	UU	118	19b. TELEPHONE NUMBER *(include area code)*

Table of Contents

Introduction

Cells in normal tissues or tumors have extensive opportunities for adhesion to their neighbors in a three-dimensional organization, and it recently became apparent that in the study of fundamental cellular processes it is important to take into account the effect of surrounding cells.

The signal transducer and activator of transcription-3 (Stat3) is activated by receptor tyrosine kinases, cytokine receptors and non-receptor tyrosine kinases. Following ligand stimulation, Stat3 is activated through phosphorylation at tyr-705 and migrates to the nucleus where it activates the transcription of genes involved in cell growth and survival[1,2]. Persistent activation of Stat3 has been demonstrated in breast and other cancers, while a constitutively active form of Stat3, Stat3C, is able to transform cultured cells[3] , further pointing to an etiologic role for Stat3 in these tumors. My project deals with the mechanism of Stat3 activation and its role in these tumors, hence the consequences of its inhibition.

We recently discovered a ***novel pathway of activation of Stat3***, a protein involved in cell division, triggered by engagement of ***E-cadherin***, an extensively studied, cell to cell adhesion molecule. Stat3 activation was due to a striking upregulation of the Rac/Cdc42 GTPases[4*] and was followed by a potent downregulation of the p53 tumor suppressor and apoptosis inhibition. Most importantly, this Stat3 activation was resistant to inhibition of a number of tyrosine kinases, including the Src family, IGF1-R, Abl, Fer and EGFR, often activated in breast and other cancers[5*]. We propose the existence of a ***novel pathway of Stat3 activation*** that is triggered by cadherin engagement, which can be especially important in tumor cells.

Another molecule with a profound significance in breast cancer and Stat3 signalling is caveolin-1. Caveolae are cholesterol-rich, 50-100nm flask-shaped invaginations of the plasma membrane, with caveolins (cav1-3), the marker proteins of caveolae, embedded in their lipid bilayer[6-8]**.** The human cav1 gene is found in a tumor suppressor locus on chromosome 7q31.1, which is commonly deleted in a variety of cancers. This led to the hypothesis that this region may encode a tumor suppressor gene[9-11]**.** Cav1 recruits many receptor and non-receptor tyrosine kinases and through binding to its scaffolding-domain, cav1 sequesters the kinases in an inactive form, thereby preventing their involvement in signaling pathways[8]**.** The examination of the effect of this inhibition upon Stat3 activity is very important in Stat3 signalling as well as breast cancer Biology.

These novel aspects of Stat3 biology, namely Stat3 activation triggered by specific cadherin engagement, or Stat3 inhibtion by cav1, could be promising prognostic markers, as well as predictive targets for the treatment of tumors which may be ***resistant*** to inhibition of many ***tyrosine kinase oncogenes*** known to be ***hyperactive in breast cancer***, such as the ErbB2 drug ***Herceptin***.

Body

Specific Aim 1. Examination of the upstream activators of Stat3 in confluent cells

Engagement of cadherin-11 increases Stat3 activity

Most of the studies on cadherin signaling have focussed on the E-cadherin, cell adhesion molecule and member of the classical type I cadherin family. Although both E-cadherin and cadherin-11, a prototype, type II classical cadherin, bind to p120 and β-catenin, they have fundamental differences in their function:

Early results showed that continued expression of ***E***-cadherin is required for cells to remain tightly associated within the epithelium, so that loss of E-cadherin function leads to metastasis of breast cancer[12,13]. In sharp contrast, cadherin-11 was shown to be elevated in a number of cancers. In addition, cadherin-11 has been linked to breast cancer metastasis[14,15] and more recent findings show that it promotes the metastasis of prostate cancer cells specifically to the bone[16]. Therefore, examination of the mechanism of cadherin-11 action is of paramount importance in the study of cell to cell adhesion as well as metastasis.

As stated in the introduction, our lab recently demonstrated that engagement of E-cadherin causes a dramatic increase in Stat3 activity[5,17,18*]. However, further examination of cell lines which are known to lack E-cadherin, such as the Chinese hamster ovary and the cervical carcinoma A431D, revealed a great increase in Stat3 activity with density (Arulanandam, Geletu, Raptis et al, unpublished observations). This prompted us to examine the involvement of other calcium-dependent adhesion molecules, such as cadherin-11, using the mouse fibroblast line Balb/c3T3. These cells express high amounts of Cadherin-11, but not E-cadherin (Fig. 1A lanes 2-3)[4*].

As shown before for a number of normal cell lines[5]*, Stat3-ptyr705 levels were almost undetectable in sparsely growing, Balb/c3T3 cells (Fig. 1B, lanes 1-2). However, density caused a dramatic increase, which peaked at 2-3 days after confluence (Fig. 1B, lanes 3-5) to levels approximately half the levels present in cells transformed by the potent Stat3 activator, v-Src (Fig. 1A, lane 6). Probing for total Stat3 revealed a modest increase with cell density (Fig. 1B), possibly due to the fact that Stat3 activates its own promoter[19], although the differences were not as big as the Stat3-tyr705 phosphorylation observed. This activation was specific to Stat3, since the levels of Erk1/2 remained unaffected by cell density, as shown before for E-cadherin[20]*. The above results indicate that cell density causes a specific increase in Stat3-ptyr705 levels in mouse Balb/c3T3 fibroblasts.

We next investigated whether the Stat3 activation is a direct consequence of the engagement of cadherin-11, or whether cadherin interactions are simply required to bring adjacent cell surfaces into proximity, to initiate signals which are not immediate effects of cadherin ligation. To definitively answer this question, we made use of a recombinant cadherin-11 fragment, encompassing the two distal, extracellular domains of cadherin-11 (11/EC12) to functionalize petri dishes by covalent immobilization (Fig.2A). This fragment has been shown to retain biological activity when attached onto surfaces and is recognized specifically by cadherin-11 expressing cells[21]. Plastic, 3cm petri dishes were coated with increasing amounts of purified 11/EC12 fragment, from 1 to 1,000μg/ml, and 30,000 Balb/c3T3 cells were plated on these surfaces[22]*. Detergent cell extracts were prepared 48 hours later, when cells were 30% confluent and probed for Stat3-ptyr705 as above. As shown in Fig. 2B, there was a dramatic and graded increase in Stat3-ptyr705 levels, in proportion to the amounts of 11/EC12 used to decorate these surfaces when Balb/c3T3 cells were plated (lanes 2-5), while there was no increase in Stat3-ptyr705 when Balb/c 3T3 cells were plated on petri dishes coated with the corresponding fragment derived from E-cadherin (E/EC12), as a control (Fig. 2B, lane 1). As a further control, normal mouse breast epithelial HC11 cells were plated on surfaces coated with 11/EC12 or on the corresponding, E-cadherin fragment E/EC12, and Balb/c3T3 cells were plated on surfaces coated with the E/EC12 fragment. As expected, there was no increase in Stat3-ptyr705 when HC11 cells, which are naturally devoid of cadherin-11, were grown on surfaces coated with 11/EC12 (Fig. 2B, lanes 7 and 8), while there was an increase upon growth of HC11 cells on E/EC12-coated surfaces (lane 9). Similar results were obtained with the 10T1/2, mouse fibroblasts, which also express cadherin 11 (not shown). The increase was specific to Stat3, since no increase in Erk1/2 upon plating of Balb/c 3T3 cells on 11/EC12-coated surfaces was noted (Fig. 2B). The above findings demonstrate a dramatic increase in Stat3-ptyr705 upon direct cadherin-11 engagement in mouse fibroblasts, which was specific to Stat3 and proportional to the density of 11/EC12 present on the culture surface, indicating that, in the appropriate cellular context, cadherin-11 engagement is sufficient to activate Stat3, in the absence of direct cell to cell contact.

To examine the contribution of cadherin-11 in the density-dependent, Stat3 activation in Balb/c3T3 cells, cadherin-11 was knocked-down using a shRNA expressed with a retroviral vector (Fig. 3). The results showed that this treatment essentially eliminated cadherin-11 (Fig. 3A lane 1-2), thus demonstrating the effectiveness of this particular shRNA. Most importantly, examination of Stat3-ptyr705 levels showed an almost total elimination of Stat3 activity as well upon cadherin-11 knockdown, even at higher densities (Fig. 3B). These findings demonstrate that cadherin-11 is the main cadherin activating Stat3 in Balb/c3T3 cells, which makes it into a suitable system for the study of the role of cadherins upon transformation by oncogenes such as vSrc (Geletu, Raptis et al, in preparation).

Cadherin-11 plays a positive role in cell survival, proliferation and migration

Previous results have shown that Stat3 signaling can induce anti-apoptotic genes, such as Bcl-xL and mcl-1[23,24], while it downregulates the p53 promotor [25], thus protecting tumor cells from apoptosis. To examine the functional consequences of the cadherin-11 mediated, Stat3 activation, we examined the effect of cadherin-11 knockdown in Balbc/3T3 cells. Following infection with a retroviral vector expressing a cadherin-11 shRNA, apoptosis was examined by terminal deoxynucleotidyl transferase biotin –dUTP nick end labeling (TUNEL) staining at different densities, as before[26]*. The results showed that cadherin-11 deficient, Balb/c3T3 cells become apoptotic when confluent (Fig. 3C, panel a-b) while no apoptosis was noted in the parental Balb/c3T3, even at high densities (Fig. 3C, panel c-d). These findings are in keeping with previous data

indicating that direct Stat3 inhibition in mouse fibroblasts using cell permeable peptides[5]* or peptidomimetics blocking the Stat3-SH2 domain[27]*, pharmacological inhibitors[27]*, or genetic ablation[26]*, in densely growing cultures induces apoptosis.

To further determine the role of cadherin-11 upon the cellular phenotype, we evaluated the effect of cadherin-11 downregulation upon the rate of cell proliferation and migration. As shown in Fig. 3D, cadherin-11 knockdown cells had a doubling time of 30 hrs, while the doubling time of the parental Balb/c3T3 was 24 hrs. In addition, the rate of migration of cadherin-11 knockdown cells was lower compared to the parental Balb/c3T3 (Fig. 3E c-d, vs a-b), indicating that cadherin-11 plays a positive role in both cell proliferation and migration.

The fact that cadherin-11 may actually activate Stat3, although, contrary to E-cadherin, cadherin-11 promotes metastasis, may point to Stat3 as a central ***survival***, rather than metastasis, factor, which would have important therapeutic implications. Most importantly cadherin-11 inhibition would be expected to induce apoptosis in metastatic cells specifically, while normal cells expressing E-cadherin would be spared.

The above data are also echoed by additional evidence on another cadherin involved in metastasis, the N-cadherin. In fact, ***Ncad*** overexpression and engagement has been reported to be associated with a highly ***invasive*** phenotype, and motility in mammary cell lines[28-31], since normal squamous epithelial cell lines acquired migratory properties upon transfection with Ncad[32]. Moreover, in certain tumour lines, such as MCF7 breast cancer cells which express Ecad and are not motile, transfected Ncad conferred a migratory phenotype, despite the presence of the endogenous Ecad[29,31]. My results demonstrated that N-cadherin also can activate Stat3: In Embryonal-stem (ES) cells where E-cadherin was ablated (null cells[4]*) and N-cadherin re-expressed (Ncad-addback)(not shown), density did cause a dramatic increase in Stat3-ptyr705 and transcriptional activity through upregulation of members of the IL6 family of cytokines. These results taken together demonstrate the generality of the phenomenon of Stat3 upregulation by cadherin engagement, which appears to be critical in cellular survival of a number of tissue types. These results will be shortly submitted for publication to *Oncogene* (see reportable outcomes below). A preliminary report has been presented at the 101th annual meeting of the American association for Cancer research, Washington, DC. April 2010 (unpublished data).

Unexpected difficulties: The cadherin-11 antibodies we used initially (Invitrogen) had poor specificity. We tested a large number of antibodies from different companies, but the results were disappointing. Attempts to examine the effect of infection of the shRNA-cadherin11 retroviral vector by examining cadherin-11 mRNA levels by RT-PCR met with poor success, likely because the mRNA is not completely degraded. Finally, we produced our own antibodies in collaboration with Dr. Ferracci and these were employed for most Western blotting and immunohistochemistry experiments.

Specific Aim 2: Examination of the role of Stat3 in confluent cultures: Effect of Stat3 upon p53

Cell density causes a dramatic increase in cav1 levels

In our attempt to decipher the interrelationship between Stat3 and p53, we discovered another potential player: Caveolin 1 (cav1), a 22 KDa membrane protein is the major protein responsible for the organization and maintenance of caveolae microdomains[6,8]**.** Cav1 recruits many receptor and non-receptor tyrosine kinases and through binding to its scaffolding-domain, cav1 sequesters the kinases in an inactive form, thereby preventing their involvement in signaling pathways[8]. Early results demonstrated that cell density can increase cav1 levels[33], but the levels of cav1 at confluences beyond 100% had not been examined. To examine the effect of extensive cell to cell adhesion upon cav1 levels, NIH3T3 cells were grown to 70% confluence and over several days thereafter cell extracts were probed for cav1 by western blotting. Our results show that cav1 levels were almost undetectable in sparsely growing cells (Fig. 4A, lanes 1-2) while density caused a dramatic increase (Fig. 4A, lanes 3-5). These results demonstrate that cell density must be taken into account in experiments measuring cav1 levels in a given cell line.

cav1 downregulation increases Stat3-ptyr705 phosphorylation and activity

Previous results indicated that reduction of cav1 levels increases the activity of Erk, perhaps through an effect upon the caveolin scaffolding domain (CSD)[33,34]. Since the Erk and Stat3 pathways are often coordinately regulated by growth factors and oncogens, we investigated the effect of cav1 upon Stat3-ptyr705 phosphorylation. Cav1 was downregulated using a commercially available cav1 shRNA retroviral construct, expressed in NIH3T3 cell line. As shown in Fig. 4B, cav1 knockdown caused an increase in Stat3 ptyr705, at all densities examined. This finding argues for cav1 as a negative regulator of Stat3 activity.

cav1 up-regulation decreases Stat3 activity and induces apoptosis through the scaffolding domain

Previous data demonstrate that p53 up-regulates caveolin-1 gene expression[35], while, in a positive feedback loop, caveolin-1 expression increases the activity of p53[36]. Since Stat3 downregulates p53 by direct promotor binding[25], we explored the potential involvement of Stat3 in p53 upregulation by cav1 (Fig. 4C). wtCav1, fused to red fluorescence protein (wt-cav1-mRFP), or the same construct with a mutation in the scaffolding domain (F92A/V94A CSD-mRFP) known to be necessary for sequestration and downregulation of growth factor receptors[37] as well as for p53 upregulation by cav1[36], were expressed in NIH3T3 or MCF7 cells. The results demonstrated a potent reduction in Stat3-ptyr705 levels upon cav1 overexpression in both cell lines, indicating that cav1 down-regulates Stat3 activity (Fig. 5A, lanes 3-4 and B, lane 3). Interestingly, the cav1 levels in NIH3T3 cells transfected with CSD-mRFP were similar to the parental line (Fig. 5A, lanes 5-6), indicating that the CSD-domain is important for Stat3 downregulation by cav1. Since Stat3 is known to inhibit p53 transcription through promotor binding[25], these data also point to the possibility that cav1 may, in fact, activate p53 through Stat3 inhibition.

To examine whether cav1 overexpression can also cause apoptosis, MCF7 cells transfected with the wt-cav1-mRFP or CSD-mRFP (F92A/V94A) were stained for TUNEL. Our results revealed extensive apoptotic death in MCF7 cells upon wt-cav1 expression (Fig. 5C, a-b). Similar results were obtained when we observed by morphology of the cells MCF7 (Fig. 5D, panel a-b) and NIH3T3 (Fig. 5E, panel a-b) wt-cav1mRFP or with a construct containing Enhanced Green Fluorescence protein fused to wt-cav1 (EGFP-cav1) expression.

In sharp contrast, NIH3T3 or MCF7 cells transfected with the cav1 scaffolding domain mutant did not display any of the morphological characteristics indicative of apoptosis at any point, up to 2 weeks after transfection (Fig. 5C, c-d and 5D, c-d). As expected, the control plasmids expressing EGFP (Fig. 5E, panel c-d) or mRFP alone (not shown) did not induce apoptosis. These data indicate that cav1 inhibits Stat3 and induces apoptosis by a mechanism which involves the scaffolding domain. Therefore, our findings point to cav1 as a potent inhibitor of Stat3 activity, and hint at the possibility that Stat3 downregulation by cav1 may be behind the apoptosis observed upon cav1 transfection. In addition, since the Stat3 downregulation by cav1 could upregulate p53, this would also explain the p53 upregulation by cav1 overexpression. Taken together, the above data reveal the presence of a potent, negative regulatory loop between cav1, p53 and Stat3 that leads to apoptosis.

Stat3 overexpression can protect from cav1-mediated apoptosis

Several studies have shown that Stat3 is responsible for transcribing anti-apoptotic genes such as Bcl-Xl and Mcl-1 that promote cell survival[23,38,39]. Since Stat3 promotes cell survival, we examined whether Stat3 could rescue cells from cav1-mediated apoptosis. Therefore, we co-transfected NIH3T3 mouse fibroblasts with EGFP-cav1 and a plasmid expressing the constitutively active form of Stat3, Stat3C (a gift of Dr. Bromberg), and the morphology of the cells was observed over 2 weeks. The results showed that Stat3C co-expression could overcome apoptosis triggered by cav1 (Fig. 5F).

Downregulation of Stat3 upregulates cav1 levels

Although examination of the cav1 promotor did not reveal any *bona fide* Stat3 consensus binding site, a Stat3 binding site is present in cav1 intron 2. Such a functional, Stat3 binding site is present in the fourth intron of the Wnt5a gene[40]. In addition, 2 sp1 transcription factor binding sites exist in the human cav1 gene, where Stat3 may bind in conjunction with sp1, in a manner previously described for the NHE3[41] and VEGF[42] promotors. In fact, our results demonstrated for the first time that, in a feedback loop, Stat3 inhibition following infection with an

Adenovirus vector expressing a Stat3-specific, shRNA, resulted in a dramatic increase in cav1 levels (Fig. 5G), indicating that Stat3 also downregulates cav1 expression. Since p53 upregulates cav1[35], and Stat3 blocks the p53 promotor[25], it is possible that Stat3 may block cav1 simply by downregulating p53, rather than downregulating the cav1 promotor directly. Whether the increase in cav1 through Stat3 inhibition is a transcriptional effect will be examined by measuring cav1 mRNA level following Stat3 downregulation. Whether these are, in fact Stat3 binding sites in vivo will be examined by chromatin immunoprecipitation assays. These results are in preparation for publication. Preliminary reports were presented at the AACR annual meeting in April, 2011, and at the research day of Queen's University (unpublished data).

The above work led to two interesting spinoffs:

1. **Stat3 is a positive regulator of gap junctional intercellular communication in cultured, human lung carcinoma cells:**

Our observation that Stat3 activity is increased by cell confluence led us to examine the effect of Stat3 upon gap junctional, intercellular communication (GJIC), which is dependent upon cadherin engagement. The results turned out to be very interesting:

Neoplastic transformation by oncogenes such as activated Src is known to suppress gap junctional, intercellular communication (GJIC). One of the Src effector pathways leading to GJIC suppression and transformation is the Ras/Raf/Mek/Erk, so that inhibition of this pathway in vSrc-transformed cells was shown to restore GJIC[43]. Stat3 is part of a distinct Src downstream effector pathway required for neoplasia, therefore we decided to examine its role in Src-mediated GJIC suppression. Unfortunately, testing of a number of breast cancer lines even lines with low Src activity levels such as MDA-MB-231[5]* revealed the absence of gap junctions. In addition, the normal human breast epithelial line, MCF-10A and the HC11 mouse breast epithelial line have low GJIC, possibly due to their requirement for growth factors, known GJIC suppressors. For this reason, to examine the effect of Src upon gap junctional, intercellular communication in cancer, we made use of non-small-cell lung cancer cell lines, two of which have high GJIC. Our results unequivocally demonstrated that Stat3 inhibition in cells expressing high Src levels, or in cells where GJIC was suppressed through exogenous Src transduction, did not restore GJIC. On the contrary, Stat3 downregulation in normal lung epithelial or in the NSCLC lines displaying extensive GJIC suppressed junctional permeability. Taken together, these findings demonstrate that although Stat3 is generally growth promoting and in an activated form it can act as an oncogene, it is ***required*** for gap junctional communication both in normal epithelial cells and in certain tumor lines that retain extensive communication. These results were submitted for publication in the Journal *Lung Cancer* (manuscript attached, unpublished data).

2. **Activated phosphatidylinositol-3 kinase; an oncogene that increases gap junctional communication**

The Stat3 requirement for gap junctional communication hinted at the possibility that it might be related to its anti-apoptotic action. Therefore, we decided to examine the effect of PI3 kinase, a survival factor activated by a variety of oncogenes such as Src, upon GJIC.

GJIC is known to be blocked in cells transformed by oncogenes such as the middle Tumor antigen of polyoma virus (mT), an oncoprotein which associates with, activates and is tyrosine-phosphorylated by cSrc family members. Specific mT phosphotyrosines provide docking sites for the phosphotyrosine binding (PTB) domain of Shc (mT-tyr250) and the SH2 domain of the phosphatidylinositol 3-kinase (PI-3k, mT-tyr315), resulting in the activation of their downstream signaling cascades, Ras/Raf/Erk and PI-3 kinase/Akt, respectively.

To examine the effect of these mT-initiated pathways upon gap junctional communication and neoplasia, GJIC was assessed in mT-mutant-expressing, rat liver epithelial T51B cells which normally have extensive GJIC, using a novel technique of *in situ* electroporation we developed. The results show that although even low levels of wt-mT are sufficient to interrupt gap junctional communication, GJIC suppression still requires an intact tyr250 site that is activation of the Ras pathway. In sharp contrast, activation of the PI-3 kinase pathway is definitely *not* required for GJIC suppression. It is remarkable that T51B cells expressing a mutant deficient in binding of Shc, hence activation of the Ras pathway, are still morphologically transformed

and do grow into tumors in syngeneic rats, albeit with an altered morphology. These results indicate that GJIC suppression requires Ras but not PI-3 kinase/Akt signalling, and is independent of full neoplastic conversion in rat liver epithelial cells.

Since PI3k activation by mT increases GJIC, we examined whether PI3k might have a positive role upon GJIC. The results showed that PI3k pharmacological inhibition eliminates GJIC, concomitant with apoptosis induction. We next expressed a form of PI3k rendered constitutively active through the addition of a myristylation signal (myr-PI3k). The results demonstrated that myr-PI3k causes an increase in GJIC. Therefore PI3k, although in an activated form it can act as an oncogene, it plays a positive role upon gap junctional, intercellular communication. This manuscript is in preparation (see reportable outcomes below). Preliminary reports were presented at the annual AACR meeting (April, 2011, Orlando, Florida) and the International congress on gap junctions (August 2011, Ghent, Belgium) (unpublished data).

Specific Aim 3. Examination of the incidence of Stat3 activation, in conjunction with Rac1 and p53 levels in primary tumors, and correlation with the type of tumor, resistance to Herceptin, disease stage and outcome.

This part of the project is ongoing as a planned collaboration with Dr. Bruce Elliott's lab. We initially prepared and stained a number of tumors manually by Immunohistochemistry. However, soon thereafter the Department of Pathology acquired an apparatus for automated staining which provides more robust staining conditions. The set up of the new imaging system (ARIOL) for scoring of the arrays and quantitating the results of staining intensity using algorithms specific for nuclear, cytoplasmic or membranous staining has been completed. This was one of only three systems available in Canada. We also introduced additional specificity controls for staining required for this integrated imaging approach. We are now doing an analysis of arrays of ~300 specimens, as a concerted effort involving a large number of basic researchers and clinicians.

Using a tissue microarray (TMA) of formalin-fixed paraffin embedded tissues, we so far examined 63 primary invasive breast cancers, for which clinico-pathological data were available, for pErk, Ki67, cyclin D1, p53 and Her2. Histologic (H) scores (% positive tumor area x staining intensity 0-3) were manually determined by two pathologists independently. Excellent replicability was observed between H scores for each marker compared on replicate slides. Each TMA slide was then scanned into the Ariol Imaging System, algorithms were trained for each marker, and H scores were calculated. Excellent concordance between manual and automated Ariol scores was observed for all markers, based on both Pearson correlation coefficients for continuous data and Kappa statistics for dichotomized data (+ve versus –ve stain). Interestingly, a statistically significant association of pERK positivity with absence of Lymphovascular involvement and lymph node negativity was observed. pERK positivity was also associated with poorly-differentiated high-grade tumors, consistent with a role for pERK in early, pre-metastatic lesions. p53 over-expression, characteristic of dysfunctional p53 in breast cancer, was also associated with high tumor grade. Thus automated quantitation of immunostaining yields objectively reliable results that are comparable to standardized pathological scoring metrics, and moreover suggest biologically meaningful associations with clinico-pathological data. We anticipate that a large number of data from this part of the project will be generated in the next year of the program. The results on representative sections are attached (Fig.6) (Unpublished data).

The Rb pathway in breast cancer

Rb somatic mutations have been noted in a number of cancers including breast cancer. The prognosis and treatment of breast cancer is significantly informed by a number of biomarkers, and the Rb pathway plays a prominent role [reviewed in[44]]. In particular, the status of the Estrogen receptor-α (ER) is an important determinant in treatment: ER-positive breast cancer has a more favorable prognosis and can be treated with selective inhibitors (e.g. Tamoxifen or aromatase inhibitors). Still, a significant number of ER-positive cancers fail hormonal therapy and a great deal of effort has been expended in identifying pathways leading to Tamoxifen or aromatase inhibitor resistance. Recent reports demonstrated that the selective CDK4/6 inhibitor (hence Rb activator), PD-0332991, could be especially valuable in ER+ breast cancers that are resistant to endocrine therapy, and is now being tested in phase II clinical trials[45]. I was invited to write a review on this topic, which was recently accepted (preprint attached).

Key Research Accomplishments

- Engagement of cadherin-11 increases Stat3 activity in mouse Balb/c3T3 fibroblasts.
- Cadherin-11 plays a positive role in cell survival.
- Cell density causes a dramatic increase in cav1 levels.
- cav1 downregulation increases Stat3-ptyr705.
- cav1 up-regulation decreases Stat3 activity and induces apoptosis through the scaffolding domain
- Stat3 prevents cav1-mediated apoptosis.
- Downregulation of Stat3 upregulates cav1 levels.
- Stat3 is *required* for gap junctional communication both in normal epithelial cells and in certain tumor lines.
- Constitutively active PI3k, although oncogenic, plays a positive role upon gap junctional, intercellular communication.

Reportable Outcomes

Award

American Association for Cancer Research, Minority Scholar in Cancer Research Award. AACR 102nd Annual Meeting 2011, taking place in April 2-6, 2011 in Orlando, FL. (I presented a poster, #6 & 7 below).

Papers published or in press

1. **Raptis L, Arulanandam R, Geletu M, Turkson J**. **(**2011). The R(h)oads to Stat3: Stat3 activation by the Rho GTPases. Exp Cell Res. 317(13):1787-95

2. **Geletu, M. and Raptis, L**. (2011). Viral oncogenes and the retinoblastoma family. In: *Retinoblastoma*, Govindasamy Kumaramanickavel Editor. *InTech*, Croatia. In press (Open access, Book chapter). Retrieved from http://www.intechweb.org/subject/....

Manuscripts submitted or in preparation

1. **Geletu M, Chaize C, Arulanandam R, Anagnostopoulou A and Raptis, L.** Src activity and gap junctional communication in cultured, human lung carcinoma cells. Manuscript submitted to *Lung Cancer*.

2. **Arulanandam, R*., Geletu, M*., Chevalier, S., Feracci, H. and Raptis, L**. Cadherin-11 engagement activates Stat3 throughRac/Cdc42 and IL6 and promotes survival of mouse fibroblasts. Manuscript in the last stages of preparation for submission to *Oncogene*.
   *Equal contribution

3. **Geletu, M., Greer, S., and Raptis, L.** Differential effects of polyoma virus middle tumor antigen mutants upon gap junctional, intercellular communication. In preparation for submission to the *Journal of Virology.*

Abstract with oral presentation

Geletu, M, Greer, S., and Raptis, L. 2011. Differential effects of polyoma virus middle tumor antigen mutants upon gap junctional, intercellular communication**.** Annual resident and postdoctoral fellow research day March 10, Department of Pathology, Queen's University, Kingston, Ontario, Canada.

Abstracts with poster presentation

1. **Rozanne Arulanandam, Mulu Geletu, Adina Vultur, and Leda Raptis.** 2009. The Simian Virus 40 Large Tumor antigen requires Src for full neoplastic transformation. 100th annual meeting of the American association for Cancer research, Denver, Colorado.

2. **D'Abreo C, Arulanandam R, Geletu M and Raptis L.** 2010. Activated Src increases total Rac levels and requires Rac and IL6 for full neoplastic transformation. 101th annual meeting of the American association for Cancer research, Washington, DC.

3. **Arulanandam, R., Geletu, M., Vultur, A., Cao, J., Larue, L., Feracci, H. and Raptis, L.** 2010. Cadherin-cadherin engagement promotes cell survival via Rac/Cdc42 and Stat3. 101th annual meeting of the American association for Cancer research, Washington, DC.

4. **Mulu Geletu, Reva Mohan, Rozanne Arulanandam, Adina Vultur, and Leda Raptis.** 2010. Reciprocal regulation of Stat3 and the caveolae protein, cav-1. 101th annual meeting of the American association for Cancer research, Washington, DC.

5. **J. Cass, R. Arulanandam, M. Geletu, B. Starova, E. Carefoot, S. SenGupta, B.E. Elliott, and, L. Raptis.** A novel cadherin-dependent Rac/Stat3 pathway in invasive breast cancer. (2010). 101th annual meeting of the American association for Cancer research, Washington, DC.

6. **Mulu Geletu**, **Reva Mohan, Rozanne Arulanandam, Bharat Joshi, Ivan Nabi, Leda Raptis.** 2011.Reciprocal regulation of Stat3 and caveolin-1 in normal fibroblasts and breast carcinoma lines. 102th annual meeting of the American association for Cancer research, April 2-6, 2011, Orlando, Florida, USA

7. **Greer, S., Geletu, M. and Raptis, L**,. 2011. Differential effects of polyoma virus middle tumor antigen mutants upon gap junctional, intercellular communication. 102th annual meeting of the American association for Cancer research, April 2-6, 2011, Orlando, Florida, USA.

8. **Mulu Geletu, Reva Mohan, Rozanne Arulanandam, Bharat Joshi, Ivan Nabi, Leda Raptis.** 2011.Reciprocal regulation of Stat3 and caveolin-1 in normal fibroblasts and breast carcinoma lines. The Fourteenth Annual Scientific Meeting for Health Science Research Trainees May 31, 2011 Faculty of Health Sciences, Queen's University.

9. **Mulu Geletu**, **Reva Mohan, Rozanne Arulanandam, Bharat Joshi, Ivan Nabi, Leda Raptis.** 2011.Reciprocal regulation of Stat3 and caveolin-1 in normal fibroblasts and breast carcinoma lines. Department of Defense (DOD) Breast Cancer Research Program (BCRP) sixth Era of Hope Conference, August 2-5, 2011, Orlando, Florida, USA

10. **Geletu, M. Greer, S. and Raptis, L**. 2011 Activated phosphatidylinositol-3 kinase; an oncogene that increases gap junctional communication. International Gap Junction Conference, August 6-11, Ghent, Belgium

Conclusions

The relevance of interactions observed in ***densely*** growing, cultured cells to human cancer is clearly evident from findings demonstrating a close correspondence of genes expressed in prostate cancer LNCaP cells cultured to ***high***, but not low, densities, with genes associated with prostate cancer *in vivo*[46].

Our results bring to light a robust Stat3 activation by cadherin-11 engagement. The fact that cadherin-11 may actually activate Stat3, although, contrary to E-cadherin, cadherin-11 promotes metastasis, may point to Stat3 as a central survival, rather than metastasis, factor. Most importantly cadherin-11 inhibition could induce apoptosis in metastatic cells specifically, while normal cell expressing E-cadherin would be spared.

We also demonstrated that cav-1 downregulation activates Stat3, while cav1 overexpression downregulates Stat3 and induces growth retardation or apoptosis, which was inhibited by co-expression of the constitutively active form of Stat3, Stat3C. Therefore, cav1 may be a potent inhibitor of Stat3 activity. Our results further demonstrate for the first time that, in a feedback loop, Stat3 inhibition results in a dramatic increase in cav1 levels, indicating that Stat3 also downregulates cav1 expression. The above findings reveal the presence of a potent, negative regulatory loop between cav1, p53 and Stat3 that plays a crucial role in cellular survival. Therefore, these novel pathways of Stat3 activation that are triggered by specific cadherin engagement, or Stat3 inhibtion by cav1, could be promising prognostic markers, as well as predictive targets for the treatment of tumors which may be ***resistant*** to inhibition of many ***tyrosine kinase oncogenes*** known to be ***hyperactive*** in ***breast cancer***, such as the ErbB2 inhibitor ***Herceptin***.

Mentorship:

My mentor, Dr. Leda Raptis was diagnosed with breast cancer in April, 2010. She went through 3 major operations and six cycles of very aggressive chemotherapy. For this reason, the submission of some of my papers has been delayed. She is now back to work and I will complete the last part of the project as planned.

Numbers followed by a star refer to publications from our group

Figure 1

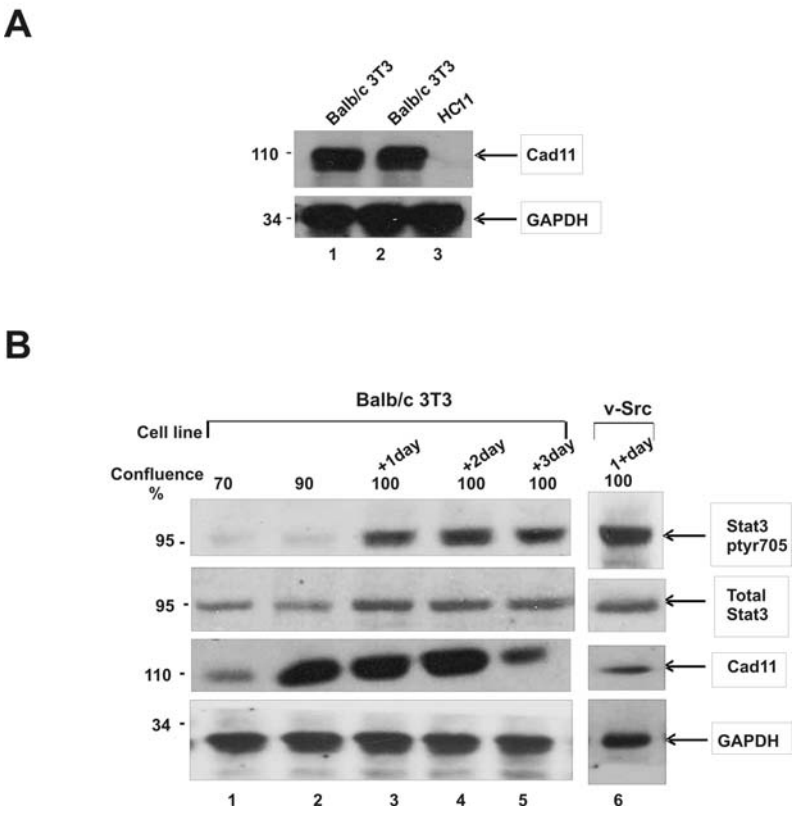

Figure 1.

A: Balb/c 3T3 cells express high amounts of cadherin-11

Protein Extracts from Balb/c3T3, mouse fibroblasts or the HC11, mouse breast epithelial cells were examined by Western blotting using a cadherin-11 antibody (1A, lanes 1-3). Note the high amounts of cadherin-11, compared to HC11 mouse breast epithelial cells.

B: Cell density upregulates Stat3-ptyr705 levels in Balb/c3T3 cells.

Balb/c3T3 fibroblasts before (lanes 1-5) or after (lane 6) vSrc expression were grown to increasing densities and lysates probed for Stat3-ptyr705, total Stat3, Cadherin-11or GAPDH as a loading control, as indicated.

Figure 2

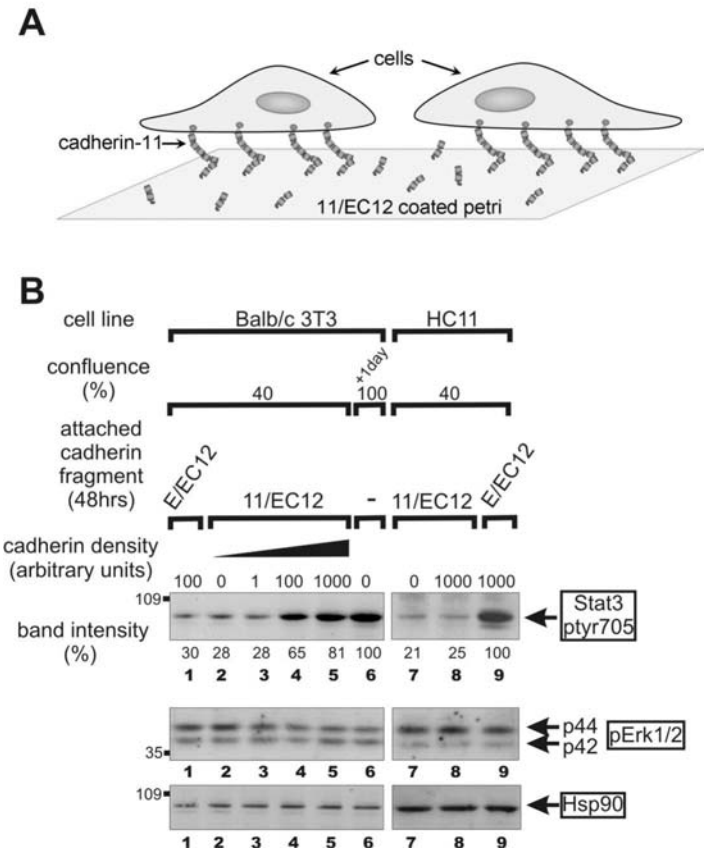

Figure 2. Cadherin-11 engagement is sufficient to activate Stat3 in Balb/c3T3 fibroblasts
A: Schematic drawing of fibroblasts plated at low density in plastic petris coated with a cadherin-11 fragment encompassing the two outermost EC domains (11/EC12) [47].
B: Balb/c3T3 cells were grown in plastic 3cm dishes, coated with increasing amounts of the cadherin-11 fragment, 11/EC12, as indicated (lanes 2-5). 48 hours later, cell lysates were probed for Stat3-ptyr705, phospho-Erk1/2 or Hsp90 as a loading control, as indicated. As controls, Balb/c 3T3 cells, which are devoid of E-cadherin (Fig. 1A), were grown on a surface coated with the corresponding E-cadherin fragment (E/EC12, lane 1) and HC11 cells which are devoid of cadherin-11 were grown on surfaces coated by 11/EC12 (lanes 7 and 8), or by E/EC12, as a control (lane 9). Numbers under the lanes refer to band intensities obtained by densitometric scanning.

Figure 3

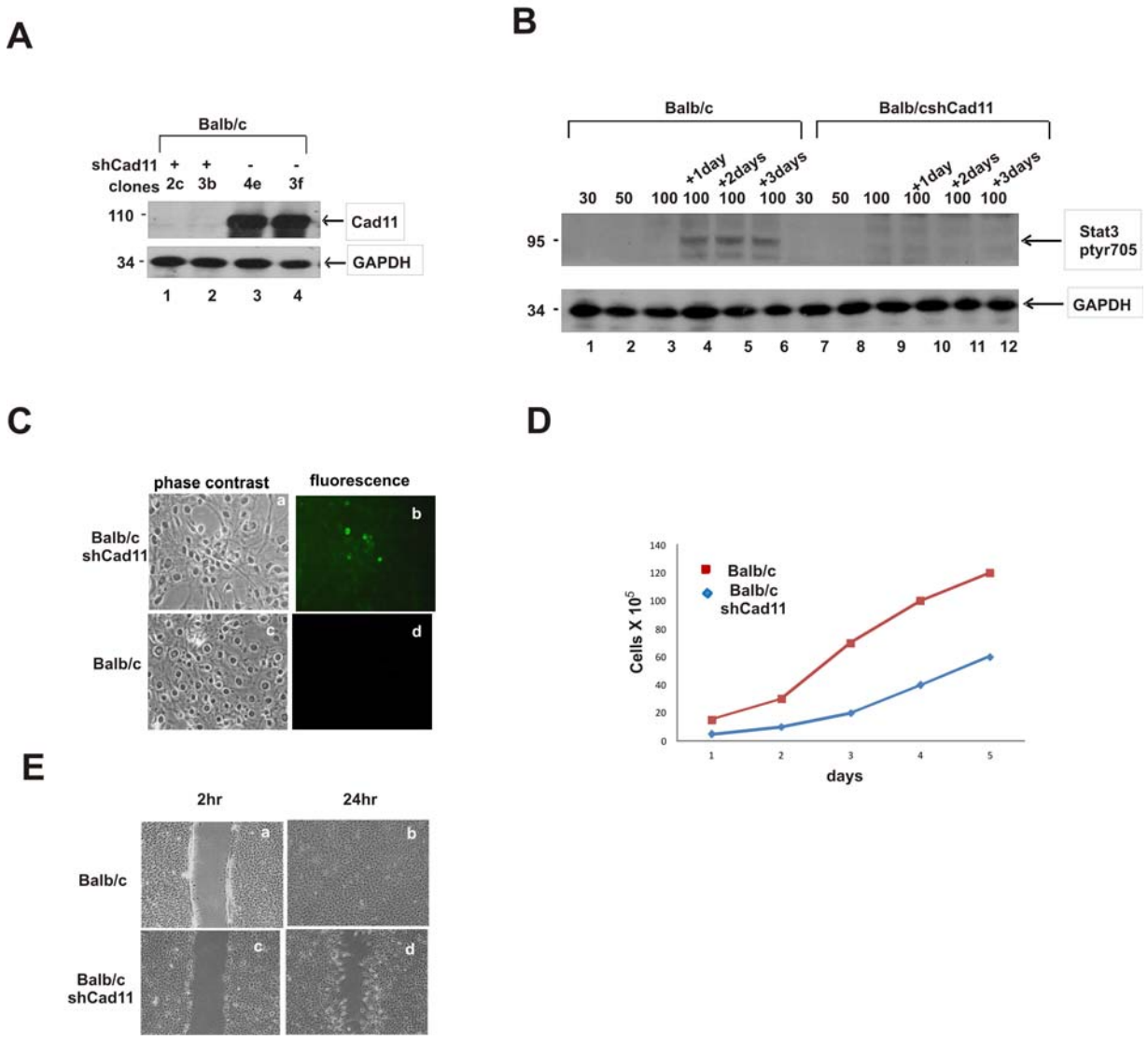

Figure 3. Cadherin-11 plays a positive role in Stat3-ptyr705, cell survival, proliferation and migration

A: **Stable expression of the cadherin-11 shRNA construct dramatically reduces cadherin-11 levels.** Balb/c 3T3 mouse fibroblasts were infected with the supernatant of the psi-2 cadherin-11 shRNA packaging line which produces the retrovirus carrying the *cadherin-11 shRNA* gene and stably selected using puromycin as a selection marker. Infected cells and the parental cell lines were grown to 100% confluence, lysates resolved by gel electrophoresis and immunoblots probed for cadherin 11 and GAPDH as a loading control.

B: Cadherin-11 knockdown causes a dramatic reduction in Stat3-ptyr705 levels in Balb/c3T3 cells: Balb/c3T3 cells before (lanes 1-6) or after cadherin-11 knockdown (lanes 7-12) were grown to differenr densities and lysates probed for Stat3-ptyr705.

C: Cadherin-11 knockdown with sh-RNA induces apoptosis. Balb/c3T3 cells after (panel a-b) or before cadherin-11 knockdown (panel c-d) were grown to a density of 2 days post-confluence and apoptosis examined by TUNEL staining**.**

D: Cadherin-11 knockdown with sh-RNA reduces the rate of cell proliferation: Balb/c and Balb/c sh-cadherin-11 cells were grown in Petri dishes in 10% serum and cell numbers obtained over several days, as indicated.

E: Cadherin-11 knockdown with sh-RNA reduces the rate of cell migration: Balb/c and Balb/c sh-cadherin-11 cells were cultured to confluence before a scratch was made through the monolayer using a plastic pipette tip. Cells were photographed at 2hr (panels a, c,) or 24 h (panel b, d,) after 12 h of culturing in 0.5% fetal calf serum.

Figure 4

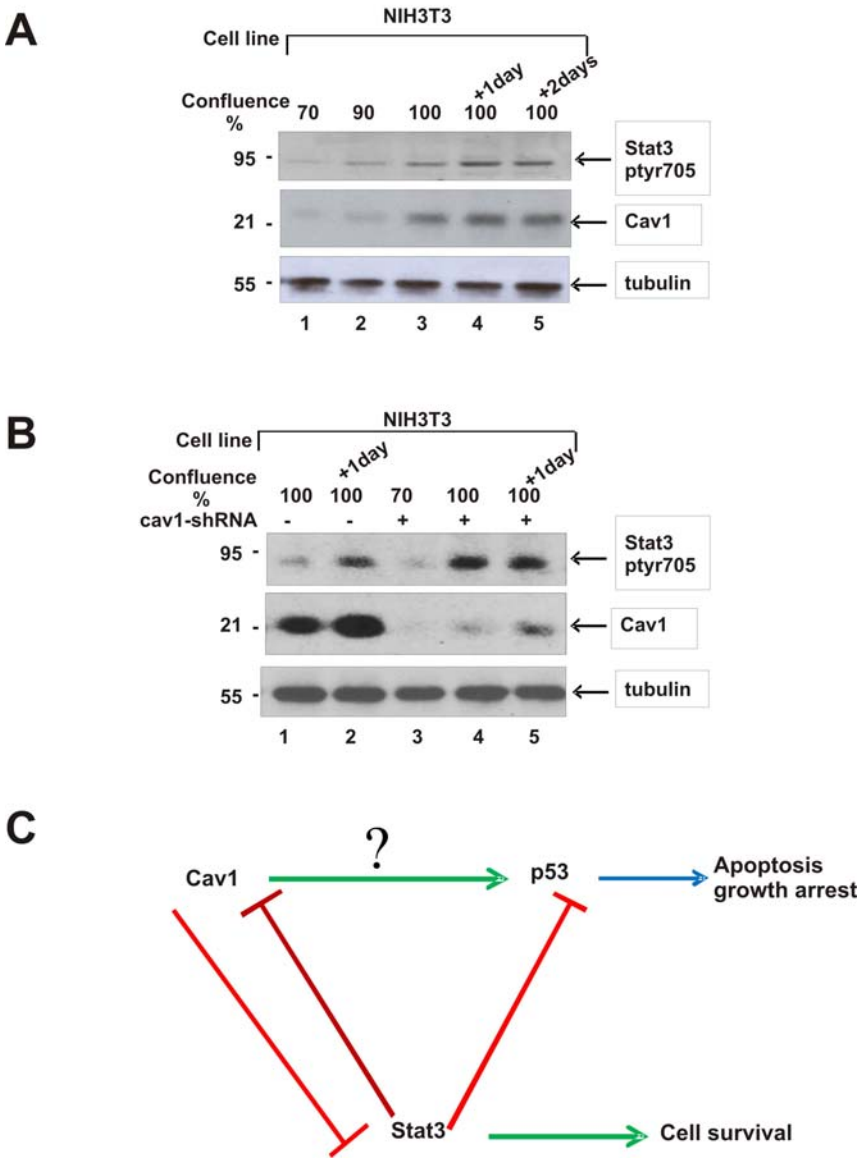

Figure 4. Stat3 activity and cav1 levels increase with cell density.
A: Lysates from NIH3T3 mouse fibroblasts grown to different densities were probed for Stat3-ptyr705, cav1 or tubulin as a loading control. Note that both Stat3-ptyr705 and cav1 levels increase with cell density, peaking at post-confluence.

B: Cav1 downregulation increases Stat3-ptyr705 activity. NIH3T3 mouse fibroblasts were infected with the supernatant of the psi-2 cav1 shRNA packaging line, which produces the retrovirus carrying the *cav1 shRNA* gene and stably selected using puromycin as a selection marker. Infected cells (lanes 3-5) and the parental line (lane 1-2) were grown to different densities and lysates probed for total cav1, ptyr-705 Stat3 or tubulin as a loading control.

C: Model of the cav1, Stat3 and p53 interactioon: cav1 can downregulate Stat3, through the scaffolding domain. Stat3 on the other hand can downregulate p53, although the possibility that cav1 upregulates p53 in a Stat3-independent manner cannot be excluded. At the same time, Stat3 downregulates cav1 (Fig. 5G).

Figure 5

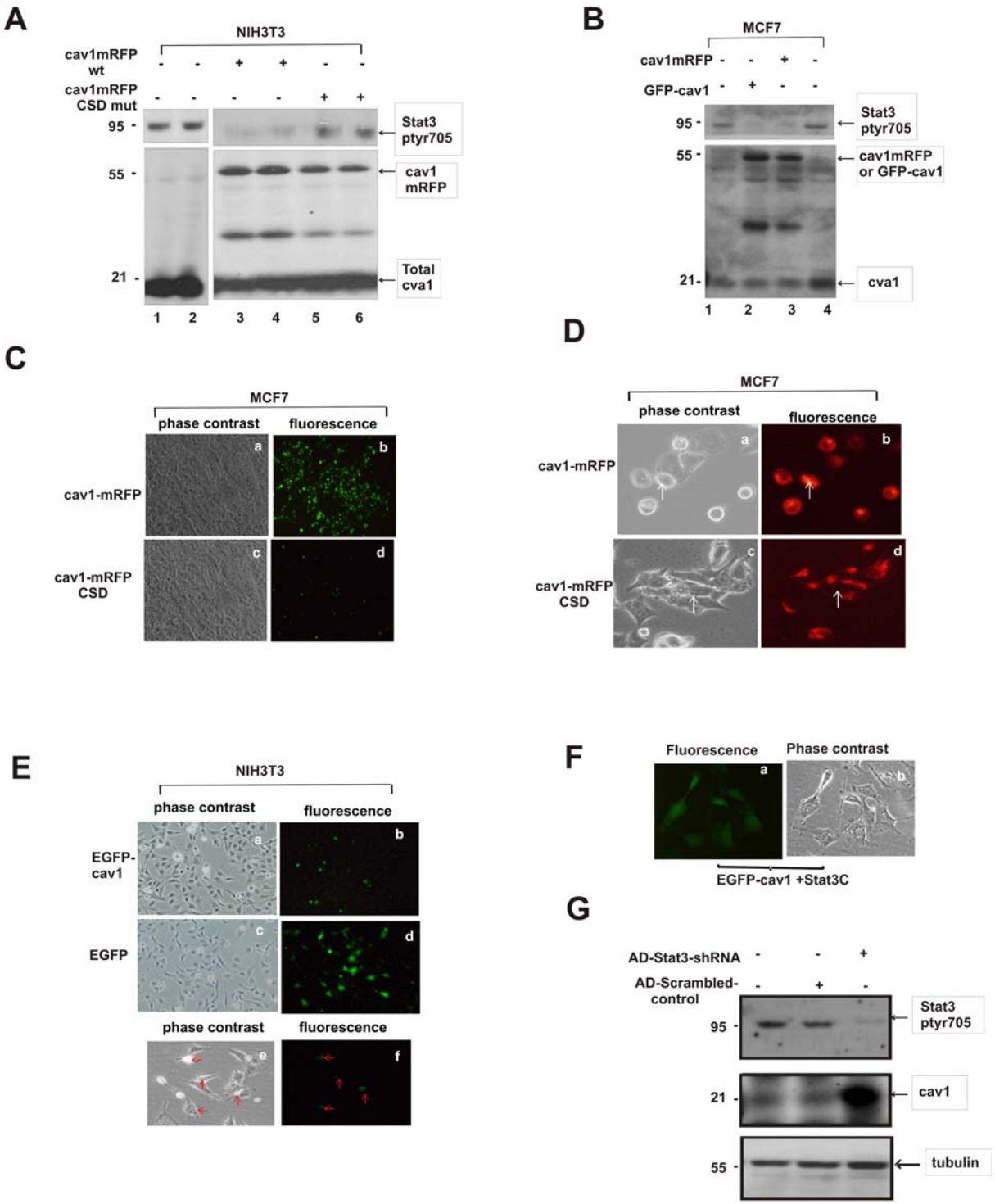

Figure 5. Cav1 upregulation decreases Stat3 activity and induces apoptosis through the scaffolding domain

A: NIH3T3 and **B:** MCF7 cells were transfected with the cav1-mRFP or GFP-cav1, or CSD-cav1mRFP (expressing the scaffolding domain mutant) plasmids. Lysates were prepared at different densities and Western blots probed for Stat3-ptyr705 or cav1. Note the cav1-mRFP or GFP-cav1 bands (at 55kDa), indicating cav1-mRFP or GFP-cav1 expression, which corresponds to a decrease in Stat3-ptyr705 levels. Bottom band represents endogenously expressed cav1.

cav1 overexpression induces apoptosis

C: MCF-7 cells were transfected with the cav1mRFP or CSD-cav1mRFP plasmids. Cells were selected with G418. Apoptosis were examined by TUNEL staining.

Over expression of cav1 scaffolding domain mutant (CSD) does not induce apoptosis
D: MCF-7 cells were transfected with the cav1mRFP or SCD-cav1mRFP plasmids. Cells were selected with G418 and stable clones were photographed under phase contrast (panels a, c) or fluorescence illumination (panels b,d). Note the changes in morphology in a-b, indicating apoptosis. Magnification:240x.
E: NIH3T3 cells were transfected with the EGFP-cav1 plasmid, or EGFP as a control. 48 hours later cells were photographed under phase contrast (panels a,c) or fluorescence illumination (panels b,d). Note the changes in morphology, indicating apoptosis. Magnification: A:140x B: 240x (panels e, f).

Stat3C co-expression rescues cells from cav1-induced apoptosis.
F: NIH3T3 fibroblasts were co-transfected with the EGFP-cav1 and Stat3C plasmids. 96 hours later cells were photographed under phase contrast or fluorescence illumination. Note the normal morphology, indicating absence of apoptosis. Magnification: 240x .

Downregulation of Stat3 upregulates cav1 levels.
G: HeLa cells were infected with adenoviral constructs coding for a Stat3 siRNA (Adenovirus Stat3i) or a control vector coding for a scrambled version of the Stat3 siRNA gene (Adenovirus Stat3sc). Cell lysates were prepared approximately 36 hours after infection and the Western blots were probed for phospho-Stat3, total cav1 and tubulun as loading control. The Stat3i adenovirus vector effectively downregulated Stat3-ptyr705. This decrease in pStat3 corresponds to a significant increase in cav1 expression.

Figure 6

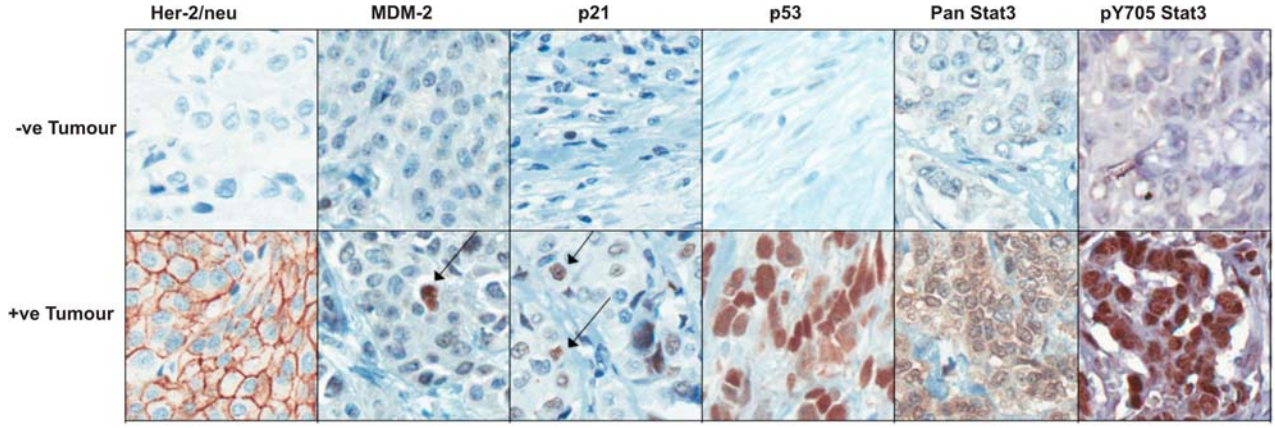

Figure 6. Immunohistochemical staining of a human breast carcinoma TMA: Representative positive and negative cores. Sections are 6 microns thick and tissue was formalin fixed and paraffin embedded. Antibodies used include Her-2/neu, MDM-2, p21, p53, pan Stat3 and pY705 Stat3. Arrows indicate select positive cells for MDM-2 and p21.

Reference List

1. Yu,H., Pardoll,D., & Jove,R. STATs in cancer inflammation and immunity: a leading role for STAT3. *Nat. Rev. Cancer* **9**, 798-809 (2009).

2. Frank,D.A. STAT3 as a central mediator of neoplastic cellular transformation. *Cancer Lett.* **251**, 199-210 (2007).

3. McLemore,M.L. *et al.* STAT-3 activation is required for normal G-CSF-dependent proliferation and granulocytic differentiation. *Immunity.* **14**, 193-204 (2001).

4. Arulanandam,R. *et al.* Cadherin-cadherin engagement promotes survival via Rac/Cdc42 and Stat3. *Molecular Cancer Research* **17**, 1310-1327 (2009).

5. Vultur,A. *et al.* Cell to cell adhesion modulates Stat3 activity in normal and breast carcinoma cells. *Oncogene* **23**, 2600-2616 (2004).

6. Cohen,A.W., Hnasko,R., Schubert,W., & Lisanti,M.P. Role of caveolae and caveolins in health and disease. *Physiol Rev.* **84**, 1341-1379 (2004).

7. Goetz,J.G., Lajoie,P., Wiseman,S.M., & Nabi,I.R. Caveolin-1 in tumor progression: the good, the bad and the ugly. *Cancer Metastasis Rev.* **27**, 715-735 (2008).

8. Patel,H.H., Murray,F., & Insel,P.A. Caveolae as organizers of pharmacologically relevant signal transduction molecules. *Annu. Rev. Pharmacol. Toxicol.* **48**, 359-391 (2008).

9. Kerr,J. *et al.* Allelic loss on chromosome 7q in ovarian adenocarcinomas: two critical regions and a rearrangement of the PLANH1 locus. *Oncogene* **13**, 1815-1818 (1996).

10. Matsuura,K. *et al.* Loss of heterozygosity of chromosome 9p21 and 7q31 is correlated with high incidence of recurrent tumor in head and neck squamous cell carcinoma. *Anticancer Res.* **18**, 453-458 (1998).

11. Zenklusen,J.C., Oshimura,M., Barrett,J.C., & Conti,C.J. Inhibition of tumorigenicity of a murine squamous cell carcinoma (SCC) cell line by a putative tumor suppressor gene on human chromosome 7. *Oncogene* **9**, 2817-2825 (1994).

12. Oka,H. *et al.* Expression of E-cadherin cell adhesion molecules in human breast cancer tissues and its relationship to metastasis. *Cancer Res.* **53**, 1696-1701 (1993).

13. Kowalski,P.J., Rubin,M.A., & Kleer,C.G. E-cadherin expression in primary carcinomas of the breast and its distant metastases. *Breast Cancer Res.* **5**, R217-R222 (2003).

14. Pishvaian,M.J. *et al.* Cadherin-11 is expressed in invasive breast cancer cell lines. *Cancer Res.* **59**, 947-952 (1999).

15. Feltes,C.M., Kudo,A., Blaschuk,O., & Byers,S.W. An alternatively spliced cadherin-11 enhances human breast cancer cell invasion. *Cancer Res.* **62**, 6688-6697 (2002).

16. Chu,K. *et al.* Cadherin-11 promotes the metastasis of prostate cancer cells to bone. *Mol. Cancer Res.* **6**, 1259-1267 (2008).

17. Vultur,A. *et al.* Stat3 is required for full neoplastic transformation by the Simian Virus 40 Large Tumor antigen. *Molecular Biology of the Cell* **16**, 3832-3846 (2005).

18. Raptis,L. *et al.* Beyond structure, to survival: Stat3 activation by cadherin engagement. *Biochemistry and Cell Biology* **87**, 835-843 (2009).

19. Narimatsu,M. *et al.* Tissue-specific autoregulation of the stat3 gene and its role in interleukin-6-induced survival signals in T cells. *Mol. Cell. Biol.* **21**, 6615-6625 (2001).

20. Arulanandam,R., Geletu,M., Feracci,H., & Raptis,L. RacV12 requires gp130 for Stat3 activation, cell proliferation and migration. *Experimental Cell Research* **316**, 875-886 (2010).

21. Perret,E. *et al.* Fast dissociation kinetics between individual E-cadherin fragments revealed by flow chamber analysis. *EMBO J.* **21**, 2537-2546 (2002).

22. Arulanandam,R. *et al.* Cadherin-cadherin engagement promotes survival via Rac/Cdc42 and Stat3. *Molecular Cancer Research* **17**, 1310-1327 (2009).

23. Epling-Burnette,P.K. *et al.* Inhibition of STAT3 signaling leads to apoptosis of leukemic large granular lymphocytes and decreased Mcl-1 expression. *J. Clin. Invest.* **107**, 351-362 (2001).

24. Grandis,J.R. *et al.* Constitutive activation of Stat3 signaling abrogates apoptosis in squamous cell carcinogenesis in vivo. *Proc. Nat. Acad. Sci. USA* **97**, 4227-4232 (2000).

25. Niu,G. *et al.* Role of Stat3 in regulating p53 expression and function. *Mol. Cell Biol.* **25**, 7432-7440 (2005).

26. Vultur,A. *et al.* Stat3 is required for full neoplastic transformation by the Simian Virus 40 Large Tumor antigen. *Molecular Biology of the Cell* **16**, 3832-3846 (2005).

27. Anagnostopoulou,A. *et al.* Differential effects of Stat3 inhibition in sparse vs confluent normal and breast cancer cells. *Cancer Lett.* **242**, 120-132 (2006).

28. Hazan,R.B., Qiao,R., Keren,R., Badano,I., & Suyama,K. Cadherin switch in tumor progression. *Ann. N. Y. Acad. Sci.* **1014**, 155-163 (2004).

29. Hazan,R.B., Phillips,G.R., Qiao,R.F., Norton,L., & Aaronson,S.A. Exogenous expression of N-cadherin in breast cancer cells induces cell migration, invasion, and metastasis. *J. Cell Biol.* **148**, 779-790 (2000).

30. Li,G., Satyamoorthy,K., & Herlyn,M. N-cadherin-mediated intercellular interactions promote survival and migration of melanoma cells. *Cancer Res.* **61**, 3819-3825 (2001).

31. Nieman,M.T., Prudoff,R.S., Johnson,K.R., & Wheelock,M.J. N-cadherin promotes motility in human breast cancer cells regardless of their E-cadherin expression. *J. Cell Biol.* **147**, 631-644 (1999).

32. Islam,S., Carey,T.E., Wolf,G.T., Wheelock,M.J., & Johnson,K.R. Expression of N-cadherin by human squamous carcinoma cells induces a scattered fibroblastic phenotype with disrupted cell-cell adhesion. *J. Cell Biol.* **135**, 1643-1654 (1996).

33. Galbiati,F. *et al.* Targeted downregulation of caveolin-1 is sufficient to drive cell transformation and hyperactivate the p42/44 MAP kinase cascade. *EMBO J.* **17**, 6633-6648 (1998).

34. Chen,X. & Resh,M.D. Cholesterol depletion from the plasma membrane triggers ligand-independent activation of the epidermal growth factor receptor. *J. Biol. Chem.* **277**, 49631-49637 (2002).

35. Razani,B. *et al.* Caveolin-1 expression is down-regulated in cells transformed by the human papilloma virus in a p53-dependent manner. Replacement of caveolin-1 expression suppresses HPV-mediated cell transformation. *Biochemistry* **39**, 13916-13924 (2000).

36. Galbiati,F. *et al.* Caveolin-1 expression negatively regulates cell cycle progression by inducing G(0)/G(1) arrest via a p53/p21(WAF1/Cip1)-dependent mechanism. *Mol. Biol. Cell* **12**, 2229-2244 (2001).

37. Goetz,J.G. *et al.* Concerted regulation of focal adhesion dynamics by galectin-3 and tyrosine-phosphorylated caveolin-1. *J. Cell Biol.* **180**, 1261-1275 (2008).

38. Altieri,D.C. Survivin, cancer networks and pathway-directed drug discovery. *Nat. Rev. Cancer* **8**, 61-70 (2008).

39. Catlett-Falcone,R. *et al.* Constitutive activation of Stat3 signaling confers resistance to apoptosis in human U266 myeloma cells. *Immunity* **10**, 105-115 (1999).

40. Katoh,M. & Katoh,M. STAT3-induced WNT5A signaling loop in embryonic stem cells, adult normal tissues, chronic persistent inflammation, rheumatoid arthritis and cancer (Review). *Int. J. Mol. Med.* **19**, 273-278 (2007).

41. Su,H.W., Wang,S.W., Ghishan,F.K., Kiela,P.R., & Tang,M.J. Cell confluency-induced Stat3 activation regulates NHE3 expression by recruiting Sp1 and Sp3 to the proximal NHE3 promoter region during epithelial dome formation. *Am. J. Physiol Cell Physiol* **296**, C13-C24 (2009).

42. Loeffler,S., Fayard,B., Weis,J., & Weissenberger,J. Interleukin-6 induces transcriptional activation of vascular endothelial growth factor (VEGF) in astrocytes in vivo and regulates VEGF promoter activity in glioblastoma cells via direct interaction between STAT3 and Sp1. *Int. J. Cancer* **115**, 202-213 (2005).

43. Ito,S. *et al.* v-Src requires Ras signaling for the suppression of gap junctional intercellular communication. *Oncogene* **25**, 2420-2424 (2006).

44. Musgrove,E.A. & Sutherland,R.L. Biological determinants of endocrine resistance in breast cancer. *Nat. Rev. Cancer* **9**, 631-643 (2009).

45. Thangavel,C. *et al.* Therapeutically activating RB: reestablishing cell cycle control in endocrine therapy-resistant breast cancer. *Endocr. Relat Cancer* **18**, 333-345 (2011).

46. Chen,Q. *et al.* Gene expression in the LNCaP human prostate cancer progression model: progression associated expression in vitro corresponds to expression changes associated with prostate cancer progression in vivo. *Cancer Lett.* **244**, 274-288 (2006).

47. Boggon,T.J. *et al.* C-cadherin ectodomain structure and implications for cell adhesion mechanisms. *Science* **296**, 1308-1313 (2002).

Appendices: Attached

Control/Tracking Number: 11-A-3260-AACR
Activity: Abstract Submission
Current Date/Time: 11/12/2010 10:23:57 AM
Mulu Geletu[1], Reva Mohan[1], Rozanne Arulanandam[1], Bharat Joshi[2], Ivan Robert Nabi[2], Leda Helen Raptis[1]. [1]Queen's Univerity, Kingston, ON, Canada; [2]The University of British Columbia, Vancouver, BC, Canada
102th annual meeting of the American association for Cancer research, April 2-6, 2011, Orlando, Florida, USA

Title: Reciprocal regulation of Stat3 and caveolin-1 in normal fibroblasts and breast carcinoma lines

Abstract:
Membrane tyrosine kinases known to activate the signal transducer and activator of transcription-3 (Stat3) concentrate in caveolae, where they are sequestered in an inactive state through binding to the main caveolae protein, caveolin-1 (cav1). We previously demonstrated that cell-to-cell adhesion can cause a dramatic increase in Stat3 activity in cultured cells. Therefore, to examine the effect of cav1 upon Stat3, experiments were conducted at several confluences. Our results indicate that cav-1 downregulation through expression of anti-sense or shRNA constructs or treatment of cells with the pharmacological inhibitor, methyl-cyclo-dextran which destroys caveolae, activates Stat3 as well as Erk1/2, at all densities. Conversely, cav1 overexpression downregulates Stat3 and induces growth retardation or apoptosis in NIH3T3 fibroblasts and in breast cancer lines. In all cases, apoptosis was inhibited by co-expression of the constitutively active form of Stat3, Stat3C. Taken together, these findings point to cav1 as an inhibitor of Stat3 activity. In addition, it was previously demonstrated that cav1 upregulates p53, although the exact mechanism is unclear. Since Stat3 is known to inhibit p53 transcription through promotor binding, these data also point to the possibility that cav1 upregulation may, in fact, activate p53 through Stat3 inhibition. Our results further demonstrate for the first time that, in a feedback loop, Stat3 inhibition results in a dramatic increase in cav1 levels, indicating that Stat3 also downregulates cav1 expression. The above findings reveal the presence of a potent, negative regulatory loop between cav1, p53 and Stat3 that plays a crucial role in cellular survival.

:

Geletu, M., Greer, S. and Raptis , L.

International Gap Junction Conference, August 6-11, Ghent, Belgium

Title: **Activated phosphatidylinositol-3 kinase: An oncogene that increases gap junctional communication**

Gap junctional, intercellular communication (GJIC) is blocked in cells transformed by oncogenes such as the middle Tumor antigen of polyoma virus (mT), an oncoprotein which associates with, activates and is tyrosine-phosphorylated by cSrc family members. Specific mT phosphotyrosines provide docking sites for the phosphotyrosine binding (PTB) domain of Shc (mT-tyr250) and the SH2 domain of the phosphatidylinositol 3-kinase (PI-3k, mT-tyr315), resulting in the activation of their downstream signaling cascades, Ras/Raf/Erk and PI-3 kinase/Akt, respectively.

To examine the effect of these mT-initiated pathways upon gap junctional communication and neoplasia, GJIC was assessed in mT-mutant-expressing, rat liver epithelial T51B cells which normally have extensive GJIC, using a novel technique of *in situ* electroporation we developed. The results show that although even low levels of wt-mT are sufficient to interrupt gap junctional communication, GJIC suppression still requires an intact tyr250 site, that is activation of the Ras pathway. In sharp contrast, activation of the PI-3 kinase pathway is definitely *not* required for GJIC suppression. It is remarkable that T51B cells expressing a mutant deficient in binding of Shc, hence activation of the Ras pathway, are still morphologically transformed and do grow into tumors in syngeneic rats, albeit with an altered morphology. These results indicate that GJIC suppression requires Ras but not PI-3 kinase/Akt signalling, and is independent of full neoplastic conversion in rat liver epithelial cells.

Since PI3k activation by mT increases GJIC, we examined whether PI3k might have a positive ole upon GJIC. The results showed that PI3k pharmacological inhibition eliminates GJIC, concomitant with apoptosis induction. We next expressed a form of PI3k rendered constitutively active through the addition of a myristylation signal (myr-PI3k). The results demonstrated that myr-PI3k causes an increase in GJIC. Therefore PI3k, although in an activated form it can act as an oncogene, it plays a positive role upon gap junctional, intercellular communication.

Greer, S., **Geletu, M.** and Raptis, L.
102th annual meeting of the American association for Cancer research, April 2-6, 2011, Orlando, Florida, USA

Title: Differential effects of polyoma virus middle tumor antigen mutants upon gap junctional, intercellular communication.

Gap junctions are channels that connect the cytoplasm of adjacent cells. Gap junctional, intercellular communication (GJIC) is blocked in cells transformed by oncogenes such as the middle Tumor antigen of polyoma virus (mT), an oncoprotein which associates with and is tyrosine-phosphorylated by cSrc family members. Specific phosphotyrosines provide docking sites for the phosphotyrosine binding domain of Shc (mT-tyr250) and the SH2 domain of the phosphatidylinositol 3-kinase (mT-tyr315), resulting in the activation of their downstream signaling cascades, Ras/Raf/Erk and PI-3 kinase/Akt, respectively.

To examine the effect of these mT-initiated pathways upon gap junctional communication and neoplasia, GJIC was assessed in mT-mutant-expressing, rat liver epithelial T51B cells which normally have extensive GJIC, using a novel technique of *in situ* electroporation we developed. The results show that although low levels of wt-mT are sufficient to interrupt gap junctional communication, GJIC suppression still requires an intact tyr250 site, that is activation of the Ras pathway. In sharp contrast, activation of the PI-3 kinase pathway is *not* required for GJIC suppression. It is remarkable that T51B cells expressing a mutant deficient in binding of Shc, hence activation of the Ras pathway, are still morphologically transformed and do grow into tumors in syngeneic rats, albeit with an altered morphology. These results indicate that GJIC suppression requires Ras but not PI-3 kinase/Akt signalling, and is independent of neoplastic conversion in rat liver epithelial cells.

Mulu Geletu, Reva Mohan, Rozanne Arulanandam, Leda Raptis.
Queen's University, Kingston, ON, Canada

Department of Defense (DOD) Breast Cancer Research Program (BCRP) sixth Era of Hope Conference, August 2-5, 2011, Orlando, Florida, USA

Title: Reciprocal regulation of Stat3 and caveolin-1 in normal fibroblasts and breast carcinoma lines

Abstract

Membrane tyrosine kinases known to activate the signal transducer and activator of transcription-3 (Stat3) concentrate in caveolae, where they are sequestered in an inactive state through binding to the main caveolae protein, caveolin-1 (cav1). Activation of Stat3 has been demonstrated in breast and other cancers, while a constitutively active form of Stat3, Stat3C, is able to transform cultured cells, further pointing to an etiologic role for Stat3 in these tumors. However, the exact mechanism of its activation as well as the role of Stat3 in these tumors, remain to be determined. Our objective is to examine the effect of cav1 upon Stat3.

We previously demonstrated that cell-to-cell adhesion can cause a dramatic increase in Stat3 activity in cultured cells. Therefore, to examine the effect of cav1 upon Stat3, experiments were conducted at several cell confluences. Our results indicate that cav-1 downregulation through expression of full-length, anti-sense or shRNA constructs or treatment of cells with the pharmacological inhibitor, methyl-cyclo-dextran (MCD) which destroys caveolae, activates Stat3 as well as Erk1/2, at all densities. Conversely, cav1 overexpression downregulates Stat3 and induces growth retardation or apoptosis in NIH3T3 fibroblasts and in breast cancer lines. In all cases, apoptosis was inhibited by co-expression of the constitutively active form of Stat3, Stat3C. In addition, it was previously demonstrated that cav1 upregulates the tumor suppressor p53, although the exact mechanism is unclear. Since Stat3 is known to inhibit p53 transcription through promotor binding, these data also point to the possibility that cav1 upregulation may, in fact, activate p53 through Stat3 inhibition.

Taken together, our findings so far point to cav1 as an inhibitor of Stat3 activity. Our results further demonstrate for the first time that, in a feedback loop, Stat3 inhibition results in a dramatic increase in cav1 levels, indicating that Stat3 also downregulates cav1 expression. The above findings reveal the presence of a potent, negative regulatory loop between cav1, p53 and Stat3 that plays a crucial role in cellular survival (Figure 1).

Stat3 plays a pivotal role in promoting cancer cell survival, proliferation, invasion and angiogenesis. We have brought to light a novel pathway leading from E-cadherin engagement to Stat3 activation and cav1 and p53 downregulation, which is a key for the decision between cell division and apoptosis. Most importantly, this pathway could be a promising target for the treatment of cancers where inhibitors of tyrosine kinases, such as Herceptin, are ineffective.

Mulu Geletu, Reva Mohan, Rozanne Arulanandam, Adina Vultur, and Leda Raptis.

Department of Pathology, Queenôs University, Kingston, Ontario, Canada.
American Association of Cancer Research Annual meeting, Washington, DC., April 2010.

Title: Reciprocal regulation of Stat3 and the caveolae protein, cav-1

Caveolae are cholesterol-rich, flask-shaped invaginations of the plasma membrane with many roles in the cell, including the regulation of signal transduction. Caveolin 1 (Cav1) is the major protein responsible for the organization and maintenance of caveolae microdomains. Cav1 recruits many receptor and non-receptor tyrosine kinases and through binding to its scaffolding-domain, Cav1 sequesters the kinases in an inactive form, thereby preventing their involvement in signaling pathways. One important downstream target of many tyrosine kinases (Src, EGF, PDGF, IL6 and others) is the signal transducer and activator of transcription-3 (Stat3). Stat3 is a cytoplasmic signal transducer which is activated by tyrosine-705 phosphorylation by a number of kinases, then migrates to the nucleus to initiate transcription of genes involved in cell division and survival. Despite extensive evidence on the role of cav1 in signal transduction, its effect upon Stat3 is still obscure.

We previously demonstrated that cell-to-cell adhesion, as occurs in confluent cultures, can cause a dramatic increase in Stat3 phosphorylation and activity in cultured cells (Oncogene 23:2600, MBC 16:3832). Therefore, to examine effects upon Stat3, cell density has to be taken into account. Our results now indicate that cav-1 downregulation through expression of an anti-sense construct, or treatment with the pharmacological inhibitor, methyl-cyclo-dextran which removes cholesterol from the membrane and destroys caveolae, caused a strong activation of Stat3 as well as Erk1/2, at all densities examined. Conversely, cav1 overexpression downregulated Stat3 and induced apoptosis in NIH3T3 fibroblasts both before and after transformation by the Simian Virus 40 Large Tumor antigen, as well as in HeLa cells. In all cases, apoptosis was prevented by co-expression of the constitutively active form of Stat3, Stat3C. Taken together, these findings point to ***cav1*** as an ***inhibitor*** of ***Stat3*** activity.

It was previously demonstrated that cav1 upregulates p53 gene activity. Since Stat3 is known to inhibit p53 transcription by direct binding to the p53 promotor, these data also point to the possibility that cav1 may, in fact, activate p53 through *Stat3* inhibition.

Our results also demonstrate for the first time that, in a feedback loop, ***Stat3*** inhibition following infection with an Adenovirus vector expressing a Stat3-specific, shRNA, results in a dramatic ***in***crease in cav1 levels, indicating that Stat3 also downregulates cav1 expression. Since p53 also upregulates cav1, and Stat3 blocks the p53 promotor, it is possible that Stat3 may block cav1 simply by downregulating p53, rather than downregulating the cav1 promotor directly. The above findings taken together reveal the presence of a potent, negative regulatory loop between cav1 and Stat3 activity that plays a crucial role in cellular survival. (supported by CIHR, CBCF-Ontario chapter, US Army breast cancer program NSERC and BCAK).

D'Abreo C, Arulanandam R, Geletu M and Raptis L.
Abstract Number: 10-A-4866-AACR
American Association of Cancer Research Annual meeting, Washington, DC., April 2010.

Activated Src increases total Rac levels and requires Rac and IL6 for full neoplastic transformation

Activated Src (vSrc) was previously shown to activate Rac through the exchange factors Vav2 and Tiam, and to require Rac for neoplastic transformation, but the exact mechanism remains unclear. Since Src requires the function of the Signal transducer and activator of transcription-3 (Stat3), a Rac target for transformation, we explored the potential role of the Rac/Stat3 axis in transformation by vSrc. In fact, we recently demonstrated a dramatic increase in the activity of Stat3 in breast carcinoma as well as normal epithelial cells and fibroblasts, as a consequence of cell to cell adhesion (Oncogene 23:2600).
In light of these findings, we revisited the question of the role of Rac and Stat3 in vSrc transformation. The results showed that, as previously demonstrated, vSrc expressing mouse fibroblasts had higher Rac activity, at all densities examined. Unexpectedly, our results also demonstrate for the first time a dramatic surge in total Rac upon Src expression, which was at least in part responsible for the Stat3 activity increase. Moreover, Rac activation caused an increase in levels of cytokines of the IL6 family, which was required for Stat3 activation, as shown by the fact that knockdown of gp130, the common receptor subunit of this family, reduced Stat3 activation and neoplastic transformation. Besides transformation, the Rac/IL6/Stat3 axis was required for apoptosis inhibition upon vSrc expression. (supported by CIHR, CBCF-Ontario chapter, US Army breast cancer program, NSERC and Breast Cancer Action Kingston).

Arulanandam, R., Geletu, M., Vultur, A., Cao, J., Larue, L., Feracci, H. and Raptis, L.

American Association of Cancer Research Annual meeting, Washington, DC., April 2010.

Title: Cadherin-cadherin engagement promotes cell survival via Rac/Cdc42 and Stat3

Stat3 (signal transducer and activator of transcription-3) is activated by a number of receptor and non-receptor tyrosine kinases, while a constitutively active form of Stat3 alone is sufficient to induce neoplastic transformation. We recently demonstrated a dramatic increase in the activity of Stat3 in breast carcinoma as well as normal epithelial cells and fibroblasts, as a consequence of cell to cell adhesion (Oncogene 23:2600). Given the generally accepted, positive role of Stat3 in proliferation, the Stat3 activity increase observed in confluent cells, that is when cells do not divide, was an unexpected observation. Interestingly, by plating cells onto surfaces coated with fragments encompassing the two outermost domains of E-cadherin and cadherin-11, two members of the classical type I and II cadherin family of surface receptors, responsible for the formation of cell to cell junctions, we demonstrated that cadherin engagement *per se* can directly activate Stat3, in the absence of cell to cell contact. Examination of the mechanism of the cadherin-mediated, Stat3 activation unexpectedly revealed for the first time a dramatic surge in total Rac1 and Cdc42 protein levels by cadherin engagement, and a proportional increase in Rac1 and Cdc42 activity. Therefore, to examine the potential role of Rac/Cdc42 in the density-dependent, Stat3 activation, the ability of mutationally activated Rac^{V12} to activate Stat3 at high cell densities was examined. The results revealed a dramatic increase in protein levels and activity of both the endogenous Rac and Rac^{V12} with cell density, which was due to inhibition of proteasomal degradation in both cases. In addition, Rac^{V12}-expressing cells had higher Stat3, tyrosine-705 phosphorylation and activity levels at all densities, indicating that Rac^{V12} is, in fact, able to activate Stat3. Further examination of the mechanism of Stat3 activation showed that both cadherin engagement and Rac^{V12} expression caused a surge in mRNA of Interleukin-6 (IL6) family cytokines, known potent Stat3 activators. Knockdown of gp130, the common subunit of this family reduced Stat3 activity in densely growing normal, as well as in Rac^{V12}-transformed cells, indicating that the IL6 family may be responsible for the Stat3 activation both by cadherin engagement and Rac mutational activation. Indeed, Rac knockdown reduced the density-mediated, Stat3 activation, indicating that Rac is responsible for the Stat3 stimulation observed upon cadherin ligation. Inhibition of cadherin interactions using a peptide, a soluble cadherin fragment or genetic ablation induced apoptosis, pointing to a significant role of this pathway in cell survival signalling, a finding which could also have important therapeutic implications. (supported by CIHR, CBCF-Ontario chapter, US Army breast cancer program, NSERC and Breast Cancer Action Kingston).

Jamaica Cass, Rozanne Arulanandam, Mulu Geletu, Blerta Starova, Esther Carefoot, Sandip Sengupta, Bruce Elliott, Leda Raptis

American Association of Cancer Research Annual meeting, Washington, DC., April 2010.

Title: A novel cadherin-dependent Rac/Stat3 pathway in invasive breast cancer

Stat (signal transducer and activator of transcription) 3 is a transcription factor involved in a number of signaling pathways activated by receptor and non-receptor tyrosine kinases. Constitutively active Stat3 alone is sufficient to induce tumorigenesis. We have previously shown that Stat3 can also be activated by engagement of the epithelial adhesion molecule E-cadherin (Arulanandam, R. et al., MCR, 2009). An additional novel finding in this study was that levels of total and activated Rac1 proteins increase dramatically, thereby causing the Stat3 stimulation. Interestingly, Stat3 expression was independently found to downregulate p53 expression in several epithelial and fibroblast cell lines. These findings suggest a novel Cadherin/Rac1/Stat3-dependent pathway that causes sustained downregulation of p53, resulting in uncontrolled growth and survival. As a first step to test this hypothesis in human cancer, we are assessing the expression profiles and localization of these molecules in murine breast epithelial and carcinoma cell lines, and in human breast cancer tissues. The results revealed that at low cell density in 2-D culture conditions, E-cadherins and b-catenin showed strong cytoplasmic and perinuclear localization, respectively. In contrast, at high cell density both markers showed strong localization to the plasma membrane. On the other hand, a breast carcinoma cell line showed cytoplasmic staining of pan-cadherin and nuclear staining of b-catenin under both low and high cell density conditions. Western blotting revealed that levels of pan and activated (pY705) Stat3, and Rac1 were increased at high compared to low cell densities, consistent with a cadherin-dependent activation of this pathway. We are currently extrapolating these findings to a 3-D culture model in which mammary epithelial cells (EPH4) form acini-like spheroids with hollow lumen surrounded by a well-polarized outer layer of cells that is in direct contact with matrix. Under these conditions, total Stat3 levels are sustained for 4-6 days followed by a transient increase in cyclin D1 expression. We are also performing immunohistochemical analyses of these molecular biomarkers on a cohort of human breast cancer tissues (n=59) to test associations of protein expression profiles in human cancer. Preliminary results have shown increased expression of active Stat3 in breast tumours compared to normal mammoplasty tissues. In addition, increased expression of p53 was observed in a subset (17%) of these breast cancers. Detailed ARIOL imaging analysis are currently in progress to evaluate relative expression levels and associations of Stat3 and p53 in breast cancer tissues. Our findings suggests a novel pathway by which Stat3 activation causes a dramatic decrease in p53 levels, resulting in increased proliferation and survival of cancer cells. (Supported by US Army breast cancer program, CIHR and CBCRA).

Src activity and gap junctional intercellular communication in cultured, human lung carcinoma cells

Geletu, M., Greer, S., Arulanandam, R., Tomai, E. and Raptis, L.*

[1] Departments of Microbiology and Immunology and Pathology, Queen's University, Kingston, Ontario, Canada K7L3N6.

*Corresponding author.
Phone number: (613) 533-2462 (office/lab)
(613) 533-2450 (secretary)
FAX number: (613) 533-6796.
e-mail: raptisl@queensu.ca

Running Title: gap junctions and Src in lung cancer

Key words: electroporation, Indium-Tin oxide, gap junctions, Stat3, cell to cell adhesion

Abstract

Neoplastic transformation by a number of oncogenes such as Src suppresses gap junctional, intercellular communication (GJIC). However, the role of Src upon GJIC in small cell lung cancer (NSCLC) has not been defined. Immunohistochemical analysis revealed high Src activity in NSCLC biopsy samples compared to normal tissues. Here we explored the potential effect of Src upon GJIC in a number of NSCLC lines, by assessing the levels of tyr418 phosphorylated Src. Gap junctional communication was examined by electroporating a fluorescent dye into cells grown on a transparent electrode, followed by observation of the migration of the dye to the adjacent, nonelectroporated cells under fluorescence illumination. The results demonstrate a dramatic increase in the levels of connexin-43, a ubiquitous gap junction protein with cell density in normal cells. However, the majority of cell lines examined (11/13) had low GJIC even at high densities. An inverse relationship between Src activity levels and GJIC was observed in the majority of cell lines; in four lines with high Src activity gap junctional communication was absent (A549, CALU-1, CALU-6 and SW-900), while two lines with extensive GJIC (QU-DB and SK-LuCi-6) had high GJIC levels. Nevertheless, additional factors must be responsible for gap junction closure, since Src inhibition did not restore GJIC in the four lines with high Src activity, while two other lines had no GJIC despite the fact that Src-ptyr418 levels were very low (BH-E, LC-T). Src effector pathways leading to GJIC suppression include the Ras/Erk and Cas, that is their inhibition reinstates GJIC in Src-expressing cells. We examined the role of a distinct Src effector, Stat3. The results demonstrate that Stat3 inhibition in cells expressing high Src levels, or in cells where GJIC was suppressed through exogenous Src transduction, did not restore GJIC. On the contrary, Stat3 downregulation in normal lung epithelial or in the NSCLC lines displaying extensive GJIC suppressed junctional permeability. Taken together, these findings demonstrate that although Stat3 is generally growth promoting and in an activated form it can act as an oncogene, it is ***required*** for gap junctional communication both in normal epithelial cells and in certain tumor lines that retain extensive communication.

Introduction

Gap junctions are plasma membrane channels that provide a path of direct communication between the interiors of neighboring cells. They are formed by the connexin (Cx) family of proteins. An increase in cell proliferation correlates with a reduction in gap junctional, intercellular communication (GJIC, reviewed in [33]. In fact, a number of oncogenes such as v-Src [20], the polyoma virus middle Tumor antigen (mT [9,27], the activated chaperone Hsp90N [17], vRas [8,10] and others have been shown to interrupt junctional communication.

A body of evidence has indicated that expression of the Src tyrosine kinase leads to gap junction closure, through phosphorylation of the ubiquitous connexin, Cx43. Src exerts its effect either through direct tyrosine phosphorylation of Cx43, or indirectly, through activation of the Erk1/2 or Protein kinase C family kinases that phosphorylate Cx43 at Ser/thr (reviewed in [25]. Examination of levels of tyr-418 phosphorylated, ie activated Src in a number of Non Small Cell Lung Cancer (NSCLC) biopsies previously showed the presence of higher Src activity than the surrounding, non tumor lung tissue [22,40]. However, the effect of Src upon GJIC and its contribution to GJIC suppression in NSCLC lines and tissues that may express other oncogenes in addition to Src, remains to be determined.

The Signal Transducer and Activator of transcription-3 (Stat3), is a cytoplasmic transcription factor and an important Src downstream effector. Following phosphorylation on tyr-705 by Src, as well as by Growth factor or cytokine receptors, Stat3 normally dimerises through a reciprocal SH2 domain-phosphotyrosine interaction and translocates to the nucleus, where it induces the transcription of specific genes [39]. Examination of Stat3 levels in a number of cultured NSCLC lines demonstrated that Src is a major Stat3 activator in these cells, transducing signals from EGFR and IL6 that lead to apoptosis inhibition [29]. However, we and others previously demonstrated that cell to cell adhesion caused by confluence of cultured cells causes a dramatic increase in Stat3 activity levels [26], therefore cell density has to be taken into account in the examination of the effect of different factors upon Stat3 activity. In the present report this was achieved by assessing Stat3 activity levels at a range of densities.

We previously assessed GJIC in a number of lung cancer lines [31]. In this work GJIC was examined using an apparatus where cells were grown on a glass slide, half of which was coated with electrically conductive, optically transparent, indium-tin oxide. An electrode was placed on top of the cells and an electric pulse which opens transient pores on the plasma membrane was applied in the presence of the fluorescent dye, Lucifer yellow. The dye penetrates into the cells growing on the conductive part of the slide, and its migration through gap junctions to the non-electroporated cells growing on the non-conductive area is then microscopically observed under fluorescence illumination. Although this technique is adequate for a number of lines, the turbulence generated as the electrode is removed can cause cell detachment, which makes GJIC examination problematic. In the present communication we revisited the question of GJIC levels in lung cancer lines using an improved technique, where the upper electrode is eliminated. This approach is valuable for the electroporation of tumor-derived lines especially at high densities, when cell adhesion to the substratum may be weak. Interestingly, the results revealed that cell density *per se* triggers a dramatic increase in both Cx43 levels and GJIC. Two NSCLC lines, QU-DB and SK-LuCi-6 were found to have extensive GJIC, similar to control, normal lung epithelial cells, while GJIC in 9 other lines, such as A549 was very low or undetectable. Investigation of the mechanism of gap junction closure revealed an inverse relation between Src activity levels and GJIC in the majority of cell lines. However,

two lines with low Src activity (BH-E, LC-T) had no GJIC, indicating that other oncogene(s) may be responsible for gap junction closure in these lines. Further examination of the mechanism of GJIC suppression led to the discovery that, unlike Ras inhibition in Src-transformed fibroblasts [19], Stat3 inhibition in A549 cells that have high Src activity, or in Src-transduced, SK-LuCi-6 cells, does not restore GJIC. On the contrary, Stat3 inhibition in NSCLC cells displaying extensive GJIC (QU-DB, SK-LuCi-6) suppressed junctional permeability, indicating that Stat3 function is actually ***required*** for the maintenance of gap junction function in these lung cancer lines.

Materials and methods

Examination of gap junctional communication

To examine gap junctional communication by *in situ* electroporation, it is important to be able to reliably distinguish cells that were loaded with Lucifer yellow directly by electroporation, from cells that received the dye from neighbouring cells by diffusion through gap junctions. This was achieved using a slide where a 3 mm-wide strip of ITO had been removed by etching with acids, leaving two co-planar electrodes, supported by the same glass slide substrate [2]. In a further improvement (Fig. 1), the coating was removed from the glass surface in lines of ~20 μm wide, to define electrode and non-conducting regions. Etching was done using a laser beam, so that the nonconductive glass underneath is exposed. It was important to ensure that only the 800Å coating was removed, without affecting the glass, so that cell growth would be unaffected across the line. This was achieved with a UV laser operating at a 355 nanometer wavelength using approximately 1 watt of output power with 60% of the energy delivered to the surface of the glass. The beam was manipulated by mirrors on a pair of galvanometers to produce the desired pattern.

To form the two electrodes, the coating was removed in a straight line in the middle [**2**]. A dam of nonconductive plastic [**3**] was bonded onto this line, to divert the current upwards, thus creating a sharp transition in electric field intensity between electroporated and non-electroporated sections. To provide areas where the cells are not electroporated, the ITO was also removed in two parallel lines ([**4**], [**4*a***]). A plastic chamber was bonded onto the slide, to form a container for the cells and electroporation solutions [**5**]. Current flows inwards from each contact point [**6** and **6*a***], via a conductive highway under the well [**5**] electroporating cells in area [***d***] then over the barrier ([**8**], arrowheads) to the other side, in area [***a***]. In this configuration, cells which acquired LY by electroporation (growing in [***a***] and [***d***]) and cells into which LY traveled through gap junctions ([***b***] and [***c***]) both grow on ITO, separated only by a laser-etched line of ~20 μm. Extensive experimentation showed that in this setup the electroporation intensity is uniform across the electroporated area (Fig. 2B and Fig. 3).

Cells were plated in the chamber and when they reached the appropriate density (90% confluence, to 5 days post-confluence), the growth medium was replaced with Calcium-free DMEM supplemented with 5 mg/ml Lucifer yellow [**7**]. The slide/chamber was placed into a holder where electrical contacts were established and a set of electrical pulses delivered to the cells. Extensive experimentation indicated that 10 pulse pairs, each pulse of 18 volts peak value, 100 μs length and spaced 0.5 seconds apart, with one of each pair having a polarity opposite to that of its partner gave optimal results. Following a 5 min incubation at 37^{o}C, the unincorporated dye was washed with Calcium-free DMEM supplemented with 10% dialysed fetal calf serum and cells observed and photographed under fluorescence and phase contrast illumination.

Cell lines, culture techniques and Stat3 inactivation

All cells were grown in DMEM with 10% fetal calf serum. Confluence was estimated visually and quantitated by imaging analysis of live cells under phase contrast using the MCID-elite software (Imaging Research, St. Catharine's Ont.). Stat3 was inactivated using two approaches: **(1).** Treatment with 50 μM CPA7 [$PtCl_3(NO_2)(NH_3)_2$] [21] for 24 hrs **(2)**. Expression of shRNA, delivered with a lentivirus vector [15]. Stat3 transcriptional activity was measured as described, by transient transfection of the p*Luc*TKS3 construct [32]. As a control, cells were co-transfected with the reporter pRLSRE, which contains two copies of the serum response element (SRE) of the c-fos promoter, subcloned into the *Renilla* luciferase reporter, pRL-null (Promega) [34]. The firefly and *Renilla* luciferases utilize different substrates and thus can be assayed independently in the same lysates using this kit. Following transfection, cells were plated to different densities and luciferase activity determined. Western blotting was conducted as before [18] on proteins extracted from cell pellets, using antibodies to Cx43 (a generous gift of Dr. Elisavet Kardami, University of Manitoba), Hsp90 (Stressgen #SPA-830) GAPDH (---), or tubulin as loading controls, followed by secondary antibodies and ECL reagents, according to the manufacturer's protocol (Biosource).

Cells were cultured from surgically explanted tumors as previously described [31].

Src was inactivated using 3 approaches: Dasatinib (???), PD180970 (0.2 μM with redosing every 12 hours for a total of 24 hours), or SU6656 (5μM for 24 hrs).

Results

Cell density modulates GJIC and connexin-43 protein levels

A number of reports showed that gap junction function is dependent upon cell to cell contact and the assembly of adherens junctions [14,37]. Since the opportunity for cell to cell adhesion is expected to increase with cell density, we examined the effect of cell density upon GJIC. To this effect, we at first took advantage of the normal mouse lung type II line, E10 that has extensive GJIC, an even and flat morphology and good adhesion to the substratum even at high densities [36] (Fig. 2A). Cells were plated in electroporation chambers and when 90% confluent or at 3 days post-confluence Lucifer yellow was electroporated and the movement of the dye through gap junctions observed under fluorescence and phase contrast illumination (see Materials and Methods). The results revealed that, although cells at 90% confluence did display some gap junction transfer (Fig. 2B, ***a-b***, GJIC ~1.5), GJIC increased to ~6 at 3 days post-confluence (Fig. 2B, ***c-d***), while at intermediate densities GJIC displayed intermediate values. These results indicate that confluence beyond 100% causes a dramatic increase in GJIC.

We next examined the levels of Cx43, a widely expressed gap junction protein, at different cell densities. Cells were plated in plastic petri dishes at a confluence of 40% and at different times thereafter, up to 5 days post confluence (Fig. 2A), total protein extracts were probed for Cx43 by Western blotting. To ensure that the growth medium was not depleted of nutrients, it was changed every day. As shown in Fig. 2C (top panel), cell density caused a dramatic increase in Cx43 levels, which plateaued at ~3 days post-confluence (lane 5). To further examine the importance of time of cell to cell contact required to form the gap junctions, we repeated the experiment by plating different numbers of cells ($0.4x10^6$, $0.6\ x10^6$, $1.1\ x10^6$ or $1.5\ x10^6$ per 3 cm petri, respectively), so that they would reach densities equivalent to 80% and 3, 4 and 5 days postconfluence, respectively after 36 hrs, and at that time Cx43 levels were examined. As shown in Fig. 2D, very similar results were obtained, indicating that it is the extent of cell to cell contact, regardless of time in culture beyond 36 hrs, that is responsible for the increase in Cx43 levels with cell density.

GJIC and connexin-43 in NSCLC lines or freshly explanted tumor cells

In light of the above findings, we examined GJIC levels at different densities up to 4 days post-confluence in a panel of human lung cancer lines [31]. As shown in Table I, two NSCLC lines, QU-DB and SK-LuCi-6 had extensive GJIC (6.3 and 6.5, respectively, Fig. 3A and Table I) which increased with density, while 11 other NSCLC lines had very low GJIC even at high densities (e.g. A549, Fig. 3B and Table I). In addition, primary cells explanted and cultured from a poorly differentiated adenocarcinoma had no GJIC. Interestingly, fibroblasts cultured from the same tumor had extensive communication, as expected for normal cells, although they constitute parts of the same tissue (Fig. 4). Primary cells and fibroblasts, freshly explanted from two other tumor specimens (a moderately differentiated adenosquamous carcinoma and adenocarcinoma, respectively) gave similar results (not shown).

Examination of Cx43 levels in the lung cancer lines by Western blotting showed that QU-DB cells had levels similar to E10, which increased dramatically with cell density, while Cx43 levels in A549 cells were undetectable (Fig. 5A). SK-LuCi-6 cells had levels similar to QU-DB, while all other NSCLC lines examined had very low Cx43. The above data taken together indicate that, besides normal epithelial cells, cell density causes a dramatic increase in

GJIC and Cx43 protein levels in two lung carcinoma lines which have extensive GJIC. Nevertheless, the majority of lung cancer lines examined (11/13) had very low or no detectable communication, even at high cell densities (Table I).

Src activity and GJIC suppression in lung cancer lines

Src was previously found to be overexpressed in a number of lung cancer biopsy samples compared to normal tissues [22,40]. As a first step in the elucidation of the potential effect of Src upon GJIC in NSCLC, we assessed Src levels in the NSCLC lines. In fact, it has been previously reported that cell to cell adhesion may dramatically increase the activity of a prominent Src effector, Stat3 ([32], reviewed in [26]). For this reason, we examined Src activity at different densities from 50% of confluence up to 7 days post confluence, the densities where Stat3, tyr705 phosphorylation and activity was previously shown to be upregulated in a large number of lines [35]. Extracts from cells grown to different densities were probed for the tyr-418 phosphorylated form of Src which correlates with its activity using a phospho-specific antibody. As shown in Fig. 5 (B-D), Src-ptyr418 levels in A549 cells were high, similar to the levels in vSrc-transformed E10 (panel D, lanes 1 vs 3), while levels in QU-DB cells were low, similar to E10 (panel C, 3 vs 8). Interestingly, cell density had no effect upon Src-ptyr418 or total Src protein levels in A549 or QU-DB cells (panel B, 1-4 and 5-8) or any other line examined, indicating that density does ***not*** affect cSrc activity in these cells.

We next examined Src-ptyr418 levels in the NSCLC lines. As shown in Fig. 5C, lines CALU-1, SW-900 and CALU-6 had Src levels similar to A549, and LC-T, BH-E and SK-LuCi-6 had low levels, similar to QU-DB. Examination of gap junctional communication revealed that five lines with high Src-ptyr418 had no detectable GJIC (CALU-1, SW-900, CALU-6, A549), consistent with the known Src effect of GJIC suppression. In addition, two lines with high GJIC (QU-DB and SK-LuCi-6) had undetectable Src-418 levels. Taken together, these data point to an inverse relationship between Src activity levels and GJIC. However, two lines with very low Src-418 levels (LC-T and BH-E) had undetectable GJIC levels indicating that possibly other, Src-independent factors may be responsible for gap junction closure in these lines. Primary cells from the three tumors were found to have high Src activity, as shown before for biopsy tissues, while tumor-derived fibroblasts had low levels, similar to E10 (not shown).

To further explore the contribution of activated Src upon GJIC suppression, Src was downregulated with the Src-selective, pharmacological inhibitors Dasatinib, PD180970 or SU6656 [34] in A549 cells (see Materials and Methods). As shown in **Fig. 5D**, Dasatinib treatment caused a dramatic reduction in Src-ptyr418 levels. However, Src inhibition did not produce any detectable increase in GJIC. Similar results were obtained following treatment with PD180970 and SU6656, and with CALU-1 and CALU-6 cells (not shown). These findings indicate that possibly other oncogenes besides Src, or other factors may be important contributors to GJIC suppression in these lines.

Stat3 is a positive regulator of GJIC in lung cancer lines

The mechanism of GJIC suppression in A549 cells was examined further. Previous results indicated that downregulation of the cRas protooncogene product in vSrc [19]- or mT [11]-transformed fibroblasts restores GJIC, underlining the importance of the Ras pathway in GJIC reduction by activated Src. Stat3 is at the core of another pathway emanating from the Src kinase. To explore the potential contribution of Stat3 to the Src-induced suppression of gap junctional communication, we at first examined the correlation between Src-ptyr418 and Stat3-

ptyr705 levels in 9 NSCLC lines. As shown before for a number of cell types [26], density was found to cause an increase in Stat3-ptyr705 levels in A549 cells (Fig. 5B), therefore Stat3-ptyr705 levels were assessed at a range of densities in all cell lines. The results showed elevated Stat3-ptyr705 levels in lines with high Src-ptyr418 (A549, also CALU-1, SW-900 and CALU-6), indicating that Src may be an important Stat3 activator in these lines. At the same time, QU-DB, SK-LuCi-6 and BH-E had low levels of both Src-ptyr418 and Stat3-ptyr705. However, line LCT had undetectable Src-ptyr418 levels, although Stat3-ptyr705 was high, indicating that other, Src independent factor(s) may be responsible for the Stat3-ptyr705 increase in this line.

To examine the contribution of Stat3 to GJIC suppression by Src, we assessed the effect of Stat3 inhibition upon GJIC in cells that express high Src activity levels (A549, CALU-1, SW-900 and CALU-6). As shown in Fig. 5E, treatment with the Stat3 inhibitor, CPA7 for 24 hrs [21], or expression of a Stat3 specific, shRNA, essentially eliminated Stat3, tyr705 phosphorylation in this line. Unexpectedly however, CPA7 treatment (Fig. 3A, ***d-f***), or expression of the sh-Stat3 lentivirus vector (Fig. 3A, ***g-i***) did not increase junctional permeability in A549 cells (Table II). Similar results were obtained with CALU-1, SW-900 and CALU-6 cells. The above data taken together indicate that the high Stat3 activity, which could be, at least in part, due to high Src activity levels, cannot be solely responsible for the lack of junctional communication in A549, lung carcinoma cells.

As Src inhibition experiments showed (Fig. 5D), A549 cells may express other oncogenes besides Src, which may contribute to gap junction closure. To examine the role of Stat3 in the Src-mediated, GJIC suppression, we expressed Src in SK-LuCi-6 cells which have low Src-ptyr418 levels and extensive GJIC, using a retroviral vector [24]. As expected, Src expression disrupted gap junctional permeability. Subsequent Stat3 inhibition with CPA7 or shRNA did not restore GJIC, in keeping with the data from A549 cells (Table II). The above findings taken together indicate that Stat3 cannot be part of a pathway leading to Src-induced, gap junction closure in SK-LuCi-6-Src cells.

We then explored the potential importance of Stat3 function in the maintenance of gap junctional permeability, by assessing the effect of Stat3 inhibition upon GJIC levels in QU-DB cells which have low Src activity and extensive GJIC. Unexpectedly, as shown in Fig. 3A, Stat3 downregulation through CPA7 treatment essentially ***abolished*** GJIC in QU-DB cells. Reduction of Stat3 levels through infection with the sh-Stat3 lentivirus vector gave similar results (panels ***g-i***). Stat3 downregulation in SK-LuCi-6 cells also caused a dramatic ***de***crease in GJIC (Table II). The above data taken together reveal that, rather than increasing GJIC, Stat3 inhibition eliminates junctional permeability, that is Stat3 activity is actually required for gap junction function, in two cultured lung carcinoma lines which display extensive GJIC.

Discussion

Extensive data demonstrated that oncogenes such as mT, Src or Ras can suppress gap junctional, intercellular communication [9,10]. Moreover, it was shown that lower levels of these gene products were sufficient to interrupt gap junctions than the levels necessary for full transformation [12,27], indicating that a decrease in junctional communication may be an early event in neoplastic conversion. In this communication we explored the correlation between the activity of Src, the prototypical oncogene known to be hyperactive in NSCLC, and GJIC in normal epithelial, in established lung cancer lines as well as in cultured primary lung tumor cells, using an improved procedure for GJIC examination. Our results indicated that cell density *per se* increases both GJIC and connexin 43 levels. Still, the majority of the lines tested (11/13) had very low or no GJIC even at high densities.

Src may suppress GJIC in certain cell lines and primary tumor cells

Given the significance of density in GJIC assessment, to measure the impact of Src upon GJIC we at first examined the effect of density upon Src activity. We and others previously demonstrated that cell confluence induces a dramatic increase in the activity of the prominent Src effector, Stat3 [26,34,35]. Interestingly, our results revealed the absence of an increase in Src protein levels or activity with cell density in NSCLC lines, which implies that, although Src is a known potent Stat3 activator, other kinase(s) must be responsible for the density-induced increase in Stat3-ptyr705 levels. In fact, our previous data demonstrated that in HC11 mouse breast epithelial cells, engagement of the E-cadherin, cell to cell adhesion molecule, causes a dramatic increase in the levels of the cellular Rac GTPase. This leads to an increase in the levels of interleukin-6 (IL6) family cytokines, potent Stat3 activators [6,7]. Whether the Rac/IL6 axis is responsible for the density-induced, Stat3 upregulation in the lung carcinoma lines as well is currently under investigation.

Examination of Src activity in the NSCLC lines revealed an inverse correlation between Src, tyr418 phosphorylation levels and GJIC. Although the number of samples is too low to allow statistical correlations, since Src is known to suppress gap junctional communication in cultured cells such as rodent fibroblasts, it is tempting to speculate that Src may be responsible, at least in part, for gap junction closure in these lines. Still, Src inhibition did not restore GJIC in three lines with high Src activity, A549, CALU-1 and CALU-6, indicating that, in addition to Src, these cells may express other factors responsible for GJIC closure. Furthermore, two lines with low Src-ptyr418 levels (BH-E, LC-T) had no detectable communication, indicating that other, Src-independent factors may be responsible for the lack of GJIC in these lines.

We also examined GJIC in freshly explanted, primary cells from 3 NSCLC specimens. Since the senescence process can reduce or abolish GJIC [38], cells were plated in electroporation chambers immediately after surgery at densities of ~80%, so that they would reach confluence within 1-2 days and GJIC examined every day for up to 10 days. No gap junctions were ever detected in any of the preparations. Src-418 levels were high in cells from all three tumor specimens, indicating that Src may have played a role in GJIC suppression. However, the possibility that the initiation of the senescence process even a day after surgery may have affected GJIC cannot be excluded.

Stat3 does not transmit Src signals to gap junction closure

Several signal transducers besides Stat3 are known to be downstream effectors of the Src kinase such as Ras/Raf/Erk, PI3k/Akt the Crk-associated substrate (Cas) and others [1]. Constitutively active Ras is neoplastically transforming and can suppress GJIC [10,12]. Similarly, constitutively active Stat3 can transform established lines [23], but the effect of Stat3 upon GJIC in NSCLC is unknown. Examination of the mechanism of Src-mediated, GJIC suppression previously indicated that inhibition of Ras in Src-transformed, rat fibroblasts reinstated gap junctional permeability, despite the fact that Cx43 was phosphorylated [19]. Conversely, mT expression in Ras-deficient cells did not suppress GJIC [11]. These data taken together indicate that Ras signalling is part of a Src-induced pathway leading to GJIC suppression. Similarly, it was shown that Cas is required for the Src-induced, reduction in gap junctional communication [28]. In sharp contrast, our present data demonstrate that Stat3 inhibition in A549 cells did not restore GJIC. It is certainly possible that other oncogenes present are responsible for the GJIC suppression, since inhibition of Src itself did not restore

GJIC. However, the fact that Src expression in SK-LuCi-6 cells eliminated GJIC, and that communication was not reinstated by Stat3 inhibition, shows that a role of Stat3 in the Src-induced, GJIC suppression in these cells is unlikely.

Stat3 plays a positive role in gap junctional communication

The fact that cell density upregulates Stat3 concomitant with an increase in both Cx43 and GJIC prompted us to explore a potential positive role of Stat3 upon GJIC. Interestingly, Stat3 inhibition in two NSCLC lines which exhibit extensive GJIC (QU-DB, SK-LuCi-6) abolished junctional permeability, indicating that Stat3 plays a role in the maintenance of GJIC function. This conclusion is in agreement with a previous report indicating that Stat3 inhibition eliminated GJIC in normal rat liver epithelial cells as well [15]. Taken together, these findings demonstrate that although Stat3 is generally growth promoting and in an activated form it can act as an oncogene, it is ***required*** for gap junctional communication both in normal epithelial cells and in certain tumor lines that retain GJIC. The possible role of Stat3 in the GJIC and Cx43 increase is currently under investigation.

Our data also show high Stat3 activity in four NSCLC lines (A549, CALU-1, CALU-6, SW-900) presumably, at least in part, due to the high Src activity. However, despite the fact that Stat3 promotes GJIC, the Src-mediated, Stat3 activation does not lead to an increase in gap junctional permeability. This could be due to Cx43 phosphorylation by Src, either directly or indirectly [25] , so that the net effect of Src expression is gap junction closure.

Results from a number of labs demonstrated that Stat3 activates a number of anti-apoptotic genes [39]. Induction of apoptosis was shown to lead to a loss of cell coupling, probably due to caspase-3 mediated degradation of Cx43, in primary bovine lens epithelial and mouse NIH3T3 fibroblasts [30]. Interestingly, we previously demonstrated that Stat3 inhibition in cells transformed by Src or the Large Tumor antigen of Simian Virus 40 leads to apoptosis [4,34], possibly due to activation by Src of the transcription factor E2F family, a potent apoptosis inducer. Therefore, apoptosis induction brought about through Stat3 downregulation in cells with high Src may have accentuated gap junction closure.

In a previous report it was shown that Src inhibition increases Stat3 activity in certain NSCLC lines [13]. However, this was not evident in our system; treatment with Dasatinib, PD180970 or SU6656 at different concentrations and up to 72 hrs reduced Stat3, ptyr705 levels in all lines we examined (e.g. Fig. 5D)

The SK-LuCi-6 line originated from a biopsy of a large cell anaplastic lung carcinoma, which was rapidly metastatic [5]. Assuming that the establishment process did not eliminate tumor genes, it appears that the oncogenes that were responsible for tumor induction and may still be expressed in these cells are not able to suppress GJIC. This work may establish a correlation between Src activity, Stat3 and GJIC that could be important in the development of chemotherapeutic drugs.

Acknowledgements

We would like to thank Dr. Mike Baird and Shallyn Littlefield for CPA7 synthesis, the Center for manufacturing of advanced ceramics and nanomaterials of Queen's University for laser etching services and Kevin Firth, P.Eng., of Ask Sciences products, Kingston, Ontario for engineering design. We are grateful to Dr Elissavet Kardami (University of Manitoba, Canada) for a generous gift of connexin-43 antibody. The financial assistance of the Canadian Institutes of Health Research (CIHR), the Canadian Breast Cancer Foundation (Ontario Chapter), the

Natural Sciences and Engineering Research Council of Canada (NSERC), the Canadian Breast Cancer Research Alliance, the Ontario Centers of Excellence, the Breast Cancer Action Kingston and the Clare Nelson bequest fund through grants to LR is gratefully acknowledged. RA was supported by a Canada Graduate Scholarships Doctoral award from CIHR, the Ontario Women's Health Scholars Award from the Ontario Council on Graduate Studies and a Queen's University Graduate Award. SG was the recipient of an NSERC summer studentship. MG was supported by a postdoctoral fellowship from the US army Breast Cancer Program, the Ministry of Research and Innovation of the Province of Ontario and the Advisory Research Committee of Queen's University.

Author Disclosure Statement: The authors do not have any conflict of interest.

Table I
GJIC in normal epithelial and lung cancer cell lines

	Cell line	Confluence[α]	GJIC[β]
Normal epithelial	**E10**	90%	1.5±0.5
		100+3d	6±1
Lung cancer lines	**QU-DB**	90%	1±0.2
		100+3d	6.3±1
	SK-LuCi-6	90%	1.8±0.2
		100+3d	6.5±1
	A549	90%	0.1±0.1
		100+3d	0
	SK-MES	100+3d	0.8±0.2
	SK-Lu-1	100+3d	1.1±0.2
	CALU-1	100+3d	0
	LC-T	100+3d	0
	SW-900	100+3d	0
	BHE	100+3d	0
	CALU-6	100+3d	0
	FR-E	100+3d	0
	WT-E	100+3d	0
	SW-1573	100+3d	0
	SK-LuCi-6-Src	100+3d	0
Primary[γ] tumor		100+3d	0
fibroblasts[γ]		100+3d	5.8±1.2

[α]Confluence was quantitated by imaging analysis (see Materials and Methods).

[β]GJIC was assessed by *in situ* electroporation at the indicated confluence (see Materials and Methods, Fig. 1). Quantitation was achieved by dividing the number of cells into which the dye had transferred through gap junctions (denoted by dots), by the number of cells at the edge of the electroporated area (denoted by stars, Fig. 2B and 3A). Numbers are averages of at least three experiments, where transfer from more than 200 cells was examined.

[γ]Immediately after surgery, cells were placed in culture and GJIC examined. After 8-10 weeks in culture, most of the tumor cells had died while the fibroblasts present in the initial suspension predominated. These cells did not express cytokeratins, contrary to tumor cells.

Table II

Effect of Stat3 downregulation upon GJIC

A. Cells expressing activated Src

Cell line	Treatment[α]	Stat3[β] (%)	GJIC[γ]
A549	DMSO	93±12	0.5 ±0.1
"	CPA7	3±1	0.1 ±0.1
"	sh-Stat3	22±3	0.1 ±0.1
E10-Src	DMSO	100±15	0.8 ±0.2
	CPA7	5±1	0.1 ±0.1
	sh-Stat3	18±3	0.2 ±0.1
SK-LuCi-6-Src	DMSO	100±12	0.6 ±0.1
"	CPA7	3±1	0.1 ±0.1
	sh-Stat3	22±3	0.3 ±0.1

B. **Cells with extensive junctional communication**

Cell line	Treatment	Stat3 (%)	GJIC
E10	DMSO	55±11	6.±0.4
"	CPA7	4.2±1.2	0.2±0.1
"	sh-Stat3	11±2	1.0±0.2
QU-DB	DMSO	47±11	6.3±0.4
"	CPA7	2±0.5	0.2±0.1
"	sh-Stat3	8±3	0.8±0.2
SK-LuCi-6	DMSO	52±10	6.5±1
"	CPA7	2.8±1.2	0.3±0.1
"	sh-Stat3	16±2	1±0.2

[α] Cells were treated with 50 μM CPA7 for 24 hrs, or infected with a lentivirus vector expressing a Stat3-specific, shRNA (see Materials and Methods).

[β] Stat3-tyr705 levels were measured by Western blotting. Numbers represent relative values obtained by quantitation analysis, with the average of the values for v-Src expressing, E10 cells taken as 100%. Averages of at least three experiments ±SEM are shown. Data from sparsely growing cells are presented, but the relative increases were the same regardless of cell density [34]. The transcriptional activity values obtained paralleled the Stat3-705 phosphorylation levels indicated (Fig. 5E, see Materials and Methods).

[γ]GJIC was assessed as in Table I, at 3 days after confluence.

Figures

Figure 1

The electroporation apparatus
A: Top view

Cells are grown on a glass slide (**1**), coated with conductive and transparent indium-tin oxide [ITO, (**1*a***)]. The ITO coating is laser-etched in a straight line in the middle (**2**), essentially forming two electrodes. A dam of Teflon (**3**) is used to divert the current upwards, thus creating a sharp transition in electric field intensity. A plastic chamber is bonded onto the slide, to form a container for the cells and LY (**5**). To provide areas where the cells are not electroporated, the ITO was also removed in two parallel lines [(**4**), (**4a**)]. Current from a pulse generator flows inwards from each contact point (**6** and **6*a***) to area (***d***) then over the barrier [(**3**), arrowheads] to the other side, electroporating cells in area (***a***). For clarity, the front part of the chamber is removed.

B: Side view

The slide (**1**) with the cells growing on the ITO coated [(**1*a***), light green] and etched, bare glass regions is shown. When electroporation medium (**7**) is added to the chamber to a level above the height of the dam (**3**) then an electrical path (arrowheads) between the electrodes (**6**) and (**6*a***) and the cells (9) growing in this area is formed. Note that the size of the cells and the ITO layer (**1*a***) are shown exaggerated for clarity although the actual thickness of the ITO (800 Å) is much less than the thickness of the cells.

Figure 2

Cell density increases Cx43 levels and GJIC

A. E10 cells were plated in 3 cm petris, grown to different densities and photographed under phase-contrast illumination. Magnification: 240x.

B. E10 cells were plated in electroporation chambers and subjected to a pulse in the presence of Lucifer yellow when 90% confluent (***a,b***) or 3 days after confluence (***c,d***). Arrows point to the position of the edge of the electroporated area. In ***b*** and ***d***, stars mark cells loaded with the dye at the edge of the electroporated area and dots mark cells where the dye transferred through gap junctions. In ***d***, only cells in the lower part of the photograph were marked, to better visualize the gradient of fluorescence. Magnification: 220x.

C. E10 cells were plated in 3 cm plates and when they reached the indicated densities, detergent cell extracts were probed for Cx43 (top) or Hsp90 (bottom) as a control. Arrows point to the position of Cx43 or Hsp90, respectively.

D. Different numbers of E10 cells as indicated were plated in 3 cm plates and cell extracts were prepared 24 hrs later and probed for Cx43 (top) or Hsp90 (bottom) as a control. Arrows point to the position of Cx43 or Hsp90, respectively.

Figure 3

A. Stat3 downregulation eliminates gap junctional permeability in human lung carcinoma QU-DB cells

QU-DB cells were plated on conductive ITO-coated glass and Lucifer yellow electroporated following treatment with the DMSO carrier alone (***a-c***) or CPA7 (***d-f***), or infection with the sh-Stat3 lentiviral vector (***g-i***) (see Materials and Methods). After washing the unincorporated dye, cells from the same field were photographed under fluorescence (***a, d, g***) or phase contrast (***b, e, h***) illumination. Cells at the edge of the conductive area which were loaded with LY through electroporation were marked with a star, and cells at the non-electroporated area which received LY through gap junctions were marked with a dot [27]. Arrows point to the edge of the electroporated area. ***c, f, i***: Overlay of phase-contrast and fluorescence. Magnification: 240x.

Note the extensive junctional communication in (***b***).

B. Stat3 downregulation does not increase gap junctional permeability in human lung carcinoma A549 cells

Same as above, A549 cells. Note the absence of communication, even after Stat3 downregulation (***e, h***).

Figure 4

A and B: Cells cultured from a freshly explanted tumor specimen were grown in electroporation chambers [3] and Lucifer yellow introduced with a pulse. Arrows point to the edge of the electropoirated area. Note the absence of communication. Magnification: 240x.

C and D: Following growth of the cells for 10 weeks, fibroblasts present in the original cell suspension predominated. They were plated in electroporation chambers and Lucifer yellow introduced. Note the extensive communication through gap junctions.

Figure 5

A: Cell density causes a dramatic increase in Cx43 levels in QU-DB cells.

QU-DB (lanes 5-8) or A549 (lanes 1-4) cells were grown to different densities as indicated and extracts probed for Cx43 or Hsp90 as a loading control. Note the absence of Cx43 in A549 cells.

B: Cell density does not affect Src levels.

QU-DB (lanes 5-8) or A549 (lanes 1-4) cells were grown to different densities as indicated and extracts probed for Src-ptyr418, Stat3-ptyr705 or total Src. Note the low levels of Src-ptyr418 in QU-DB cells.

C: Src-ptyr418 and Stat3-ptyr705 in NSCLC lines.

Cells were grown to 3 days postconfluence and extracts probed for Stat3-ptyr705, Src-ptyr418 total Src or GAPDH as a loading control, as indicated. Src: Src-transformed, E10 cells.

D: Dasatinib reduces Src-ptyr418 levels in A459 cells:

A549 cells were treated with the Src-selective inhibitor, Dasatinib or the DMSO carrier alone and cell extracts probed for Src-ptyr418, Stat3-ptyr705 or GAPDH as a loading control.

E: CPA7 or infection with a vector expressing Stat3 shRNA reduce Stat3-ptyr705 levels:

A549 cells were grown to different densities and treated with the Stat3 inhibitor, CPA7 (lanes 6-8) or the DMSO carrier (lanes 1-5) for 24 hrs and cell extracts probed for Stat3-ptyr705 or tubulin as a loading control. Parallel cultures were infected with a vector expressing a Stat3-specific, shRNA [16], and stable lines treated as above.

Lower panel: A549 cells were transfected with a plasmid expressing a firefly luciferase gene under control of a Stat3-responsive promotor (■) and a Stat3-independent promotor driving a *Renilla* luciferase gene (□) (see Materials and Methods). After transfection, cells were plated to different densities and treated with CPA7 or the DMSO carrier alone for 24 hrs, at which time firefly and *Renilla* luciferase activities were determined.

Reference List

[1] A. Aleshin, R.S. Finn, SRC: a century of science brought to the clinic. Neoplasia. 12 (2010) 599-607.

[2] A. Anagnostopoulou, J. Cao, A. Vultur, K.L. Firth, L. Raptis, Examination of gap junctional, intercellular communication by *in situ* electroporation on two co-planar indium-tin oxide electrodes. Molecular Oncology 1 (2007) 226-231.

[3] A. Anagnostopoulou, J. Cao, A. Vultur, K.L. Firth, L. Raptis, Examination of gap junctional, intercellular communication by *in situ* electroporation on two co-planar indium-tin oxide electrodes. Molecular Oncology 1 (2007) 226-231.

[4] A. Anagnostopoulou, A. Vultur, R. Arulanandam, J. Cao, J. Turkson, R. Jove, J.S. Kim, M. Glenn, A.D. Hamilton, L. Raptis, Role of Stat3 in normal and SV40 transformed cells. Research Trends - Trends in Cancer Research 2 (2006) 93-103.

[5] B. Anger, R. Bockman, M. Andreeff, R. Erlandson, S. Jhanwar, T. Kameya, P. Saigo, W. Wright, E.J. Beattie, Jr., H.F. Oettgen, L.J. Old, Characterization of two newly established human cell lines from patients with large-cell anaplastic lung carcinoma. Cancer 50 (1982) 1518-1529.

[6] R. Arulanandam, M. Geletu, H. Feracci, L. Raptis, RacV12 requires gp130 for Stat3 activation, cell proliferation and migration. Experimental Cell Research 316 (2010) 875-886.

[7] R. Arulanandam, A. Vultur, J. Cao, E. Carefoot, P. Truesdell, B. Elliott, L. Larue, H. Feracci, L. Raptis, Cadherin-cadherin engagement promotes survival via Rac/Cdc42 and Stat3. Molecular Cancer Research 17 (2009) 1310-1327.

[8] M.M. Atkinson, J.D. Sheridan, Altered junctional permeability between cells transformed by v-ras, v-mos, or v-src. Am.J.Physiol. 255 (1988) C674-C683.

[9] R. Azarnia, W.R. Loewenstein, Polyomavirus middle t antigen downregulates junctional cell-to-cell communication. Mol.Cell.Biol. 7 (1987) 946-950.

[10] H.L. Brownell, R. Narsimhan, M.J. Corbley, V.M. Mann, J.F. Whitfield, L. Raptis, Ras is involved in gap junction closure in mouse fibroblasts or preadipocytes but not in differentiated adipocytes. DNA & Cell Biol. 15 (1996) 443-451.

[11] H.L. Brownell, J.F. Whitfield, L. Raptis, Cellular Ras partly mediates gap junction closure by the polyoma virus middle Tumor antigen. Cancer Lett. 103 (1996) 99-106.

[12] H.L. Brownell, J.F. Whitfield, L. Raptis, Elimination of intercellular junctional communication requires lower Ras^{leu61} levels than stimulation of anchorage-independent proliferation. Cancer Detect.Prev. 21 (1997) 289-294.

[13] L.A. Byers, B. Sen, B. Saigal, L. Diao, J. Wang, M. Nanjundan, T. Cascone, G.B. Mills, J.V. Heymach, F.M. Johnson, Reciprocal regulation of c-Src and STAT3 in non-small cell lung cancer. Clin.Cancer Res. 15 (2009) 6852-6861.

[14] E.M. Frenzel, R.G. Johnson, Gap junction formation between cultured embryonic lens cells is inhibited by antibody to N-cadherin. Dev.Biol. 179 (1996) 1-16.

[15] M. Geletu, C. Chaize, R. Arulanandam, A. Vultur, C. Kowolik, A. Anagnostopoulou, R. Jove, L. Raptis, Stat3 activity is required for gap junctional permeability in normal epithelial cells and fibroblasts. DNA & Cell Biol. 28 (2009) 319-327.

[16] M. Geletu, C. Chaize, R. Arulanandam, A. Vultur, C. Kowolik, A. Anagnostopoulou, R. Jove, L. Raptis, Stat3 activity is required for gap junctional permeability in normal epithelial cells and fibroblasts. DNA & Cell Biol. 28 (2009) 319-327.

[17] N. Grammatikakis, A. Vultur, C.V. Ramana, A. Siganou, C.W. Schweinfest, L. Raptis, The role of Hsp90N, a new member of the Hsp90 family, in signal transduction and neoplastic transformation. J.Biol.Chem. 277 (2002) 8312-8320.

[18] S. Greer, R. Honeywell, M. Geletu, R. Arulanandam, L. Raptis, housekeeping gene products; levels may change with confluence of cultured cells. Journal of Immunological Methods 355 (2010) 76-79.

[19] S. Ito, Y. Ito, T. Senga, S. Hattori, S. Matsuo, M. Hamaguchi, v-Src requires Ras signaling for the suppression of gap junctional intercellular communication. Oncogene 25 (2006) 2420-2424.

[20] R. Lin, K.D. Martyn, C.V. Guyette, A.F. Lau, B.J. Warn-Cramer, v-Src tyrosine phosphorylation of connexin43: regulation of gap junction communication and effects on cell transformation. Cell Commun.Adhes. 13 (2006) 199-216.

[21] S.L. Littlefield, M.C. Baird, A. Anagnostopoulou, L. Raptis, Synthesis, characterization and Stat3 inhibitory properties of the prototypical platinum(IV) anticancer drug, [PtCl3(NO2)(NH3)2] (CPA-7). Inorg.Chem. 47 (2008) 2798-2804.

[22] T. Masaki, K. Igarashi, M. Tokuda, S. Yukimasa, F. Han, Y.J. Jin, J.Q. Li, H. Yoneyama, N. Uchida, J. Fujita, H. Yoshiji, S. Watanabe, K. Kurokohchi, S. Kuriyama, pp60c-src activation in lung adenocarcinoma. Eur.J.Cancer 39 (2003) 1447-1455.

[23] M.L. McLemore, S. Grewal, F. Liu, A. Archambault, J. Poursine-Laurent, J. Haug, D.C. Link, STAT-3 activation is required for normal G-CSF-dependent proliferation and granulocytic differentiation. Immunity. 14 (2001) 193-204.

[24] U.K. Mukhopadhyay, R. Eves, L. Jia, P. Mooney, A.S. Mak, p53 suppresses Src-induced podosome and rosette formation and cellular invasiveness through the upregulation of caldesmon. Mol.Cell Biol. 29 (2009) 3088-3098.

[25] M. Pahujaa, M. Anikin, G.S. Goldberg, Phosphorylation of connexin43 induced by Src: regulation of gap junctional communication between transformed cells. Exp.Cell Res. 313 (2007) 4083-4090.

[26] L. Raptis, R. Arulanandam, A. Vultur, M. Geletu, S. Chevalier, H. Feracci, Beyond structure, to survival: Stat3 activation by cadherin engagement. Biochemistry and Cell Biology 87 (2009) 835-843.

[27] L. Raptis, H.L. Brownell, K.L. Firth, L.W. MacKenzie, A novel technique for the study of intercellular, junctional communication; electroporation of adherent cells on a partly conductive slide. DNA & Cell Biol. 13 (1994) 963-975.

[28] Y. Shen, P.R. Khusial, X. Li, H. Ichikawa, A.P. Moreno, G.S. Goldberg, SRC utilizes Cas to block gap junctional communication mediated by connexin43. J.Biol.Chem. 282 (2007) 18914-18921.

[29] L. Song, J. Turkson, J.G. Karras, R. Jove, E.B. Haura, Activation of Stat3 by receptor tyrosine kinases and cytokines regulates survival in human non-small cell carcinoma cells. Oncogene 22 (2003) 4150-4165.

[30] C. Theiss, A. Mazur, K. Meller, H.G. Mannherz, Changes in gap junction organization and decreased coupling during induced apoptosis in lens epithelial and NIH-3T3 cells. Exp.Cell Res. 313 (2007) 38-52.

[31] E. Tomai, H.L. Brownell, T. Tufescu, K. Reid, L. Raptis, Gap junctional communication in lung carcinoma cells. Lung Cancer 23 (1999) 223-231.

[32] J. Turkson, T. Bowman, R. Garcia, E. Caldenhoven, R.P. de Groot, R. Jove, Stat3 activation by Src induces specific gene regulation and is required for cell transformation. Mol.Cell.Biol. 18 (1998) 2545-2552.

[33] M. Vinken, T. Vanhaecke, P. Papeleu, S. Snykers, T. Henkens, V. Rogiers, Connexins and their channels in cell growth and cell death. Cell Signal. 18 (2006) 592-600.

[34] A. Vultur, R. Arulanandam, J. Turkson, G. Niu, R. Jove, L. Raptis, Stat3 is required for full neoplastic transformation by the Simian Virus 40 Large Tumor antigen. Molecular Biology of the Cell 16 (2005) 3832-3846.

[35] A. Vultur, J. Cao, R. Arulanandam, J. Turkson, R. Jove, P. Greer, A. Craig, B.E. Elliott, L. Raptis, Cell to cell adhesion modulates Stat3 activity in normal and breast carcinoma cells. Oncogene 23 (2004) 2600-2616.

[36] A. Vultur, E. Tomai, K. Peebles, A.M. Malkinson, N. Grammatikakis, P.G. Forkert, L. Raptis, Gap junctional, intercellular communication in cells from urethane-induced tumors in A/J mice. DNA & Cell Biol. 22 (2003) 33-40.

[37] C.J. Wei, R. Francis, X. Xu, C.W. Lo, Connexin43 associated with an N-cadherin-containing multiprotein complex is required for gap junction formation in NIH3T3 cells. J.Biol.Chem. 280 (2005) 19925-19936.

[38] H.Q. Xie, R. Huang, V.W. Hu, Intercellular communication through gap junctions is reduced in senescent cells. Biophys.J. 62 (1992) 45-47.

[39] H. Yu, D. Pardoll, R. Jove, STATs in cancer inflammation and immunity: a leading role for STAT3. Nat.Rev.Cancer 9 (2009) 798-809.

[40] J. Zhang, S. Kalyankrishna, M. Wislez, N. Thilaganathan, B. Saigal, W. Wei, L. Ma, I.I. Wistuba, F.M. Johnson, J.M. Kurie, SRC-family kinases are activated in non-small cell lung cancer and promote the survival of epidermal growth factor receptor-dependent cell lines. Am.J.Pathol. 170 (2007) 366-376.

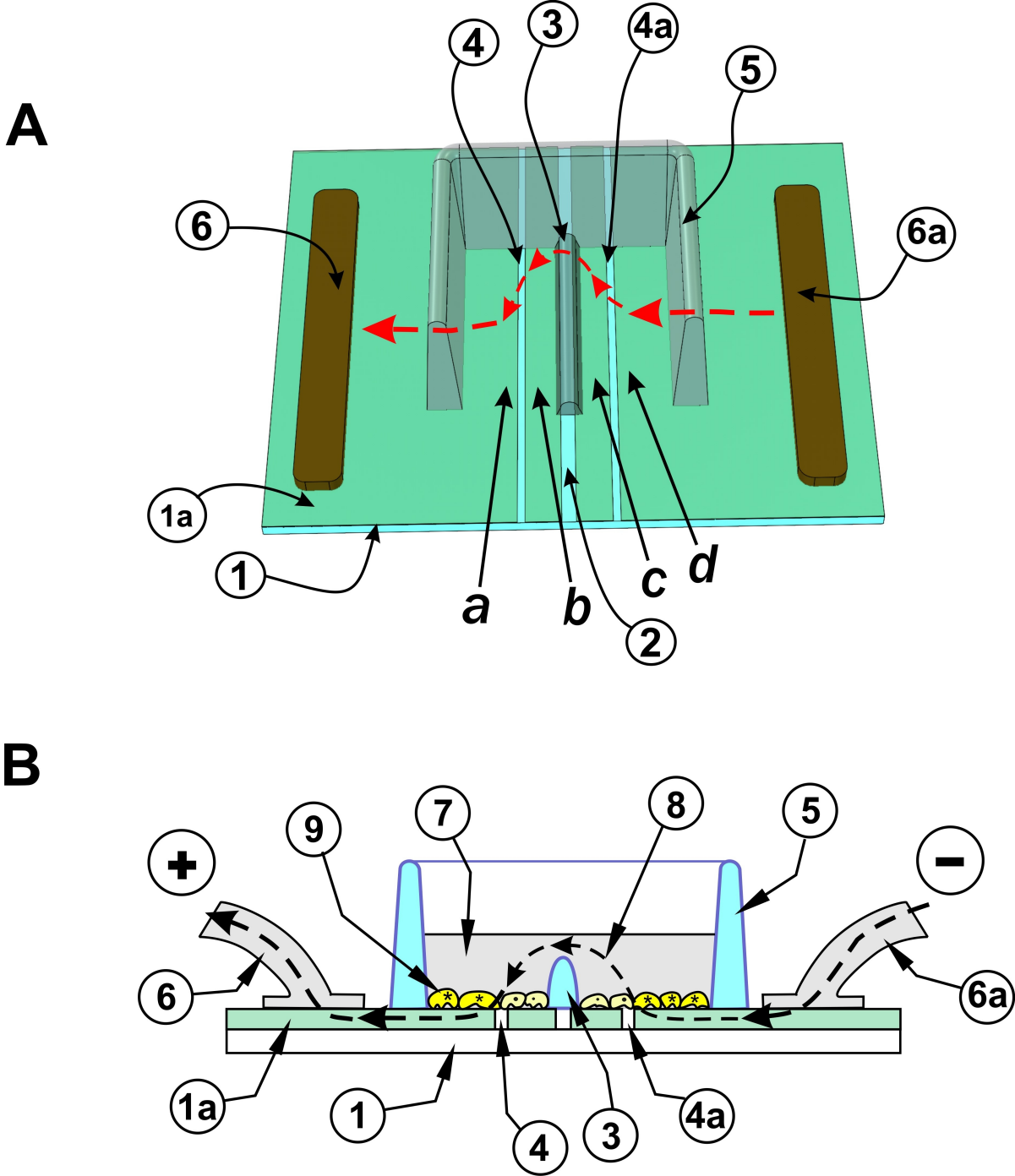
A
4
3
4a
5
6
6a
1a
1
a
b
c
d
2
B
9
7
8
5
+
−
6
6a
1a
1
4
3
4a

Figure 2

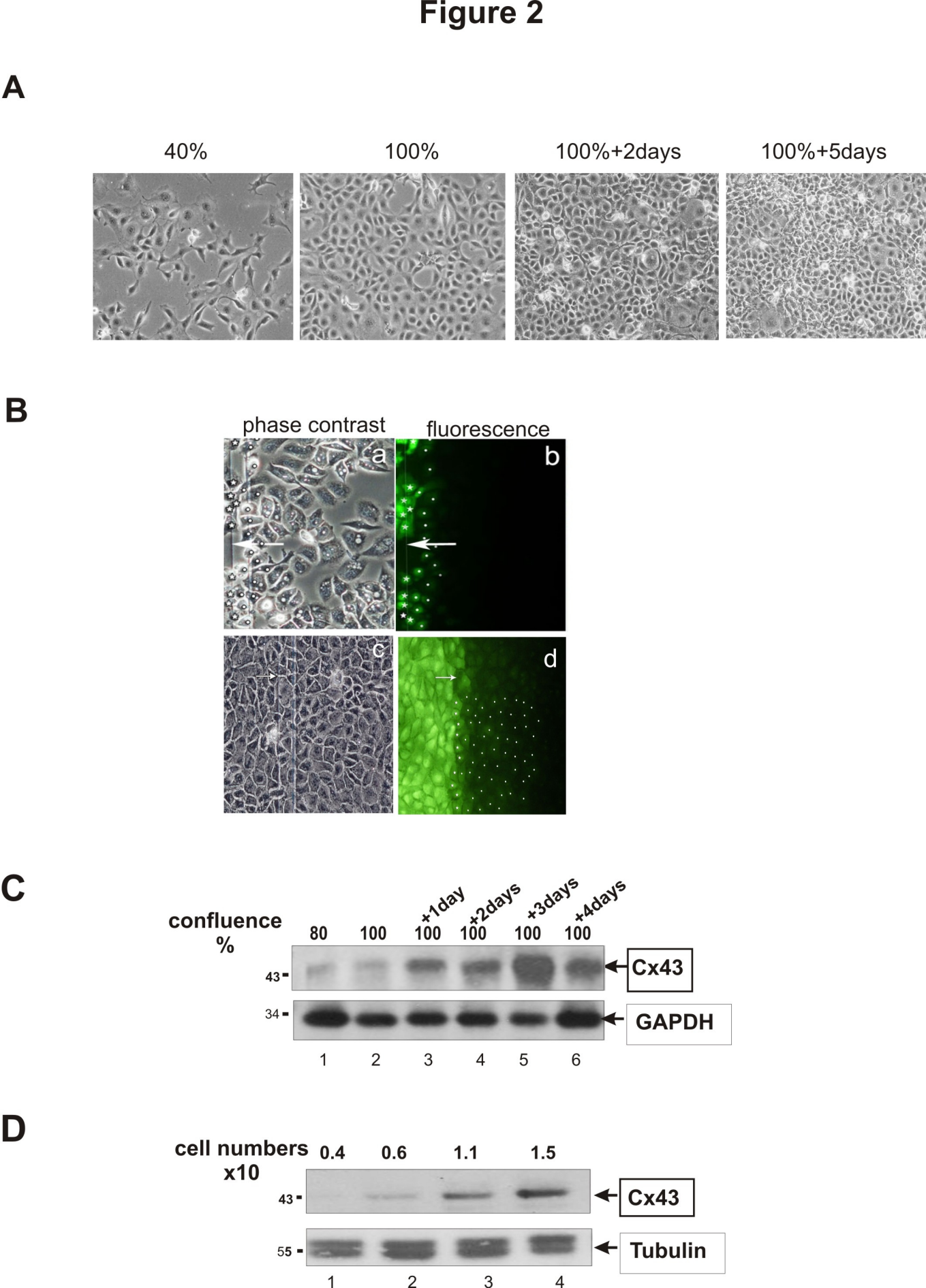
A
40%
100%
100%+2days
100%+5days
B
phase contrast
fluorescence
a
b
c
d
C
confluence %
80
100
+1day
100
+2days
100
+3days
100
+4days
100
43
Cx43
34
GAPDH
1
2
3
4
5
6
D
cell numbers x10
0.4
0.6
1.1
1.5
43
Cx43
55
Tubulin
1
2
3
4

Figure 3

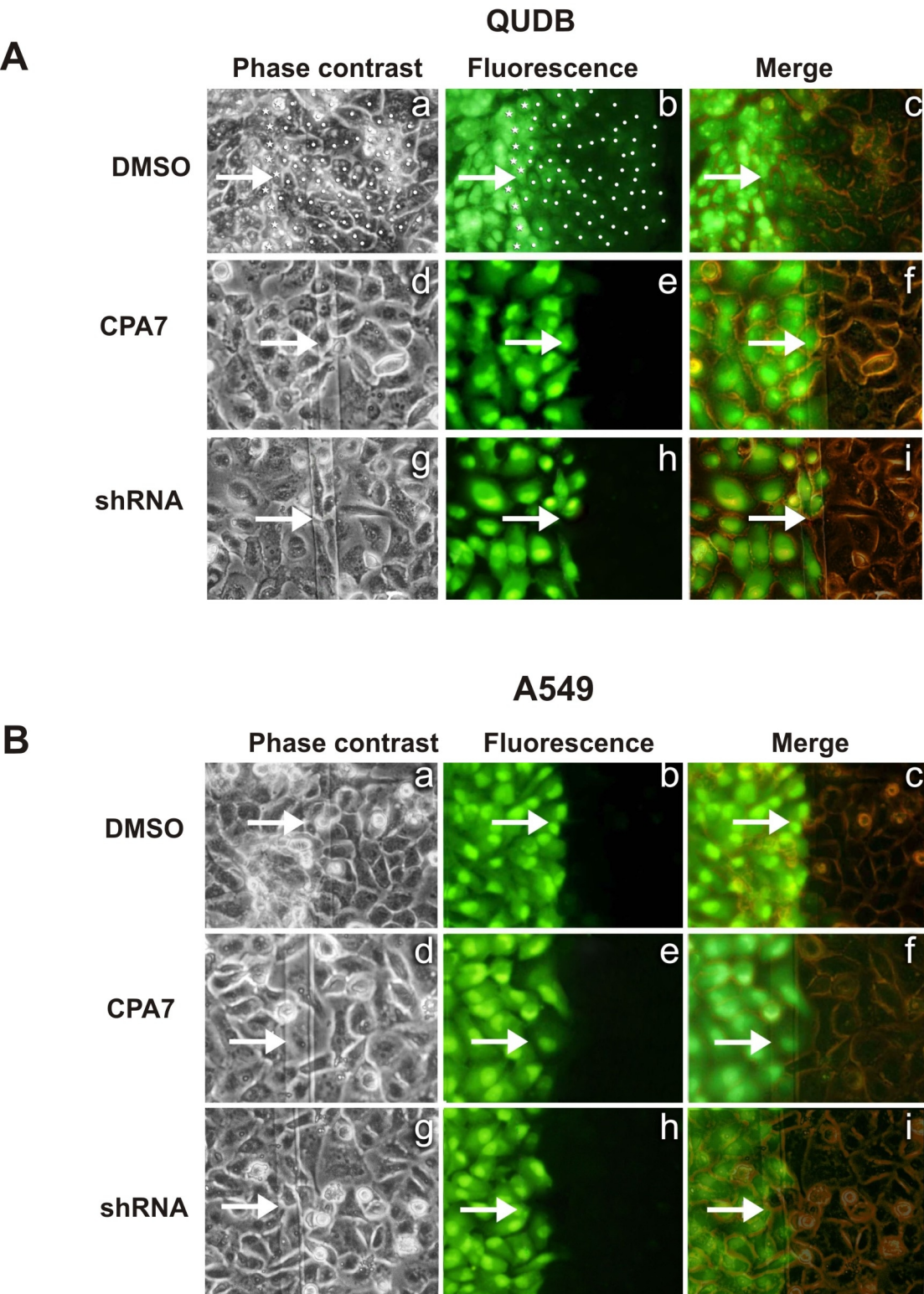
A
QUDB
Phase contrast
Fluorescence
Merge
DMSO
CPA7
shRNA
a
b
c
d
e
f
g
h
i
B
A549
Phase contrast
Fluorescence
Merge
DMSO
CPA7
shRNA
a
b
c
d
e
f
g
h
i

Figure 4

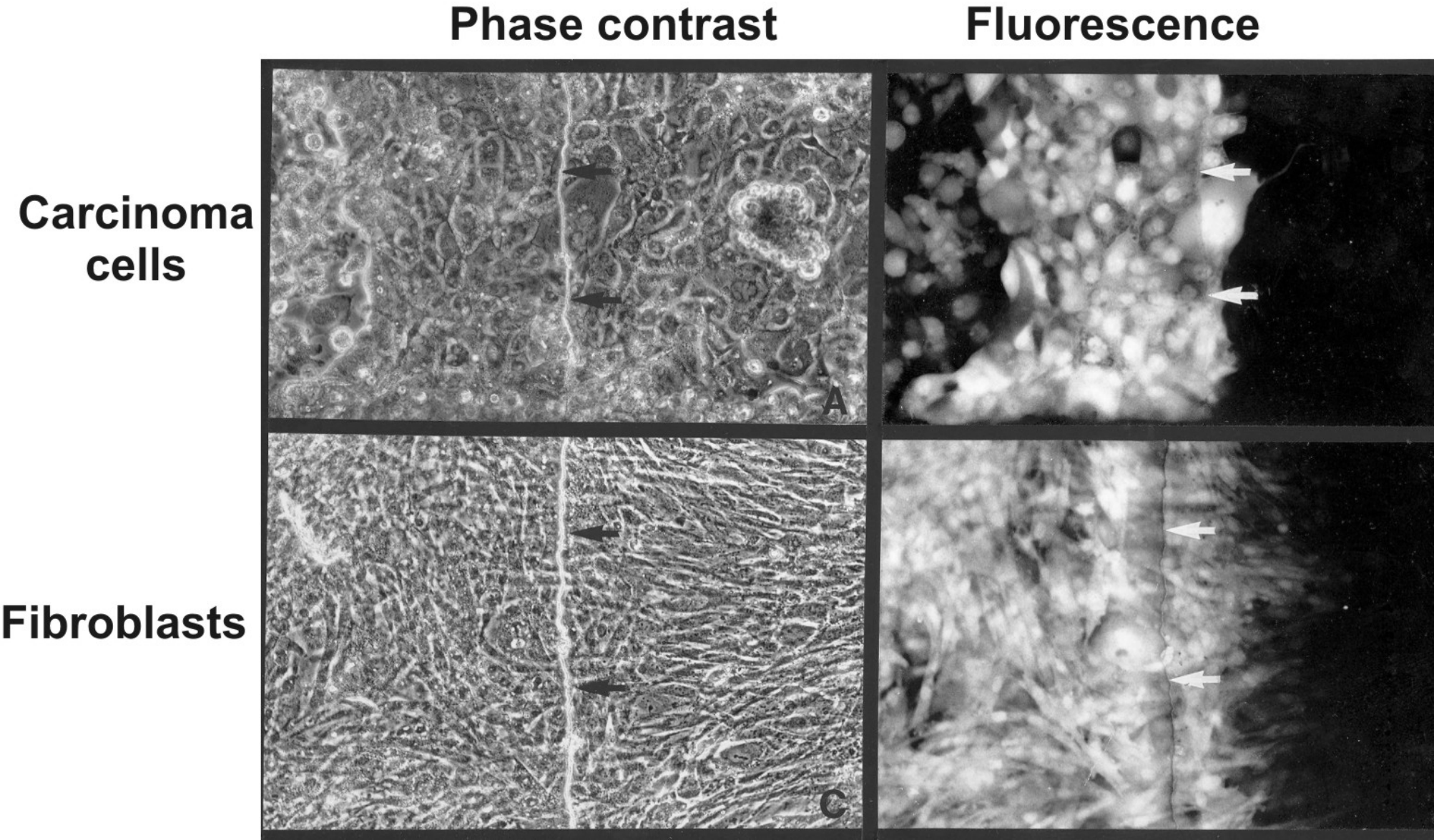
Phase contrast
Fluorescence
Carcinoma cells
Fibroblasts
A
C

Figure 5

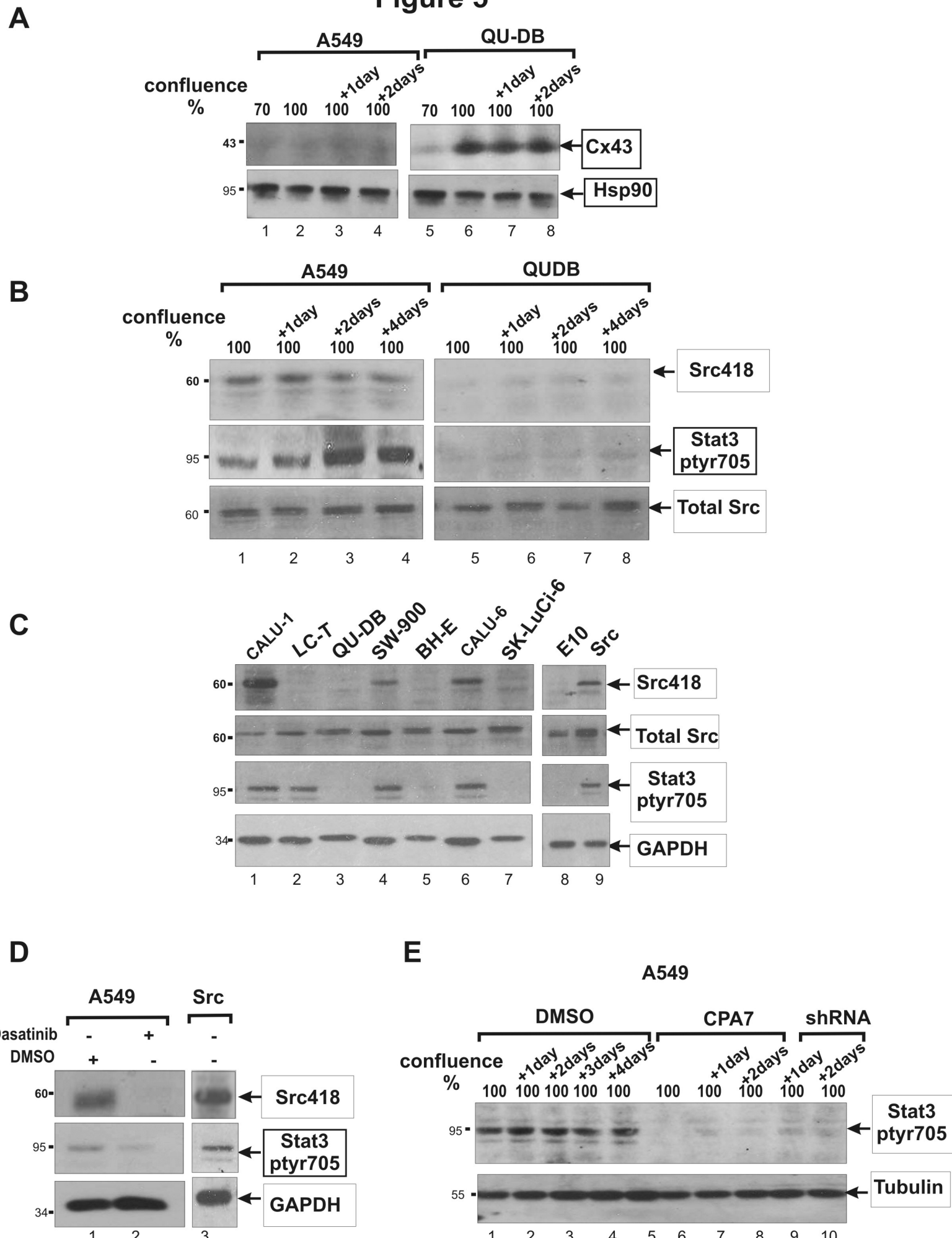
A
A549
QU-DB
confluence %
+1day
+2days
70 100 100 100 70 100 100 100
43
95
Cx43
Hsp90
1 2 3 4 5 6 7 8
B
A549
QUDB
confluence %
+1day
+2days
+4days
100 100 100 100 100 100 100 100
60
95
60
Src418
Stat3 ptyr705
Total Src
1 2 3 4 5 6 7 8
C
CALU-1
LC-T
QU-DB
SW-900
BH-E
CALU-6
SK-LuCi-6
E10
Src
60
60
95
34
Src418
Total Src
Stat3 ptyr705
GAPDH
1 2 3 4 5 6 7 8 9
D
A549
Src
Dasatinib - + -
DMSO + - -
60
95
34
Src418
Stat3 ptyr705
GAPDH
1 2 3
E
A549
DMSO
CPA7
shRNA
confluence %
+1day
+2days
+3days
+4days
100 100 100 100 100 100 100 100 100 100
95
55
Stat3 ptyr705
Tubulin
1 2 3 4 5 6 7 8 9 10

Viral oncogenes and the retinoblastoma family

Geletu, M. and Raptis, L[*].

[1] Departments of Microbiology and Immunology and Pathology, Queen's University, Kingston, Ontario, Canada K7L3N6.

[*]Corresponding author.
Phone number: (613) 533-2462 (office/lab)
(613) 533-2450 (secretary)
FAX number: (613) 533-6796.
e-mail: raptisl@queensu.ca

Running Title: DNA tumor viruses and the Rb family

Key words: Adenovirus E1A, SV40 TAg, polyoma viruses, Retinoblastoma, breast cancer

Introduction – History of viruses and cancer

The discovery of viruses is tightly linked to the most significant advances in Molecular Cell Biology, including cancer research. Cell division is a fundamental biological phenomenon, therefore it is not surprising that human cancer is an evolutionarily ancient disease, that attracted attention in early civilizations. The remains of a 4 million-old fossilized hominid show evidence of bone tumors (Diamandopoulos, 1996), while some of the oldest written accounts of cancer are recorded in the code of Hamourabi (1750 BCE), Egyptian papyri (1600 BCE) and others. Unfortunately, in ancient Egypt knowledge was the realm of priests, so the writings of the time attributed the etiology of disease to the "will of Gods". In ancient Greece, medicine was freed from the bonds of religion; Hippocrates (460-370 BCE) tried to use logical thinking to propose the humoral theory of cancer and his ideas influenced philosophers and scientists for the next ~1,800 years. During this time, knowledge of Mathematics and Physics was remarkably advanced; the acoustics of amphitheaters, built in the 5th century BC are as good as the best of today's structures. Still, these amazing minds believed in spontaneous generation of life, a theory that lasted till Louis Pasteur (1822-1895) who demonstrated that living things cannot be generated automatically (Javier and Butel, 2008).

In 1892 Ivanofsky and Beijerinck became the fathers of the new field of Virology by showing that an infectious pathogen of tobacco plants, the Tobacco Mosaic agent, retained infectivity after passage through filters of unglazed porcelaine, known to retain bacteria (Levine, 2001). These landmark discoveries were quickly followed by the discovery of the first cancer viruses, the chicken leukemia virus by Ellerman and Bang in 1908, and the Rous Sarcoma virus in 1911. Since that time, virus research and cancer research have been closely integrated, since

complicated biological problems that constitute the basic mechanisms of life are highly conserved, since they cannot change radically once solved by evolution. As viruses need to use the molecular machinery of the host to replicate, they have provided us with valuable tools to study the host, including mechanisms of cellular replication, ie cancer. Historically, two classes of viruses, the retroviruses and DNA tumor viruses have been involved in landmark discoveries in cancer, and have played a fundamental role as models in Molecular Biology, as well as experimental cancer research.

Early work by Sarah Stewart and Bernice Eddy demonstrated that the mouse polyoma virus produced in cell culture could cause tumors upon injection in newborn hamsters (Eddy et al., 1958). Soon thereafter, Vogt and Dulbecco developed tissue culture methods and it was shown that it could transform normal, cultured cells to acquire properties of cells derived from polyoma virus-induced tumors, such as growth to many layers, growth in the absence of anchorage to a solid support and tumorigenicity in syngeneic animals (Vogt and Dulbecco, 1960). At the same time, Simian Virus 40 (SV40) gained notoriety because it was found by Eddy to be a contaminant of poliomyelitis and Adenovirus vaccines, which had been administered to millions of healthy individuals worldwide. The public health implications of this revelation provided the initial impetus for an in depth study of SV40 biology. Later work showed that SV40 DNA sequences as well as infectious virus are in fact found in human tumors and may have contributed to oncogenesis. The fact that SV40 uses mostly cellular machinery to carry out important steps in viral infection, made it into a powerful probe to examine many fundamental questions in eukaryotic molecular biology.

In addition to their importance in Cell Biology, due to their potent transforming ability, DNA tumor viruses have been studied extensively. In fact, work on the mechanism of neoplasia

caused by these viruses has yielded a plethora of information on cell growth controls and led to the discovery of two families of antioncogenes, p53 and the retinoblastoma susceptibility (Rb) gene products.

Replication of DNA tumor viruses

The DNA tumor viruses belong in the papova (the name is derived from **pa**pilloma, **po**lyoma, Simian **va**cuolating viruses) or Adenovirus families. They all have non-enveloped particles and both groups are highly tumorigenic in experimental animals.

Polyoma viruses cause disease in a variety of species, with a very limited host range. The prototype of this group is the mouse polyoma virus, but three polyomaviruses have also been described in humans: JCV, the etiologic agent of progressive, multifocal leucoencephalopathy, a fatal demyelinating disease, BKV, causing nephropathy in immunocompromised individuals, (Hirsch, 2005) and SV40, the contaminant of polio vaccines, whose prevalence in humans is not clear (Garcea and Imperiale, 2003).

The response of cultured cells to DNA tumor virus infection depends upon the species being infected. In the case of SV40, monkey cells support the production of infectious virus, which leads to their death (lytic cycle), whereas rodent cells produce only the early proteins, ie the proteins expressed before viral DNA replication has commenced in a lytic infection, and acquire a neoplastically transformed phenotype. Similarly, polyoma virus grows lytically in mouse cells but transforms rat or hamster cells in culture.

Viruses of the polyoma family have circular dsDNA genomes of approximately 5,000bp, contained in icosahedral capsids. Their genome contains two coding regions, the early genes, expressed before viral DNA replication in a lytic infection, and the late genes which are

expressed after viral DNA replication is underway. Both transcription units are regulated by a common non-coding control region that contains the transcription start sites, binding sites for the transcription factors and the origin of DNA replication. The early region encodes the alternatively spliced transforming proteins large T (or Tumor)-antigen and small t-antigen, while the mouse polyoma virus also expresses a 56kDa middle tumor antigen, which is its main transforming protein. The late genes encode mostly structural coat proteins (VP1, VP2, VP3, Figure 1).

In the host species, polyomaviruses spread by lytic infection of permissive cells. Lytic infection requires the Large T-antigen, a ~100 kDa nuclear phosphoprotein which binds the origin and is essential for viral DNA replication [reviewed in (Cole, 1995a)]. Polyomaviruses rely on cellular enzymes for the replication of their DNA, since their genome does not code for replication proteins. These proteins are confined to the S phase of the cell cycle, and the large T-antigens modulate cellular signaling pathways by interacting with a plethora of cellular proteins that promote cell cycle progression into S phase. Due to this property, the Large T-antigens are also important players in the transformation of virus-infected cells. The most well-known interaction is the ability of the T-antigens to associate with, and interfere with the functions of the two tumor suppressor proteins, pRb and p53.

In non-permissive, cultured cells infection is abortive and neoplastic transformation of the cell may occur. Transformation requires expression of the early region, in particular the large T-antigen in the case of the human polyoma viruses (Fig. 1). The mouse polyoma middle-tumor antigen associates with and activates the cellular Src protein, but its Large T antigen is also important in viral DNA replication, as well as transformation in certain systems. The tumor

antigens are also key players in the highly efficient oncogenesis *in vivo* by these viruses, ie when virus is inocculated into animals or when the early region is introduced into transgenic mice.

Adenoviruses have linear dsDNA's of approximately 35,000bp enclosed in icosahedral particles with spikes on the vertices.The human Adenoviruses infect and can grow lytically in human cells but can cause tumors in rodents and transform a variety of rodent cells in culture. Their genome is linear, double-stranded DNA of ~35,000 bp with a number of transcription units. Early after infection at least four promotors are activated (E1, E2, E3, E4), while at late times there is activation of the major late promotor, coding mostly for a number of coat proteins (Fig. 2). The Adenovirus early region E1A and E1B genes are important in transformation of cultured cells and tumorigenicity, but E1A is also required in a lytic infection, for the transactivation of all other Adenoviral genes. E1A proteins bind the Rb family, while E1B associates with and inactivates p53. The Adenoviruses display extensive RNA splicing, therefore it is not surprising that splicing was discovered for the first time in Adenoviruses [(Broker, 1984), reviewed in (Shenk, 1995)].

The papillomaviruses comprise a group of nonenveloped DNA viruses that induce mostly benign lesions of the skin (warts) and mucous membranes (condylomas) in humans and animals. However, some members such as human papilloma viruses 16 and 18 have been implicated in the development of epithelial malignancies, especially cancer of the uterine cervix and other tumors of the urogenital tract. The Papillomaviruses are small, nonenveloped, icosahedral DNA viruses that replicate in the nucleus of squamous epithelial cells. The virion has a single molecule of double-stranded, circular DNA of approximately 8,000 base pairs. The E6 and E7 are the main oncogenes of the high-risk HPVs. E7 binds with and inactivates Rb, while E6 binds p53 and leads to its degradation (Howley and Lowy, 2007)

Interaction of the DNA tumor virus oncogenes with the retinoblastoma family

The demonstration that DNA tumor viruses can cause tumors in animals led to an intensive investigation into the mechanism of tumor induction. The type of tumor that developed in an animal following viral inocculation often depended upon the site of injection; early findings demonstrated that injection of Adenovirus-12 directly into the vitreous body of newborn rats, mice or baboons induced retinoblastoma-like tumors that expressed Adenovirus gene products (Kobayashi and Mukai, 1973; Mukai et al., 1977; Mukai et al., 1980; Kobayashi et al., 1982). However, no Adenovirus or JC polyoma virus was ever found in human retinoblastomas. Still, Adenovirus research and the development of monoclonal antibodies against the tumor antigens of these viruses greatly facilitated the identification of cellular proteins specifically binding the viral oncogenes. One of them was the *Rb* gene product, whose inactivation was independently demonstrated to lead to retinoblastoma formation in humans.

Seminal studies on Retinoblastoma by Knudson *et al* (Knudson, Jr., 1971) laid the foundation for the tumor suppressor hypothesis. Statistical analysis of age and family history made him conclude that two independent mutation events are required for retinoblastoma development. It was later proposed that the two mutations occurred in the two alleles of the same gene, *Rb1* that is, retinoblastoma is a recessive cancer where one abnormal chromosome was inherited, while the corresponding, wild-type chromosomal segment was lost in the tumor cells (Godbout et al., 1983; Benedict et al., 1983). Genetic linkage studies demonstrated anomalies on chromosome 13q14, close to the esterase D locus (Sparkes et al., 1983). Cloning of the retinoblastoma cDNA followed and it was shown that it encodes a 110 kDa nuclear phosphoprotein (Lee et al., 1987). Additional studies showed that the *Rb1* gene from

retinoblastoma tumors had deletions and mutations, consistent with a model where gene inactivation ie loss of function leads to tumor formation [reviewed in (Burkhart and Sage, 2008)].

Several groups tried to identify cellular proteins that bind to the E1A gene products. Branton *et al* developed a series of anti-peptide antisera and identified several co-immunoprecipitated proteins, including a doublet of approximately 105 kDa (Yee and Branton, 1985). Most importantly, these proteins could be affinity-purified from uninfected cells using E1A expressed in bacteria. This observation indicated that the 105 kDa protein(s) was of cellular, rather than viral, origin. Moreover, their expression did not depend upon Adenovirus infection, or expression of any viral proteins (Egan et al., 1988). It was further shown that residues 111-127 and 30-60 of E1A were required for binding to the 105 kDa protein (Egan et al., 1988). A breakthrough finding followed: A monoclonal antibody was raised using as an immunogen E1A that had been immunoprecipitated from E1A-expressing, 293 cells, therefore potentially containing cellular proteins bound to E1A. As it turned out, this antibody recognised the 105kDa, Rb protein. These data demonstrated that the Rb was, in fact, the 105 kDa, cellular protein associated with E1A. This observation offered the first demonstration of a physical association between an oncogene and an antioncogene (Whyte et al., 1988; Lee et al., 1987). Similar findings emerged on the SV40 system (DeCaprio et al., 1988). Most importantly, it was soon demonstrated that that TAg mutants that were unable to transform, were unable to bind Rb (e.g. E107K). These mutants disrupted the sequence LxCxE, the site of Rb binding which is present in the Large TAg's of both SV40 and polyoma, Adenovirus E1A, the human papillomavirus E7 proteins, as well as the TAg's of several other human polyoma viruses (Munger et al., 1989; Dyson et al., 1989). Taken together, these findings demonstrated the

cardinal importance of Rb binding in transformation by these oncogenes [reviewed in (DeCaprio, 2009)].

Examination of Rb's function demonstrated that Rb is unphosphorylated in quiescent (Go) cells, but its phosphorylation increases as cells progress in the cell cycle (Buchkovich et al., 1989). It was later found that it is the cyclin D/Cdk4, cyclin E/Cdk2, cyclin A/Cdk2 and cyclin B/cdc2 kinases, shown to be required for entry into the cell cycle, that phosphorylate, hence inactivate Rb (DeCaprio et al., 1992). It was also demonstrated that the SV40-TAg binds the under- or unphosphorylated form of Rb exclusively (Ludlow et al., 1990), which suggested that the Go form of Rb served a growth-suppressive function, which was overcome by TAg. In addition, overexpression of Rb inhibits cell cycle progression from G1 to S (Goodrich et al., 1991). Finally, transgenic expression of SV40-TAg under control of luteinizing hormone-β induces retinoblastomas and TAg co-precipitated Rb in lysates from tumor cells, supporting the hypothesis that retinoblastoma can develop by the inactivation of Rb function by TAg (Windle et al., 1990).

Thus, the loss of the Rb growth suppressive function can be achieved by: 1. mutation (retinoblastomas), 2. phosphorylation (cell cycle), or 3. binding to viral oncogenes. It was later shown that two Rb-related proteins that also exhibit features of cell-cycle regulators, p107 and p130, can also bind the LxCxE sequence of E1A and TAg (Ewen et al., 1992; Dumont and Branton, 1992).

Several laboratories have mapped the Rb sequences required for binding the LxCxE sequence. In fact, the two thirds, C-terminal region of Rb can bind E1A and TAg, and it is referred to as the large-pocket, while the central part of Rb (379-792) constitutes the small pocket (Kaelin, Jr. et al., 1990; Hu et al., 1990) (Fig. 3). The central part of Rb was the site of

mutations in retinoblastomas, and these forms also failed to bind E1A and TAg. This observation offers a strong correlation between loss of binding to the oncogene to loss of function (Kaelin, Jr. et al., 1990; Pietenpol et al., 1990). That is, the viral oncogenes were found to disrupt a normal function of Rb, that was necessary for tumor suppression.

Further studies on the mechanism of tumor suppression by Rb and transformation by these oncogenes led to the search for cellular proteins that could compete with TAg and E1A for Rb binding. One of these protein families is the E2F transcription factors. In fact, the hypophosphorylated form of Rb binds E2F and using Rb affinity columns it became clear that the viral oncogenes (E1A, TAg, E7) dissociate Rb from E2F (Chellappan et al., 1992; Chellappan et al., 1991). Rb binding correlated with repression of E2F transcriptional activity (Hiebert et al., 1992), and overexpression of E2F1 could promote entry into S phase in a manner similar to Adenovirus E1A (Johnson et al., 1993). Therefore, the prevailing model is that E1A could serve to dissociate Rb from E2F, while the conserved LxCxE motif plays an important role in the high affinity binding of the viral oncoproteins to Rb. In fact, a minimal peptide of 9 residues corresponding to the LxCxE motif of HPV16-E7 could compete with Rb binding to E2F and to DNA (Jones et al., 1992). There is also evidence that TAg and E1A recruit the CBP/p300 histone acetyltransferase to remodel chromatin and actively start transcription (reviewed in (DeCaprio, 2009), Fig. 4).

The crystal structure of Rb demonstrated that the A and B domains of the small pocket are bound to each other and are linked with a large area of highly conserved residues located in the fold between them. The LxCxE motif of HPV-E7 is bound to an exposed cleft within the B domain. The side chains of L,C and E make direct contact to Rb, which explains their high degree of conservation (Fig. 3B) (Xiao et al., 2003). Still, E1A and Large TAg employ a

different activity to displace E2F from Rb. The 100, N-terminal residues of LT form a J-domain, found in the family of DnaJ-Hsp40 molecular chaperones (Stubdal et al., 1997). The J domain recruits Hsc70 and activate its ATPase activity to promote chaperone activity. The J domain of Large TAg cooperates with the LxCxE motif to dissociate Rb family members from E2F4 (Kim et al., 2001).

It was also found that E2F acts in a complex with another protein, the differentiation-regulated transcription factor-polypeptide 1 (DP1), which forms a heterotrimeric complex with E2F1 and cooperates with E2F for promotor binding (Simonson and Herman, 1993). Since the original cloning, a large number of E2F and DP molecules have been identified that play a variety of roles [reviewed in (van den Heuvel and Dyson, 2008)].

Consequences of E2F activation

Besides DNA tumor virus oncogenes, a large number of tyrosine kinases such as vSrc activate the E2F transcription factor indirectly, through activation of the CDK kinases. As a result, E2F is found to be hyperactive in many cancers. Transcriptional activation of E2F targets is achieved either through active transactivation or derepression of genes having E2F-binding sites on their promoters. A detailed Microarray analysis for E2F-activated genes yielded many targets, among which is a number of membrane receptor tyrosine kinases, such as PDGFRα, IGF1R, VEGF, and others (Young et al., 2003). In fact, it has long been demonstrated that transformed cells secrete autocrine factors, able to induce anchorage-independent growth to normal cells (Raptis, 1991; Ciardiello et al., 1990). These growth factors activate the membrane signalling apparatus, including the Ras and phosphatidyl-inositol-3 kinase (PI3k) cascades, as well as the Signal-transducer and activator of transcription-3 (Stat3) pathway. Following ligand

binding, Stat3 binds to receptors of Growth factors or cytokines and is phosphorylated on tyrosine-705 by the receptor itself or by the associated Jak or Src kinases. Two Stat3 molecules subsequently dimerize through reciprocal phosphotyrosine-SH2 domain interactions, the dimer migrates to the nucleus and initiates transcription of a number of genes (Yu et al., 2009; Raptis et al., 2009). Both the PI3 kinase and Stat3 constitute potent survival signals.

As a result of E2F activation, the SV40-TAg and Adenovirus E1A have both been shown to activate and require Ras (Raptis et al., 1997) and Stat3 (Vultur et al., 2005) for neoplastic transformation, as well as the block of adipocytic differentiation (Cao et al., 2007b; Cao et al., 2007a). However, it is particularly remarkable that at the same time E2F is a potent ***apoptosis inducer***, hence the high demand of transformed cells for survival signals, normally offered by Stat3, activated by the Growth Factor receptors. Therefore, direct Stat3 inhibition induces apoptosis of E1A or Tag-transformed cells preferentially, due to their higher E2F activity levels which promotes programmed cell death through p53-dependent or independent mechanisms. These findings underscore the importance of Stat3 the survival of tumor cells, and could have significant therapeutic implications (Fig. 5).

The Rb pathway in breast cancer

Although inherited, germline mutations in the Rb gene were identified mostly in retinoblastomas, Rb somatic mutations, mimicking Rb inactivation by the DNA tumor viruses have also been noted in a number of cancers, including breast cancer, so that, despite the fact that no DNA tumor viruses have ever been found in breast cancer, E2F is frequently activated.

Unlike the majority of cancers, the prognosis and treatment of breast cancer is significantly informed by a number of biomarkers, and the Rb pathway plays a prominent role

[reviewed in (Musgrove and Sutherland, 2009)]. In particular, the status of the Estrogen receptor-α (ER) is an important determinant in treatment: ER-positive breast cancer has a more favorable prognosis and can be treated with selective ER antagonists (e.g. Tamoxifen) or aromatase inhibitors (e.g. Anastrozole), while ER-negative breast cancer is generally more aggressive, and with fewer treatment options. Still, a significant number of ER-positive cancers fail hormonal therapy and a great deal of effort has been expended in identifying pathways leading to Tamoxifen or aromatase inhibitor resistance.

In ER-positive breast cancer treatment, ER antagonists are effective at stopping cell division, indicating that such tumors are dependent upon estrogen for proliferation and survival (Musgrove and Sutherland, 2009). It was further shown that estrogen inhibition results in cell cycle arrest in the Go/ G1 phase of the cell cycle through attenuation of CDK/cyclin complexes at multiple levels (Foster et al., 2001). In particular, cyclin D1 is a direct transcriptional target of ER signalling (Eeckhoute et al., 2006). On the other hand, functional analyses have suggested that a multitude of cascades can contribute to acquired resistance to endocrine therapy, such as aberant ErbB2, Grb10 or Akt signalling (Miller et al., 2009), while p27kip1 and Rb inactivation can compromise the efficacy of ER inhibition (Cariou et al., 2000; Bosco et al., 2007). Specifically, a gene expression signature of Rb-dysfunction is associated with luminal B breast cancer, which exhibits a relatively poor response to endocrine therapy. Most importantly, recent reports demonstrated that a selective CDK4/6 inhibitor, PD-0332991 suppressed cell proliferation of a number of tamoxifen-resistant, cultured breast cancer cell lines. While ER antagonists in sensitive lines induce cell cycle arrest, CDK4/6 inhibition in tamoxifen-resistant lines induced a state having certain molecular characteristics of senescence in hormone therapy resistant cell populations. Therefore, PD-0332991 is an effective cell cycle inhibitor that could

be especially valuable in ER+ breast cancers that are resistant to endocrine therapy, and is now being tested in phase II clinical trials (Thangavel et al., 2011).

Conclusions:

Results on the mechanism of transformation by DNA tumor viruses have given valuable insights on the role of the Rb family in cell division. Evidence is now emerging that these conclusions are applicable to human cancers such as cancer of the breast, hence the Rb pathway may be an important target for chemotherapy. It is reasonable to assume that the study of the viral oncogenes will offer additional insights into the role of Rb in cancer.

Figure 1

Genomic organisation of the 5297 bp mouse polyoma virus. The early region is at the right and the late region at the left. The transcriptional enhancer and origin of DNA replication are also shown. Soon after infection, the differentially spliced, early genes (T antigens) are expressed (right side), followed by replication of viral DNA. After DNA replication, the late genes are expressed (left), coding mostly for the structural proteins, VP1, VP2, VP3. Squiggly lines indicate the introns (Cole, 1995b).

Figure 2

Transcription and translation map of Adenovirus type 2. The early mRNAs are designated E, late mRNAs are designated L. The main genes involved in transformation are the E1A and E1B at the left of the genome, giving rise to several proteins with differential splicing (not shown). [From (Broker, 1984)].

r-strand: rightwards transcribed, l-strand, leftwards transcribed.

Figure 3

A. The human pRb consists of 928 aminoacids. Deletion mutagenesis, as well as structural studies have uncovered regions that mediate its binding to individual partners. Most of them bind the pocket region. The Rb C-terminus binds specifically to E2F1 and this inhibits apoptosis. E1A binding to pRb inhibits proliferation but not apoptosis. Rb can also be phosphorylated by CDK kinases as well as CHk2 (checkpoint homologue 2) and Raf 1 and this inhibits binding of most partners (Burkhart and Sage, 2008).
B. Three-dimensional structure of the Rb/E2F complex. The helices of the A domain are shown in red and the B domain in blue. The main-chain trace of E2F is shown as a yellow worm (upper panel), while the main-chain trace of the papillomavirus E7 is shown as a green worm (lower panel) (Xiao et al., 2003).

Figure 4

Effect of TAg or Adenovirus E1A upon Rb.

A.- Active Rb binds the E2F/DP complex to repress transcription. **B**. Rb phosphorylation reduces binding to E2F/DP, permitting E2F activation. **C**. TAg or E1A binding removes Rb and permits E2F action. **D-E**: TAg or E1A can also bind the CBP/p300 histone acetyltransferase to increase gene expression. **F**. E1A can also bring Rb to CBP/p300 bound to transcription factors to repress promotors.

Figure 5

Activation of E2F through Rb inactivation by viral oncogenes such as SV40-TAg or Adenovirus E1A activates a number of kinases such as IGF1-R and Src, which would activate Stat3, a potent apoptosis inhibitor. Apoptosis inhibition leads to cell division and neoplastic transformation. Paradoxically however, E2F also induces apoptosis through both p53-dependent and independent pathways. Most importantly, Stat3 inhibition in cells with high E2F levels results in apoptosis as a result (Sears and Nevins, 2002),

.

Reference List

Benedict,W.F., Murphree,A.L., Banerjee,A., Spina,C.A., Sparkes,M.C., and Sparkes,R.S. (1983). Patient with 13 chromosome deletion: evidence that the retinoblastoma gene is a recessive cancer gene. Science *219*, 973-975.

Bosco,E.E., Wang,Y., Xu,H., Zilfou,J.T., Knudsen,K.E., Aronow,B.J., Lowe,S.W., and Knudsen,E.S. (2007). The retinoblastoma tumor suppressor modifies the therapeutic response of breast cancer. J. Clin. Invest *117*, 218-228.

Broker,T.R. (1984). Processing of RNA. In Animal virus RNA processing, D.Apirion, ed. CRC Press), pp. 181-212.

Buchkovich,K., Duffy,L.A., and Harlow,E. (1989). The retinoblastoma protein is phosphorylated during specific phases of the cell cycle. Cell *58*, 1097-1105.

Burkhart,D.L. and Sage,J. (2008). Cellular mechanisms of tumour suppression by the retinoblastoma gene. Nat. Rev. Cancer *8*, 671-682.

Cao,J., Arulanandam,R., Vultur,A., Anagnostopoulou,A., and Raptis,L. (2007a). Adenovirus E1A requires c-Ras for full neoplastic transformation or suppression of differentiation of murine preadipocytes. Molecular Carcinogenesis *46*, 284-302.

Cao,J., Arulanandam,R., Vultur,A., Anagnostopoulou,A., and Raptis,L. (2007b). Differential effects of c-Ras upon transformation, adipocytic differentiation and apoptosis mediated by the Simian Virus 40 Large Tumor Antigen. Biochemistry and Cell Biology *85*, 32-48.

Cariou,S., Donovan,J.C., Flanagan,W.M., Milic,A., Bhattacharya,N., and Slingerland,J.M. (2000). Down-regulation of p21WAF1/CIP1 or p27Kip1 abrogates antiestrogen-mediated cell cycle arrest in human breast cancer cells. Proc. Natl. Acad. Sci. U. S. A *97*, 9042-9046.

Chellappan,S., Kraus,V.B., Kroger,B., Munger,K., Howley,P.M., Phelps,W.C., and Nevins,J.R. (1992). Adenovirus E1A, simian virus 40 tumor antigen, and human papillomavirus E7 protein share the capacity to disrupt the interaction between transcription factor E2F and the retinoblastoma gene product. Proc. Nat. Acad. Sci. USA *89*, 4549-4553.

Chellappan,S.P., Hiebert,S., Mudryj,M., Horowitz,J.M., and Nevins,J.R. (1991). The E2F transcription factor is a cellular target for the RB protein. Cell *65*, 1053-1061.

Ciardiello,F., Valverius,E.M., Colucci-D'Amato,G.L., Kim,N., Bassin,R.H., and Salomon,D.S. (1990). Differential growth factor expression in transformed mouse NIH-3T3 cells. J. Cell Biochem. *42*, 45-57.

Cole,C.N. (1995b). Polyomavirinae: The viruses and their replication. In: Virology, B.N.Fields, D.M.Knipe, and Hawley P.M., eds., pp. 917-946.

DeCaprio,J.A. (2009). How the Rb tumor suppressor structure and function was revealed by the study of Adenovirus and SV40. Virology *384*, 274-284.

DeCaprio,J.A., Furukawa,Y., Ajchenbaum,F., Griffin,J.D., and Livingston,D.M. (1992). The retinoblastoma-susceptibility gene product becomes phosphorylated in multiple stages during cell cycle entry and progression. Proc. Natl. Acad. Sci. U. S. A *89*, 1795-1798.

DeCaprio,J.A., Ludlow,J.W., Figge,J., Shew,J.Y., Huang,C.M., Lee,W.H., Marsilio,E., Paucha,E., and Livingston,D.M. (1988). SV40 large tumor antigen forms a specific complex with the product of the retinoblastoma susceptibility gene. Cell *54*, 275-283.

Diamandopoulos,G.T. (1996). Cancer: an historical perspective. Anticancer Res. *16*, 1595-1602.

Dumont,D.J. and Branton,P.E. (1992). Phosphorylation of adenovirus E1A proteins by the p34cdc2 protein kinase. Virology *189*, 111-120.

Dyson,N., Duffy,L.A., and Harlow,E. (1989). In vitro assays to detect the interaction of DNA tumor virus transforming proteins with the retinoblastoma protein. Cancer cells *7*, 235-240.

Eddy,B.E., Stewart,S.E., Young,R., and Mider,G.B. (1958). Neoplasms in hamsters induced by mouse tumor agent passed in tissue culture. J. Natl. Cancer Inst. *20*, 747-761.

Eeckhoute,J., Carroll,J.S., Geistlinger,T.R., Torres-Arzayus,M.I., and Brown,M. (2006). A cell-type-specific transcriptional network required for estrogen regulation of cyclin D1 and cell cycle progression in breast cancer. Genes Dev. *20*, 2513-2526.

Egan,C., Jelsma,T.N., Howe,J.A., Bayley,S.T., Ferguson,B., and Branton,P.E. (1988). Mapping of cellular protein binding sites on the products of early region E1A of human Adenovirus type 5. Mol. Cell. Biol. *8*, 3955-3959.

Ewen,M.E., Faha,B., Harlow,E., and Livingston,D.M. (1992). Interaction of p107 with cyclin A independent of complex formation with viral oncoproteins. Science *255*, 85-87.

Foster,J.S., Henley,D.C., Bukovsky,A., Seth,P., and Wimalasena,J. (2001). Multifaceted regulation of cell cycle progression by estrogen: regulation of Cdk inhibitors and Cdc25A independent of cyclin D1-Cdk4 function. Mol. Cell Biol. *21*, 794-810.

Garcea,R.L. and Imperiale,M.J. (2003). Simian virus 40 infection of humans. J. Virol. *77*, 5039-5045.

Godbout,R., Dryja,T.P., Squire,J., Gallie,B.l., and Phillips,R.A. (1983). Somatic inactivation of genes on chromosome 13 is a common event in retinoblastoma. Nature *304*, 451-453.

Goodrich,D.W., Wang,N.P., Qian,Y.W., Lee,E.Y., and Lee,W.H. (1991). The retinoblastoma gene product regulates progression through the G1 phase of the cell cycle. Cell *67*, 293-302.

Hiebert,S.W., Chellappan,S.P., Horowitz,J.M., and Nevins,J.R. (1992). The interaction of RB with E2F coincides with an inhibition of the transcriptional activity of E2F. Genes Dev. *6*, 177-185.

Hirsch,H.H. (2005). BK virus: opportunity makes a pathogen. Clin. Infect. Dis. *41*, 354-360.

Howley,P.M. and Lowy,D.R. (2007). Papillomaviruses. In Virology, D.M.Knipe and P.M.Howley, eds.

Hu,Q.J., Dyson,N., and Harlow,E. (1990). The regions of the retinoblastoma protein needed for binding to adenovirus E1A or SV40 large T antigen are common sites for mutations. EMBO J. *9*, 1147-1155.

Javier,R.T. and Butel,J.S. (2008). The history of tumor virology. Cancer Res. *68*, 7693-7706.

Johnson,D.G., Schwarz,J.K., Cress,W.D., and Nevins,J.R. (1993). Expression of transcription factor E2F1 induces quiescent cells to enter S phase. Nature *365*, 349-352.

Jones,R.E., Heimbrook,D.C., Huber,H.E., Wegrzyn,R.J., Rotberg,N.S., Stauffer,K.J., Lumma,P.K., Garsky,V.M., and Oliff,A. (1992). Specific N-methylations of HPV-16 E7 peptides alter binding to the retinoblastoma suppressor protein. J. Biol. Chem. *267*, 908-912.

Kaelin,W.G., Jr., Ewen,M.E., and Livingston,D.M. (1990). Definition of the minimal simian virus 40 large T antigen- and adenovirus E1A-binding domain in the retinoblastoma gene product. Mol. Cell. Biol. *10*, 3761-3769.

Kim,H.Y., Ahn,B.Y., and Cho,Y. (2001). Structural basis for the inactivation of retinoblastoma tumor suppressor by SV40 large T antigen. EMBO J. *20*, 295-304.

Knudson,A.G., Jr. (1971). Mutation and cancer: statistical study of retinoblastoma. Proc. Natl. Acad. Sci. U. S. A *68*, 820-823.

Kobayashi,M., Mukai,N., Solish,S.P., and Pomeroy,M.E. (1982). A highly predictable animal model of retinoblastoma. Acta Neuropathol. *57*, 203-208.

Kobayashi,S. and Mukai,N. (1973). Retinoblastoma-like tumors induced in rats by human adenovirus. Invest Ophthalmol. *12*, 853-856.

Lee,W.H., Shew,J.Y., Hong,F.D., Sery,T.W., Donoso,L.A., Young,L.J., Bookstein,R., and Lee,E.Y. (1987). The retinoblastoma susceptibility gene encodes a nuclear phosphoprotein associated with DNA binding activity. Nature *329*, 642-645.

Levine, A. J. The origins of Virology. Fields Virology 1, 3-18. 2001.

Ludlow,J.W., Shon,J., Pipas,J.M., Livingston,D.M., and DeCaprio,J.A. (1990). The retinoblastoma susceptibility gene product undergoes cell cycle-dependent dephosphorylation and binding to and release from SV40 large T. Cell *60*, 387-396.

Miller,T.W., Perez-Torres,M., Narasanna,A., Guix,M., Stal,O., Perez-Tenorio,G., Gonzalez-Angulo,A.M., Hennessy,B.T., Mills,G.B., Kennedy,J.P., Lindsley,C.W., and Arteaga,C.L. (2009). Loss of Phosphatase and Tensin homologue deleted on chromosome 10 engages ErbB3 and insulin-like growth factor-I receptor signaling to promote antiestrogen resistance in breast cancer. Cancer Res. *69*, 4192-4201.

Mukai,N., Kalter,S.S., Cummins,L.B., Matthews,V.A., Nishida,T., and Nakajima,T. (1980). Retinal tumor induced in the baboon by human adenovirus 12. Science *210*, 1023-1025.

Mukai,N., Nakajima,T., Freddo,T., Jacobson,M., and Dunn,M. (1977). Retinoblastoma-like neoplasm induced in C3H/BifB/Ki strain mice by human adenovirus serotype 12. Acta Neuropathol. *39*, 147-155.

Munger,K., Werness,B.A., Dyson,N., Phelps,W.C., Harlow,E., and Howley,P.M. (1989). Complex formation of human papillomavirus E7 proteins with the retinoblastoma tumor suppressor gene product. EMBO J. *8*, 4099-4105.

Musgrove,E.A. and Sutherland,R.L. (2009). Biological determinants of endocrine resistance in breast cancer. Nat. Rev. Cancer *9*, 631-643.

Pietenpol,J.A., Stein,R.W., Moran,E., Yaciuk,P., Schlegel,R., Lyons,R.M., Pittelkow,M.R., Munger,K., Howley,P.M., and Moses,H.L. (1990). TGF-Beta1 Inhibition of c-myc Transcription and Growth in Keratinocytes is Abrogated by Viral Transforming Proteins with pRB Binding Domains. Cell *61*, 777-785.

Raptis,L. (1991). Polyomavirus middle tumor antigen increases responsiveness to growth factors. J. Virol. *65*, 2691-2694.

Raptis,L., Arulanandam,R., Vultur,A., Geletu,M., Chevalier,S., and Feracci,H. (2009). Beyond structure, to survival: Stat3 activation by cadherin engagement. Biochemistry and Cell Biology *87*, 835-843.

Raptis,L., Brownell,H.L., Wood,K., Corbley,M., Wang,D., and Haliotis,T. (1997). Cellular ras gene activity is required for full neoplastic transformation by Simian Virus 40. Cell Growth Differ. *8*, 891-901.

Sears,R.C. and Nevins,J.R. (2002). Signaling networks that link cell proliferation and cell fate. J. Biol. Chem. *277*, 11617-11620.

Shenk,T. (1995). Adenoviridae: The Viruses and Their Replication. In Fundamental Virology, 3rd Edition, B.N.Fields, D.M.Knipe, and P.M.Howley, eds. (Philadelphia: Lippincott-Raven).

Simonson,M.S. and Herman,W.H. (1993). Protein kinase C and protein tyrosine kinase activity contribute to mitogenic signaling by endothelin-1. Cross-talk between G protein-coupled receptors and pp60c-src. J. Biol. Chem. *268*, 9347-9357.

Sparkes,R.S., Murphree,A.L., Lingua,R.W., Sparkes,M.C., Field,L.L., Funderburk,S.J., and Benedict,W.F. (1983). Gene for hereditary retinoblastoma assigned to human chromosome 13 by linkage to esterase D. Science *219*, 971-973.

Stubdal,H., Zalvide,J., Campbell,K.S., Schweitzer,R.C., Roberts,T.M., and DeCaprio,J.A. (1997). Inactivation of RB related proteins P130 and P107 mediated by the J domain of Simian Virus 40 Large Tumor antigen. Mol. Cell. Biol. *17*, 4979-4990.

Thangavel,C., Dean,J.L., Ertel,A., Knudsen,K.E., Aldaz,C.M., Witkiewicz,A.K., Clarke,R., and Knudsen,E.S. (2011). Therapeutically activating RB: reestablishing cell cycle control in endocrine therapy-resistant breast cancer. Endocr. Relat Cancer *18*, 333-345.

van den Heuvel,S. and Dyson,N.J. (2008). Conserved functions of the pRB and E2F families. Nat. Rev. Mol. Cell Biol. *9*, 713-724.

Vogt,M. and Dulbecco,R. (1960). Virus-cell interaction with a tumor-producing virus. Proc. Natl. Acad. Sci. U. S. A *46*, 365-370.

Vultur,A., Arulanandam,R., Turkson,J., Niu,G., Jove,R., and Raptis,L. (2005). Stat3 is required for full neoplastic transformation by the Simian Virus 40 Large Tumor antigen. Molecular Biology of the Cell *16*, 3832-3846.

Whyte,P., Buchkovich,K.J., Horowitz,J.M., Friend,S.H., Raybuck,M., Weinberg,R.A., and Harlow,E. (1988). Association between an oncogene and an anti-oncogene: the adenovirus E1A proteins bind to the retinoblastoma gene product. Nature *334*, 124-129.

Windle,J.J., Albert,D.M., O'Brien,J.M., Marcus,D.M., Disteche,C.M., Bernards,R., and Mellon,P.L. (1990). Retinoblastoma in transgenic mice. Nature *343*, 665-669.

Xiao,B., Spencer,J., Clements,A., Ali-Khan,N., Mittnacht,S., Broceno,C., Burghammer,M., Perrakis,A., Marmorstein,R., and Gamblin,S.J. (2003). Crystal structure of the retinoblastoma tumor suppressor protein bound to E2F and the molecular basis of its regulation. Proc. Natl. Acad. Sci. U. S. A *100*, 2363-2368.

Yee,S.P. and Branton,P.E. (1985). Detection of cellular proteins associated with human adenovirus type 5 early region 1A polypeptides. Virology *147*, 142-153.

Young,A.P., Nagarajan,R., and Longmore,G.D. (2003). Mechanisms of transcriptional regulation by Rb-E2F segregate by biological pathway. Oncogene *22*, 7209-7217.

Yu,H., Pardoll,D., and Jove,R. (2009). STATs in cancer inflammation and immunity: a leading role for STAT3. Nat. Rev. Cancer *9*, 798-809.

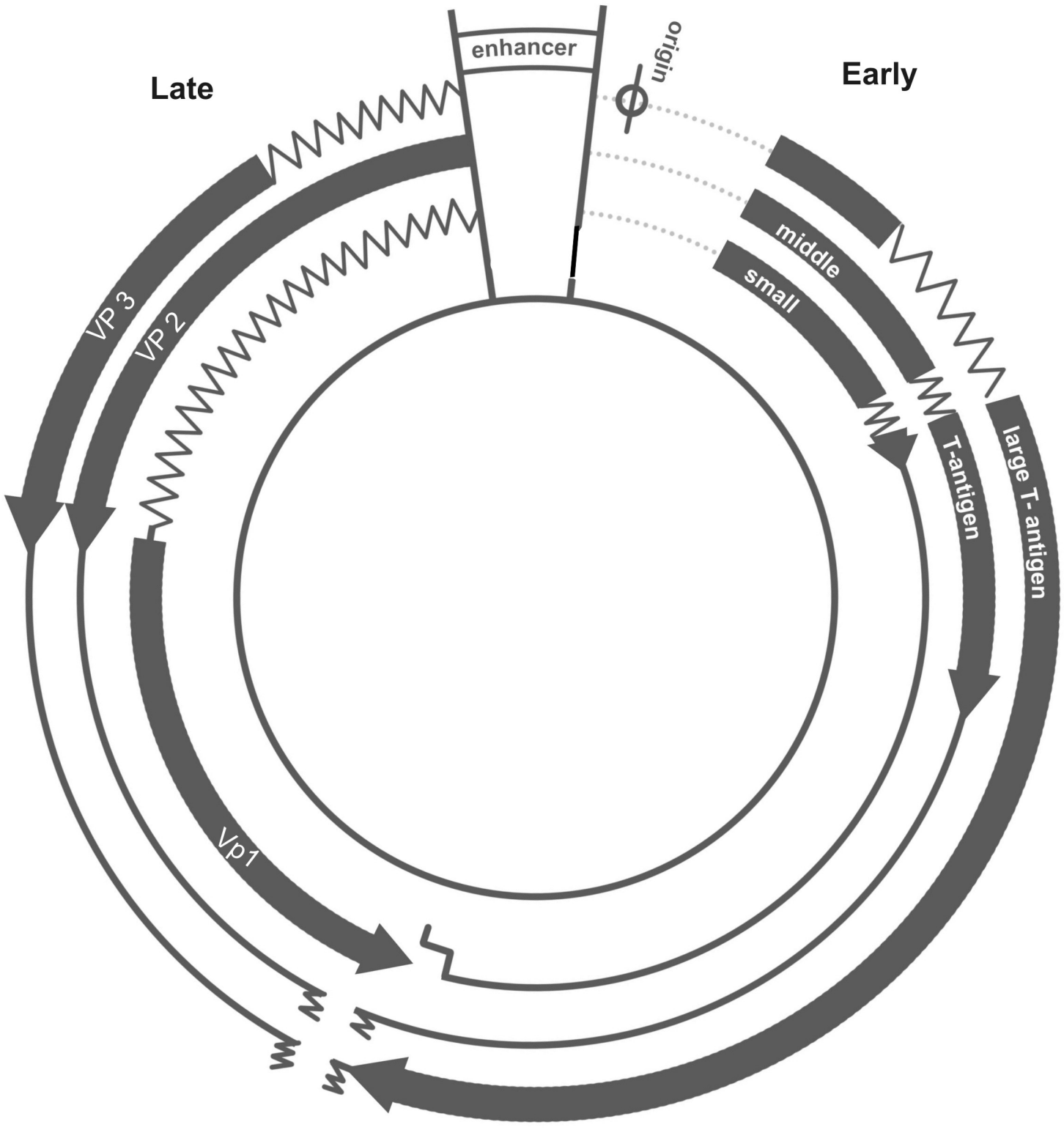
enhancer
origin
Late
Early
VP 3
VP 2
middle
small
T-antigen
large T- antigen
Vp1

Figure 1

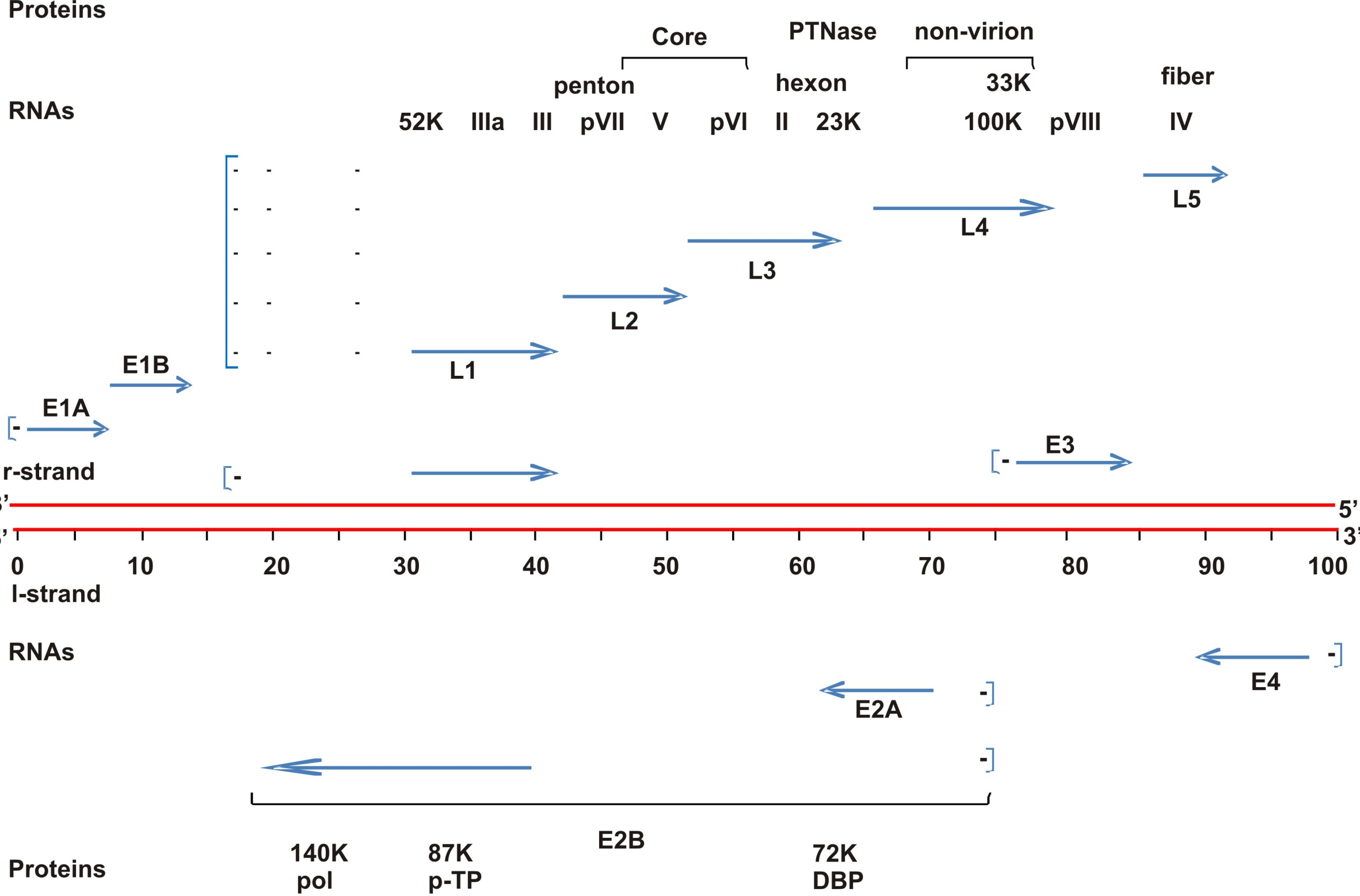
Proteins
Core
PTNase
non-virion
penton
hexon
33K
fiber
RNAs
52K
IIIa
III
pVII
V
pVI
II
23K
100K
pVIII
IV
L5
L4
L3
L2
L1
E1B
E1A
E3
r-strand
3'
5'
5'
3'
0
10
20
30
40
50
60
70
80
90
100
l-strand
RNAs
E4
E2A
E2B
Proteins
140K
pol
87K
p-TP
72K
DBP

Figure 2

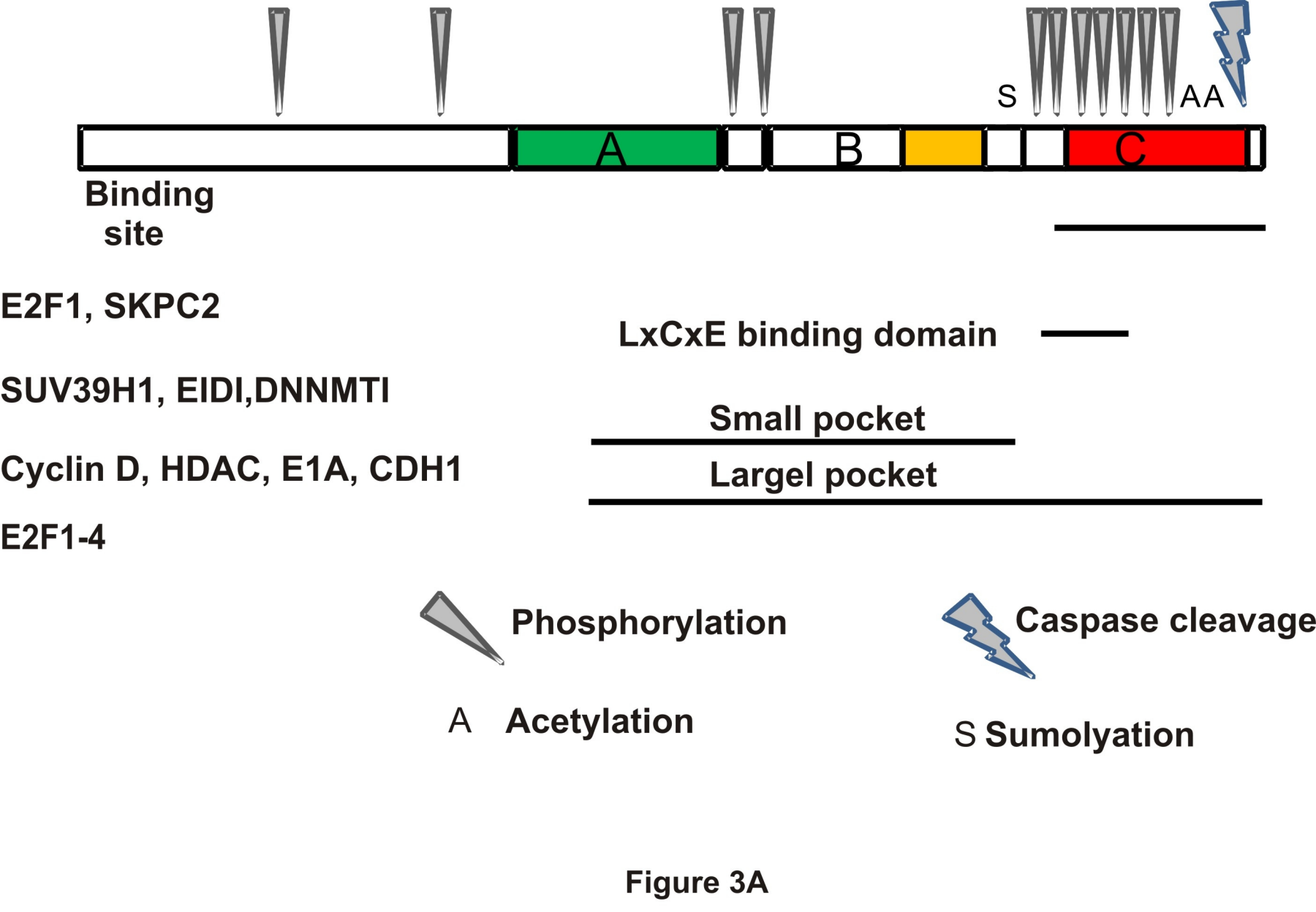
S
AA
A
B
C
Binding site
E2F1, SKPC2
LxCxE binding domain
SUV39H1, EIDI,DNNMTI
Small pocket
Cyclin D, HDAC, E1A, CDH1
Largel pocket
E2F1-4
Phosphorylation
Caspase cleavage
A Acetylation
S Sumolyation

Figure 3A

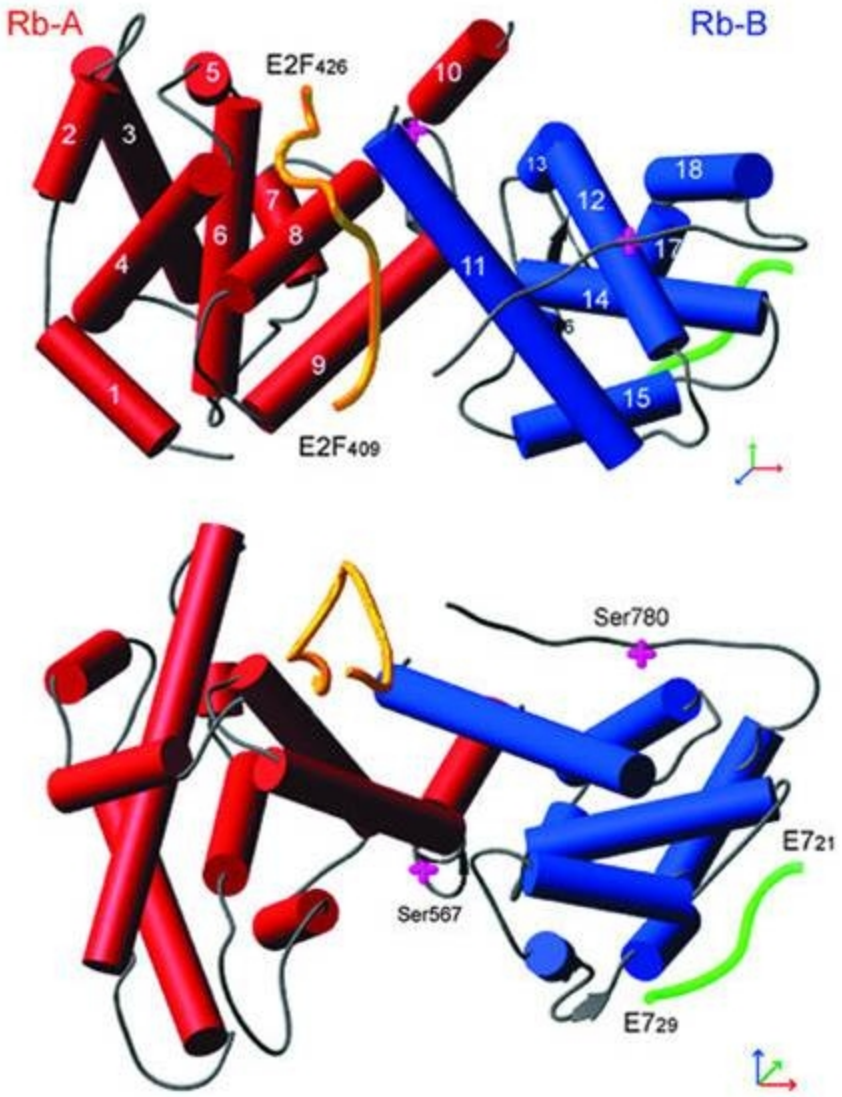

Figure 3B

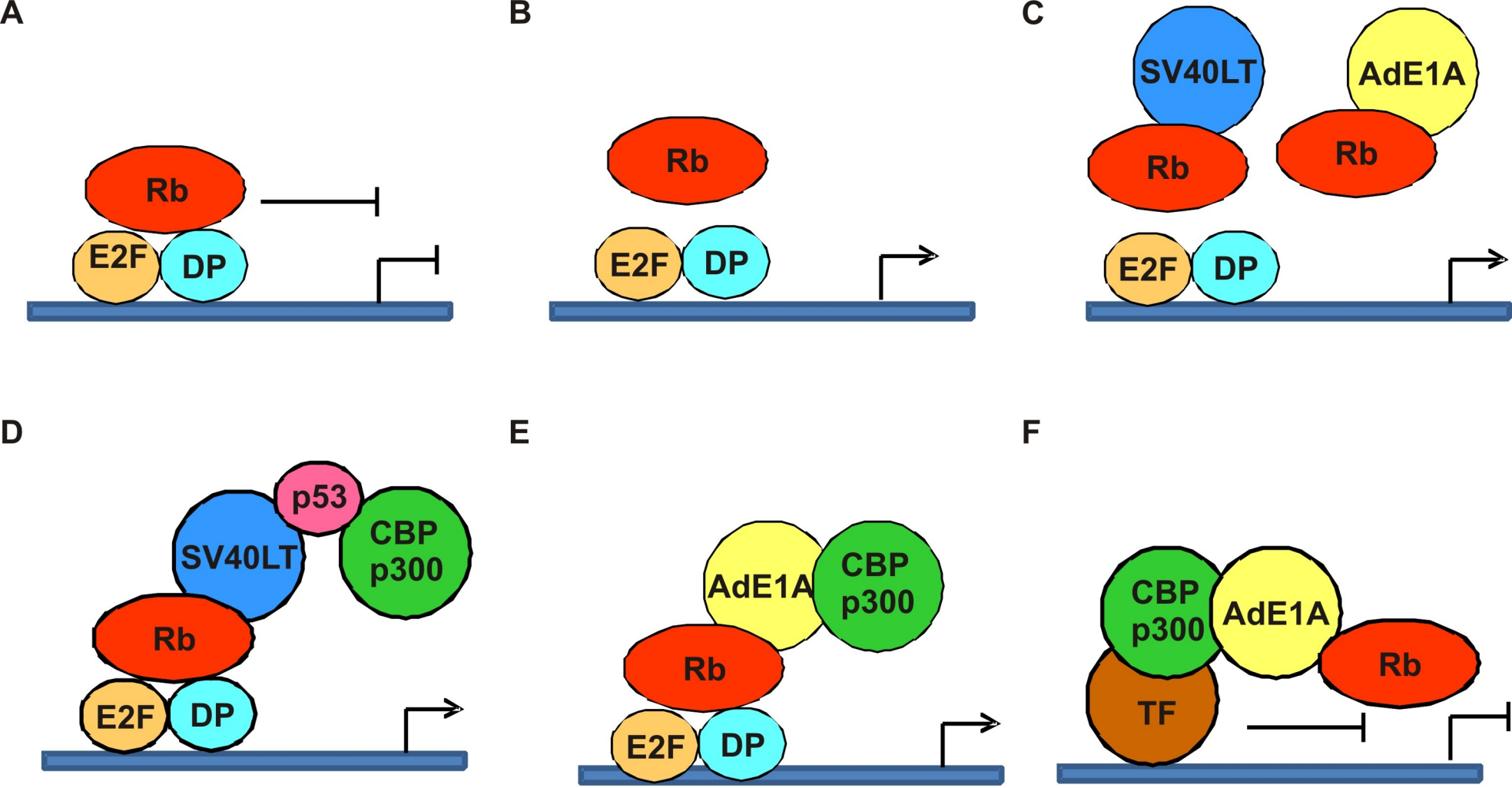
A
Rb
E2F
DP
B
Rb
E2F
DP
C
SV40LT
AdE1A
Rb
Rb
E2F
DP
D
p53
SV40LT
CBP
p300
Rb
E2F
DP
E
AdE1A
CBP
p300
Rb
E2F
DP
F
CBP
p300
AdE1A
Rb
TF

Figure 4

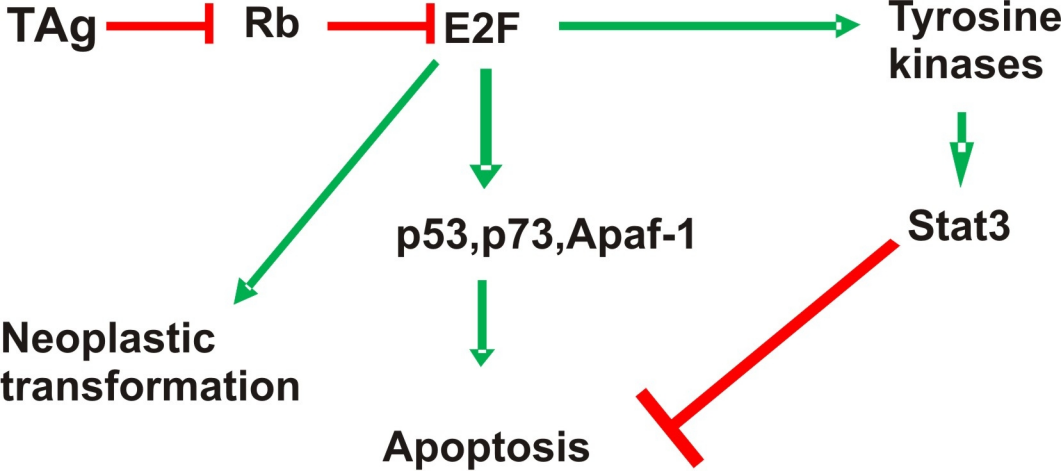
TAg
Rb
E2F
Tyrosine kinases
p53,p73,Apaf-1
Stat3
Neoplastic transformation
Apoptosis

Figure 5

EXPERIMENTAL CELL RESEARCH XX (2011) XXX–XXX

available at www.sciencedirect.com

ScienceDirect

www.elsevier.com/locate/yexcr

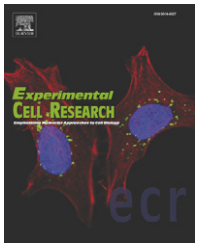

Review Article

The R(h)oads to Stat3: Stat3 activation by the Rho GTPases

Leda Raptis[a,*], *Rozanne Arulanandam*[a,1], *Mulu Geletu*[a], *James Turkson*[b]

[a] *Department of Microbiology and Immunology and Pathology, Queen's University, Kingston, Ontario, Canada K7L 3N6*
[b] *Burnett School of Biomedical Sciences, College of Medicine, University of Central Florida, Orlando, FL 32827, USA*

ARTICLE INFORMATION

Article Chronology:
Received 8 March 2011
Revised version received 9 May 2011
Accepted 10 May 2011

Keywords:
Rho GTPases
MgcRacGAP
Stat3

ABSTRACT

The signal transducer and activator of transcription-3 (Stat3) is a member of the STAT family of cytoplasmic transcription factors. Overactivation of Stat3 is detected with high frequency in human cancer and is considered a molecular abnormality that supports the tumor phenotype. Despite concerted investigative efforts, the molecular mechanisms leading to the aberrant Stat3 activation and Stat3-mediated transformation and tumorigenesis are still not clearly defined. Recent evidence reveals a crosstalk close relationship between Stat3 signaling and members of the Rho family of small GTPases, including Rac1, Cdc42 and RhoA. Specifically, Rac1, acting in a complex with the MgcRacGAP (male germ cell RacGAP), promotes tyrosine phosphorylation of Stat3 by the IL6-receptor family/Jak kinase complex, as well as its translocation to the nucleus. Studies have further revealed that the mutational activation of Rac1 and Cdc42 results in Stat3 activation, which occurs in part through the upregulation of IL6 family cytokines that in turn stimulates Stat3 through the Jak kinases. Interestingly, evidence also shows that the engagement of cadherins, cell to cell adhesion molecules, specifically induces a striking increase in Rac1 and Cdc42 protein levels and activity, which in turn results in Stat3 activation. In this review we integrate recent findings clarifying the role of the Rho family GTPases in Stat3 activation in the context of malignant progression.

Contents

* *Corresponding author at:* Department of Microbiology and Immunology, Queen's University, Botterell Hall, Room 713, Kingston, Ontario, Canada K7L 3N6. Fax: +1 613 533 6796.
E-mail address: raptisl@queensu.ca (L. Raptis).

Abbreviations: STATs, signal transducers and activators of transcription; MgcRacGAP, male germ cell RacGAP; E-cadherin, epithelial cadherin; MDCK, Madin–Darby canine kidney cells; Rho, Ras homologous GTPases, Rho; Ras, Rat sarcoma; GEF, guanine nucleotide exchange factor; GAP, GTPase activating proteins; GDI, guanine nucleotide dissociation inhibitor; CRIB, Cdc42/Rac interactive binding domain; REM, Rho effector homology domain; PAK, p21-activated kinase; ROCK, Rho-associated coiled-coil domain kinases; ROS, reactive oxygen species; LMwtPTPase, low-molecular-weight phosphatase; Cool-2, cloned out of library-2; Tiam-1, T-cell lymphoma invasion and metastasis-1; PI3-kinase, phosphatidylinositol −3 kinase; APRF, acute phase response factor; IL6, interleukin-6; EGFR, epidermal growth factor receptor; HGF, hepatocyte growth factor; VEGF, vascular endothelial growth factor; ptyr, phosphorylated tyrosine; NLS, nuclear localisation signal; Erk, extracellular-signal activated kinase 1/2; SH2, Src homology 2; JAKs, Janus kinases; NFκB, nuclear factor-kappaB.

[1] Present address: Center for Innovative Cancer Research, 3rd Floor, The Ottawa Hospital General Campus, 503 Smyth Road, Ottawa, Ontario, Canada K1H 1C4.

0014-4827/$ – see front matter © 2011 Elsevier Inc. All rights reserved.
doi:10.1016/j.yexcr.2011.05.008

Introduction

Normal or tumor tissues consist of cells which are in constant contact with their neighbors in a three-dimensional structure, and recent findings revealed that cell to cell adhesion may influence fundamental cellular processes such as cell division, differentiation and apoptosis [6,47]. In this context, recent studies have shown that the engagement of cadherins, calcium-dependent cell to cell adhesion molecules, causes a dramatic increase in the levels and activity of the signal transducer and activator of transcription-3 (Stat3), a member of the STAT family of cytoplasmic transcription factors, known to play a key role in a variety of cancers. Despite extensive efforts, the molecular mechanisms of Stat3 activation that lead to tumorigenesis are poorly understood. A family of molecules that are dramatically affected by the engagement of cadherins is the Rho, small GTPases (Rho). It has been demonstrated that mutationally activated forms of the Rac1, Cdc42 or RhoA members of this family, which are known to be important for transformation by oncogenes such as Src and Ras [21,26,45], directly or indirectly promote the phosphorylation and activation of Stat3 [13,17,54]. Recent studies further showed that cadherin engagement causes a dramatic increase in the levels and activity of both mutant and wild-type Rac1 and Cdc42, which in turn leads to Stat3 activation [2,4]. Thus, there is compelling evidence to support the notion that members of the Rho family represent critical sources of signals that promote events leading to Stat3 activation in the context of malignant progression. The Rho family of small GTPases and their role in neoplasia have been recently reviewed [16,21,26,27,45] and will not be discussed here. In this review we summarize the prevailing evidence on the mechanism of Stat3 upregulation and neoplastic transformation following activation of wild-type or mutant members of the Rho family of small GTPases.

Cadherins activate Rho GTPases

Cadherin family of cell to cell adhesion receptors

The formation of cell–cell adhesion junctions is primarily modulated by the calcium-dependent family of cadherin receptors. These plasma membrane glycoproteins control the organization, specificity and dynamics of cell adhesion, which is crucial for the development and maintenance of tissue architecture. Classical, type I cadherins include the epithelial (E)-cadherin and neuronal cadherin, which are found in most tissues [56]. Type I cadherins share low amino acid homology with type II cadherins, e.g., cadherin-11. Classical cadherins consist of three domains, an extracellular, a single-pass transmembrane and an intracellular domain (Fig. 1A). The ectodomain consists of five modules of ~100 amino acids each with internal sequence homology [23]. In the presence of calcium, the extracellular segments expressed on the surface of opposing cells interact to form the cell to cell adherens junctions, which are stabilized by cytoskeletal elements inside the cell, through a homologous carboxy-terminal, cytoplasmic region for binding to β- or γ-catenin proteins, which are linked to actin filaments [6].

The Rho GTPases

The small GTPases of the Ras (Rat sarcoma) superfamily (Ras, Rho, Arf, Rab and Ran) are ~21 kDa proteins that function as molecular switches in signaling pathways which are initiated by a variety of membrane triggers [21]. The Rho (Ras homologous) proteins are a subfamily of the Ras superfamily which are highly conserved from lower eucaryotes to plants and mammals [7]. They differ from other members of the group by the presence of a Rho-specific insert in the GTPase domain (Rac1 amino acids, 123–135), which has been suggested to be involved in the recognition of downstream effector proteins. Over 20 Rho GTPases are known, and 3 members, RhoA, Rac1 and Cdc42, are ubiquitously expressed, can stimulate cell cycle progression [41] and are crucial for Ras-induced transformation [46], while Rac1 was shown to be required for transformation by oncogenes such as Src [53,62] and Ras [33].

The Rho GTPases are best known as master regulators of the actin cytoskeleton: Rac1 and Cdc42 remodel the actin cytoskeleton at the leading edge of the cell, resulting in filopodial (Cdc42) or lamellipodial (Rac1) protrusions. RhoA, B and C on the other hand are largely responsible for orchestrating focal adhesion assembly and actomyosin-mediated cell contraction at the rear of the cell, thus permitting cell movement across these adhesive contacts and subsequent detachment by the trailing end of the cell [67]. Increases in the levels of Rho family proteins have been observed in a number of cancers [16,26].

Like Ras, most Rho family proteins act as molecular switches cycling between a GTP-bound, active form and a GDP-bound,

Please cite this article as: L. Raptis, et al., Exp. Cell. Res. (2011), doi:10.1016/j.yexcr.2011.05.008

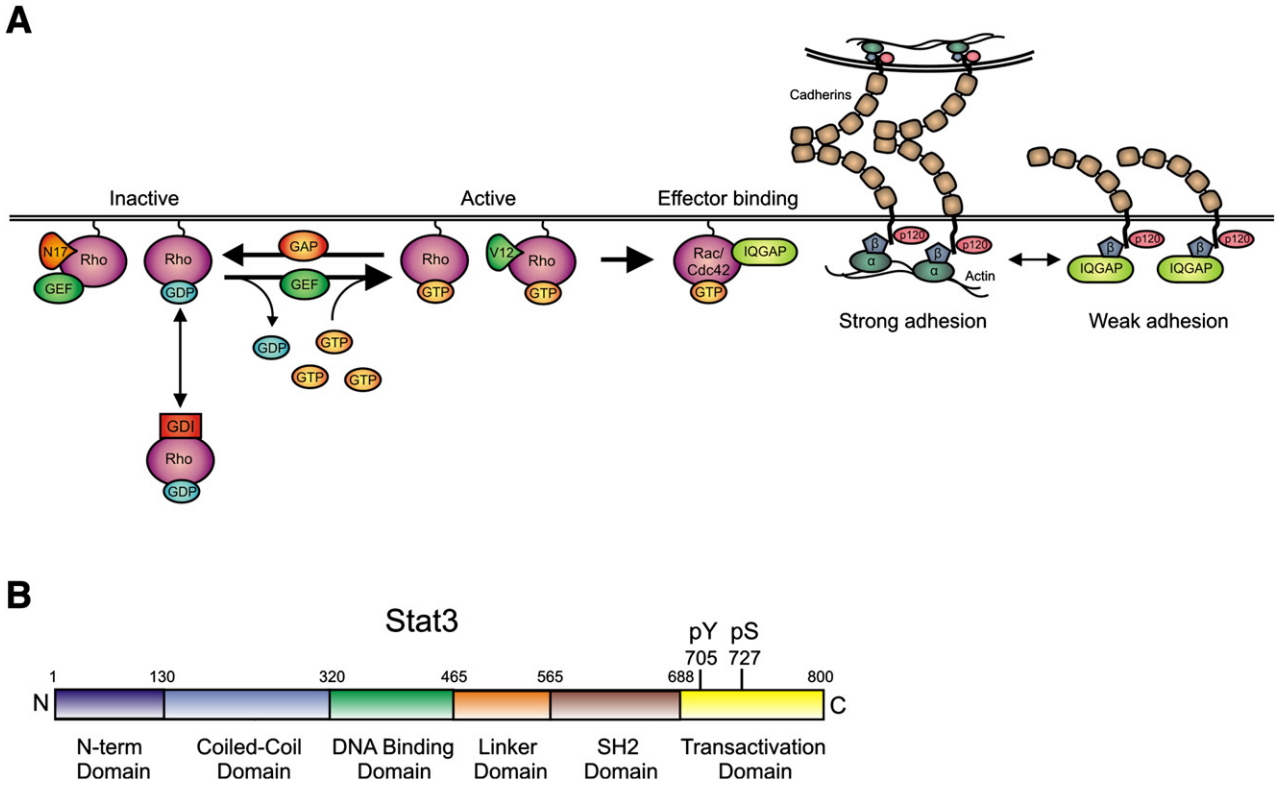

Fig. 1 – Activation of Rho GTPases (A) and Stat3 (B). (A) Rho GTPases are inactive when complexed to GDP and one of three known Rho-GDIs. Upon stimulation by extracellular factors, Rho is released from Rho-GDI and associates with the membrane through its C-terminal prenyl group. Rho-GEFs promote Rho-GTP exchange leading to the activation of various effector proteins. A Rho-GAP will then catalyze GTP hydrolysis and Rho-GDI will extract the GTPase from the membrane locking it once again in an inactive state. A substitution mutation of Thr for Asn at position 17 (Rac1 numbering) allows binding to GEF's but inhibits interactions with effectors, so that the mutant titrates out GEFs and acts as dominant-negative. On the other hand, mutation to V12 or L61 cannot hydrolyse GTP and is constitutively active. IQGAP, a Rac1 and Cdc42 effector, negatively regulates adhesion by binding to β-catenin which causes β-catenin to dissociate from the β-catenin/α-catenin complex. Activated Rac1 or Cdc42 bind IQGAP and force it to release β-catenin thus strengthening cell to cell adhesion. (B) Structure of the Stat3 transcription factor. The N-terminal, coiled-coil, DNA binding, SH2 and transactivation domains are shown, along with the tyr705 and ser727 phosphorylation sites.

inactive state [24]. GTP binding induces conformational changes which are localized within two surface loops (switch I and switch II, Rac1 amino acids 25–49 and 59–76, respectively [27]), which play an important role in GTP catalysis (Fig. 1A). The activity of Rho family proteins is regulated by three classes of proteins: guanine nucleotide exchange factors (GEFs), GTPase activating proteins (GAPs) and guanine nucleotide dissociation inhibitors (GDIs). GEFs catalyze the release of GDP from the Rho GTPases, which is the rate-limiting step in Rho activation. The free GTPase then associates with GTP, which alters the conformation of the switch regions of the enzyme to increase its affinity for the effectors (Fig. 1A). To date, over 70 Rho-GEFs have been described in humans. A substitution mutation of Thr for Asn at position 17 (Rac1 numbering) allows binding to GEFs but inhibits interactions with downstream effectors, so that these mutants titrate out the GEFs and act as dominant-negative [18]. In contrast to GEFs, the GAP proteins enhance the inherently low, intrinsic ability of the GTPases to hydrolyse the bound GTP to GDP. Therefore, GAPs promote inactivation and reverse the binding of effectors. There are over 80 mammalian Rho GAP proteins identified so far. Constitutively active mutants (e.g. Leu^{61} or Val^{12}) cannot hydrolyse GTP; therefore, they signal continuously to their effectors.

The Rho family members invariably have a C-terminal sequence ending with a -CAAX motif. Lipid modification at the C-terminus such as farnesylation, geranylgeranylation or palmitoylation promotes their membrane attachment, where they can be activated by GEFs. The GDI proteins (3 members) are cytosolic proteins that form a complex with GDP-bound Rho GTPases, so that they inhibit attachment to the membrane, hence activation by GEFs. GDIs are also able to associate with the active form and prevent binding to downstream effectors [14]. Therefore, the activation state of a given Rho family GTPase is tightly regulated and occurs in a cell-type and pathway-dependent manner, depending upon the balance of these regulators at any given moment, and this determines its downstream signaling.

Rho family proteins do not usually exert their effects directly, but instead operate through a multitude of effector proteins. The main region of Rho binding to its effectors is switch I, although regions outside switch I have been implicated in the binding of certain effectors. Over 70 effectors have been described [11]. Most Rac1 and Cdc42 effectors contain a conserved, GTPase-binding consensus site (Cdc42/Rac interactive binding or CRIB domain), while many RhoA, B, and C effectors possess an N-terminal Rho effector homology domain (REM). Many effector molecules are

Please cite this article as: L. Raptis, et al., Exp. Cell. Res. (2011), doi:10.1016/j.yexcr.2011.05.008

serine/threonine kinases. The best characterised Rac1 and Cdc42 effectors are the p21-activated kinases (PAKs [22]), while the Rho-associated coiled-coil domain kinases (ROCK-I and II) represent the best characterised RhoA effectors [49].

It is interesting to note that the small GTPases can regulate each other's activity via crosstalk. For example, oncogenic Ras needs to activate both Raf and Rac1 to transform [46]; the Tiam1, Rac1 GEF binds the Ras effector domain to activate Rac1 [33]. Similar to Tiam1, Cool-2 is activated by binding the Cdc42 effector domain, to act as a GEF for Rac1, while in a feedback loop, Rac-GTP inhibits the GEF activity of Cool-2 [19]. An additional mechanism whereby Rac1 downregulates Rho activity is through Rac1-mediated production of reactive oxygen species (ROS). ROS inhibit the low-molecular-weight phosphatase (LMwtPTPase) which normally dephosphorylates and inhibits the p190RhoGAP. Consequently, Rac1 activation reduces the activity of RhoA [40].

Cadherin engagement increases Rac1 and Cdc42 protein levels and activity

In addition to providing structure and integrity to the cell, cadherin adhesive engagement initiates intracellular signals that are communicated through the conserved cadherin tail domain to different cytoplasmic pathways. In fact, results from a number of labs indicated that Cdc42 and Rac1 are required for E-cadherin-mediated, cell–cell adhesion in MDCK cells [20], and are believed to contribute to the stability of cell–cell adhesion via their effect on cytoskeletal organization [9]: Expression of activated $Rac1^{val12}$ in canine epithelial MDCK cells induces the accumulation of E-cadherin, β-catenin and actin filaments at sites of cell–cell contact, whereas overexpression of the dominant-negative, $Rac1^{N17}$ mutant reduces their accumulation [59]. Rac1 and Cdc42 can regulate E-cadherin activity through their effector, IQGAP. IQGAP is localized to sites of cell–cell contact and negatively regulates adhesion by binding to β-catenin, which causes β-catenin to dissociate from α-catenin [32]. Rac1 and Cdc42 bind IQGAP and remove it from the β-catenin/α-catenin complex. As a result, activated Rac1 inhibits cell dissociation and scattering, and strengthens cell–cell adhesion. Interestingly, in a positive feedback mechanism, E-cadherin engagement also results in the rapid activation of Rac1 and Cdc42, in part through a PI3-kinase-mediated mechanism, while, as expected, it inhibits RhoA, through the production of ROS by Rac1 [25].

In addition to E-cadherin-mediated activation of Rac1 and Cdc42, previous reports revealed another mechanism of Rac1 regulation involving protein stability, namely, degradation through the proteasome pathway [36,44]. In fact, cadherin engagement, e.g., achieved by high cell density, led to a dramatic increase in Rac1/Cdc42 protein levels through inhibition of proteasomal degradation [2,4]. Conversely, epithelial cell scattering brought about by hepatocyte growth factor (HGF) can induce the proteasome-mediated degradation of Rac1 [36]. Moreover, a mutational analysis further indicated that constitutive activation of Rac1, as well as binding of effectors, which might be acting as ubiquitin E3 ligases, are necessary for Rac1 degradation [44]. Still, results by Arulanandam et al. indicated that although permanently activated by mutation, protein levels of $Rac1^{V12}$ and $Rac1^{L61}$ are increased dramatically with cell density [2], indicating that cell density can overcome the degradative effect of activation. The effect of cadherin engagement upon Rac1/Cdc42 levels was found to be independent from direct cell to cell contact; plating HC11 mouse breast epithelial cells sparsely on surfaces coated with a fragment encompassing the two outermost domains of E-cadherin caused a dramatic increase in Rac1 protein levels and activity, compared to cells growing on plastic [4], indicating that E-cadherin engagement per se is responsible for the increase in Rac1 and Cdc42 levels. Such a mechanism could hold true for Cdc42, which mirrored Rac1 levels and stability increases with cell density. Similarly, cadherin-11 and N-cadherin were also found to activate Rac1 in different cell lines (Arulanandam et al., in preparation). The above data taken together indicate that cadherin engagement can abolish Rac1/Cdc42 proteasomal degradation, which leads to a dramatic increase in their levels and consequently their activity, even in the absence of direct cell to cell contact.

Rho GTPases activate Stat3

The Stat3 pathway in neoplasia

Stat3 was originally discovered as the acute phase response factor (APRF) that mediates the acute phase response in the liver via the induction of the C-reactive protein [50,71]. Stat3 is activated not only by cytokine receptors, such as the receptor for the interleukin-6 (IL6) family cytokines, but also growth receptor tyrosine kinases, such as the EGFR family including Her2/Neu, and non-receptor tyrosine kinases such as Src and Abl [63], and is also activated in response to stimulation of G-protein-coupled receptors [43]. Classically, the receptor stimulation by ligand induces Stat3 binding to phosphotyrosine residues of activated receptors through its SH2 domain and its phosphorylation on a critical tyr705 residue by the receptor itself, or by associated Janus kinase (JAK, Jak1-3, Tyk2) or Src family tyrosine kinases [68], and the phosphorylation is known to mediate dimerization between two Stat3 monomers through reciprocal SH2 domain–ptyr interactions [68]. However, studies have also identified pre-existing complexes between non-phosphorylated Stat3 monomers [51]. Stat3:Stat3 dimers translocate to the nucleus where they bind to target sequences in specific promoters, although Stat3 monomers have also been detected in the nucleus. Known Stat3 upregulated genes include *Bcl-xL*, *Mcl1*, *survivin*, *Akt*, *vascular endothelial growth factor* (*VEGF*), *HGF*, *myc*, *cyclinD*, and *HIF1*, while the *p53* tumor suppressor is downregulated by Stat3 activity [69].

In contrast to normal Stat3 signaling, which is transient, hyperactive Stat3 is associated with malignant transformation and tumorigenesis. Constitutively active Stat3 is present in a large number of cancers, and studies show that aberrant Stat3 activity promotes tumor cell growth and survival, tumor angiogenesis and metastasis, and induces tumor immune evasion [68]. It was also shown that a constitutively active form of Stat3, Stat3C, is able to transform cultured cells, which further points to an etiologic role for Stat3 in cancer [10]. Of therapeutic importance, disruption of hyperactive Stat3 signaling in tumor xenografts induces tumor cell apoptosis and tumor regression with little effect upon normal tissues [65,68,70], which points to Stat3 as an important player in tumor progression.

Rac1 and MgcRacGAP mediate Stat3 ptyr705 phosphorylation and nuclear transport

Emerging evidence suggests a more complex mechanism for Stat3 activation than initially thought; recent studies indicate that Rac1

Please cite this article as: L. Raptis, et al., Exp. Cell. Res. (2011), doi:10.1016/j.yexcr.2011.05.008

plays an important role in Stat3 (as well as Stat5) tyrosine phosphorylation and nuclear translocation:

The male germ cell RacGAP (MgcRacGAP) is an evolutionarily conserved protein which binds directly to and serves as a GAP against Rac1, Rac2 and Cdc42 in vitro [61]. Studies in murine M1 leukemia cells, which differentiate into macrophages upon IL6 stimulation, show that MgcRacGAP can bind through its cysteine-rich and GAP domains to the DNA binding domain of Stat3 (aa 338–362), and that the MgcRacGAP-Stat3 association is required for Stat3, tyr705 phosphorylation following cytokine stimulation. That is, besides having Rac1-GAP activity, the MgcRacGAP, GAP domain is required for IL6-induced, Stat3 ptyr705 phosphorylation, acting as an effector of Rac1. Although MgcRacGAP is constitutively associated with Rac1, the association with Stat3 is increased upon IL6 stimulation [60]. In addition, MgcRacGAP phosphorylation at ser-387 was implicated in transformation by Src, although the exact mechanism is unclear [15].

Following their synthesis in the cytoplasm, transcription factors such as the STAT proteins have to cross the nuclear envelope in order to enter the nucleus. The exact mechanism of Stat3 translocation to the nucleus is just now beginning to emerge. Recent evidence suggests that, besides tyr705 phosphorylation, the Rac1/MgcRacGAP complex may be involved in Stat3 translocation. As a general mechanism for nuclear import, proteins larger than ~50 kDa require specific sequences, the nuclear localisation signals (NLS), or binding to NLS-containing chaperones. The best characterised NLS is the mono- or bi-partite, polybasic NLS, which is usually recognized by a family of proteins, the importin-α carriers. These associate with importin-β which docks the complex to the nuclear pore, so that the complex can migrate into the nucleus. The small GTPase, Ran-GTP, then binds importin-β, and the complex is disassembled inside the nucleus [12]. In the case of Stat1 it was recognized that it must be phosphorylated first on tyr701 and dimerized, in order to reveal a conditional NLS which can associate with importin-α5 [48]. Despite the initial assumption, however, that all STATs need to be phosphorylated to enter the nucleus, Stat3 was found to be nuclear and to shuttle between nucleus and cytoplasm, independent of tyrosine phosphorylation. Nevertheless, phosphorylation is still required to bind to specific DNA target sites [35]. It was further demonstrated that a sequence within the coiled-coil domain of Stat3 (amino acids 150–162) is necessary for nuclear translocation and is critical for the recognition of unphosphorylated as well as phosphorylated Stat3 by importins α3 and α6 [29,30,35]. However, although the 150–162 sequence was found to be indispensable for nuclear translocation of full-length Stat3, substitution of the basic amino acid cluster in this sequence did not hamper nuclear accumulation, indicating that aa 150–162 may only be part of a conformational structure that is required for nuclear import rather than a bona fide NLS [35].

In addition to this mechanism, recent evidence brought forth the role of MgcRacGAP as a nuclear chaperone for translocation of Stat3 (as well as Stat5) to the nucleus. In fact, the ternary complex between ptyrStat3, Rac1-GTP and MgcRacGAP facilitates the association with importin-α/β and nuclear translocation; mutation of the polybasic region of the MgcRacGAP NLS inhibited the nuclear translocation and transcriptional activity of Stat3 and Stat5 [28]. Therefore, Rac1 is emerging as an important regulator of Stat3 phosphorylation, nuclear import and function, acting through the MgcRacGAP/Rac/Stat3 complex (Fig. 2).

Mutationally activated Rho GTPases activate Stat3 through IL6 secretion

Data from a number of labs have demonstrated a functional role for the Rho GTPases in the activation of Stat3. An earlier study first implicated RhoA in the phosphorylation of Stat3 on ser727 in Src-transformed cells. Moreover, in vitro kinase assays using purified Stat3 as the substrate revealed that both p38 and JNK kinases, which can be activated by the Rho GTPases, phosphorylate Stat3 on ser727, while inhibition of p38 activity suppressed Stat3 activation and vSrc-mediated transformation [62]. In a subsequent report, mutationally activated RhoA was shown to activate Stat3 (but not Stat1) through phosphorylation at both tyr705 and ser727 in human cells, while this Stat3 activation, mediated by the ROCK effector, is required for RhoA-mediated transformation [5]. Further results similarly demonstrated Stat3 activation by mutationally activated forms of Rac1, Cdc42 and RhoA [13,17,54].

Despite extensive efforts, the exact mechanism of Stat3 activation by Rho's has been a matter of controversy. Simon et al. reported a direct binding between Rac1 and Stat3 in transiently transfected, Cos1 cells, while $Rac1^{N17}$ inhibited EGF-mediated, Stat3 activation [54]. On the other hand, using neutralising antibodies to inhibit IL6 binding, Faruqi et al. showed that Rac1 activates Stat3 indirectly through autocrine induction of IL-6 [17]. These results were contradicted in a later study where, using Stat3 null cells, it was demonstrated that Stat3 activation by the Rho GTPases could occur without the formation of a stable complex, and in the absence of IL6 secretion [13]. Notably, a recent report indicated that the engagement of E-cadherin, by growing the mouse breast epithelial HC11 cells to high densities, causes a dramatic increase in the levels and activity of Rac/Cdc42 ([4], see next section). Cell density was not taken into account previously, but would significantly impact studies the observations regarding the effect of Rho GTPases upon Stat3 activity. Stat3 ptyr705 levels in HC11 mouse breast epithelial cells over-expressing activated Rac^{V12} (or Rac^{Leu61}) or $Cdc42^{V12}$ mutants were compared to the parental HC11 line, both grown to different densities (from 50% confluence to 5 days post-confluence), and found to be higher at all cell densities, indicating that the activated forms of the GTPases promoted the activation of Stat3, in agreement with previous data [13,17,54]. In a similar experiment, activated $RhoA^{V13}$ was also found to activate Stat3, although to a lesser extent than $Rac1^{V12}$ or $Cdc42^{V12}$ (Arulanandam et al., unpublished). Inhibition experiments indicated that Stat3 activation by Rac^{V12}/$Cdc42^{V12}$ required NFκB and Jak activity [2]. Further examination of the mechanism showed that the addition of medium conditioned by Rac^{V12}-expressing cells to the parental line caused an increase in Stat3 activity, suggesting the presence of autocrine factor (s) that in turn promote Stat3 activation. Screening for mRNA of 86 cytokines by RT-PCR in Rac^{V12}-expressing cells indicated a significant increase in at least 3 cytokines of the IL6 family compared to untransfected HC11 cells. Furthermore, downregulation of the gp130, common receptor subunit of the family, blocked the induction of Stat3 activity in Rac^{V12}-expressing cells, indicating an important role for this family in Stat3 activation [2,4] (Fig. 2). The fact that more than one cytokine of the IL6 family appears to be involved explains the previous results where addition of neutralising antibodies to IL6 alone did not block Stat3 activation by Rac^{V12}[13]. The above results taken together demonstrate that activated forms of members of the Rho family can activate Stat3 through nuclear factor (NF)κB, gp130 and JAKs and provides a basis to explain the apparent discrepancy in the potential that Rho family GTPases promote Stat3 activation.

Please cite this article as: L. Raptis, et al., Exp. Cell. Res. (2011), doi:10.1016/j.yexcr.2011.05.008

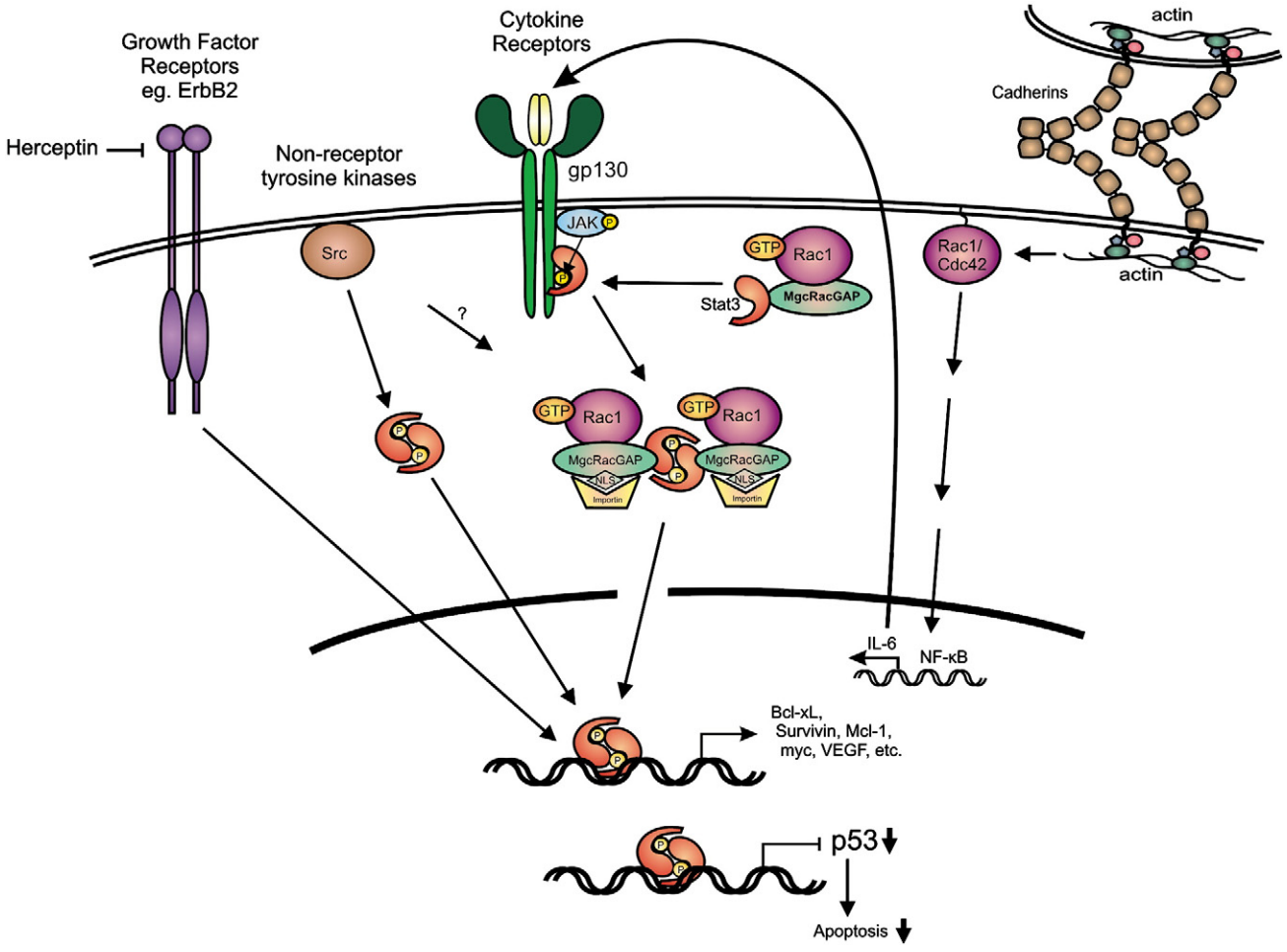

Fig. 2 – Stat3 is activated by growth factor receptors such as Her2/ErbB2 (that can be inhibited by drugs such as Herceptin), non-receptor tyrosine kinases such as Src and cytokine receptors such as the IL6 family. Activated Rac1-GTP, in a complex with MgcRacGAP and Stat3, facilitates Stat3 phosphorylation by the IL6-R/Jak complex, which results in targeting of the complex to the nuclear envelope, driven by the NLS of MgcRacGAP. The Stat3 dimer then binds specific DNA sequences to initiate transcription of Stat3 responsive genes or downregulation of other genes such as the p53 anti-oncogene. MgcRacGAP may also play a role in Stat3 activation by Src. In addition to this mechanism, cadherin engagement was shown to cause a dramatic increase in the levels of Rac1 and Cdc42 proteins and activity, which results in a transcriptional activation of IL6 through NFκB, hence Stat3 activation.

Cadherin engagement activates Stat3 through Rac1/Cdc42 and IL6

The dramatic activation of Rac1/Cdc42 following cadherin engagement [4], coupled with the ability of Rac1/Cdc42 to activate Stat3 [2], leads to the conclusion that cadherin engagement may activate Stat3 through an increase in activity of the Rho GTPases. In fact, results from a number of labs revealed that cell density causes a striking increase in the activity of Stat3 in breast carcinoma [67], melanoma [31], head and neck squamous cell carcinoma [42,55], as well as normal epithelial cells [4,57,58] and fibroblasts ([67], reviewed in [47]). Although tumor cells or cells transformed by Src or other oncogenes had higher Stat3 activity than their normal counterparts when sparse, cell density caused a further Stat3 activation [66,67]. Moreover, growing HC11 mouse breast epithelial cells on surfaces coated with E-cadherin caused a dramatic increase in Stat3 activity, demonstrating that E-cadherin engagement is sufficient to directly activate Stat3, in the absence of cell to cell contact [4]. The density-dependent Stat3 activation was strikingly greater than that brought about by serum or EGF stimulation and was not affected by inhibition or ablation of the cellular Src, Fyn, Yes, Abl, EGFR, Fer or IGF1-R kinases. As expected, this Stat3 activation is triggered by a dramatic increase in the levels of the Rac1 and Cdc42, Rho family GTPases, brought about by inhibition of proteasomal degradation [2], and a corresponding increase in their activity, following E-cadherin engagement [4]. The Rac1/Cdc42 upregulation, in turn, causes a dramatic increase in the expression of a number of cytokines of the IL6 family, which are responsible for the Stat3 activation observed.

Specificity of Stat3 activation

A key question is how and why cadherin engagement would promote the activation of Stat3, but not other pathways, such as Erk1/2. Notably, although IL-6/IL-6R typically activates extracellular-signal activated kinase 1/2 (Erk) in subconfluent cells, post-

Please cite this article as: L. Raptis, et al., Exp. Cell. Res. (2011), doi:10.1016/j.yexcr.2011.05.008

confluent cultures do not respond with Erk activation upon IL6 stimulation [4]. In the same vein, E-cadherin engagement does not lead to Erk activation. This demonstrates a rather specific Stat3 response of cells to E-cadherin engagement, despite the fact that the two pathways, Erk and Stat3, are often coordinately regulated by oncogenes and growth factor or cytokine receptors including IL-6 [4]. It is conceivable that Erk-specific phosphatases such as Cdc25A [34] may be activated at high densities or that other adaptors required for Erk activation by IL6 might be down-regulated following cadherin engagement. It is interesting to note in this context that cell density also increases Stat5, tyr694 phosphorylation and activity in K562 human chronic myelogenous leukemia cells, although the role of Rho GTPases or cadherins in this is unknown [39].

Phenotypic effects of activated Rho GTPases require Stat3

Rac1 activation was shown to stimulate survival signals through activation of the PI3k/Akt pathway [37]. However, although Rac1/Cdc42 activity is dramatically increased following cadherin engagement, no increase in Akt-473 phosphorylation was seen with cell density in HC11 cells (Arulanandam et al., unpublished results). In sharp contrast, Stat3 is dramatically upregulated at high densities and known to provide a major survival mechanism to cultured epithelial cells and fibroblasts [47,66,67]. Given the propensity of over-confluent cells to undergo growth arrest and apoptosis, it is conceivable that the Stat3 activation serves to provide a survival signal as a last effort to rescue from an impending apoptosis. Interestingly, Stat3 also enhances the resistance of tumor cells to chemotherapeutic agents [8]. The observations that cells are more resistant to inhibition of Src [1] and to chemotherapy when grown to high densities [38] are consistent with the induction of Stat3 signaling at post-confluence, which would provide a survival mechanism.

Stat3 could mediate the proliferative and migration signals provided by activated Rac1, consistent with the known function of Stat3. Thus, expression of activated $Rac1^{V12}$ or $Cdc42^{V12}$ mutants in epithelial cells was shown to increase cell migration in a "wound-healing," cell culture assay, and this process was found to require Stat3 [13] and gp130 [2]. In the same vein, Stat3 is required for the neoplastic conversion of HEK-293T cells expressing activated RhoA to anchorage independence [5].

Conclusions

In summary, while the mechanisms continue to be investigated, there is strong evidence that certain Rho GTPases are important Stat3 activators. (1) Mutational activation of Rac1, RhoA and Cdc42 leads to Stat3 activation. (2) Rac1 and Cdc42 mediate the cadherin signal that leads to activation of Stat3 through NFκB and gp130. (3) Rac1 binds MgcRacGAP and Stat3 and this complex promotes interaction with the IL6 receptor for tyr705 phosphorylation and the activation of the MgcRacGAP - NLS, thereby facilitating nuclear translocation for Stat3-mediated transcription of specific genes (Fig. 2).

The importance of cadherin engagement upon levels and activity of proteins such as Rho and Stat3 is just beginning to emerge. Cadherin engagement was also shown to activate Jak1, which is required for Stat3 activation [67]. In sharp contrast, Src was not required for Stat3 activation following cadherin engagement and its activity was unaffected by cell density [3].

Overall, the potential for the Rho GTPases to promote the pro-survival Stat3 signaling in the context of malignant transformation underscores the importance of cell–cell interactions in the tumor microenvironment in facilitating tumor progression. Due to the generally higher level of expression of E2F transcription factors which are potent apoptosis inducers [52], many tumor cells may have higher requirements for survival signals, such as provided by the cadherin/Rac1/gp130 axis. The increased dependence on Stat3 for survival would explain the increased sensitivity of cells transformed by oncogenes such as Src [64] or the large tumor antigen of simian virus 40 [66] to Stat3 inhibition, a finding which could have significant therapeutic implications.

Acknowledgments

Special thanks are due to Dr. Richard Jove for valuable advice. The financial assistance of the Canadian Institutes of Health Research (CIHR), the Canadian Breast Cancer Foundation (Ontario Chapter), the Natural Sciences and Engineering Research Council of Canada (NSERC), the Ontario Centers of Excellence, the Breast Cancer Action Kingston, the Clare Nelson bequest fund and the Canadian Breast Cancer Research Alliance (L.R.) is gratefully acknowledged. R.A. was supported by a Canada Graduate Scholarships Doctoral award from CIHR, the Ontario Women's Health Scholars Award from the Ontario Council of Graduate Studies, a Queen's University Graduate Award and a MITACS Elevate Postdoctoral fellowship. M.G. was supported by a postdoctoral fellowship from the Ministry of Research and Innovation, a postdoctoral award from the province of Ontario, and a US Army breast cancer program. JT was supported by a grant from the National Cancer Institute (CA128865).

REFERENCES

[1] A. Anagnostopoulou, A. Vultur, R. Arulanandam, J. Cao, J. Turkson, R. Jove, J.S. Kim, M. Glenn, A.D. Hamilton, L. Raptis, Differential effects of Stat3 inhibition in sparse vs confluent normal and breast cancer cells, Cancer Lett. 242 (2006) 120–132.
[2] R. Arulanandam, M. Geletu, H. Feracci, L. Raptis, RacV12 requires gp130 for Stat3 activation, cell proliferation and migration, Exp. Cell Res. 316 (2010) 875–886.
[3] R. Arulanandam, M. Geletu, L. Raptis, The simian virus 40 large tumor antigen activates cSrc and requires Src for full neoplastic transformation, Anticancer Res. 30 (2010) 47–54.
[4] R. Arulanandam, A. Vultur, J. Cao, E. Carefoot, P. Truesdell, B. Elliott, L. Larue, H. Feracci, L. Raptis, Cadherin–cadherin engagement promotes survival via Rac/Cdc42 and Stat3, Mol. Cancer Res. 17 (2009) 1310–1327.
[5] S. Aznar, P.F. Valeron, S.V. del Rincon, L.F. Perez, R. Perona, J.C. Lacal, Simultaneous tyrosine and serine phosphorylation of STAT3 transcription factor is involved in Rho A GTPase oncogenic transformation, Mol. Biol. Cell 12 (2001) 3282–3294.
[6] J.M. Benjamin, W.J. Nelson, Bench to bedside and back again: molecular mechanisms of alpha-catenin function and roles in tumorigenesis, Semin. Cancer Biol. 18 (2008) 53–64.
[7] A. Boureux, E. Vignal, S. Faure, P. Fort, Evolution of the Rho family of ras-like GTPases in eukaryotes, Mol. Biol. Evol. 24 (2007) 203–216.
[8] L.Y. Bourguignon, K. Peyrollier, W. Xia, E. Gilad, Hyaluronan–CD44 interaction activates stem cell marker Nanog, Stat-3-mediated MDR1 gene expression, and ankyrin-regulated multidrug efflux in breast and ovarian tumor cells, J. Biol. Chem. 283 (2008) 17635–17651.

Please cite this article as: L. Raptis, et al., Exp. Cell. Res. (2011), doi:10.1016/j.yexcr.2011.05.008

[9] V.M. Braga, A. Del Maschio, L. Machesky, E. DeJana, Regulation of cadherin function by Rho and Rac: modulation by junction maturation and cellular context, Mol. Biol. Cell 10 (1999) 9–22.
[10] J.F. Bromberg, M.H. Wrzeszczynska, G. Devgan, Y. Zhao, R.G. Pestell, C. Albanese, J.E. Darnell Jr., Stat3 as an oncogene, Cell 98 (1999) 295–303.
[11] X.R. Bustelo, V. Sauzeau, I.M. Berenjeno, GTP-binding proteins of the Rho/Rac family: regulation, effectors and functions in vivo, Bioessays 29 (2007) 356–370.
[12] A. Cook, F. Bono, M. Jinek, E. Conti, Structural biology of nucleocytoplasmic transport, Annu. Rev. Biochem. 76 (2007) 647–671.
[13] M. Debidda, L. Wang, H. Zang, V. Poli, Y. Zheng, A role of STAT3 in Rho GTPase-regulated cell migration and proliferation, J. Biol. Chem. 280 (2005) 17275–17285.
[14] C. DerMardirossian, G.M. Bokoch, GDIs: central regulatory molecules in Rho GTPase activation, Trends Cell Biol. 15 (2005) 356–363.
[15] N. Doki, T. Kawashima, Y. Nomura, A. Tsuchiya, C. Oneyama, T. Akagi, Y. Nojima, T. Kitamura, Constitutive phosphorylation of a Rac GAP MgcRacGAP is implicated in v-Src-induced transformation of NIH3T3 cells, Cancer Sci. 100 (2009) 1675–1679.
[16] S.I. Ellenbroek, J.G. Collard, Rho GTPases: functions and association with cancer, Clin. Exp. Metastasis 24 (2007) 657–672.
[17] T.R. Faruqi, D. Gomez, X.R. Bustelo, D. Bar-Sagi, N.C. Reich, Rac1 mediates STAT3 activation by autocrine IL-6, Proc. Natl Acad. Sci. USA 98 (2001) 9014–9019.
[18] L.A. Feig, Tools of the trade: use of dominant-inhibitory mutants of Ras-family GTPases, Nat. Cell Biol. 1 (1999) E25–E27.
[19] Q. Feng, D. Baird, X. Peng, J. Wang, T. Ly, J.L. Guan, R.A. Cerione, Cool-1 functions as an essential regulatory node for EGF receptor- and Src-mediated cell growth, Nat. Cell Biol. 8 (2006) 945–956.
[20] M. Fukata, K. Kaibuchi, Rho-family GTPases in cadherin-mediated cell–cell adhesion, Nat. Rev. Mol. Cell Biol. 2 (2001) 887–897.
[21] S.J. Heasman, A.J. Ridley, Mammalian Rho GTPases: new insights into their functions from in vivo studies, Nat. Rev. Mol. Cell Biol. 9 (2008) 690–701.
[22] C. Hofmann, M. Shepelev, J. Chernoff, The genetics of Pak, J. Cell Sci. 117 (2004) 4343–4354.
[23] P. Hulpiau, F. van Roy, Molecular evolution of the cadherin superfamily, Int. J. Biochem. Cell Biol. 41 (2009) 349–369.
[24] A.B. Jaffe, A. Hall, Rho GTPases: biochemistry and biology, Annu. Rev. Cell Dev. Biol. 21 (2005) 247–269.
[25] Z.M. Jaffer, J. Chernoff, The cross Rho'ds of cell–cell adhesion, J. Biol. Chem. 279 (2004) 35123–35126.
[26] R. Karlsson, E.D. Pedersen, Z. Wang, C. Brakebusch, Rho GTPase function in tumorigenesis, Biochim. Biophys. Acta 1796 (2009) 91–98.
[27] A.E. Karnoub, M. Symons, S.L. Campbell, C.J. Der, Molecular basis for Rho GTPase signaling specificity, Breast Cancer Res. Treat. 84 (2004) 61–71.
[28] T. Kawashima, Y.C. Bao, Y. Minoshima, Y. Nomura, T. Hatori, T. Hori, T. Fukagawa, T. Fukada, N. Takahashi, T. Nosaka, M. Inoue, T. Sato, M. Kukimoto-Niino, M. Shirouzu, S. Yokoyama, T. Kitamura, A Rac GTPase-activating protein, MgcRacGAP, is a nuclear localizing signal-containing nuclear chaperone in the activation of STAT transcription factors, Mol. Cell. Biol. 29 (2009) 1796–1813.
[29] M. Kohler, S. Ansieau, S. Prehn, A. Leutz, H. Haller, E. Hartmann, Cloning of two novel human importin-alpha subunits and analysis of the expression pattern of the importin-alpha protein family, FEBS Lett. 417 (1997) 104–108.
[30] M. Kohler, C. Speck, M. Christiansen, F.R. Bischoff, S. Prehn, H. Haller, D. Gorlich, E. Hartmann, Evidence for distinct substrate specificities of importin alpha family members in nuclear protein import, Mol. Cell. Biol. 19 (1999) 7782–7791.
[31] S. Kreis, G.A. Munz, S. Haan, P.C. Heinrich, I. Behrmann, Cell density dependent increase of constitutive signal transducers and activators of transcription 3 activity in melanoma cells is mediated by Janus kinases, Mol. Cancer Res. 5 (2007) 1331–1341.
[32] S. Kuroda, M. Fukata, M. Nakagawa, K. Fujii, T. Nakamura, T. Ookubo, I. Izawa, T. Nagase, N. Nomura, H. Tani, I. Shoji, Y. Matsuura, S. Yonehara, K. Kaibuchi, Role of IQGAP1, a target of the small GTPases Cdc42 and Rac1, in regulation of E-cadherin-mediated cell–cell adhesion, Science 281 (1998) 832–835.
[33] J.M. Lambert, Q.T. Lambert, G.W. Reuther, A. Malliri, D.P. Siderovski, J. Sondek, J.G. Collard, C.J. Der, Tiam1 mediates Ras activation of Rac by a PI(3)K-independent mechanism, Nat. Cell Biol. 4 (2002) 621–625.
[34] J.S. Lazo, K. Nemoto, K.E. Pestell, K. Cooley, E.C. Southwick, D.A. Mitchell, W. Furey, R. Gussio, D.W. Zaharevitz, B. Joo, P. Wipf, Identification of a potent and selective pharmacophore for Cdc25 dual specificity phosphatase inhibitors, Mol. Pharmacol. 61 (2002) 720–728.
[35] L. Liu, K.M. McBride, N.C. Reich, STAT3 nuclear import is independent of tyrosine phosphorylation and mediated by importin-alpha3, Proc. Natl Acad. Sci. USA 102 (2005) 8150–8155.
[36] E.A. Lynch, J. Stall, G. Schmidt, P. Chavrier, C. D'Souza-Schorey, Proteasome-mediated degradation of Rac1-GTP during epithelial cell scattering, Mol. Biol. Cell 17 (2006) 2236–2242.
[37] C. Murga, M. Zohar, H. Teramoto, J.S. Gutkind, Rac1 and RhoG promote cell survival by the activation of PI3K and Akt, independently of their ability to stimulate JNK and NF-kappaB, Oncogene 21 (2002) 207–216.
[38] T. Nakamura, Y. Kato, H. Fuji, T. Horiuchi, Y. Chiba, K. Tanaka, E-cadherin-dependent intercellular adhesion enhances chemoresistance, Int. J. Mol. Med. 12 (2003) 693–700.
[39] S. Nam, A. Williams, A. Vultur, A. List, K. Bhalla, D. Smith, F.Y. Lee, R. Jove, Dasatinib (BMS-354825) inhibits Stat5 signaling associated with apoptosis in chronic myelogenous leukemia cells, Mol. Cancer Ther. 6 (2007) 1400–1405.
[40] A.S. Nimnual, L.J. Taylor, D. Bar-Sagi, Redox-dependent downregulation of Rho by Rac, Nat. Cell Biol. 5 (2003) 236–241.
[41] M.F. Olson, A. Ashworth, A. Hall, An essential role for Rho, Rac, and Cdc42 GTPases in cell cycle progression through G1, Science 269 (1995) 1270–1272.
[42] A. Onishi, Q. Chen, J.O. Humtsoe, R.H. Kramer, STAT3 signaling is induced by intercellular adhesion in squamous cell carcinoma cells, Exp. Cell Res. 314 (2008) 377–386.
[43] S. Pelletier, F. Duhamel, P. Coulombe, M.R. Popoff, S. Meloche, Rho family GTPases are required for activation of Jak/STAT signaling by G protein-coupled receptors, Mol. Cell. Biol. 23 (2003) 1316–1333.
[44] M. Pop, K. Aktories, G. Schmidt, Isotype-specific degradation of Rac activated by the cytotoxic necrotizing factor 1, J. Biol. Chem. 279 (2004) 35840–35848.
[45] M.R. Popoff, B. Geny, Multifaceted role of Rho, Rac, Cdc42 and Ras in intercellular junctions, lessons from toxins, Biochim. Biophys. Acta 1788 (2009) 797–812.
[46] R.G. Qiu, J. Chen, D. Kirn, F. McCormick, M. Symons, An essential role for Rac in Ras transformation, Nature 374 (1995) 457–459.
[47] L. Raptis, R. Arulanandam, A. Vultur, M. Geletu, S. Chevalier, H. Feracci, Beyond structure, to survival: Stat3 activation by cadherin engagement, Biochem. Cell Biol. 87 (2009) 835–843.
[48] N.C. Reich, L. Liu, Tracking STAT nuclear traffic, Nat. Rev. Immunol. 6 (2006) 602–612.
[49] K. Riento, A.J. Ridley, Rocks: multifunctional kinases in cell behaviour, Nat. Rev. Mol. Cell Biol. 4 (2003) 446–456.
[50] J.A. Ripperger, S. Fritz, K. Richter, G.M. Hocke, F. Lottspeich, G.H. Fey, Transcription factors Stat3 and Stat5b are present in rat liver nuclei late in an acute phase response and bind interleukin-6 response elements, J. Biol. Chem. 270 (1995) 29998–30006.
[51] M. Schroder, K.M. Kroeger, H.D. Volk, K.A. Eidne, G. Grutz, Preassociation of nonactivated STAT3 molecules demonstrated in living cells using bioluminescence resonance energy transfer: a new model of STAT activation? J. Leukoc. Biol. 75 (2004) 792–797.
[52] R.C. Sears, J.R. Nevins, Signaling networks that link cell proliferation and cell fate, J. Biol. Chem. 277 (2002) 11617–11620.

Please cite this article as: L. Raptis, et al., Exp. Cell. Res. (2011), doi:10.1016/j.yexcr.2011.05.008

[53] J.M. Servitja, M.J. Marinissen, A. Sodhi, X.R. Bustelo, J.S. Gutkind, Rac1 function is required for Src-induced transformation. Evidence of a role for Tiam1 and Vav2 in Rac activation by Src, J. Biol. Chem. 278 (2003) 34339–34346.
[54] A.R. Simon, H.G. Vikis, S. Stewart, B.L. Fanburg, B.H. Cochran, K.L. Guan, Regulation of STAT3 by direct binding to the Rac1 GTPase, Science 290 (2000) 144–147.
[55] R.A. Steinman, A. Wentzel, Y. Lu, C. Stehle, J.R. Grandis, Activation of Stat3 by cell confluence reveals negative regulation of Stat3 by cdk2, Oncogene 22 (2003) 3608–3615.
[56] M.P. Stemmler, Cadherins in development and cancer, Mol. Biosyst. 4 (2008) 835–850.
[57] H.W. Su, S.W. Wang, F.K. Ghishan, P.R. Kiela, M.J. Tang, Cell confluency-induced Stat3 activation regulates NHE3 expression by recruiting Sp1 and Sp3 to the proximal NHE3 promoter region during epithelial dome formation, Am. J. Physiol. Cell Physiol. 296 (2009) C13–C24.
[58] H.W. Su, H.H. Yeh, S.W. Wang, M.R. Shen, T.L. Chen, P.R. Kiela, F.K. Ghishan, M.J. Tang, Cell confluence-induced activation of signal transducer and activator of transcription-3 (Stat3) triggers epithelial dome formation via augmentation of sodium hydrogen exchanger-3 (NHE3) expression, J. Biol. Chem. 282 (2007) 9883–9894.
[59] K. Takaishi, T. Sasaki, H. Kotani, H. Nishioka, Y. Takai, Regulation of cell–cell adhesion by rac and rho small G proteins in MDCK cells, J. Cell Biol. 139 (1997) 1047–1059.
[60] Y. Tonozuka, Y. Minoshima, Y.C. Bao, Y. Moon, Y. Tsubono, T. Hatori, H. Nakajima, T. Nosaka, T. Kawashima, T. Kitamura, A GTPase-activating protein binds STAT3 and is required for IL-6-induced STAT3 activation and for differentiation of a leukemic cell line, Blood 104 (2004) 3550–3557.
[61] A. Toure, O. Dorseuil, L. Morin, P. Timmons, B. Jegou, L. Reibel, G. Gacon, MgcRacGAP, a new human GTPase-activating protein for Rac and Cdc42 similar to Drosophila rotundRacGAP gene product, is expressed in male germ cells, J. Biol. Chem. 273 (1998) 6019–6023.
[62] J. Turkson, T. Bowman, J. Adnane, Y. Zhang, J.Y. Djeu, M. Sekharam, D.A. Frank, L.B. Holzman, J. Wu, S. Sebti, R. Jove, Requirement for Ras/Rac1-mediated p38 and c-Jun N-terminal kinase signaling in Stat3 transcriptional activity induced by the Src oncoprotein, Mol. Cell. Biol. 19 (1999) 7519–7528.
[63] J. Turkson, T. Bowman, R. Garcia, E. Caldenhoven, R.P. de Groot, R. Jove, Stat3 activation by Src induces specific gene regulation and is required for cell transformation, Mol. Cell. Biol. 18 (1998) 2545–2552.
[64] J. Turkson, S. Zhang, L.B. Mora, A. Burns, S. Sebti, R. Jove, A novel platinum compound that inhibits constitutive Stat3 signaling and induces cell cycle arrest and apoptosis of malignant cells, J. Biol. Chem. 280 (2005) 32979–32988.
[65] J. Turkson, S. Zhang, J. Palmer, H. Kay, J. Stanko, L.B. Mora, S. Sebti, H. Yu, R. Jove, Inhibition of constitutive signal transducer and activator of transcription 3 activation by novel platinum complexes with potent antitumor activity, Mol. Cancer Ther. 3 (2004) 1533–1542.
[66] A. Vultur, R. Arulanandam, J. Turkson, G. Niu, R. Jove, L. Raptis, Stat3 is required for full neoplastic transformation by the Simian Virus 40 Large Tumor antigen, Mol. Biol. Cell 16 (2005) 3832–3846.
[67] A. Vultur, J. Cao, R. Arulanandam, J. Turkson, R. Jove, P. Greer, A. Craig, B.E. Elliott, L. Raptis, Cell to cell adhesion modulates Stat3 activity in normal and breast carcinoma cells, Oncogene 23 (2004) 2600–2616.
[68] H. Yu, R. Jove, The STATs of cancer—new molecular targets come of age, Nat. Rev. Cancer 4 (2004) 97–105.
[69] H. Yu, D. Pardoll, R. Jove, STATs in cancer inflammation and immunity: a leading role for STAT3, Nat. Rev. Cancer 9 (2009) 798–809.
[70] P. Yue, J. Turkson, Targeting STAT3 in cancer: how successful are we? Expert Opin. Investig. Drugs 18 (2009) 45–56.
[71] D. Zhang, M. Sun, D. Samols, I. Kushner, STAT3 participates in transcriptional activation of the C-reactive protein gene by interleukin-6, J. Biol. Chem. 271 (1996) 9503–9509.

Please cite this article as: L. Raptis, et al., Exp. Cell. Res. (2011), doi:10.1016/j.yexcr.2011.05.008

DNA AND CELL BIOLOGY
Volume 28, Number 7, 2009

Pp. 319–327
DOI: 10.1089/dna.2008.0833

Stat3 Activity Is Required for Gap Junctional Permeability in Normal Rat Liver Epithelial Cells

Mulu Geletu,[1,*] Chrystele Chaize,[1,*] Rozanne Arulanandam,[1] Adina Vultur,[2] Claudia Kowolik,[2] Aikaterini Anagnostopoulou,[1] Richard Jove,[2] and Leda Raptis[1]

Neoplastic transformation by oncogenes such as activated Src is known to suppress gap junctional, intercellular communication (GJIC). One of the Src effector pathways leading to GJIC suppression and transformation is the Ras/Raf/Mek/Erk, so that inhibition of this pathway in vSrc-transformed cells restores GJIC. A distinct Src downstream effector required for neoplasia is the signal transducer and activator of transcription-3 (Stat3). To examine the role of Stat3 upon the Src-mediated, GJIC suppression, Stat3 was downregulated in rat liver epithelial cells expressing activated Src through treatment with the CPA7, Stat3 inhibitor, or through infection with a retroviral vector expressing a Stat3-specific shRNA. GJIC was examined by electroporating the fluorescent dye, Lucifer yellow, into cells grown on two coplanar electrodes of electrically conductive, optically transparent, indium-tin oxide, followed by observation of the migration of the dye to the adjacent, nonelectroporated cells under fluorescence illumination. The results demonstrate that, contrary to inhibition of the Ras pathway, Stat3 inhibition in cells expressing activated Src does not restore GJIC. On the contrary, Stat3 inhibition in normal cells with high GJIC levels eliminated junctional permeability. Therefore, Stat3's function is actually required for the maintenance of junctional permeability, although Stat3 generally promotes growth and in an activated form can act as an oncogene.

Introduction

The signal transducer and activator of transcription-3 (Stat3) is a cytoplasmic protein that is activated by cytokines and receptor tyrosine kinases, as well as the nonreceptor tyrosine kinase Src (reviewed in Yu and Jove, 2004, and Frank, 2007). In an unstimulated cell, Stat3 is latent in the cytoplasm. Subsequent to binding to an activated receptor through its Src homology 2 domain, Stat3 becomes activated through phosphorylation at a critical tyrosine (tyr705). This activates Stat3 by stabilizing the association of two monomers through reciprocal Src homology 2-phosphotyrosine interactions. The Stat3 dimer then migrates to the nucleus, where it binds to target sequences, leading to the transcriptional activation of specific genes that play a role in cell proliferation and survival, such as *myc*, cyclin D, *Bcl-xL*, survivin, hepatocyte growth factor (Hung and Elliott, 2001), and others (Yu and Jove, 2004). The investigation of the role of Stat3 in neoplasia gained momentum when it was found to be activated in a number of tumor cell lines and carcinomas (Germain and Frank, 2007). The fact that a constitutively active form of Stat3 alone is sufficient to induce transformation (Bromberg *et al.*, 1999) points to an etiological role for Stat3 in neoplasia.

Gap junctions are plasma membrane channels that enable the passage of small molecules between the interiors of adjacent cells. A reduction in gap junctional, intercellular communication (GJIC) is believed to lead to an increase in cell proliferation (reviewed in Vinken *et al.*, 2006). In fact, a number of oncogenes such as v-Src (Lin *et al.*, 2006), the polyoma virus middle tumor antigen (Azarnia and Loewenstein, 1987; Raptis *et al.*, 1994), the simian virus 40 large tumor antigen (Khoo *et al.*, 1998), Hsp90N (Grammatikakis *et al.*, 2002), and vRas (Brownell *et al.*, 1996a; Atkinson and Sheridan, 1988) have been shown to interrupt junctional communication. Interestingly, a loss of GJIC also accompanies the cessation of proliferation and differentiation of murine preadipocytes (Azarnia and Russell, 1985; Brownell *et al.*, 1996a; Anagnostopoulou *et al.*, 2007) and apoptosis in bovine lens epithelial cells and mouse fibroblasts (Theiss *et al.*, 2007). Gap junctions are formed by the connexin (Cx) family of proteins that consists of at least 20 members in mammals (Vinken *et al.*, 2006). Oncogenes such as Src phosphorylate Cx43, both directly and indirectly, leading to

[1]Departments of Microbiology and Immunology and Pathology, Queen's University, Kingston, Canada.
[2]Molecular Medicine, City of Hope National Medical Center, Duarte, California.
*These two authors contributed equally to this work.

GJIC suppression (reviewed in Pahujaa *et al.*, 2007). Despite the extensive literature on the effect of viral or cellular oncogenes upon GJIC, the effect of Stat3 upon GJIC is at present unknown.

We previously reported on a technique where GJIC of adherent cells can be examined by *in situ* electroporation: Cells are grown on two coplanar electrodes, consisting of glass coated with conductive indium-tin oxide (ITO) (Anagnostopoulou *et al.*, 2007). The electrodes are separated by a barrier that diverts the electric field, rendering it vertical to the cell layer. An electric pulse is applied in the presence of the tracking dye, Lucifer yellow (LY). The pulse causes the introduction of LY into the cells growing on the electrodes by opening transient pores on the membrane, and the subsequent migration of the dye to adjacent, nonelectroporated cells growing on uncoated glass is microscopically observed under fluorescence illumination. Dye transfer through gap junctions can be precisely quantitated in this way, simultaneously and in a large number of cells, without any detectable disturbance to cellular metabolism (reviewed in Raptis *et al.*, 2008). Although this technique is adequate for many adherent cell lines, cells at the edge of the electrodes, adjacent to the nonconductive area, receive slightly higher amounts of current, which could result in cellular damage. In addition, slight differences in adhesion and growth of the cells on bare glass, as opposed to ITO, might create artifacts. To overcome these problems, we modified the geometry of the slide, so that both electroporated and nonelectroporated cells grow on conductive ITO, while the electric field intensity is essentially uniform over the entire electroporated area. This technique was used to examine the role of Stat3 upon GJIC levels in rat liver epithelial cells. The results demonstrate that, unlike Ras inhibition (Ito *et al.*, 2006), Stat3 inhibition in cells expressing activated Src does not increase GJIC. On the contrary, inhibition of Stat3 activity in cells with extensive GJIC causes a dramatic reduction in junctional communication, concomitant with apoptosis induction. Therefore, Stat3's function is actually required for the maintenance of junctional permeability, although Stat3 generally promotes growth and in an activated form can act as an oncogene.

Materials and Methods

Cell lines and culture techniques

Cells were grown in Dulbecco's modified Eagle's medium (DMEM) supplemented with 10% fetal calf serum (ICN; Biomedicals, Costa Mesa, CA). T51B is a normal rat liver epithelial line. Src was activated in this line by stable expression of a construct expressing the middle tumor antigen of polyoma virus (line T51B-Src) (Royal *et al.*, 1996). Confluence was estimated visually and quantitated by imaging analysis of live cells under phase contrast using a Leitz Diaplan microscope and the MCID-elite software (Imaging Research, St. Catharines, Canada).

For Stat3 downregulation, cells grown to different densities were treated with 50 μM CPA7, and diluted in growth medium from a 20 mM stock in 50% DMSO for 24 h. Control cells were treated with the same amount of the DMSO carrier (0.00125%) alone; however, no effect of DMSO was noted upon the activity of Stat3 or GJIC at this concentration. Apoptosis was assessed by morphological observation and poly-ADP-ribose polymerase (PARP)–cleavage analysis. For a more precise quantitation, cells were fixed with ethanol and stained with propidium iodide, and the percentage of cells with a subG1 DNA content was assessed by fluorescence-activated cell sorting (FACS) analysis (Vultur *et al.*, 2004).

Examination of gap junctional communication

The setup is described in Figure 1. Cells are grown and electroporated on a glass slide (1), coated with conductive and transparent ITO (1a) with a surface resistivity of 20 Ω/square (Colorado Concept Coatings, Loveland, CO) (Tomai *et al.*, 1998). The ITO was etched to define electrode and nonconducting regions, which were electrically isolated from each other by removing the ITO coating in lines of ~20 μm wide from the glass surface. It was important to ensure that only the 800 Å coating was removed, without affecting the glass, so that cell growth would be unaffected across the line. This was achieved with a UV laser operating at a 355 nm wavelength using 1 W of output power with 60% of the energy delivered to the surface of the glass. The spot size was 20 μm across with a spot overlap of 90%. The beam was manipulated by mirrors on a pair of galvanometers to produce the desired pattern. Waverunner™ software were used to define the pattern and control the system (Nutfield Technology, Inc., Windham, NH).

To form the two electrodes, the ITO coating was removed in a straight line in the middle (2). A dam of nonconductive Teflon (3) was used to divert the current upward, thus creating a sharp transition in electric field intensity. To provide areas where the cells are not electroporated, the ITO was also etched in two rectangles (4 and 4a). Current flows inward from each contact point (5 and 5a), via a conductive highway between the rectangles (red arrows), spreading in a direction parallel to the middle barrier, then over the barrier (arrowheads [6]) to the other side, electroporating cells in areas (7 and 7a). A polypropylene chamber is bonded onto the slide, to form a container for the cells and LY (9). Cells were plated in the chamber, and 2 days after confluence the growth medium was replaced with calcium-free DMEM containing 5 mg/mL LY. The slide/chamber was placed into a holder where electrical contacts were established, and a set of electrical pulses delivered to the cells. Extensive experimentation indicated that eight pulse pairs, each pulse of 24 V peak value, 300 μs length, and spaced 0.5 s apart, with one of each pair having a polarity opposite to that of its partner gave optimal results. After a 5-min incubation at 37°C, the unincorporated dye was washed with calcium-free DMEM, and cells were observed and photographed under fluorescence and phase contrast illumination. To better pin-point the position of the edge of the electroporated area, cells were also observed and photographed under combined fluorescence and phase-contrast illumination. In this configuration, cells that acquired LY by electroporation (growing in 7 and 7a) and cells into which LY traveled through gap junctions (8 and 8a) both grow on ITO, separated only by a laser-etched line of ~20 μm (Fig. 1B, C). The equipment is available from Cell Projects Ltd. (Harrietsham, United Kingdom).

Lentivirus vector production

293T cells were plated at a density of 4×10^6 cells per 10-cm culture dish. The cells were cotransfected by calcium phos-

phate coprecipitation with 15 μg of pLKO1-Stat3 shRNA (Sigma, St. Louis, MO) and 10 μg of pPACK packaging plasmid mix (SBI, Mountain View, CA). The culture medium was replaced with fresh medium after 6 h. The supernatant was collected 16 h after the transfection and stored at −80°C. To determine the vector titers, 10^5 HT1080 cells were seeded in a six-well plate and infected with various dilutions of the vector in the presence of 4 μg/mL polybrene. The culture medium was replaced 48 h later with fresh medium containing puromycin at a concentration of 1.5 μg/mL. Puromycin-resistant colonies were counted 10 days after transduction. To examine the efficiency of Stat3 downregulation, cells were infected at 5 pfu/cell and extracts probed for total Stat3 (Cell Signalling). For GJIC examination, cells were plated in electroporation chambers and infected with 5 pfu/cell at densities of ~80%. Two days after confluence, cells were electroporated with LY for GJIC examination as described above.

Western blotting

Cells were grown to different densities, and proteins extracted as described before (Raptis *et al.*, 2000). Fifty micrograms of clarified cell extract was resolved on a 10% polyacrylamide-SDS gel and transferred to a nitrocellulose membrane (Bio-Rad, Hercules, CA). The membranes were probed with antibodies against the tyrosine-705 phosphorylated form of Stat3 (Cell Signalling, Cat.# 9131L, used at a dilution of 1:2000), against anti-Cx43 (BD-Transduction, Cat.#610061 used at a dilution of 1:250), or PARP (Roche, Basel, Switzerland; Cat.# 1 835 238, used at 1:1000), followed by secondary antibodies: alkaline phosphatase-conjugated goat anti-mouse antibody (Biosource, Cat.#AMI3405, for anti-Cx43 and Hsp90) or goat anti-rabbit antibody (Biosource, Cat. #ALI4405, for tyr705 phosphorylated form of Stat3 [Stat3-ptyr705] and PARP), both used at a 1:10,000 dilution. The bands were viewed using enhanced chemiluminescence, according to the manufacturer's instructions (PerkinElmer Life Sciences, Cat.# NEL602). As a control for protein loading, parallel blots were routinely probed with a mouse monoclonal anti-Hsp90 antibody (Stressgen, Cat.# SPA-830, used at 1:5000), followed by a secondary antibody and enhanced chemiluminescence detection as above.

Luciferase assays for Stat3 transcriptional activity

Cells were transfected with a Stat3-specific reporter plasmid (p*Luc*TKS3) that harbors seven copies of a sequence corresponding to the Stat3-specific binding site in the C-reactive gene promoter (termed APRE, TTCCCGAA) upstream from a firefly luciferase coding sequence (Turkson *et al.*, 1998) and the pRLSRE plasmid that contains two copies of the serum response element of the *c-fos* promoter, subcloned into the *Renilla* luciferase reporter, pRL-null (Turkson

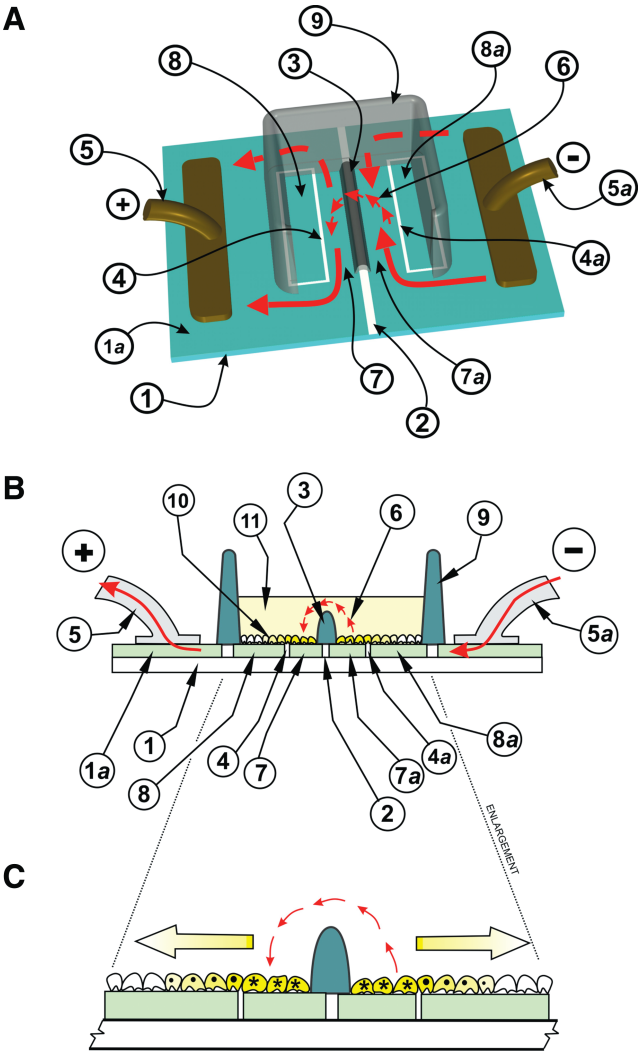

FIG. 1. The electroporation apparatus. (**A**) Top view. Cells are grown on a glass slide (1), coated with conductive and transparent indium-tin oxide (ITO, [1a]). The ITO coating is laser-etched in a straight line in the middle (2), essentially forming two electrodes. A dam of Teflon (3) is used to divert the current upward, thus creating a sharp transition in electric field intensity. To provide nonconductive areas, the ITO is also etched in two rectangles (4 and 4a). Current from a pulse generator flows inward from each contact point (5 and 5a), via a conductive highway between the rectangles (red arrows), spreading in a direction parallel to the middle barrier, then over the barrier (arrowheads [6]) to the other side, electroporating cells in areas 7 and 7a. A plastic chamber is bonded onto the slide, to form a container for the cells and Lucifer yellow (LY) (8). For clarity, the front part of the chamber is removed. (**B**) Side view. The slide (1) with the cells (10) growing on the ITO-coated (1a, light green) and etched bare glass regions (4 and 4a) is shown. When electroporation medium containing LY (11) is added to the chamber to a level above the height of the dam (3), an electrical path between the electrodes 7 and 7a and the cells (10) growing in this area is formed. Note that the ITO layer (1a) is shown with exaggerated thickness for clarity although its actual thickness (800 Å) is much less than the thickness of the cells. (**C**) The area of electroporated (7 and 7a) and nonelectroporated (8 and 8a) cells is shown enlarged. Stars denote cells (yellow) at the edge of the electroporated area that were loaded with LY by electroporation. Dots denote cells where the dye transferred through gap junctions. Large arrows show the direction of dye transfer through gap junctions. Note that the size and thickness of the cells are exaggerated for clarity. Color images available online at www.liebertonline.com/dna.

et al., 2001). Both luciferase activities were measured in total cell extracts according to the manufacturer's protocol (Promega, Cat. # E4030).

Results

Stat3 downregulation does not restore gap junctional communication in cells expressing activated Src

A body of evidence has indicated that the Src oncogene product downregulates gap junctional communication through a variety of mechanisms, including activation of the Ras/Raf/Mek/Erk pathway. As a result, inhibition of this pathway restores GJIC in vSrc-transformed cells (Ito *et al.*, 2006; Pahujaa *et al.*, 2007). Since Stat3 is also activated by and is required for transformation by vSrc (Turkson *et al.*, 1998), we used the rat liver epithelial line T51B transformed by activated Src (line T51B-Src) as a model to explore the possible role of Stat3 in suppressing gap junctional communication.

To examine gap junctional communication by *in situ* electroporation, it is important to be able to reliably distinguish cells that were loaded with LY by electroporation, from cells that received the dye from neighboring cells through gap junctions. That is, a sharp transition in electrical field intensity between electroporated and nonelectroporated areas must be established. This was achieved by etching the ITO in the pattern shown in Figure 1, and adding a dam to divert the electric field upward. To examine GJIC, cells were plated in the electroporation chambers (Fig. 1) and at 2 days postconfluence an electrical pulse was applied in the presence of the tracer, LY (see Materials and Methods). As shown in Figure 2, T51B cells have extensive GJIC (Fig. 2A, panels a and b), which is dramatically reduced after activated Src expression (Fig. 2B, panels a and b; Table 1).

To examine the effect of Stat3 downregulation, cells were treated with the platinum compound, CPA7, previously shown to be an effective Stat3 inhibitor (Turkson *et al.*, 2004; Littlefield *et al.*, 2008). The degree of Stat3 inactivation was assessed by probing Western blots with an antibody specific for the Stat3-ptyr705, as well as by measuring the reduction in Stat3 transcriptional activity. Since it was previously demonstrated that cell-to-cell adhesion dramatically activates Stat3 even in vSrc-transformed cells (Vultur *et al.*, 2004), tests were conducted at different densities; cells were plated in 3-cm Petri dishes at a confluence of 50%, and at different times thereafter, up to 5 days postconfluence, total protein extracts were probed for the Stat3-ptyr705 by Western blotting, using Hsp90 as a loading control (see Materials and Methods). To ensure that the growth medium was not depleted of nutrients, it was changed every day. As shown in Figure 3A, treatment of T51B-Src cells with 50 μM CPA7 for 24 h essentially eliminated Stat3-tyr705 phosphorylation at all cell densities examined (lanes 1–6 vs. 7–12). In addition, examination of Stat3 transcriptional activity in T51B-Src cells transfected with a luciferase gene construct under control of a Stat3-specific promoter (p*Luc*TKS3 plasmid; see Materials and Methods) revealed a dramatic decrease upon CPA7 treatment, while CPA7 did not affect Stat3-independent transcription from *c-fos*, serum response element promoter, indicating that this compound is selective for Stat3 (Fig. 3B) (Turkson *et al.*, 2004).

After Stat3 downregulation, GJIC was examined as above at 2 days postconfluence. Unexpectedly, the results showed that Stat3 inhibition did not reinstate GJIC in T51B-Src cells (Fig. 2B, panels c and d; Table 1). To further substantiate these findings, we downregulated Stat3 expression through infection with a lentivirus vector carrying an shRNA against Stat3 (sh-Stat3; see Materials and Methods). In addition, sh-Stat3 expression, which caused a reduction in Stat3-ptyr705 levels to 28% at all cell densities examined, did not increase GJIC (Fig. 2B, panels e and f; Table 1), in agreement with the CPA7 data. The above findings taken together indicate that, contrary to Ras, high Stat3 activity, which could be, at least in part, due to high Src activity levels, cannot be responsible for the lack of junctional communication in T51B-Src cells.

Stat3 is required for gap junctional communication

To further investigate whether Stat3 might, in fact, play a positive role upon gap junctional communication, we examined the effect of Stat3 inhibition in normal T51B cells that have extensive GJIC. Cells were plated in electroporation chambers and treated with 50 μM CPA7 or the DMSO carrier alone for 24 h, and gap junctional communication was examined through LY electroporation as above. Interestingly, the results showed that CPA7 treatment essentially abolished GJIC (Fig. 2A, panels c and d; Table 1). Similarly, reduction of Stat3 levels through infection with the sh-Stat3 lentivirus vector resulted in a dramatic reduction in GJIC in T51B cells (Fig. 2A, panels e and f; Table 1). The above data taken together reveal that, rather than increasing GJIC, Stat3 inhibition eliminates junctional permeability, indicating that Stat3 activity is required for gap junction function in normal epithelial cells that display extensive GJIC.

Stat3 inhibition leads to a reduction in Cx43 levels

Various reports showed that gap junction function is dependent upon cell-to-cell adhesion and the assembly of adherent junctions (Frenzel and Johnson, 1996; Wei *et al.*, 2005). Since the surface area of contact is expected to increase with cell density, we examined the effect of cell density upon the levels of Cx43, a widely expressed gap junction protein, in T51B cells. Cells were plated at a density of 50%, and at different times thereafter extracts were probed with an antibody against Cx43 (see Materials and Methods). The results revealed a dramatic increase in Cx43 levels, which plateaued at ~1–2 days after 100% confluence, indicating that cell-to-cell contact can cause a significant increase in Cx43 levels.

It was previously demonstrated that Cx43 has a short half-life (Beardslee *et al.*, 1998). To examine the effect of Stat3 inhibition upon Cx43 protein levels, lysates from T51B cells grown to different densities and treated with CPA7 were probed for Cx43 by Western blotting. As shown in Figure 4A (lanes 8–14), CPA7 treatment caused a dramatic reduction in Cx43 levels, at all densities examined, concomitant with GJIC reduction. These findings indicate that, besides GJIC, Stat3 activity is required for the maintenance of Cx43 levels as well.

Apoptosis of adherent cells causes cell rounding and a reduction in the area of cell to cell to contact. Since these morphological changes could affect GJIC, the cellular phenotype regarding apoptosis was examined after Stat3 inhibition. T51B cells were grown to 3 days postconfluence, and after Stat3 inhibition with CPA7, apoptosis was examined by PARP-cleavage analysis, and by examination of the percentage of cells with subG1 DNA content by FACS (see

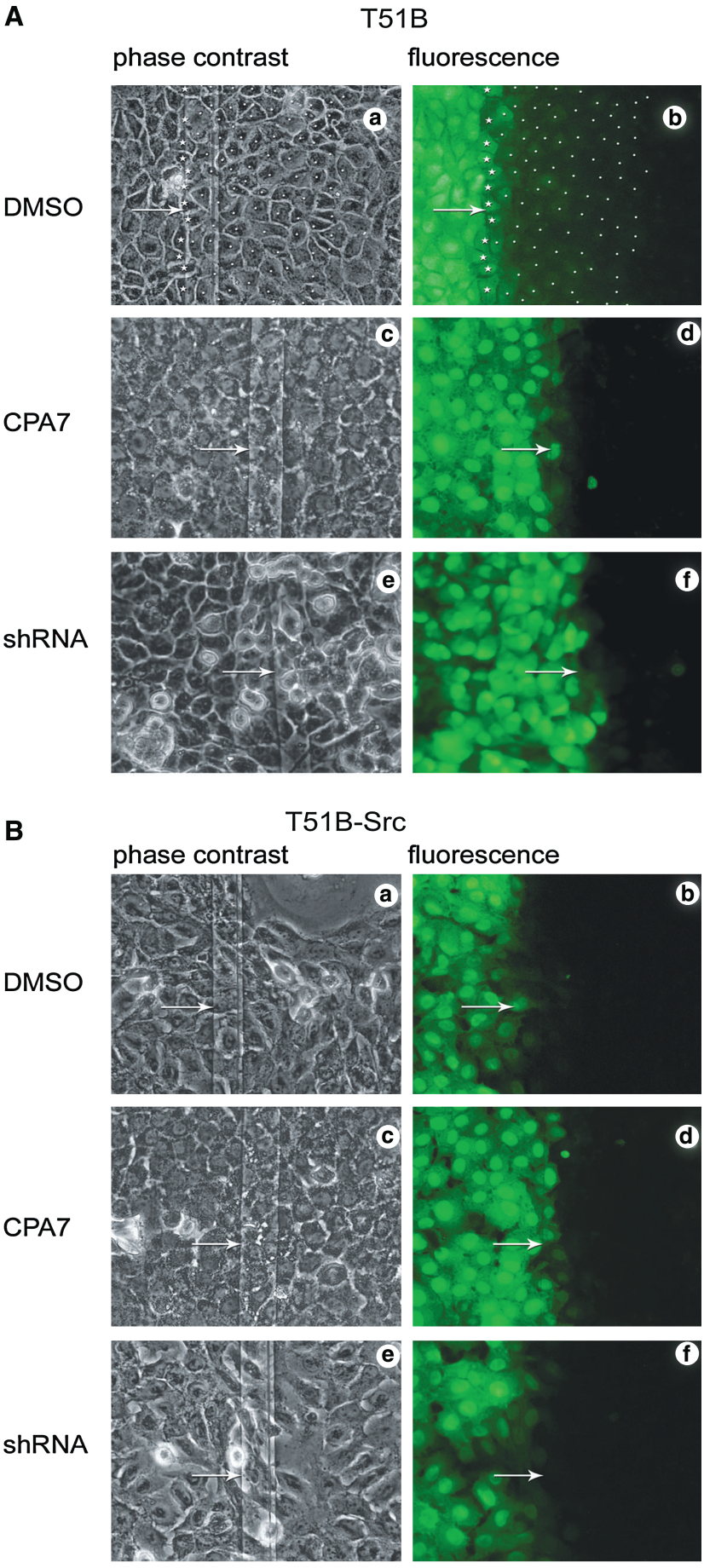

FIG. 2. (**A**) Stat3 downregulation eliminates gap junctional permeability in rat liver epithelial T51B cells. T51B cells were plated on conductive ITO-coated glass and LY electroporated after treatment with the DMSO carrier alone (**a**, **b**), or CPA7 (**c**, **d**), or infection with the sh-Stat3 lentiviral vector (**e**, **f**) (see Materials and Methods). After washing the unincorporated dye, cells from the same field were photographed under fluorescence (**b**, **d**, **f**) or phase contrast (**a**, **c**, **e**) illumination. Cells at the edge of the conductive area that were loaded with LY through electroporation were marked with a star (**a**, **b**), and cells at the nonelectroporated area that received LY through gap junctions were marked with a dot (Raptis *et al.*, 2006). Magnification, 240×. Note the extensive junctional communication in (**b**). (**B**) Stat3 downregulation does not increase gap junctional permeability in vSrc-transformed rat liver epithelial T51B cells. Same as above, T51B-Src cells. After pulse application, cells were photographed under phase contrast (**a**, **c**, **e**), or fluorescence (**b**, **d**, **f**) illumination. Magnification, 240×. Note the absence of communication, even after Stat3 downregulation (**d**, **f**). Color images available online at www.liebertonline.com/dna.

Table 1. Effect of Signal Transducer and Activator of Transcription-3 Downregulation upon Gap Junctional, Intercellular Communication

Cell line	*Treatment*[a]	*Stat3*[b] *(%)*	*GJIC*[c]	*Apoptosis % subG1*[d]
T51B	DMSO	52 ± 9	6.0 ± 2	2 ± 1
	CPA7	3 ± 2	0.2 ± 0.1	30 ± 11
	sh-Stat3	12 ± 3	0.9 ± 0.1	24 ± 9
T51B-Src	DMSO	100 ± 12	0.2 ± 0.1	5 ± 2
	CPA7	4 ± 1	0.1 ± 0.1	61 ± 12
	sh-Stat3	28 ± 3	0.1 ± 0.1	48 ± 14

[a]Cells were treated with 50 μM CPA7 or the DMSO carrier (0.00125%) for 24 h, or infected with a lentivirus vector expressing a Stat3-specific shRNA (see Materials and Methods).

[b]Stat3-ptyr705 levels were measured by Western blotting. Numbers represent relative values obtained by quantitation analysis, with the average of the values for v-Src-expressing T51B cells taken as 100%. Averages of at least three experiments ± SEM are shown. Data from sparsely growing cells are presented, but the relative increases were the same regardless of cell density (Vultur *et al.*, 2005). The transcriptional activity values obtained paralleled the Stat3-705 phosphorylation levels indicated (Fig. 3B; see Materials and Methods).

[c]GJIC was assessed by *in situ* electroporation 2 days after confluence, which was determined visually and by imaging analysis (Fig. 1; see Materials and Methods). Quantitation was achieved by dividing the number of cells into which dye had transferred through gap junctions (denoted by dots), by the number of cells at the edge of the electroporated area (denoted by stars, Fig. 2A, panels a and b). Numbers are averages of at least three experiments, where transfer from more than 200 cells was examined.

[d]After treatment, fixed cells were stained with propidium iodide and their subG1 profile was examined by fluorescence-activated cell sorting analysis (see Materials and Methods).

Materials and Methods). The results show that CPA7 treatment did result in an increase in PARP cleavage, indicating apoptosis (Fig. 4B). In addition, FACS analysis showed a substantial increase in cells with subG1 DNA content upon CPA7 treatment, or after infection with the sh-Stat3 lentivirus vector (Table 1). These findings indicate that Stat3 inhibition at high cell densities causes apoptosis, consistent with previous data regarding mouse fibroblasts and breast cancer lines (Anagnostopoulou *et al.*, 2006a, 2006b), and hint at a possible link between GJIC reduction and apoptosis induced by Stat3 inhibition.

Discussion

Results from a number of labs indicated that, constitutively active forms of Ras can suppress GJIC (Atkinson and Sheridan, 1988; Brownell *et al.*, 1996a). Moreover, this reduction in junctional permeability could be effected at lower levels than the levels required for full neoplastic conversion by this oncogene (Brownell *et al.*, 1997). Similarly, oncogenes such as the activated form of the Hsp90 chaperone, Hsp90N, which can activate the Raf protooncogene product, although unable to fully transform, can eliminate junctional permeability in normal rat F111 fibroblasts (Grammatikakis *et al.*, 2002), which stresses the role of oncogenes as GJIC suppressors. The prototype oncogene vSrc also suppresses GJIC, through direct phosphorylation of Cx43 at tyr247 and tyr265 (Lampe and Lau, 2004; Warn-Cramer and Lau, 2004), or indirectly through activation of the Protein kinase C or the Ras/Raf/Mek/Erk pathways (Zhou *et al.*, 1999; Lampe *et al.*, 2000; Shah *et al.*, 2002; Bao *et al.*, 2004; Griner and Kazanietz, 2007). It was further demonstrated that the suppression of gap junctional permeability by vSrc or middle tumor antigen, an oncogene whose function depends upon binding to and activation of cSrc (Dilworth, 2002), requires cRas signaling (Brownell *et al.*, 1996b), and independent from Erk action

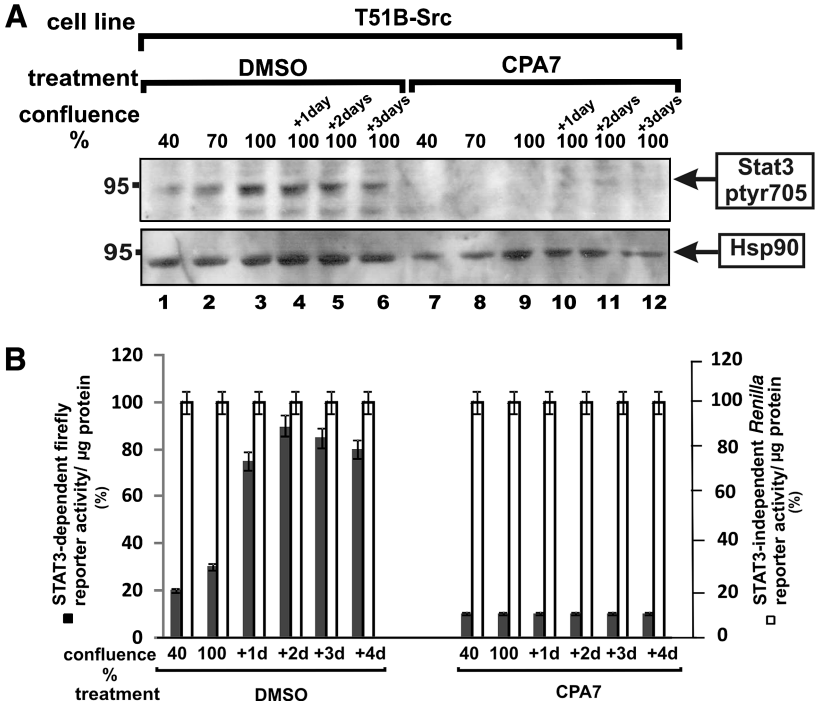

FIG. 3. CPA7 treatment eliminates Stat3-tyr705 phosphorylation and transcriptional activity in T51B-Src cells. (**A**) T51B-Src cells were grown to different densities from 40% confluence to 3 days postconfluence as indicated and treated with 50 μM CPA7 (lanes 7–12) or the DMSO carrier alone (0.00125%, lanes 1–7) for 24 h, at which time cell extracts were probed for Stat3-ptyr705 or Hsp90 as a loading control. (**B**) T51B-Src cells were transfected with a plasmid expressing a firefly luciferase gene under control of a Stat3 responsive promoter (■), and a Stat3 independent promoter driving a *Renilla* luciferase gene (□) (see Materials and Methods). After transfection, cells were plated to different densities and treated with CPA7 or the DMSO carrier alone for 24 h, at which time firefly and *Renilla* luciferase activities were determined.

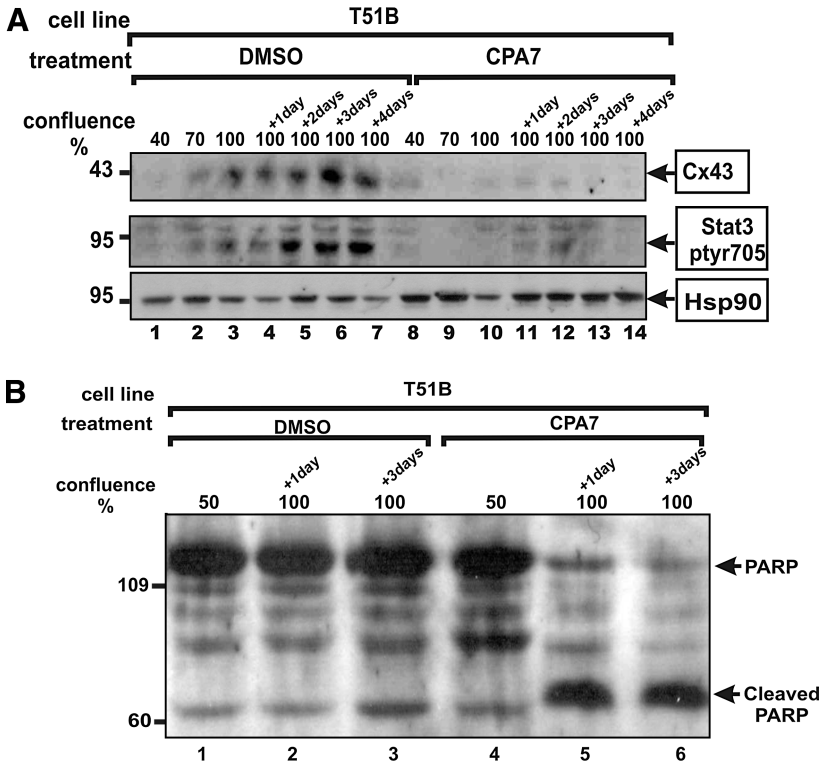

FIG. 4. (**A**) Stat3 inhibition reduces Cx43 levels. T51B cells were plated in 3-cm Petri dishes, grown to different densities and treated with CPA7 (lanes 8–14) or the DMSO carrier (0.00125%) alone (lanes 1–7), as indicated. Cell extracts were probed for Cx43 (top), Stat3 (middle), or Hsp90 as a loading control. Arrows point to the position of Cx43, Stat3-ptyr705, or Hsp90, respectively. (**B**) PARP-cleavage analysis: to assess apoptosis induction, T51B cells were grown to different densities and treated with CPA7 (lanes 4–6) or the DMSO carrier (0.00125%) alone (lanes 1–3) as indicated, and cell extracts probed with an antibody to PARP. Arrows point to the position of PARP (113 kDa) and cleaved PARP (89 kDa), respectively.

(Ito *et al.*, 2006). Since the Ras and Stat3 pathways are often coordinately regulated by growth factors or oncogenes, we looked for a possible role of Stat3 in the suppression of junctional communication. Unexpectedly, our findings indicated that, contrary to Ras downregulation, Stat3 inhibition does not restore junctional permeability in T51B cells transformed by activated Src. On the contrary, our results revealed that Stat3 inhibition eliminated GJIC in normal fibroblasts and epithelial cells that have extensive GJIC. These findings stress the role of Stat3 as a positive regulator of gap junctional communication. This is in sharp contrast to the effect of cRas, which was shown to cause gap junction closure in normal fibroblasts (Brownell *et al.*, 1996a). Therefore, Src has a dual role upon GJIC—acting as an inhibitor through direct or indirect phosphorylation of Cx43, and an activator through activation of Stat3. In the presence of high Src activity the former prevails, so that the net effect is gap junction closure.

Besides its role in promoting growth, Stat3 activates a number of antiapoptotic genes, such as survivin (Gritsko *et al.*, 2006), *Bcl-xL*, and *Mcl-1* (Yu and Jove, 2004). Apoptotic death is accompanied by dramatic shape changes, such as rounding, which force the cell to give up all its intercellular contacts, including the gap junctions. In fact, it was recently demonstrated that induction of apoptosis by cycloheximide, etoposide, or puromycin led to a rapid loss of cell coupling, most probably due to caspase-3-mediated degradation of Cx43, in primary bovine lens epithelial cells and NIH3T3 fibroblasts (Theiss *et al.*, 2007). Our results show that Stat3 inhibition, which in densely growing cells induces apoptosis (Anagnostopoulou *et al.*, 2006a), results in a dramatic reduction in Cx43 levels and GJIC, which is consistent with the above observations. In any event, our findings demonstrate that the function of Stat3, although it is generally growth promoting and in an activated form can act as an oncogene, is actually required for the maintenance of junctional permeability. The interruption of gap junctional communication upon Stat3 inhibition would therefore confine the apoptotic event to single cells, and this might be essential for the maintenance of tissue integrity.

Acknowledgments

We would like to thank Dr. Mike Baird and Shalyn Littlefield for CPA7 synthesis, the Center for Manufacturing of Advanced Ceramics and Nanomaterials of Queen's University for laser etching services, Dr. Elissavet Kardami for a generous gift of Cx43 antibody, and Kevin Firth, P.Eng., Ask Sciences products, Kingston, Ontario, for engineering design. The financial assistance of the Canadian Institutes of Health Research, the Canadian Breast Cancer Foundation (Ontario Chapter), the Natural Sciences and Engineering Research Council of Canada, the Canadian Breast Cancer Research Alliance, the Ontario Centers of Excellence, the Breast Cancer Action Kingston, and the Clare Nelson bequest fund through grants to LR is gratefully acknowledged. RA was supported by a Canada Graduate Scholarships Doctoral award from the Canadian Institutes of Health Research, an Ontario Women's Health Scholars Award from the Ontario Council on Graduate Studies, and a Queen's University Graduate Award. AV was supported by studentships and a postdoctoral fellowship from NSERC, the Ontario Graduate Studentship Program, and a Queen's University Graduate Award. MG was supported by postdoctoral fellowships from the U.S. Army Breast Cancer Program and from the Ministry of Research and Innovation of the Province of Ontario and the Advisory Research Committee of Queen's University. AA was supported by a traineeship from the U.S. Army Breast Cancer Program.

Disclosure Statement

The authors do not have any conflict of interest.

References

Anagnostopoulou, A., Cao, J., Vultur, A., Firth, K.L., and Raptis, L. (2007). Examination of gap junctional, intercellular communication by *in situ* electroporation on two co-planar indium-tin oxide electrodes. Mol Oncol **1,** 226–231.

Anagnostopoulou, A., Vultur, A., Arulanandam, R., Cao, J., Turkson, J., Jove, R., Kim, J.S., Glenn, M., Hamilton, A.D., and Raptis, L. (2006a). Differential effects of Stat3 inhibition in sparse vs confluent normal and breast cancer cells. Cancer Lett **242,** 120–132.

Anagnostopoulou, A., Vultur, A., Arulanandam, R., Cao, J., Turkson, J., Jove, R., Kim, J.S., Glenn, M., Hamilton, A.D., and Raptis, L. (2006b). Role of Stat3 in normal and SV40 transformed cells. Trends in Cancer Res **2,** 93–103.

Atkinson, M.M., and Sheridan, J.D. (1988). Altered junctional permeability between cells transformed by v-ras, v-mos, or v-src. Am J Physiol **255,** C674–C683.

Azarnia, R., and Loewenstein, W.R. (1987). Polyomavirus middle t antigen downregulates junctional cell-to-cell communication. Mol Cell Biol **7,** 946–950.

Azarnia, R., and Russell, T.R. (1985). Cyclic AMP effects on cell-to-cell junctional membrane permeability during adipocytic differentiation of 3T3-L1 fibroblasts. J Cell Biol **100,** 265–269.

Bao, X., Reuss, L., and Altenberg, G.A. (2004). Regulation of purified and reconstituted connexin 43 hemichannels by protein kinase C-mediated phosphorylation of Serine 368. J Biol Chem **279,** 20058–20066.

Beardslee, M.A., Laing, J.G., Beyer, E.C., and Saffitz, J.E. (1998). Rapid turnover of connexin43 in the adult rat heart. Circ Res **83,** 629–635.

Bromberg, J.F., Wrzeszczynska, M.H., Devgan, G., Zhao, Y., Pestell, R.G., Albanese, C., and Darnell, J.E., Jr. (1999). Stat3 as an oncogene. Cell **98,** 295–303.

Brownell, H.L., Narsimhan, R., Corbley, M.J., Mann, V.M., Whitfield, J.F., and Raptis, L. (1996a). Ras is involved in gap junction closure in mouse fibroblasts or preadipocytes but not in differentiated adipocytes. DNA Cell Biol **15,** 443–451.

Brownell, H.L., Whitfield, J.F., and Raptis, L. (1996b). Cellular Ras partly mediates gap junction closure by the polyoma virus middle tumor antigen. Cancer Lett **103,** 99–106.

Brownell, H.L., Whitfield, J.F., and Raptis, L. (1997). Elimination of intercellular junctional communication requires lower Ras^{leu61} levels than stimulation of anchorage-independent proliferation. Cancer Detect Prev **21,** 289–294.

Dilworth, S.M. (2002). Polyoma virus middle T antigen and its role in identifying cancer-related molecules. Nat Rev Cancer **2,** 951–956.

Frank, D.A. (2007). Stat3 as a central mediator of neoplastic cellular transformation. Cancer Lett **251,** 199–210.

Frenzel, E.M., and Johnson, R.G. (1996). Gap junction formation between cultured embryonic lens cells is inhibited by antibody to N-cadherin. Dev Biol **179,** 1–16.

Germain, D., and Frank, D.A. (2007). Targeting the cytoplasmic and nuclear functions of signal transducers and activators of transcription 3 for cancer therapy. Clin Cancer Res **13,** 5665–5669.

Grammatikakis, N., Vultur, A., Ramana, C.V., Siganou, A., Schweinfest, C.W., and Raptis, L. (2002). The role of Hsp90N, a new member of the Hsp90 family, in signal transduction and neoplastic transformation. J Biol Chem **277,** 8312–8320.

Griner, E.M., and Kazanietz, M.G. (2007). Protein kinase C and other diacylglycerol effectors in cancer. Nat Rev Cancer **7,** 281–294.

Gritsko, T., Williams, A., Turkson, J., Kaneko, S., Bowman, T., Huang, M., Nam, S., Eweis, I., Diaz, N., Sullivan, D., Yoder, S., Enkemann, S., Eschrich, S., Lee, J.H., Beam, C.A., Cheng, J., Minton, S., Muro-Cacho, C.A., and Jove, R. (2006). Persistent activation of Stat3 signaling induces survivin gene expression and confers resistance to apoptosis in human breast cancer cells. Clin Cancer Res **12,** 11–19.

Hung, W., and Elliott, B. (2001). Co-operative effect of c-Src tyrosine kinase and Stat3 in activation of hepatocyte growth factor expression in mammary carcinoma cells. J Biol Chem **276,** 12395–12403.

Ito, S., Ito, Y., Senga, T., Hattori, S., Matsuo, S., and Hamaguchi, M. (2006). v-Src requires Ras signaling for the suppression of gap junctional intercellular communication. Oncogene **25,** 2420–2424.

Khoo, N.K., Zhang, Y., Bechberger, J.F., Bond, S.L., Hum, K., and Lala, P.K. (1998). SV40 tag transformation of the normal invasive trophoblast results in a premalignant phenotype. II. Changes in gap junctional intercellular communication. Int J Cancer **77,** 440–448.

Lampe, P.D., and Lau, A.F. (2004). The effects of connexin phosphorylation on gap junctional communication. Int J Biochem Cell Biol **36,** 1171–1186.

Lampe, P.D., Tenbroek, E.M., Burt, J.M., Kurata, W.E., Johnson, R.G., and Lau, A.F. (2000). Phosphorylation of connexin43 on serine368 by protein kinase C regulates gap junctional communication. J Cell Biol **149,** 1503–1512.

Lin, R., Martyn, K.D., Guyette, C.V., Lau, A.F., and Warn-Cramer, B.J. (2006). v-Src tyrosine phosphorylation of connexin43: regulation of gap junction communication and effects on cell transformation. Cell Commun Adhes **13,** 199–216.

Littlefield, S.L., Baird, M.C., Anagnostopoulou, A., and Raptis, L. (2008). Synthesis, characterization and Stat3 inhibitory properties of the prototypical platinum(IV) anticancer drug, [PtCl3(NO2)(NH3)2] (CPA-7). Inorg Chem **47,** 2798–2804.

Pahujaa, M., Anikin, M., and Goldberg, G.S. (2007). Phosphorylation of connexin43 induced by Src: regulation of gap junctional communication between transformed cells. Exp Cell Res **313,** 4083–4090.

Raptis, L., Brownell, H.L., Firth, K.L., and Mackenzie, L.W. (1994). A novel technique for the study of intercellular, junctional communication; electroporation of adherent cells on a partly conductive slide. DNA Cell Biol **13,** 963–975.

Raptis, L., Brownell, H.L., Vultur, A.M., Ross, G., Tremblay, E., and Elliott, B.E. (2000). Specific inhibition of growth factor-stimulated ERK1/2 activation in intact cells by electroporation of a Grb2-SH2 binding peptide. Cell Growth Differ **11,** 293–303.

Raptis, L., Vultur, A., Brownell, H.L., and Firth, K.L. (2006). Dissecting pathways; *in situ* electroporation for the study of signal transduction and gap junctional communication. In *Cell Biology: A Laboratory Handbook*, Volume 2, Chapter 44. J.E. Celis, ed. (Elsevier Academic Press, Burlington, MA), pp. 341–354.

Raptis, L., Vultur, A., Brownell, H.L., Tomai, E., Anagnostopoulou, A., Arulanandam, R., Cao, J., and Firth, K.L. (2008). Electroporation of adherent cells *in situ* for the study of signal transduction and gap junctional communication. In *Electroporation Protocols*, Chapter 12. S. Li, ed. (The Humana Press Inc., Totowa, NJ), pp. 167–183.

Royal, I., Raptis, L., Druker, B.J., and Marceau, N. (1996). Downregulation of cytokeratin 14 gene expression by the polyoma virus middle T antigen is dependent on c-src association but independent of full transformation in rat liver nonparenchymal epithelial cells. Cell Growth Differ **7,** 737–743.

Shah, M.M., Martinez, A.M., and Fletcher, W.H. (2002). The connexin43 gap junction protein is phosphorylated by protein kinase A and protein kinase C: *in vivo* and *in vitro* studies. Mol Cell Biochem **238,** 57–68.

Theiss, C., Mazur, A., Meller, K., and Mannherz, H.G. (2007). Changes in gap junction organization and decreased coupling during induced apoptosis in lens epithelial and NIH-3T3 cells. Exp Cell Res **313,** 38–52.

Tomai, E., Brownell, H.L., Tufescu, T., Reid, K., Raptis, S., Campling, B.G., and Raptis, L. (1998). A functional assay for intercellular, junctional communication in cultured human lung carcinoma cells. Lab Invest **78,** 639–640.

Turkson, J., Bowman, T., Garcia, R., Caldenhoven, E., De Groot, R.P., and Jove, R. (1998). Stat3 activation by Src induces specific gene regulation and is required for cell transformation. Mol Cell Biol **18,** 2545–2552.

Turkson, J., Ryan, D., Kim, J.S., Zhang, Y., Chen, Z., Haura, E., Laudano, A., Sebti, S., Hamilton, A.D., and Jove, R. (2001). Phosphotyrosyl peptides block Stat3-mediated DNA binding activity, gene regulation, and cell transformation. J Biol Chem **276,** 45443–45455.

Turkson, J., Zhang, S., Palmer, J., Kay, H., Stanko, J., Mora, L.B., Sebti, S., Yu, H., and Jove, R. (2004). Inhibition of constitutive signal transducer and activator of transcription 3 activation by novel platinum complexes with potent antitumor activity. Mol Cancer Ther **3,** 1533–1542.

Vinken, M., Vanhaecke, T., Papeleu, P., Snykers, S., Henkens, T., and Rogiers, V. (2006). Connexins and their channels in cell growth and cell death. Cell Signal **18,** 592–600.

Vultur, A., Arulanandam, R., Turkson, J., Niu, G., Jove, R., and Raptis, L. (2005). Stat3 is required for full neoplastic transformation by the Simian Virus 40 Large Tumor antigen. Mol Biol Cell **16,** 3832–3846.

Vultur, A., Cao, J., Arulanandam, R., Turkson, J., Jove, R., Greer, P., Craig, A., Elliott, B.E., and Raptis, L. (2004). Cell to cell adhesion modulates Stat3 activity in normal and breast carcinoma cells. Oncogene **23,** 2600–2616.

Warn-Cramer, B.J., and Lau, A.F. (2004). Regulation of gap junctions by tyrosine protein kinases. Biochim Biophys Acta **1662,** 81–95.

Wei, C.J., Francis, R., Xu, X., and Lo, C.W. (2005). Connexin43 associated with an N-cadherin-containing multiprotein complex is required for gap junction formation in NIH3T3 cells. J Biol Chem **280,** 19925–19936.

Yu, H., and Jove, R. (2004). The STATs of cancer—new molecular targets come of age. Nat Rev Cancer **4,** 97–105.

Zhou, L., Kasperek, E.M., and Nicholson, B.J. (1999). Dissection of the molecular basis of pp60(v-src) induced gating of connexin 43 gap junction channels. J Cell Biol **144,** 1033–1045.

Address correspondence to:
Leda Raptis, Ph.D.
Departments of Microbiology and Immunology and Pathology
Queen's University
Botterell Hall, Stuart St. 18
K7L3N6 Kingston, Ontario
Canada

E-mail: raptisl@queensu.ca

Received for publication November 14, 2008; received in revised form January 26, 2009; accepted April 6, 2009.

EXPERIMENTAL CELL RESEARCH 316 (2010) 875–886

available at www.sciencedirect.com

ScienceDirect

www.elsevier.com/locate/yexcr

Research Article

Activated Rac1 requires gp130 for Stat3 activation, cell proliferation and migration

Rozanne Arulanandam[a], *Mulu Geletu*[a], *Hélène Feracci*[b], *Leda Raptis*[a,*]

[a] *Departments of Microbiology and Immunology and Pathology and Molecular Medicine, and Queen's University Cancer Institute, Queen's University, Botterell Hall, Rm. 713, Kingston, Ontario, Canada K7L 3N6*
[b] *Université Bordeaux 1, Centre de Recherche Paul Pascal, CNRS UPR 8641, 33600 Pessac, France*

ARTICLE INFORMATION

Article Chronology:
Received 31 August 2009
Revised version received
15 October 2009
Accepted 16 October 2009
Available online 21 October 2009

Keywords:
Rac/Cdc42
Stat3
IL6
gp130
Erk1/2
Cell migration

ABSTRACT

Rac1 (Rac) is a member of the Rho family of small GTPases which controls cell migration by regulating the organization of actin filaments. Previous results suggested that mutationally activated forms of the Rho GTPases can activate the Signal Transducer and Activator of Transcription-3 (Stat3), but the exact mechanism is a matter of controversy. We recently demonstrated that Stat3 activity of cultured cells increases dramatically following E-cadherin engagement. To better understand this pathway, we now compared Stat3 activity levels in mouse HC11 cells before and after expression of the mutationally activated Rac1 (Rac^{V12}), at different cell densities. The results revealed for the first time a dramatic increase in protein levels and activity of both the endogenous Rac and Rac^{V12} with cell density, which was due to inhibition of proteasomal degradation. In addition, Rac^{V12}-expressing cells had higher Stat3, tyrosine-705 phosphorylation and activity levels at all densities, indicating that Rac^{V12} is able to activate Stat3. Further examination of the mechanism of Stat3 activation showed that Rac^{V12} expression caused a surge in mRNA of Interleukin-6 (IL6) family cytokines, known potent Stat3 activators. Knockdown of gp130, the common subunit of this family reduced Stat3 activity, indicating that these cytokines may be responsible for the Stat3 activation by Rac^{V12}. The upregulation of IL6 family cytokines was required for cell migration and proliferation induced by Rac^{V12}, as shown by gp130 knockdown experiments, thus demonstrating that the gp130/Stat3 axis represents an essential effector of activated Rac for the regulation of key cellular functions.

Introduction

Rho family GTPases are intracellular molecular switches cycling between the active, GTP-bound state and the inactive, GDP-bound form [1]. Upon activation, the Rho GTPases can activate a distinct panel of effectors to regulate cellular functions. In fact, the Rho family members RhoA, Rac1 and Cdc42 are best known as master regulators of the actin cytoskeleton, promoting the formation of stress fibers, lamellipodia or filopodia, respectively. In addition, Rho GTPases are known growth stimulators that act by modulating key cell cycle regulators, such as cyclin D1 and the transcription factor Nuclear Factor-kappaB (NFkB), at the transcriptional level [2,3].

The Signal Transducers and Activators of Transcription (STATs) were discovered as latent cytoplasmic transcription factors that are activated by a number of cytokines and growth factors. Among

* *Corresponding author.* Fax: +1 613 533 6796.
E-mail address: raptisl@queensu.ca (L. Raptis).

Abbreviations: STATs, Signal Transducers and Activators of Transcription; IL6, Interleukin-6; ptyr, phosphorylated tyrosine; Erk, Extracellular-signal activated kinase; SH2, Src homology 2; JAKs, Janus kinases; Hsp90, Heat shock protein 90; NFkB, Nuclear Factor-kappaB; IKK, IkappaB kinase

0014-4827/$ – see front matter © 2009 Elsevier Inc. All rights reserved.
doi:10.1016/j.yexcr.2009.10.017

seven mammalian STAT genes identified, Stat3 is found to be overexpressed in a number of tumor cell lines and carcinomas [4]. The fact that a constitutively active form of Stat3 alone is sufficient to transform cultured fibroblasts to anchorage-independence and tumorigenicity points to an etiological role for Stat3 in neoplasia [5]. Like other STAT proteins, Stat3 is latent in the cytoplasm in an unstimulated cell. Following ligand engagement and receptor phosphorylation, Stat3 binds the activated receptor through its Src homology 2 (SH2) domain and is activated through phosphorylation by the receptor itself or by the associated JAKs (Janus kinases) or Src family kinases. Phosphorylation at a critical tyrosine, tyr-705 activates Stat3 by stabilizing the association of two monomers through reciprocal SH2-phosphotyrosine interactions. The Stat3 dimer then migrates to the nucleus where it binds to target sequences, leading to the transcriptional activation of specific genes, such as myc, Bcl-xL, cyclin D, survivin, Hepatocyte Growth Factor [6] and to the downregulation of the p53 antioncogene [7,8].

Previous results suggested a functional link between the Rho GTPases and Stat3 but the mechanism is still unclear. Indeed, while in one study it was reported that mutationally activated Rac1 can directly interact with Stat3 in co-immunoprecipitation assays [9], other data showed that Rac1 indirectly activates Stat3 through autocrine induction of interleukin-6 (IL-6) [10], while another group reported that the Rho GTPases can activate Stat3 independent from IL6 action [11]. We and others recently demonstrated a dramatic increase in the activity of Stat3 triggered by cell to cell contact in a variety of cell lines [12–16]. For this reason, the modulation of Stat3-ptyr705 levels by cell density must be taken into account in experiments assessing the effect of proto-oncogenes such as the Rho GTPases upon Stat3 function.

In this communication, we revisited the question of the mechanism of Stat3 activation by Rac1 and Cdc42, in light of the above findings. The results indicate that cell density alone causes a dramatic increase in protein levels and activity of both the endogenous cRac1 (Rac) and Cdc42, and the mutationally activated Rac1 (Rac^{V12}) and $Cdc42^{V12}$ in mouse HC11 epithelial cells, through inhibition of proteasomal degradation. Furthermore, lines expressing activated Rac^{V12} had higher Stat3 activity levels at all cell densities examined, indicating that Rac^{V12} is, in fact, able to activate Stat3. The Stat3 increase was mediated through the expression of IL6 family cytokines, as shown through knockdown of the gp130, common subunit of the family. Gp130 function and Stat3 activation were required for cell migration and increase in proliferation induced by mutationally activated Rac and Cdc42, as shown by genetic knockdown experiments, thus demonstrating that the gp130/Stat3 axis represents an essential effector of activated Rac in the regulation of both of these essential cellular functions.

Materials and methods

Cell lines, culture techniques and gene expression

The normal mouse mammary epithelial line HC11 is a prolactin-responsive cell clone originally isolated from the COMMA-1D mouse mammary epithelial cell line derived from a female Balb/c mouse in mid-gestation [17]. Cell confluence was estimated visually and quantitated by imaging analysis of live cells under phase contrast using a Leitz Diaplan microscope and the MCID-elite software (Imaging Research, St. Catharine's Ont.).

For NFkB inhibition, cells were treated with 20 μM IKK-inhibitorIII (BMS-345541) or 20 μM/ml CAPE (EMD Biosciences). JAK-inhibitor-1 (EMD Biosciences) or MG132 (Sigma) were added at the indicated concentrations. Treatment with the JAK-inhibitor-1 was for 24 h and with MG132 for 8 h. The CPA7, platinum Stat3 inhibitor was prepared as described [18] and used at a 50 μM concentration. Cell viability was assessed by trypan blue exclusion and by replating cells in medium lacking the inhibitors. IL6 was purchased from Invitrogen.

For gp130 knockdown, a mouse pSM2 retroviral target gene shRNA set (Cat#. RMM4530-NM_010560, Supplementary Table S1) was purchased from Open Biosystems. V2MM-70734 was the most efficient. Infected cells were selected for puromycin resistance. Rac^{V12} was expressed with a retroviral vector (a gift of Dr John Collard, [19]). Rac^{L61}, $Cdc42^{V12}$ and wtRac1 were expressed through plasmid transfection under control of the CMV promotor (plasmids were a gift of Dr. Graham Côté, Queen's University). Transient transfections for wtRac1 and Rac^{L61} expression were performed with Lipofectamine Plus (Invitrogen). To effectively compare the consequences of wtRac1 vs. Rac^{L61} expression upon Stat3 activity, HC11 cells were transfected with each of their respective plasmids and the next day plated at 3×10^6 cells/3 cm petri, equivalent to 2 days post-confluence, as before [20]. 24 h later, cell extracts were prepared and Western blots probed with the indicated antibodies.

For neutralisation of IL6 the #ab6672 antibody (Abcam) was used, while for neutralisation of LIF we used the antibody #L9152 (Sigma), at concentrations of 0.425 μM/ml and 1 ng/ml, respectively, according to the manufacturers' protocols.

Western blotting and immunoprecipitation

Detergent cell extracts were prepared as described [12]. Following a careful protein determination (BCA-1 Protein assay kit, Sigma), 30 or 100 μg of clarified cell extract were submitted to SDS-PAGE, as indicated. Blots were cut into strips and probed with antibodies specific for the tyr-705 phosphorylated Stat3 (Cell Signalling), total Stat3 (Cell Signalling), the dually phosphorylated form of Extracellular-signal activated kinase Erk1/2 (Biosource), survivin (Cell Signalling), p21 (Biosource), gp130 (Sigma) or Heat shock protein 90 (Hsp90, Stressgen) followed by alkaline phosphatase, or Horseradish Peroxidase-conjugated secondary antibodies (Jackson Labs). Rac1 and Cdc42 antibodies (BD Transduction Labs) recognised both the endogenous and mutant Rac or Cdc42, respectively. To examine the degree of Rac ubiquitination, extracts were immunoprecipitated with anti-ubiquitin antibodies (Biomol) and blotted against Rac1 or myc-tag (for Rac^{L61}, antibody 9E10, Sigma). In all cases, bands were visualized using enhanced chemiluminescence (PerkinElmer Life Sciences), or SuperSignal West Femto Maximum Sensitivity Substrate (Pierce). Quantitation was achieved by fluorimager analysis using the FluorChem program (AlphaInnotech Corp). In all cases Stat3-ptyr705 band intensities were normalized to Hsp90 levels of the same samples. Jak1 phosphorylation was examined by immunoprecipitation against total Jak1, followed by blotting with a Jak-ptyr1022/1023 antibody (Cell Signalling).

Rac/Cdc42 activation assays were performed using GST-PAK pull-down assays with the Rac/Cdc42 activation assay kit

(Cytoskeleton, #BK035). Briefly, the beads were coated with glutathione-S-transferase (GST) fused to the binding domain of p21-activated kinase, PAK (PAK-PBD) in pulldown assays. Adding twice the amount of PBD-coated beads did not increase the signal, indicating that the amount of binding partner used in the detection was not limiting.

Photoshop (Adobe) or Corel Draw software were used for the organization of non-adjusted, original images and blots.

qRT-PCR assays

For quantitative RT-PCR, the delta ct (Dct) value was calculated from the given ct value by the formula: $Dct = (ct_{sample} - ct_{control})$. For the qRT-PCR cytokine array, we used the PAMM-021A kit (SA Biosciences) with an RT-PCR for IL6 run in parallel, according to the manufacturer's protocol.

Results

Cell density inhibits cRac1 proteasomal degradation

We recently demonstrated that cell–cell contacts through E-cadherin engagement in HC11, normal mouse breast epithelial cells causes a dramatic increase in the cellular Rac1 (Rac) and Cdc42 protein levels [20]. To explore the possibility that the increase in Rac/Cdc42 with cell density (Figs. 1A and B, lanes 1–7) might be due to inhibition of proteasome-mediated degradation, we at first made use of the MG132 proteasome inhibitor [21]. As shown in Fig. 2A, MG132 treatment of sparsely growing HC11 cells caused a substantial increase in Rac protein levels, as well as the $p21^{CIP/WAF}$, p53 substrate serving as a positive control [22]. This observation points to a role for the proteasome in Rac degradation. At the same time, the levels of phosphorylated, i.e. activated extracellular-signal activated kinase (Erk1/2) remained unchanged following MG132 treatment, suggesting that Rac may be selectively degraded by the proteasome.

We next examined the effect of ubiquitin overexpression upon Rac protein levels, by transfecting HC11 cells with a plasmid consisting of a CMV promotor driving the transcription of an mRNA encoding a multimeric precursor molecule composed of eight, NH2-terminal hexa-histidine tagged ubiquitin units [23]. The results revealed that ubiquitin overexpression caused a reduction in Rac total protein levels which was more pronounced at lower cell densities, while pErk1/2 levels remained unaffected (Fig. 2B).

To further investigate whether Rac itself might be a substrate of the proteasome in sparsely growing cells, we examined whether Rac is modified by ubiquitin tagging. To this effect, we searched for the presence of Rac in the pool of ubiquitinated proteins, by probing anti-ubiquitin immunoprecipitates from HC11 cells for Rac by Western blotting. As shown in Fig. 2C, a diffuse band of ubiquitin-tagged Rac, consistent with short chain polyubiquitination [24], was detected in immunoprecipitates from HC11 cells grown to 30% confluence (lane 5). This band was very weak at 100% confluence (lane 6), possibly due to inhibition of ubiquitination at high cell densities. When the anti-ubiquitin antibody was omitted (lane 1) or replaced with normal mouse IgG (lane 3) or an unrelated, control mouse monoclonal antibody (not shown), no Rac was found in the immunoprecipitates from 30% confluent cultures. The above data taken together indicate that Rac itself is, in fact, a substrate of the proteasome in sparsely growing HC11 cultures, and that cell confluence inhibits Rac ubiquitination and proteasomal degradation.

Cell density upregulates activated Rac^{V12} levels through inhibition of proteasomal degradation

It was previously shown that the active, GTP-bound form of Rac is preferentially degraded by the proteasome [25]. Therefore, to examine the impact of cell density upon the levels of mutationally activated Rac^{V12} or Rac^{L61}, the latter labelled with a myc-tag, these genes were stably expressed in HC11 cells (see Materials and methods). A number of colonies were picked and, since cell density affects Rac protein levels (Fig. 1), screening for total Rac or myc-Rac by Western blotting was performed at 40% confluence. Three clones from each, expressing high Rac levels (H-Rac^{V12} and H-Rac^{L61}) were used for further study. Cells were plated in 3 cm dishes and when 30% confluent and at different times thereafter, Rac protein levels were evaluated by Western blotting. As shown in Fig. 1A (lanes 8–14), the levels of Rac^{V12} increased dramatically with cell density (lane 8 vs. 14). H-Rac^{V12} cells had ~3× higher total Rac levels than the parental HC11, at all densities examined. Two other Rac^{V12} and three Rac^{L61}-expressing clones gave the same results (not shown). The above results taken together indicate that, similar to cRac1 [20], activated Rac^{V12} and Rac^{L61} are also subject to density-dependent upregulation.

The effect of cell density upon Rac^{V12} activity was examined next. Cells were plated in petri dishes and when ~30% confluent, and over several days thereafter, Rac activity was measured by assessing the binding between Rac-GTP and its effector p21-activated kinase (PAK) in cell extracts using pull-down assays (see Materials and methods). As shown in Fig. 1, there was a dramatic increase in Rac activity with cell density, in both the parental line (lanes 1–7), and in Rac^{V12}-expressing, H-Rac^{V12} cells, at all densities examined (lanes 8–14), in parallel with Rac protein levels. Clones expressing the mutationally activated, $Cdc42^{V12}$ gave similar results (Fig. 1B). The above findings taken together indicate that cell density, besides an increase in total Rac/Cdc42 protein levels, it also causes a dramatic increase in both Rac/Cdc42 and Rac^{V12}/$Cdc42^{V12}$ activity. It follows that, cell density has to be taken into account when the effect of Rac^{V12} upon Stat3 is examined.

To better control the degree of cell–cell contact, irrespective of differences in cell growth patterns, we repeated the experiments by plating different numbers of HC11 or H-Rac^{V12} cells (0.4×10^6, 0.7×10^6, 1.0×10^6, 1.3×10^6, 1.8×10^6 or 2.5×10^6 per 3 cm petri, respectively), so that they would reach the same densities as above within 24 h [20]. At that time, cells were lysed and Rac protein levels and activity analysed as above. In all cases, very similar results were obtained, indicating that it is the extent of cell–cell contact, regardless of time in culture beyond 24 h, that is responsible for the increase in Rac protein and activity (not shown).

The potential role of ubiquitination upon the levels of the mutationally activated, Rac^{V12} was examined next. As for Rac in HC11 cells (Fig. 2C, lanes 5 and 6), anti-ubiquitin immunoprecipitates of Rac^{V12}-expressing cells grown to different densities were probed with an anti-Rac1 antibody. As shown in Fig. 2C (lane 8), a diffuse band of ubiquitin-tagged Rac [24], was detected in immunoprecipitates from cells grown to 30% confluence. Cells grown to 100% confluence on the other hand, had very low levels

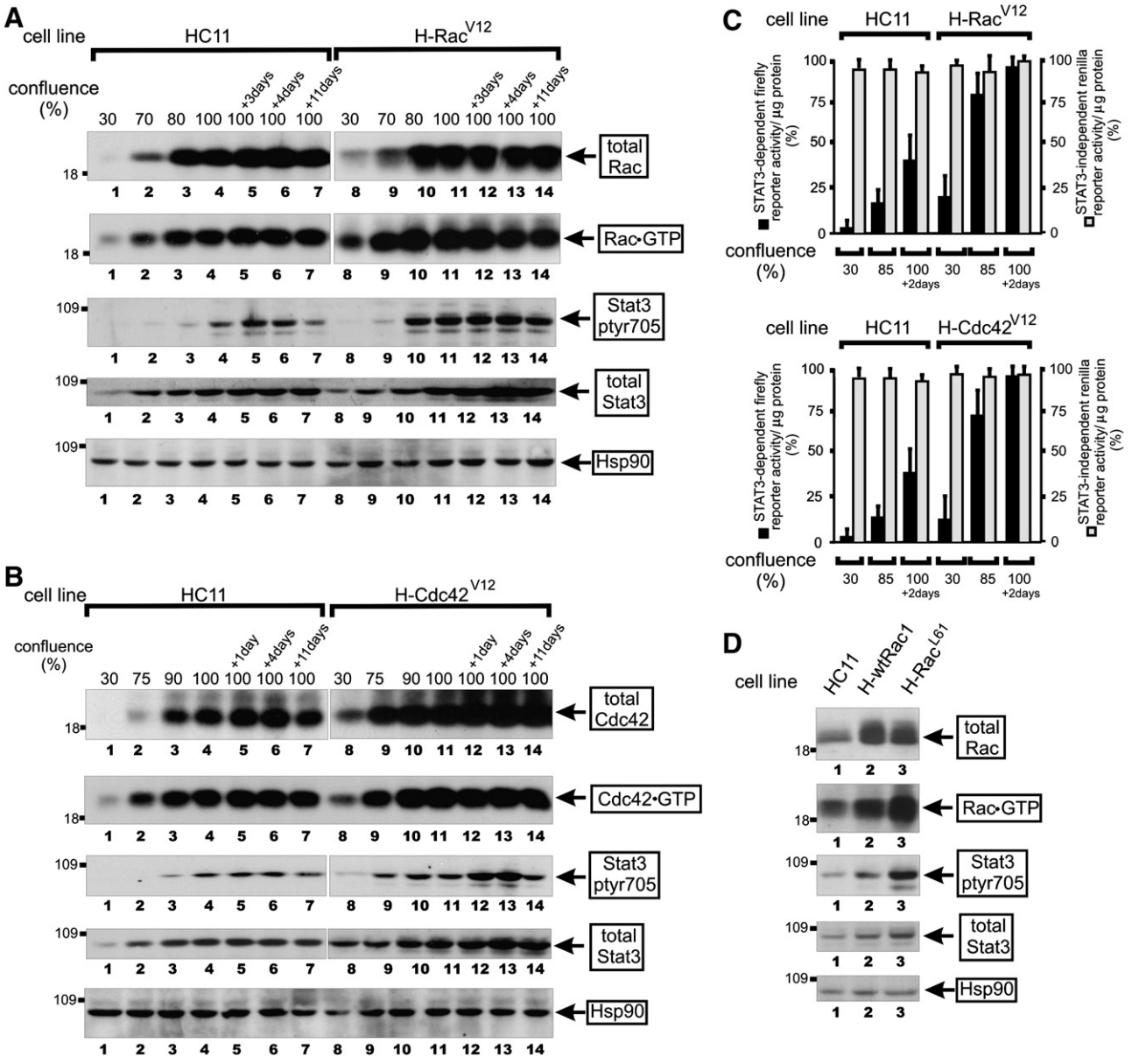

Fig. 1 – Rac^{V12} and Cdc42^{V12} activate Stat3 in HC11 cells at all cell densities. (A) Both endogenous and mutant Rac^{V12} protein levels and activity are dramatically increased by cell density, while Rac^{V12} expression increases Stat3-ptyr705 levels at all cell densities. HC11 cells (lanes 1–7) or their counterparts stably expressing activated Rac^{V12} (lanes 8–14) were grown to increasing densities, up to 11 days post-confluence. Detergent cell lysates were probed for total Rac, active Rac-GTP, Stat3-ptyr705, total Stat3 or Hsp90 as a loading control, as indicated (see Materials and methods). Numbers at the left refer to molecular weight markers. (B) Both endogenous and mutant Cdc42^{V12} protein levels and activity are dramatically increased by cell density, while Cdc42^{V12} expression increases Stat3-ptyr705 levels at all cell densities. HC11 cells (lanes 1–7) or their counterparts stably expressing activated Cdc42^{V12} (lanes 8–14) were grown to increasing densities, up to 11 days post-confluence. Detergent cell lysates were probed for total Cdc42, active Cdc42-GTP, Stat3-ptyr705, total Stat3 or Hsp90 as a loading control, as indicated. (C) Rac^{V12} and Cdc42^{V12}-expression increases Stat3 transcriptional activity. HC11 and Rac^{V12} (top panel)- and Cdc42 ^{V12} (bottom panel)-expressing cells were transfected with the Stat3-dependent p*Luc*TKS3 and the Stat3-independent pRLSRE reporters and grown to the indicated densities. Firefly (■) or *Renilla* (□) luciferase activities were determined in detergent cell extracts [12]. Values shown represent luciferase units expressed as a percentage of the highest value obtained, means ± s.e.m. of at least 3 experiments, each performed in triplicate. (D) Rac^{L61} is more effective than wtRac1 at increasing Stat3-705 phosphorylation. HC11 cells (lane 1), or their counterparts transfected with wtRac1 (lane 2) or Rac^{L61} (lane 3) were plated at 3×10^6 cells/3 cm plate (see Materials and methods) and detergent cell lysates probed for total Rac, active Rac-GTP, Stat3-ptyr705, total Stat3 or Hsp90 as a loading control, as indicated. Numbers at the left refer to molecular weight markers.

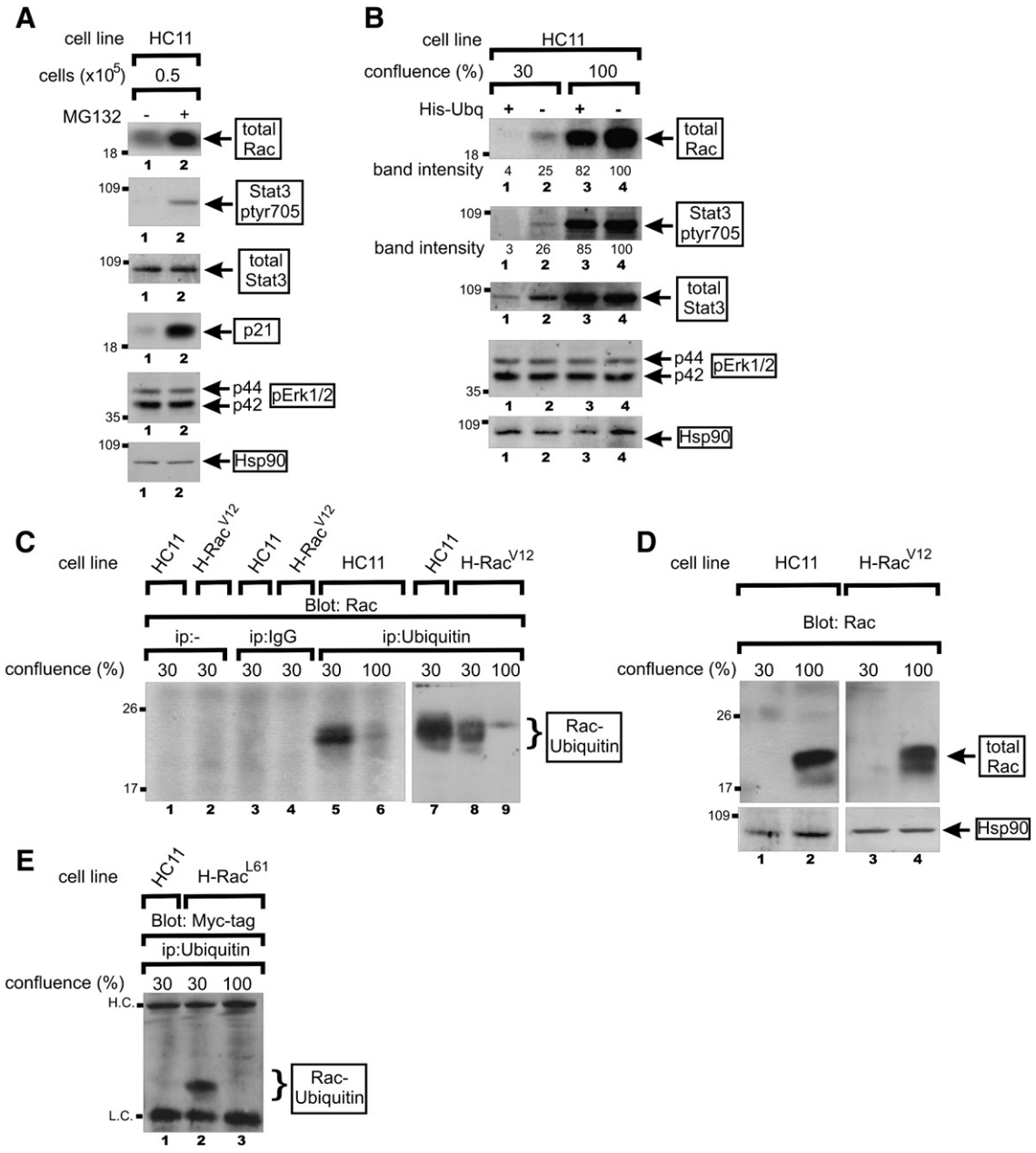

Fig. 2 – Cell density inhibits the proteasomal degradation of Rac. (A) The proteasome inhibitor, MG132 increases total Rac and Stat3-ptyr705 levels. Sparsely growing HC11 cells were treated with 10 mM of the proteasome inhibitor, MG132 (lane 2), or buffer alone (lane 1) for 8 h. Detergent cell extracts were probed for total Rac, Stat3-ptyr705, total Stat3, p21$^{CIP/WAF}$, pErk1/2 or Hsp90 as a loading control, as indicated. (B) Ubiquitin overexpression leads to Rac degradation. HC11 cells were transfected with a plasmid consisting of a CMV promotor driving the transcription of an mRNA encoding eight ubiquitin units with a his6 tag (His-Ubq, lanes 1 and 3) and grown to 30% (lanes 1 and 2) or 100% (lanes 3 and 4) confluence. Extracts were probed for Rac, Stat3-ptyr705, total Stat3, pErk1/2 or Hsp90, as indicated. Numbers under the lanes refer to total Rac or Stat3-ptyr705 band intensities obtained through quantitation by fluorimager analysis and normalized to Hsp90 levels, with the peak value of the control, HC11 cells grown to confluence (lane 4) taken as 100% (see Materials and methods). (C–E) Rac is ubiquitinated *in vivo*, at low cell densities. HC11 or H-Rac^{V12} cells were grown to 30% or 100% confluence and anti-ubiquitin immunoprecipitates of detergent cell extracts (lanes 5–9) blotted against Rac1. As a control, extracts from cells grown to 30% confluence were immunoprecipitated with normal rabbit serum (lanes 3–4) or buffer alone (lanes 1–2). Bracket points to the ubiquitinated Rac. (D) Extracts from HC11 or H-Rac^{V12} cells grown to 30% or 100% confluence were blotted against Rac1. (E) HC11 cells before (lane 1) or after (lanes 2 and 3) expression of a myc-tagged, L61 mutant were grown to 30% or 100% confluence and anti-ubiquitin immunoprecipitates of detergent cell extracts blotted against the myc-tag. H.C., L.C.: IgG heavy and light chains, respectively. Bracket points to the ubiquitinated Rac.

of ubiquitin-tagged Rac (lane 9), consistent with inhibition of ubiquitination at high cell densities. When the anti-ubiquitin antibody was omitted (lane 2) or replaced with normal mouse IgG (lane 4), no Rac^{V12} was detected in the immunoprecipitates. At the same time, total Rac protein levels were much higher at high densities, both in the HC11 and H-Rac^{V12} cell lines (Fig. 2D). Taken together, these data strongly suggest that Rac^{V12} itself is a substrate of the proteasome, in sparsely growing cells exclusively. To ensure that it is the mutationally activated Rac which is ubiquitinated, we made use of the myc-tagged, Rac^{L61}. As shown in Fig. 2E, blotting anti-ubiquitin immunoprecipitates from H-Rac^{L61} cells, expressing a myc-tagged Rac^{L61}, grown to 30% confluence, with an anti-myc-tag antibody, yielded a strong band (lane 2), while at 100% confluence no myc-tagged band was detected (lane 3). The above data taken together indicate that cell density can cause a dramatic increase in both Rac, and Rac^{V12} and RacL61 protein levels, through inhibition of proteasomal degradation.

Mutationally activated Rac^{V12} and $Cdc42^{V12}$ can activate Stat3

Previous results demonstrated that Rac^{V12} expression leads to activation of Stat3. However, the effect of cell density was not taken into account in any previous report, and this could be a source of apparently conflicting results [9–11]. To definitively demonstrate the effect of Rac^{V12} upon Stat3 activity, H-Rac^{V12} cells were plated in 3 cm dishes and at different times thereafter Stat3-ptyr705 levels measured by western blotting and compared to the parental HC11. As shown in Fig. 1A (lanes 8–14), H-Rac^{V12} cells had higher Stat3-ptyr705 levels at all cell densities examined. Similar results were obtained with Rac^{L61} (not shown), while overexpression of the cellular Rac1 (wtRac1, Fig. 1D) had a substantially reduced effect upon Stat3-ptyr705 levels, compared to Rac^{V12} or Rac^{L61}. Examination of the levels of total Stat3 protein revealed a modest increase with cell density, as previously reported [12], and with Rac^{V12} or $Cdc42^{V12}$ expression (Figs. 1A, B, D), possibly due to the fact that the Stat3 promotor itself is one of the Stat3 targets [26], although the differences were not as pronounced as the Stat3-tyr705 phosphorylation observed. Stat3 transcriptional activity also increased upon Rac^{V12} or $Cdc42^{V12}$ expression (Fig. 1C), following the pattern of Stat3-tyr705 phosphorylation (Figs. 1A and B).

The effect of Rac ubiquitination upon Stat3-ptyr705 levels was examined next. As shown in Fig. 2A, treatment with MG132, which increased Rac levels, also increased the levels of Stat3-ptyr705, while expression of his-ubiquitin, which reduced Rac levels, had a proportional effect upon Stat3-ptyr705 (Fig. 2B). $Cdc42^{V12}$ mirrored the effect of Rac^{V12} regarding Stat3 activation (Fig. 1B, lanes 8–14). The above results taken together indicate that mutationally activated forms of both Rho family GTPases are indeed able to activate Stat3, above and beyond the activation due to cell density.

NFkB and JAKs are required for the Rac^{V12}-mediated, Stat3 activation

Early data showed that Rac1 can activate NFkB [27]. To examine whether NFkB may be actually required for the Rac^{V12}-mediated Stat3 activation, sparsely growing HC11 cells were trypsinised and plated to a high density (2.5×10^6 cells/3 cm petri). Following attachment, cells were treated with the Ikappa Kinase (IKK)-inhibitor-III (BMS-345541) or the DMSO carrier alone, for 48 h. As shown in Fig. 3A, treatment with the inhibitor caused a dramatic reduction in Stat3-ptyr705 levels, in both the parental HC11 (lanes 3 vs. 2) and H-Rac^{V12} (lanes 5 vs. 4) cells. Similar results were obtained with caffeic acid phenethyl ester (CAPE), another known inhibitor of NFkB activity (not shown). These data indicate that both the cell density-mediated, and Rac^{V12}-mediated increase in Stat3-tyr705 phosphorylation requires NFkB. On the other hand, Rac levels were unaffected by NFkB inhibition (Fig. 3A), which further reinforces the conclusion that NFkB is downstream of Rac, i.e., it is required for the Rac-mediated, Stat3 activation exclusively.

To explore the role of Jak1 in the Rac^{V12}-mediated, Stat3 activation, we at first investigated whether Jak1 is activated by Rac^{V12}, by examining Jak1 phosphorylation at tyr1022/1023, shown to be important in the regulation of Jak1 activity [28,29]. Jak1 phosphorylation at 1022/1023 was measured by blotting lysates from H-Rac^{V12} and HC11 cells with a phospho-specific antibody (see Materials and methods). As shown in Fig. 3B, there was a ~2 fold increase in Jak1, 1022/1023 phosphorylation upon Rac^{V12} expression at 1 day after 100% confluence (lanes 3 vs. 4), which paralleled the phosphorylation of Stat3 at this density (Fig. 3A, lanes 2 vs. 4), while at 30% confluence the difference was more pronounced (Fig. 3B, lane 1 vs. 2). To examine whether Jak1 is actually required for the Rac^{V12}-mediated increase in Stat3 activity, HC11 cells grown to densities of 1 day post-confluence were treated with the pan-JAK inhibitor, JAK inhibitor 1. The results showed a dramatic reduction in Stat3-ptyr705 levels, which essentially plateaued at 2 μM of inhibitor, consistent with previous findings [20], while Rac levels remained unaffected (Fig. 3C, lanes 1–6). Similar results were obtained with the AG490 JAK inhibitor ([30], not shown). These findings suggest that the JAK kinases are required for the Rac^{V12}-mediated increase in Stat3-ptyr705 levels.

Rac^{V12} triggers cytokine gene expression and requires gp130 for Stat3 activation

To explore the possibility that the Rac^{V12}-induced, Stat3 activation may be mediated by autocrine factors, medium conditioned by sparsely growing, H-Rac^{V12} cells was added to the parental HC11 cells growing to a low density and Stat3-ptyr705 examined. The results revealed a 3-fold increase in Stat3-ptyr705, indicating the presence of autocrine factors (not shown). To explore the nature of the cytokines responsible, we conducted a quantitative RT-PCR array experiment for 86 cytokines, comparing mRNA levels in H-Rac^{V12} cells with levels in the parental HC11 line (see Materials and methods). Given the effect of density upon Stat3 levels, to examine the effect of Rac^{V12} *per se*, we compared cells expressing Rac^{V12} with the parental HC11, while both were grown to densities of 40%. The results revealed an increase in mRNA levels of two cytokines of the IL6 family, IL6 (18-fold) and Leukemia inhibitory factor (LIF) (~10-fold), known to act through the common gp130 subunit, shared by a number of Stat3 activating cytokines [31] (Supplementary Table S2). In fact, addition of neutralising antibodies against two members of the family, IL6 and LIF separately reduced Stat3-ptyr705 levels by approximately 30%, while a combination of the two caused a reduction of ~50% (Fig. 4A, top panel). To further demonstrate the requirement for IL6 family cytokines for the Rac^{V12}-mediated, Stat3 activation, the levels of gp130 were reduced through stable expression of a specific shRNA, using a retroviral vector (see

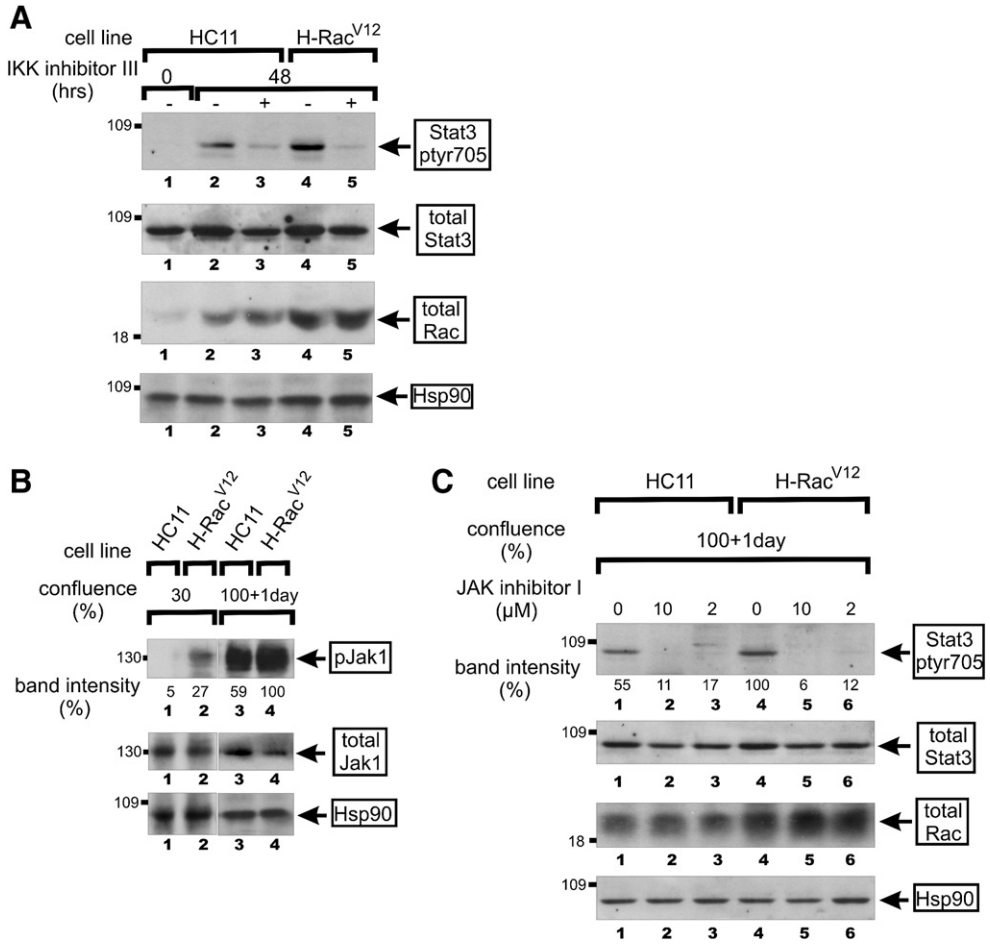

Fig. 3 – Rac^{V12}-dependent Stat3-ptyr705 phosphorylation requires JAK and NFkB. (A) The IKK inhibitor III inhibits the density-mediated, Stat3, tyr705 phosphorylation in both HC11 and H-Rac^{V12} cells. HC11 (lanes 1–3) or Rac^{V12} (lanes 4 and 5) cells were trypsinised and plated at a high density (2.5×10^6 cells/3 cm plate). Following attachment 30 min later, cells were treated with the IKK inhibitor III (lanes 3 and 5), or the DMSO carrier (lanes 2 and 4). Cell extracts were probed for Stat3-ptyr705, total Stat3, Rac or Hsp90, as a loading control. Lane 1: HC11 cells immediately after attachment to the plastic. (B) Rac^{V12}-expression increases Jak11022/1023 phosphorylation. Lysates from HC11 (lanes 1 and 3) or H-Rac^{V12} (lanes 2 and 4) cells were grown to 30% confluence (lanes 1 and 2), or 1 day after confluence (lanes 3 and 4) and probed for p-Jak1022/1023, total Jak1 or Hsp90 as a loading control, as indicated. (C) JAK inhibitor 1 reduces the Rac^{V12}-dependent, Stat3-tyr705 phosphorylation. HC11 (lanes 1–3) or Rac^{V12} (lanes 4–6) cells were grown to a high density and treated with 0 (lanes 1 and 4), 10 (lanes 2 and 5) or 2 (lanes 3 and 6) μg/ml JAK inhibitor 1. Cell lysates were probed for Stat3-ptyr705, total Stat3, Rac or Hsp90 as a loading control, as indicated.

Materials and methods). As shown in Fig. 4A, gp130 knockdown reduced Stat3-ptyr705 levels in H-Rac^{V12} cells (line H-Rac^{V12}-sh*gp130*) at all densities examined (lanes 1–3 vs. 4–6), pointing to the possibility that the two IL6 family cytokines play an important role in the activation of Stat3 by Rac^{V12}.

Rac^{V12}-induced IL6 upregulation is unable to activate Erk1/2 in confluent cultures

Results from a number of labs indicated that, in addition to Stat3, IL6 is able to activate the Erk1/2 kinase (Erk) [32]. Since Rac^{V12} expression leads to IL6 upregulation, we investigated whether Rac^{V12} can activate Erk. H-Rac^{V12} and HC11 cells were grown to 30% confluence, serum-starved for 24 h and levels of the dually phosphorylated, i.e. activated Erk1/2 (pErk) examined by Western immunoblotting. As shown in Fig. 4B, pErk levels were higher in H-Rac^{V12} cells when grown to 30% confluence than the parental HC11 (lane 2 vs. 1). At high density however, there was no Erk activity increase upon Rac^{V12} expression (lanes 4 vs. 3), although Stat3 phosphorylation was increased (Fig. 1A). To investigate whether the Erk activation by Rac^{V12} might be due to the IL6 family cytokines produced, pErk levels were examined in the gp130 knockdown cells. As shown in Fig. 4B (lanes 5–8), sh*gp130*-expressing cells had low pErk levels, even after Rac^{V12} expression (lane 6 vs. 2), indicating that IL6 activity is required for pErk upregulation by Rac^{V12}. To further verify the effect of IL6 upon Erk, we directly examined the role of density upon the activation of Erk by purified IL6. HC11 cells were grown to densities of 60% or 2 days after confluence, stimulated with IL6 for 15 min and Erk activity examined by probing for pErk (Fig. 4B, right panel). The results demonstrated that although IL6 could activate Erk in subconfluent cultures (lane 2 vs. 1), as previously reported [32], there was no Erk activity increase upon IL6 addition in cells grown to high confluence (lane 4). The above

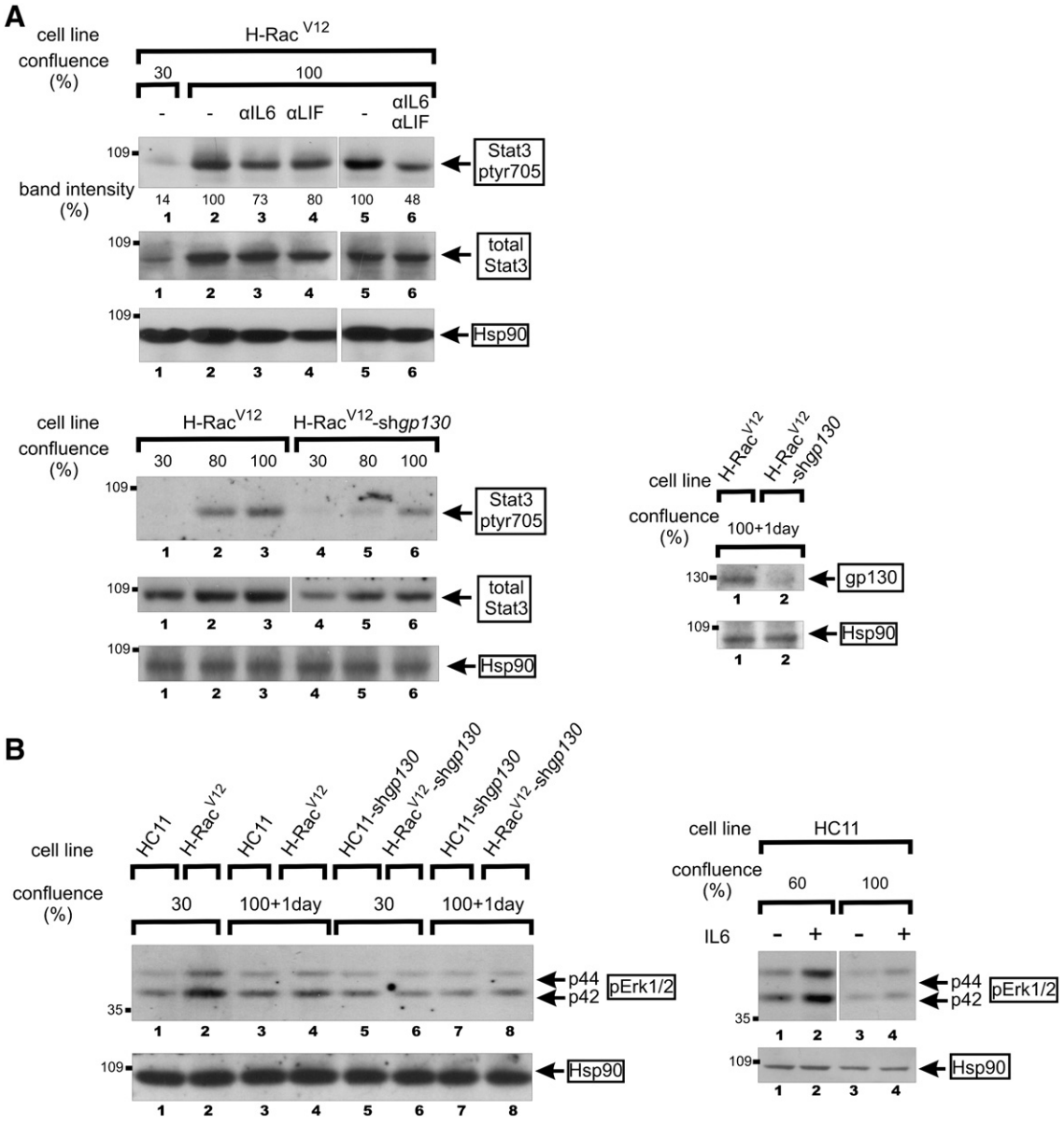

Fig. 4 – gp130 is required for the Rac^{V12}-mediated, Stat3 activation. (A) Top: reduction in Stat3-ptyr705 levels by neutralising antibodies to IL6 and LIF. Rac^{V12} cells were grown to 30% confluence (lane 1) or 1 day post-confluence and an antibody to IL6 (lane 3) or to LIF (lane 4), or a combination of the two (lane 6) added to the growth medium for 6 h. Detergent cell extracts were blotted for Stat3-ptyr705, total Stat3 or Hsp90 as a loading control. Lanes 2 and 5: control lanes, cells treated with buffer alone. Bottom panel: lysates from H-Rac^{V12} cells before (lanes 1–3) or after (lanes 4–6) expression of a gp130-specific, shRNA were probed for Stat3-ptyr705, total Stat3 or Hsp90 as a loading control, as indicated. Right panel: lysates from H-Rac^{V12} cells, before (lane 1) or after (lane 2) knockdown of gp130 were probed for gp130 or Hsp90 as a loading control, as indicated. (B) Rac^{V12} does not activate Erk at high cell densities. Left panel: extracts from the indicated cell lines, before (lanes 1–4) or after (lanes 5–8) expression of the gp130-specific, shRNA were probed for pErk1/2 or Hsp90 as a loading control, as indicated. Right panel: IL6 was added at 10 ng/ml for 15 min to HC11 cells grown to 60% (lane 2) or 100% (lane 4) confluence and cell extracts probed for Erk1/2 or Hsp90 as a loading control, as indicated.

findings clearly indicate that, although Rac^{V12} induces the expression of IL6, a known Erk activator, IL6 is unable to activate Erk in cells grown to high densities. This observation explains earlier data indicating that pErk levels are unaffected by confluence in a number of cellular systems [12], and reveals a profound effect of cell to cell adhesion upon the response of HC11 cells to IL6.

Rac^{V12}-induced cell proliferation and migration require IL6 family cytokines

The Rho family GTPases are known to play a role in the control of cell proliferation [33]. To examine the effect of IL6 family cytokines upon the Rac^{V12}-induced cell proliferation, HC11, H-*sh*gp130, H-Rac^{V12} and H-Rac^{V12}- sh*gp130* cells were plated in 3 cm dishes and their

growth rate determined. As shown in Fig. 5A, sh*gp130* expression caused a ~2.2 fold reduction in the growth rate of both H-Rac^{V12} cells and the parental HC11, indicating that gp130 is an essential component of a pathway leading to Rac-induced cell proliferation.

It is well established that increased Rac activity can increase cell motility through the formation of lamellipodia at the leading edge of cells in a wound healing assay [34]. To examine the role of the gp130 subunit in the Rac-induced cell migration, HC11, H-Rac^{V12}, H-sh*gp130* and H-Rac^{V12}-sh*gp130* cells were plated in plastic petri dishes. At 2 days post-confluence, a scratch-wound was introduced to the monolayer using a plastic pipette tip, and the cells allowed to migrate into the gap. As shown in Figs. 5B and C, Rac^{V12}-expressing cells were able to move faster to the open wound than the parental HC11 (panel f vs. b). However, gp130 downregulation abolished this effect (panel h), indicating that gp130 is an integral component of the Rac^{V12} pathway leading to the increase in cell migration. gp130 shRNA expression in the parental HC11 line also decreased cell migration (panel d). Although H-Rac^{V12} cells grow faster than H-Rac^{V12}-sh*gp130*, the accelerated growth rate cannot account for the increase in rate of migration and gap closure. Downregulation of Stat3 through shRNA knockdown [35], or treatment with the CPA7 inhibitor [18] caused a similar decrease in cell migration of H-Rac^{V12} cells (not shown), as previously reported in other systems [11]. These findings indicate that gp130 is required for cell migration triggered by the cellular Rac, and that expression of the mutationally activated Rac^{V12} cannot overcome the gp130 knockdown. Taken together, these results demonstrate that gp130 represents an essential effector of activated Rac in the regulation of both cell proliferation and migration.

Discussion

We previously demonstrated that cell to cell adhesion induces a dramatic increase in the levels of Stat3 activity, which peaks at

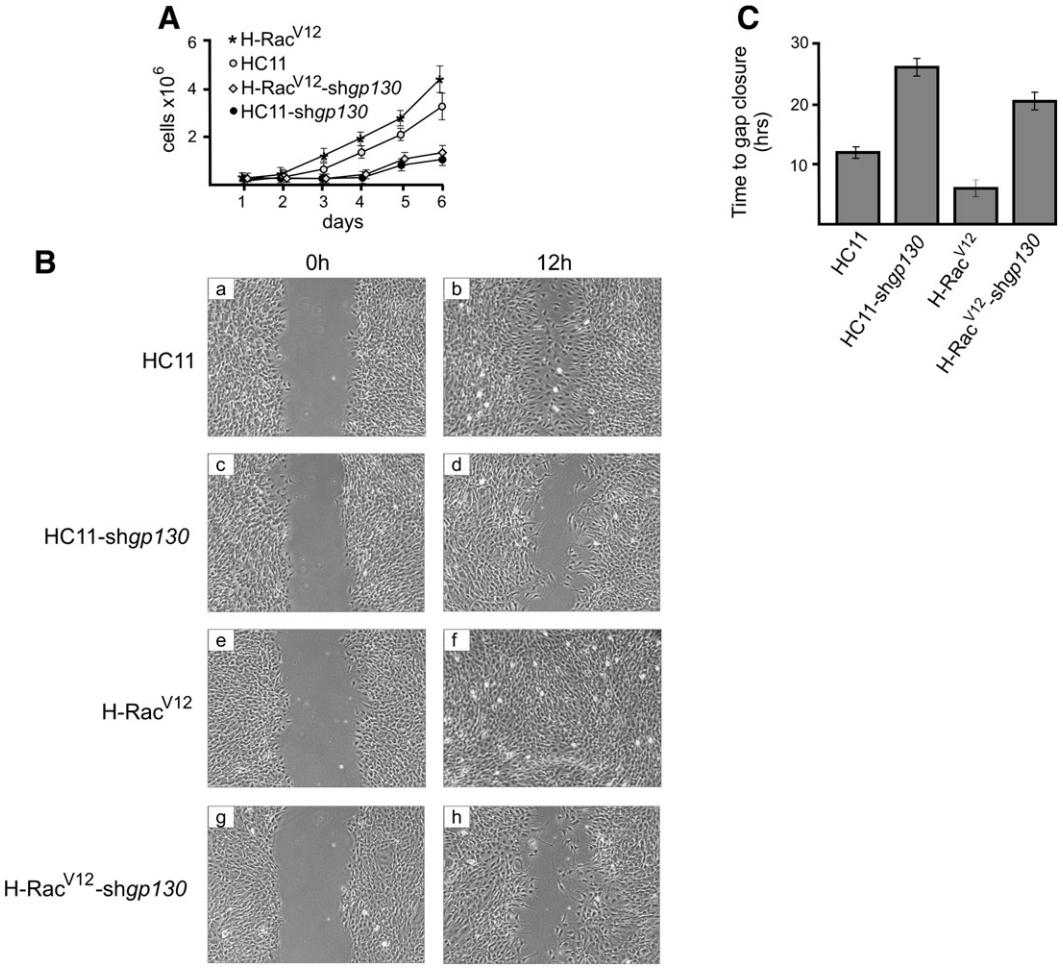

Fig. 5 – Rac-induced cell migration and proliferation require gp130. (A) Cell proliferation: HC11, H-sh*gp130*, H-Rac^{V12}, or H-Rac^{V12}-sh*gp130* cells were grown in Petri dishes in 10% serum and cell numbers obtained over several days, as indicated. Values represent averages of 3 independent experiments. (B) Cell migration: HC11, HC11-sh*gp130*, H-Rac^{V12} or H-Rac^{V12}-sh*gp130* cells were cultured to confluence before a scratch was made through the monolayer using a plastic pipette tip. Cells were photographed at 0 (panels a, c, e, g) or 24 h (panels b, d, f, h) after 12 h of culturing in 0.5% fetal calf serum. (C) Quantitation of the time (h) required by the different cell lines for gap junction closure. HC11, HC11-sh*gp130*, H-Rac^{V12} or H-Rac^{V12}-sh*gp130* cells were cultured to confluence before a scratch was made through the monolayer using a plastic pipette tip. The time taken for gap junction closure was determined by microscopic observation. Numbers represent averages of 3 independent experiments.

approximately 2 days after 100% confluence [12,36] (reviewed in [37]. An important piece of information that came out of these studies is that cell density must be taken into account in experiments to assess the effect of an oncogene upon Stat3 activity. Therefore, to investigate the effect of activated Rac upon Stat3, Stat3 activity levels were examined at different cell densities, following expression of two mutationally activated Rac constructs, Rac^{V12} and Rac^{L61}. The results revealed that Stat3 activity was increased with activated Rac expression at all cell densities examined, indicating that activated Rac can, in fact, activate Stat3, above and beyond the activation due to cell density.

These observations raise important questions: (1) What is the mechanism of increase in Rac and Rac^{V12} levels with cell density? (2) What is the mechanism of Stat3 activation by Rac^{V12}? (3) What is the functional significance of the Stat3 activation in Rac^{V12}-expressing cells?

Cell density inhibits the proteasomal degradation of Rac

We previously demonstrated that cell density increases Rac levels [20]. Our data now indicate that this increase could be due to inhibition of Rac proteasomal degradation with confluence. In fact, previous results indicated that Rac can be degraded through the proteasome pathway [25]. A mutational analysis further indicated that constitutive activation of Rac, as well as binding of effectors, which might be acting as ubiquitin E3 ligases, are necessary for Rac degradation [25]. Our results, demonstrating that, although activated, Rac^{V12} and Rac^{L61} protein levels are increased dramatically with cell density, indicate that cell density can overcome the degradative effect of activation. These findings extend and reinforce previous data indicating that epithelial cell scattering brought about by Hepatocyte Growth factor can induce the proteasome-mediated degradation of Rac1 [24]. A similar mechanism could hold true for Cdc42, which mirrored Rac levels and stability increases with cell density.

IL6 family cytokines transmit the signal from activated Rac^{V12} to Stat3

Although earlier reports [9] indicated that Rac can directly interact with Stat3 in co-expression/co-immunoprecipitation assays, later findings unequivocally demonstrated that Stat3 activation by the Rho GTPases can occur without the formation of a stable complex ([11] and data not shown). In addition, data by Faruqi et al. [10] demonstrated that Rac^{V12} could indirectly activate Stat3 through autocrine induction of IL6. However, through the use of specific antibodies added to the medium it was later demonstrated that Stat3 activation can occur independently of IL6 stimulation [11]. To resolve this apparent controversy, we examined mRNA levels for 86 cytokines in an array analysis. The results revealed an increase in two cytokines of the IL6 family (IL6 and LIF), indicating that this family may be involved in Stat3 activation by mutationally activated Rac. Furthermore, downregulation of gp130, the common subunit of the family, abolished the Rac^{V12}-mediated, Stat3 activation indicating that this subunit is actually required for Stat3 activation. The fact that the LIF also, rather than IL6 alone, is upregulated by Rac^{V12} explains earlier data indicating that IL6-specific antibodies did not reduce Stat3 activity [11], since these antibodies, directed against the unique extracellular subunit of IL6 would inhibit IL6 exclusively, while LIF would still be free to activate Stat3. In any event, these results demonstrate that the total Stat3 activity in the cell is the sum of effects of both cell to cell adhesion, plus the Stat3 activating, Rac^{V12} or $Cdc42^{V12}$ oncogene present.

Previous results indicated that IL6 activates Erk, as well as Stat3. Since Rac^{V12} causes the upregulation of IL6 family cytokines, it is expected that Rac^{V12} expression would activate Erk. However, although Rac^{V12}-expressing cells had higher pErk levels than the parental HC11, when sparsely grown, there was no pErk increase in H-Rac^{V12} cells grown to high densities. To solve this apparent paradox, HC11 cells were grown to different densities and stimulated with IL6. Indeed IL6 itself, although able to activate Erk in subconfluent cultures, was unable to do so once cells reached confluence (Fig. 4B), although Stat3 was still activated (Fig. 1). It is possible that Erk-specific phosphatases such as Cdc25A are activated at high cell densities [38], or that other adaptors required for Erk activation by IL6, or phosphorylation of IL6-R sites, are downregulated following cadherin engagement and establishment of cell to cell contacts. In any event, these results further demonstrate that, despite the fact that these two pathways are often both activated by oncogenes, cytokines or growth factors, they are not coordinately regulated by IL6 in densely growing cells.

Gp130 is required for Rac-mediated cell proliferation and migration

It is well established that Rac activation can increase cell motility, in part due to regulation of the actin cytoskeleton. However, the role of the IL6/Stat3 axis in this effect has not been examined. Our results showed that, as observed before [34], Rac^{V12}-expressing, HC11 cells were able to move faster into an open wound intro-

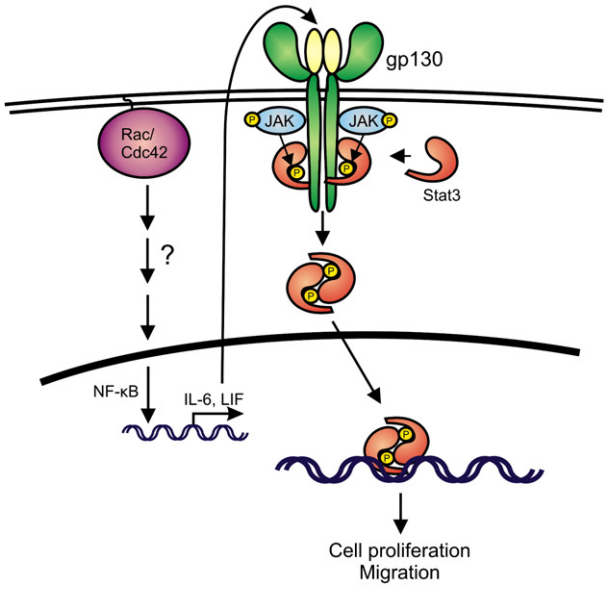

Fig. 6 – Proposed model for Rac/Cdc42-mediated, Stat3 activation. Constitutively active Rac/Cdc42 activates Stat3 through induction of IL6 family cytokines, such as IL6 and LIF which possess the common subunit, gp130. This leads to activation of their respective receptors, Jak activation and phosphorylation of Stat3, resulting in cell proliferation and migration.

duced with a plastic pipette tip into a cell monolayer than the parental line [1]. Furthermore, the Rac-mediated motility required the activity of IL6 family cytokines, since downregulation of the gp130, common subunit of the family, reduced the rate of migration. The fact that activated Rac^{V12} upregulates IL6 and Stat3, gives further credence to the model of Stat3 activation by cadherin engagement, *via* Rac and IL6 [20].

Conclusions

Our results definitively demonstrate that activated Rac/Cdc42 expression leads to Stat3 activation, by a mechanism requiring NFkB, gp130 and JAK. This pathway is required for cell proliferation and migration, that is the gp130/Stat3 axis represents an essential effector of activated Rac for the regulation of key cellular functions (Fig. 6).

Acknowledgments

Special thanks are due to Dr. Richard Jove and Dr. James Turkson for valuable advice. We would like to thank Dr. John Collard for the Rac^{V12} vector and Dr. Graham Côté for the Rac^{L61}, wtRac1 and $Cdc42^{V12}$ vectors and Dr. Harriet Feilotter and Xiao Zhang of the Queen's University Laboratory for Molecular Pathology/Microarray Facility for qRT-PCR array analysis.

The financial assistance of the Canadian Institutes of Health Research (CIHR), the Canadian Breast Cancer Foundation (Ontario Chapter), the Natural Sciences and Engineering Research Council of Canada (NSERC), the Ontario Centers of Excellence, the Canadian Breast Cancer Research Alliance, the Breast Cancer Action Kingston and the Clare Nelson bequest fund (LR) and the Fondation pour la Recherche Médicale, Région Aquitaine and the Association pour la Recherche contre le Cancer (HF), is gratefully acknowledged. RA was supported by a Canada Graduate Scholarships Doctoral award from CIHR, the Ontario Women's Health Scholars Award from the Ontario Council of Graduate Studies and a Queen's University Graduate Award (QGA). MG was supported by a postdoctoral fellowship from the US Department of Defense breast cancer research program (BCRP-CDMRP), a postdoctoral fellowship from the Ministry of Research and Innovation of the Province of Ontario and the Advisory Research Committee of Queen's University.

Appendix A. Supplementary data

Supplementary data associated with this article can be found, in the online version, at doi:10.1016/j.yexcr.2009.10.017.

REFERENCES

[1] S. Etienne-Manneville, A. Hall, Rho GTPases in cell biology, Nature 420 (2002) 629–635.
[2] R. Perona, S. Montaner, L. Saniger, I. Sanchez-Perez, R. Bravo, J.C. Lacal, Activation of the nuclear factor-kappaB by Rho, CDC42, and Rac-1 proteins, Genes Dev. 11 (1997) 463–475.
[3] D. Joyce, B. Bouzahzah, M. Fu, C. Albanese, M. D'Amico, J. Steer, J.U. Klein, R.J. Lee, J.E. Segall, J.K. Westwick, C.J. Der, R.G. Pestell, Integration of Rac-dependent regulation of cyclin D1 transcription through a nuclear factor-kappaB-dependent pathway, J. Biol. Chem. 274 (1999) 25245–25249.
[4] D.A. Frank, STAT3 as a central mediator of neoplastic cellular transformation, Cancer Lett. 251 (2007) 199–210.
[5] J.F. Bromberg, M.H. Wrzeszczynska, G. Devgan, Y. Zhao, R.G. Pestell, C. Albanese, J.E. Darnell Jr., Stat3 as an oncogene, Cell 98 (1999) 295–303.
[6] W. Hung, B. Elliott, Co-operative effect of c-Src tyrosine kinase and Stat3 in activation of hepatocyte growth factor expression in mammary carcinoma cells, J. Biol. Chem. 276 (2001) 12395–12403.
[7] G. Niu, K.L. Wright, Y. Ma, G.M. Wright, M. Huang, R. Irby, J. Briggs, J. Karras, W.D. Cress, D. Pardoll, R. Jove, J. Chen, H. Yu, Role of Stat3 in regulating p53 expression and function, Mol. Cell. Biol. 25 (2005) 7432–7440.
[8] H. Yu, R. Jove, The STATs of cancer—new molecular targets come of age, Nat. Rev., Cancer 4 (2004) 97–105.
[9] A.R. Simon, H.G. Vikis, S. Stewart, B.L. Fanburg, B.H. Cochran, K.L. Guan, Regulation of STAT3 by direct binding to the Rac1 GTPase, Science 290 (2000) 144–147.
[10] T.R. Faruqi, D. Gomez, X.R. Bustelo, D. Bar-Sagi, N.C. Reich, Rac1 mediates STAT3 activation by autocrine IL-6, Proc. Nat. Acad. Sci. U. S. A. 98 (2001) 9014–9019.
[11] M. Debidda, L. Wang, H. Zang, V. Poli, Y. Zheng, A role of STAT3 in Rho GTPase-regulated cell migration and proliferation, J. Biol. Chem. 280 (2005) 17275–17285.
[12] A. Vultur, J. Cao, R. Arulanandam, J. Turkson, R. Jove, P. Greer, A. Craig, B.E. Elliott, L. Raptis, Cell to cell adhesion modulates Stat3 activity in normal and breast carcinoma cells, Oncogene 23 (2004) 2600–2616.
[13] A. Onishi, Q. Chen, J.O. Humtsoe, R.H. Kramer, STAT3 signaling is induced by intercellular adhesion in squamous cell carcinoma cells, Exp. Cell Res. 314 (2008) 377–386.
[14] R.A. Steinman, A. Wentzel, Y. Lu, C. Stehle, J.R. Grandis, Activation of Stat3 by cell confluence reveals negative regulation of Stat3 by cdk2, Oncogene 22 (2003) 3608–3615.
[15] H.W. Su, H.H. Yeh, S.W. Wang, M.R. Shen, T.L. Chen, P.R. Kiela, F.K. Ghishan, M.J. Tang, Cell confluence-induced activation of signal transducer and activator of transcription-3 (Stat3) triggers epithelial dome formation via augmentation of sodium hydrogen exchanger-3 (NHE3) expression, J. Biol. Chem. 282 (2007) 9883–9894.
[16] S. Kreis, G.A. Munz, S. Haan, P.C. Heinrich, I. Behrmann, Cell density dependent increase of constitutive signal transducers and activators of transcription 3 activity in melanoma cells is mediated by Janus kinases, Mol. Cancer Res. 5 (2007) 1331–1341.
[17] R.K. Ball, R.R. Friis, C.A. Schoenenberger, W. Doppler, B. Groner, Prolactin regulation of beta-casein gene expression and of a cytosolic 120-kd protein in a cloned mouse mammary epithelial cell line, EMBO J. 7 (1988) 2089–2095.
[18] S.L. Littlefield, M.C. Baird, A. Anagnostopoulou, L. Raptis, Synthesis, characterization and Stat3 inhibitory properties of the prototypical platinum(IV) anticancer drug, [PtCl3(NO2)(NH3)2] (CPA-7), Inorg. Chem. 47 (2008) 2798–2804.
[19] E.E. Sander, S. van Delft, J.P. ten Klooster, T. Reid, R.A. van der Kammen, F. Michiels, J.G. Collard, Matrix-dependent Tiam1/Rac signaling in epithelial cells promotes either cell–cell adhesion or cell migration and is regulated by phosphatidylinositol 3-kinase, J. Cell Biol. 143 (1998) 1385–1398.
[20] R. Arulanandam, A. Vultur, J. Cao, E. Carefoot, P. Truesdell, B. Elliott, L. Larue, H. Feracci, L. Raptis, Cadherin–cadherin engagement promotes survival via Rac/Cdc42 and Stat3, Mol. Cancer Res. 17 (2009) 1310–1327.
[21] S. Tsubuki, Y. Saito, M. Tomioka, H. Ito, S. Kawashima, Differential inhibition of calpain and proteasome activities by peptidyl aldehydes of di-leucine and tri-leucine, J. Biochem. 119 (1996) 572–576.
[22] Q. Zhu, G. Wani, J. Yao, S. Patnaik, Q.E. Wang, M.A. El Mahdy, M. Praetorius-Ibba, A.A. Wani, The ubiquitin–proteasome system

regulates p53-mediated transcription at p21waf1 promoter, Oncogene 26 (2007) 4199–4208.
[23] M. Treier, L.M. Staszewski, D. Bohmann, Ubiquitin-dependent c-Jun degradation in vivo is mediated by the delta domain, Cell 78 (1994) 787–798.
[24] E.A. Lynch, J. Stall, G. Schmidt, P. Chavrier, C. D'Souza-Schorey, Proteasome-mediated degradation of Rac1-GTP during epithelial cell scattering, Mol. Biol. Cell 17 (2006) 2236–2242.
[25] M. Pop, K. Aktories, G. Schmidt, Isotype-specific degradation of Rac activated by the cytotoxic necrotizing factor 1, J. Biol. Chem. 279 (2004) 35840–35848.
[26] M. Narimatsu, H. Maeda, S. Itoh, T. Atsumi, T. Ohtani, K. Nishida, M. Itoh, D. Kamimura, S.J. Park, K. Mizuno, J. Miyazaki, M. Hibi, K. Ishihara, K. Nakajima, T. Hirano, Tissue-specific autoregulation of the stat3 gene and its role in interleukin-6-induced survival signals in T cells, Mol. Cell. Biol. 21 (2001) 6615–6625.
[27] D.J. Sulciner, K. Irani, Z.X. Yu, V.J. Ferrans, P. Goldschmidt-Clermont, T. Finkel, rac1 regulates a cytokine-stimulated, redox-dependent pathway necessary for NF-kappaB activation, Mol. Cell. Biol. 16 (1996) 7115–7121.
[28] M.C. Gauzzi, L. Velazquez, R. McKendry, K.E. Mogensen, M. Fellous, S. Pellegrini, Interferon-alpha-dependent activation of Tyk2 requires phosphorylation of positive regulatory tyrosines by another kinase, J. Biol. Chem. 271 (1996) 20494–20500.
[29] W.J. Leonard, J.J. O'Shea, Jaks and STATs: biological implications, Annu. Rev. Immunol. 16 (1998) 293–322.
[30] Y. Zhang, J. Turkson, C. Carter-Su, T. Smithgall, A. Levitzki, A. Kraker, J.J. Krolewski, P. Medveczky, R. Jove, Activation of Stat3 in v-Src transformed fibroblasts requires cooperation of Jak1 kinase activity, J. Biol. Chem. 275 (2000) 24935–24944.
[31] D. Hilfiker-Kleiner, A. Hilfiker, M. Fuchs, K. Kaminski, A. Schaefer, B. Schieffer, A. Hillmer, A. Schmiedl, Z. Ding, E. Podewski, E. Podewski, V. Poli, M.D. Schneider, R. Schulz, J.K. Park, K.C. Wollert, H. Drexler, Signal transducer and activator of transcription 3 is required for myocardial capillary growth, control of interstitial matrix deposition, and heart protection from ischemic injury, Circ. Res. 95 (2004) 187–195.
[32] P. Fischer, D. Hilfiker-Kleiner, Role of gp130-mediated signalling pathways in the heart and its impact on potential therapeutic aspects, Br. J. Pharmacol. 153 (Suppl. 1) (2008) S414–S427.
[33] F. Guo, Y. Zheng, Involvement of Rho family GTPases in p19Arf- and p53-mediated proliferation of primary mouse embryonic fibroblasts, Mol. Cell Biol. 24 (2004) 1426–1438.
[34] C.D. Nobes, A. Hall, Rho GTPases control polarity, protrusion, and adhesion during cell movement, J. Cell Biol. 144 (1999) 1235–1244.
[35] M. Geletu, C. Chaize, R. Arulanandam, A. Vultur, C. Kowolik, A. Anagnostopoulou, R. Jove, L. Raptis, Stat3 activity is required for gap junctional permeability in normal epithelial cells and fibroblasts, DNA Cell Biol. 28 (2009) 319–327.
[36] A. Vultur, R. Arulanandam, J. Turkson, G. Niu, R. Jove, L. Raptis, Stat3 is required for full neoplastic transformation by the Simian Virus 40 Large Tumor antigen, Mol. Biol. Cell 16 (2005) 3832–3846.
[37] L. Raptis, R. Arulanandam, A. Vultur, M. Geletu, S. Chevalier, H. Feracci, Beyond structure, to survival: Stat3 activation by cadherin engagement, Biochem. Cell Biol. 87 (2009) 835–843.
[38] J.S. Lazo, K. Nemoto, K.E. Pestell, K. Cooley, E.C. Southwick, D.A. Mitchell, W. Furey, R. Gussio, D.W. Zaharevitz, B. Joo, P. Wipf, Identification of a potent and selective pharmacophore for Cdc25 dual specificity phosphatase inhibitors, Mol. Pharmacol. 61 (2002) 720–728.

Journal of Immunological Methods 355 (2010) 76–79

Contents lists available at ScienceDirect

Journal of Immunological Methods

journal homepage: www.elsevier.com/locate/jim

Technical note

Housekeeping genes; expression levels may change with density of cultured cells

Samantha Greer [1], Rice Honeywell [1], Mulu Geletu, Rozanne Arulanandam, Leda Raptis *

Department of Microbiology and Immunology, Queen's University, Kingston, Ontario, Canada K7L 3N6
Department of Pathology and Molecular Medicine, and Queen's University Cancer Institute, Queen's University, Kingston, Ontario, Canada K7L 3N6

ARTICLE INFO

Article history:
Received 9 September 2009
Received in revised form 5 February 2010
Accepted 10 February 2010
Available online 19 February 2010

Keywords:
α-tubulin
GAPDH
Hsp90
β-actin
Gel electrophoresis
Cell confluence

ABSTRACT

Western blotting is a powerful technique to characterize a multitude of cellular proteins. As an internal control, the blots are commonly probed for "housekeeping" gene products. In this communication, we show that cell confluence significantly affects the levels of two such widely used proteins, α-tubulin and Glyceraldehyde-3-Phosphate Dehydrogenase. On the other hand the levels of heat-shock protein-90 and β-actin remained unchanged at a wide range of cell densities, making these proteins into more reliable loading controls.

1. Introduction

Western immunoblotting is a powerful technique to detect and characterize a multitude of proteins. Since the first trials in 1979 (Towbin et al., 1979), Western blotting methods have been used extensively to examine protein levels in different cells or tissues (Kurien and Scofield, 2003). Proteins are usually resolved by sodium-dodecylsulphate-polyacrylamide gel electrophoresis (SDS-PAGE) at first, then transferred electrophoretically to a membrane. The subsequent detection of the membrane-bound proteins using specific antibodies has evolved into a powerful tool for cell biology. The experimental protocol invariably involves the comparison of levels of a given protein or its modifications under study between different cell preparations. For this reason, it is necessary to ensure that all lanes of the gel were loaded with equal amounts of total protein and this can be achieved by determining protein concentrations in the cell lysates. However, as an internal control, and to take protein degradation into account, it is also necessary to probe for a protein which is not expected to change with the different conditions ("housekeeping" gene product). In fact, antibodies to a number of such proteins have been commercially developed. Most are also very abundant proteins in the cell, such as β-actin, heat-shock protein-90 (Hsp90), Glyceraldehyde-3-Phosphate Dehydrogenase (GAPDH) and α-tubulin, to name a few.

Cells in normal tissues or in tumors have extensive opportunities for adhesion to their neighbors in a three-dimensional organization. This is reproduced *in vitro* by culturing cells in dishes to high densities; such dense cultures, albeit only two dimensional, may in part mimic some of the physiological signals that occur *in vivo*. In fact, cell to cell adhesion in cultured, normal epithelial cells and fibroblasts triggers an increase in activity of the Rac1 and Cdc42, Rho family GTPases (Etienne-Manneville and Hall, 2002), which plateaus at a confluence of ~90%. Rac1/Cdc42, in turn, were found to cause a dramatic increase in the phosphorylation of the Signal transducer and activator of transcription-3 at tyr705 (Stat3-ptyr705) (Arulanandam et al., 2009). The peak is usually at 1–

* Corresponding author. Department of Microbiology and Immunology, Queen's University Botterell Hall, Rm. 713 Kingston, Ontario Canada K7L3N6. Tel.: +1 613 533 2462; fax: +1 613 533 6796.
E-mail address: raptisl@queensu.ca (L. Raptis).
[1] The first two authors contributed equally to this work.

0022-1759/$ – see front matter © 2010 Elsevier B.V. All rights reserved.
doi:10.1016/j.jim.2010.02.006

2 days after confluence, depending upon the cells' growth rate (Vultur et al., 2004; Raptis et al., 2009). In such experiments, it is important to employ a gene product whose levels are not affected by cell density, as a control for protein loading.

In our search for a suitable marker, we examined the effect of cell density upon the levels of a number of commonly used housekeeping gene products. The results showed that the levels of GAPDH and α-tubulin increased gradually with cell density starting at 10% confluence and plateauing at ~90%. Hsp90 and β-actin levels on the other hand did not change with cell density, from 10% confluence up to 5 days after confluence, indicating that these proteins may be appropriate controls. This is the first report on the effect of density of cultured cells upon the levels of certain commonly used, housekeeping gene products.

2. Materials and methods

2.1. Cell growth, protein extraction, and Western blotting

Mouse NIH3T3 fibroblasts (subclone DL+10) were previously described (Vultur et al., 2004). They were grown to different densities in Dulbecco's modification of Eagle's medium supplemented with 5% calf serum. Cells were scraped with a rubber policeman into 1.8 mL microcentrifuge tubes, washed with cold phosphate-buffered saline (PBS) and the cell pellet resuspended in the different extraction buffers. Three buffers were used: NP-40 [50 mM Hepes pH 7.4, 150 mM NaCl, 10 mM EDTA, 10 mM $Na_4P_2O_7$, 1% NP-40, 100 mM NaF, 2 mM Na_3VO_4, 0.5 mM phenylmethylsulphonyl fluoride (PMSF), 10 μg/mL aprotinin, 10 μg/mL leupeptin], radioimmunoassay precipitation assay buffer [RIPA, 150 mM NaCl, 1% NP-40, 50 mM Tris, pH 8.0, 0.5% sodium deoxycholate, 0.1% sodium dodecyl sulphate (SDS), 5 mM NaF, 2 mM Na_3VO_4, 1.25 mM PMSF, 10 μg/mL aprotinin, 10 μg/mL leupeptin] and SDS buffer [1% SDS, 10 mM ethylene-diaminetetraacetic acid, 80 mM Tris, pH 8.1, 5 mM NaF, 2 mM Na_3VO_4, 1.25 mM PMSF, 10 μg/mL aprotinin, 10 μg/mL leupeptin]. To optimize protein quantitation, the amount of extraction buffer was proportional to cell numbers, 100 μL/10^6 cells. Following extraction, NP-40 and RIPA lysates were clarified by centrifugation. SDS extracts on the other hand were passed through a syringe to break up the DNA and liquefy the preparation. Protein determination followed on clarified

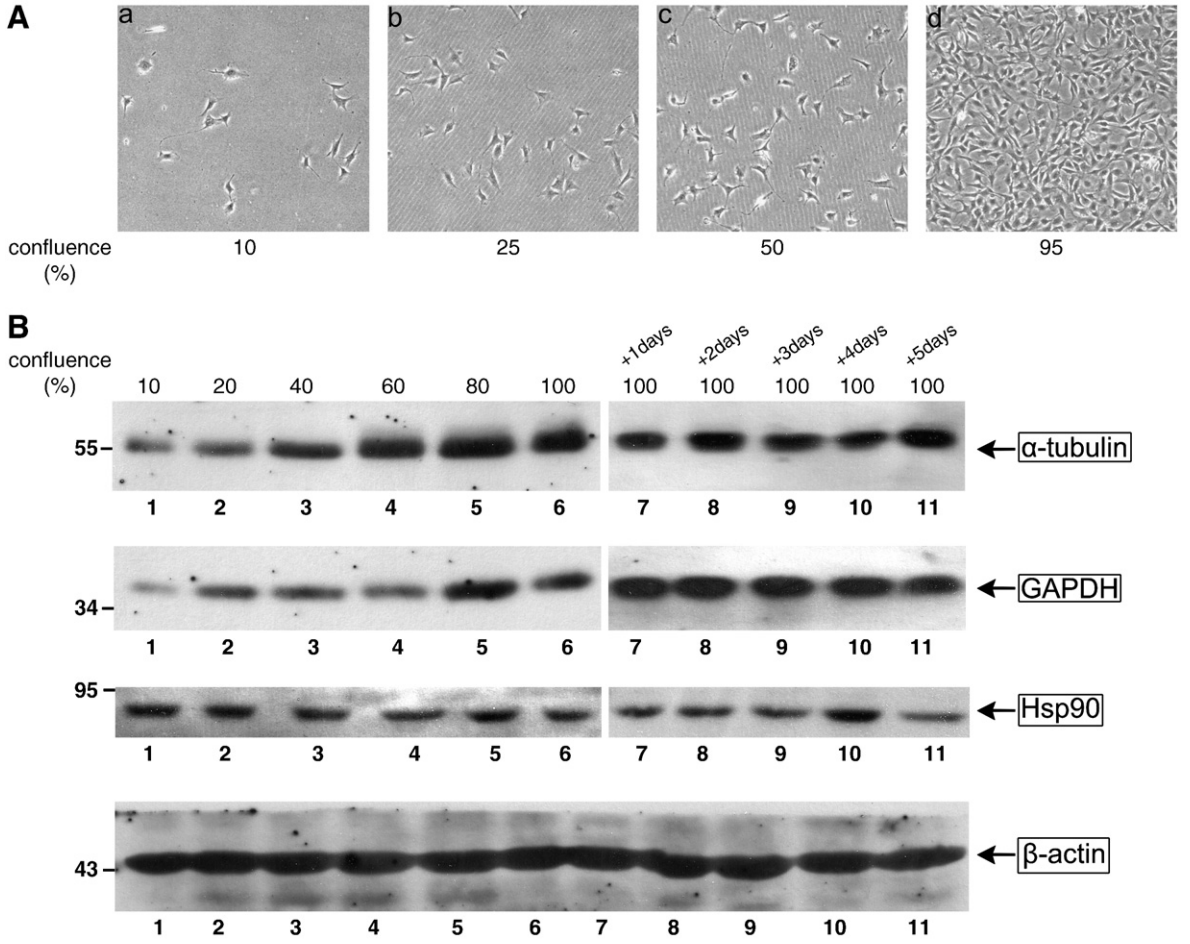

Fig. 1. α-tubulin and GAPDH levels increase with cell density, while Hsp90 and β-actin levels remain unaffected. A. NIH3T3 fibroblasts grown to the indicated confluences were photographed under phase-contrast illumination. Magnification: 140×. B. RIPA extracts from NIH3T3 cells grown to different densities were resolved by gel electrophoresis and blots probed for α-tubulin, GAPDH, Hsp90 or β-actin, as indicated. Numbers at the left refer to molecular weight markers. 30 μg total protein were loaded per lane.

extracts and 30 μg protein from each preparation were loaded onto SDS-PAGE gels. Lysates were clarified by centrifugation (10,000 *g*, 20 min) and protein determination conducted using the bicinchoninic acid kit (Sigma, Cat.# BCA1-1KT) for the NP-40 or RIPA extracts or the *DC* protein assay kit II (Bio-Rad, Cat.# 500-0112) for the SDS extracts. Proteins were resolved by SDS-PAGE and electrophoretically transferred to a nitrocellulose membrane (Bio-Rad). Blots were probed with antibodies to α-tubulin (Cell Signaling, Cat.# 2125), GAPDH (Cell Signaling, Cat.# 2118), Hsp90 (Stressgen, Cat.# SPA-830) and β-actin (Biovision, Cat.# 3598-199), followed by alkaline phosphatase-conjugated secondary antibodies and ECL reagents, according to the manufacturer's protocols (Biosource, Pierce). Bands were visualized using enhanced chemiluminescence (PerkinElmer Life Sciences, Cat.# NEL602), or SuperSignal West Femto Maximum Sensitivity Substrate (Pierce, Cat.# 34095). Quantitation was achieved by fluorimager analysis using the FluorChem program (AlphaInnotech Corp.).

3. Results and discussion

Mouse NIH3T3 fibroblasts were grown in tissue culture dishes at different densities, ranging from 10% confluence to 5 days after 100% confluence (Fig. 1A). To eliminate any effects of extraction efficiency differences, we used three commonly employed lysis buffers. In initial experiments, cells were lysed directly on the plate and protein determination conducted on extracts clarified by centrifugation. However, significant amounts of serum proteins (mainly bovine serum albumin) present in the growth medium were found to attach non-specifically to the plastic tissue culture dish and be eluted with the detergent-containing extraction buffer. The amounts were found to vary from 2.22 μg/cm^2 to 9.46 μg/cm^2 for cells grown in 5% calf serum, and they could disturb the determination of protein concentration in the lysate significantly, especially at lower cell densities. To avoid this problem, cells were scraped in ice-cold PBS, transferred into microcentrifuge tubes, washed once in PBS and the extraction

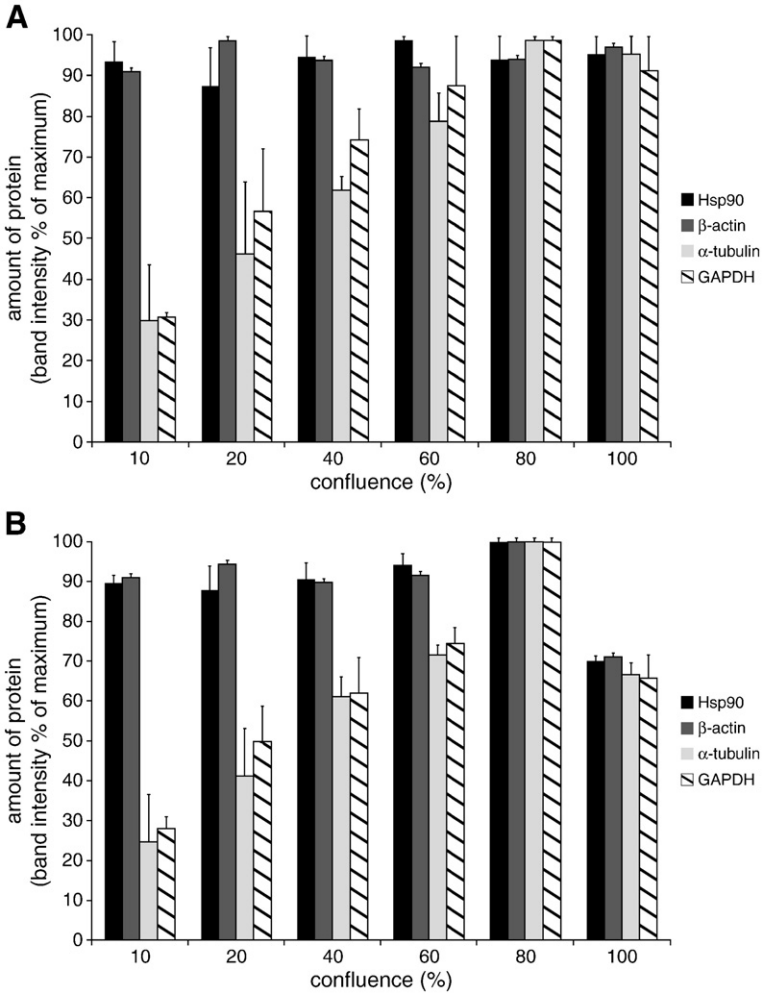

Fig. 2. Quantitation of protein levels at different densities. A. The results of quantitation of band intensity of the different proteins are presented, loading 30 μg total protein per lane. Values shown represent units expressed as a percentage of the highest value obtained for each protein, means ± s.e.m. of at least 3 experiments, each performed in triplicate, with each extraction buffer. B. The results of quantitation of band intensity of the different proteins are presented, loading the protein from 60,000 cells per lane. Values shown represent units expressed as a percentage of the highest value obtained for each protein, means ± s.e.m. of 3 experiments, each performed in triplicate, with each extraction buffer.

buffer added to cell pellets for 10 min with vigorous pipetting. Three different, commonly employed buffers were used, NP-40, RIPA and SDS (see Materials and methods) and 30 μg total protein loaded per lane. As shown in Fig. 1B and Fig. 2A, there was a ~3× increase in the amount of α-tubulin detected in cells grown to 100%, compared to 10% confluence. A similar increase was seen in the levels of GAPDH, and it was the same regardless of extraction method used. However, Hsp90 and β-actin levels remained essentially unchanged with cell density. Similar results were obtained with a number of other cell lines, such as the A549 and SK-Luci-6 lung carcinoma (Tomai et al., 1999), the MDA-MB-468, MDA-MB-231 and MDA-MB-453 breast carcinoma (Vultur et al., 2004), normal mouse breast epithelial HC11 (Arulanandam et al., 2009), rat liver epithelial T51B (Geletu et al., 2009), and mouse primary and spontaneously established fibroblasts, before and after transformation by the middle tumor antigen of polyoma virus (Raptis et al., 1985) or the large tumor antigen of Simian Virus 40 (Vultur et al., 2005).

Since the content per cell of many proteins may change with cell density, these experiments were repeated, loading the protein from an equal number of cells (60,000) per lane (Fig. 2B). This amounted to 30 μg protein for actively growing NIH3T3 cells, i.e. at confluences of up to 75%, while the same number of cells at 100% confluence had 23.3 μg as expected, due to the higher proportion of cells in Go/G1. The results showed that at densities of up to ~75% Hsp90 and β-actin levels were unchanged with density, while the levels of GAPDH and α-tubulin increased as above. However, at confluences equal to or greater than 100% the amounts of all housekeeping proteins examined were lower compared to cells grown to 75% confluence, indicating that their levels are proportional to the amount of cellular protein loaded, regardless of cell numbers.

To compare the efficiency of extraction with the different buffers, the levels of these proteins remaining in the pellets were assessed; following NP-40 or RIPA extraction, the pellets were solubilised by resuspending in SDS buffer and the amounts of residual α-tubulin and GAPDH quantitated by Western blotting. Pellets from cells extracted with NP-40 contained approximately equal amounts of α-tubulin as the supernatants, and twice the amounts present in the pellets from cells extracted with RIPA buffer, indicating that the RIPA buffer can extract ~2× higher amounts of α-tubulin than the NP-40. However, no GAPDH was detected in any of the pellets, indicating that both buffers can extract most of this cytosolic protein.

Conclusions

In this communication we examined the levels of four gene products which are commonly used as loading controls in Western blotting experiments. The results revealed that levels of α-tubulin and GAPDH increased significantly with cell confluence from 10% to 100%, which shows that these proteins may be unsuitable as loading controls for Western blotting experiments requiring growth of cells to subconfluence. On the other hand, our results demonstrate that Hsp90 and β-actin levels were essentially unaffected by cell confluence, making these proteins into reliable gel loading controls for a wide range of cell densities.

Acknowledgements

The financial assistance of the Canadian Institutes of Health Research (CIHR), the Canadian Breast Cancer Foundation (Ontario Chapter), the Natural Sciences and Engineering Research Council of Canada (NSERC), the Ontario Centres of Excellence, the Breast Cancer Action Kingston, the Clare Nelson bequest fund and the Canadian Breast Cancer Research Alliance through grants to LR is gratefully acknowledged. RA was supported by a Canada Graduate Scholarships Doctoral award from CIHR, the Ontario Women's Health Scholars Award from the Ontario Council on Graduate Studies and a Queen's University Graduate Award (QGA). SG was supported by an NSERC USRA award. MG was supported by a fellowship from the Ministry of Research and Innovation of the Province of Ontario and a postdoctoral fellowship from the US Army breast cancer program.

References

Arulanandam, R., Vultur, A., Cao, J., Carefoot, E., Truesdell, P., Elliott, B., Larue, L., Feracci, H., Raptis, L., 2009. Cadherin–cadherin engagement promotes survival via Rac/Cdc42 and Stat3. Mol. Cancer Res. 17, 1310.

Etienne-Manneville, S., Hall, A., 2002. Rho GTPases in cell biology. Nature 420, 629.

Geletu, M., Chaize, C., Arulanandam, R., Vultur, A., Kowolik, C., Anagnostopoulou, A., Jove, R., Raptis, L., 2009. Stat3 activity is required for gap junctional permeability in normal epithelial cells and fibroblasts. DNA Cell Biol. 28, 319.

Kurien, B.T., Scofield, R.H., 2003. Protein blotting: a review. J. Immunol. Methods 274, 1.

Raptis, L., Arulanandam, R., Vultur, A., Geletu, M., Chevalier, S., Feracci, H., 2009. Beyond structure, to survival: Stat3 activation by cadherin engagement. Biochem. Cell Biol. 87, 835.

Raptis, L., Lamfrom, H., Benjamin, T.L., 1985. Regulation of cellular phenotype and expression of polyomavirus middle T antigen in rat fibroblasts. Mol. Cell. Biol. 5, 2476.

Tomai, E., Brownell, H.L., Tufescu, T., Reid, K., Raptis, L., 1999. Gap junctional communication in lung carcinoma cells. Lung Cancer 23, 223.

Towbin, H., Staehelin, T., Gordon, J., 1979. Electrophoretic transfer of proteins from polyacrylamide gels to nitrocellulose sheets: procedure and some applications. Proc. Natl. Acad. Sci. U. S. A 76, 4350.

Vultur, A., Arulanandam, R., Turkson, J., Niu, G., Jove, R., Raptis, L., 2005. Stat3 is required for full neoplastic transformation by the Simian Virus 40 Large Tumor antigen. Mol. Biol. Cell 16, 3832.

Vultur, A., Cao, J., Arulanandam, R., Turkson, J., Jove, R., Greer, P., Craig, A., Elliott, B.E., Raptis, L., 2004. Cell to cell adhesion modulates Stat3 activity in normal and breast carcinoma cells. Oncogene 23, 2600.